Identification and characterization of a HY5-BBX transcriptional module regulating light and karrikin signaling

Inaugural-Dissertation
to obtain the academic degree
Doctor rerum naturalium (Dr. rer. nat.)

Submitted to the Department of Biology, Chemistry, Pharmacy
of Freie Universität Berlin

by

Katharina Bursch, M.Sc.

Berlin, 2021

December 2016 to July 2021

This work was conducted under supervision of Dr. Henrik Johansson at the Institute of Biology, Department of Applied Genetics at the Freie Universität Berlin.

1st Reviewer: Dr. Henrik Johansson

2nd Reviewer: Prof. Dr. Thomas Schmülling

Date of defense 13.10.2021

Statement of Authorship

Herewith I certify that I have prepared and written this thesis independently and that I have not used any sources and aids other than those indicated by me.

Berlin, July 2021 Katharina Bursch

Acknowledgements

I would like to express my deepest gratitude to Dr. Henrik Johansson for giving me the opportunity to collaborate with him and work in his lab on the projects comprising this dissertation. I could not have wished for a better supervisor and mentor.

Further, I wish to thank Prof. Dr. Thomas Schmülling, not only for reviewing this work, but also for his constant support throughout the last years.

Many thanks to my student assistants Miriam Lohr and Ella Niemann for your work and effort in the lab. Without your help, I might still be genotyping the last mutants for this research project.

Special thanks to all the people, who keep the applied genetics research running, to the technicians, the gardeners, the secretary, and the lab technicians. I am extremely grateful to Cordula Braatz. You have never let me down when I underestimated the amount of work of my planned experiments. With your “we can do it”-attitude you helped me to get through the hardest times within the last years.

I had a great pleasure to work with, learn from, and collaborate with all the current and former members of the applied genetics. Special thanks to Jan-Erik, Anne, Daniela, Georgie and Venja for all the professional and emotional support.

I would also like to thank my family. Thanks to my parents, my brother, and my grandparents that you always supported me and never let me forget that you are there when I need you. Finally, I am extremely grateful to Tino for being by my side and constantly convincing me that I can make it until the end of this thesis.

Summary

When a dark grown seedling perceives the full spectrum of light for the first time its developmental program is changed from skotomorphogenic to photomorphogenic growth. This transition is accompanied by massive transcriptomic changes. The bZIP transcription factor ELONGATED HYPOCOTYL 5 (HY5) is a major positive regulator of photomorphogenesis. Its protein amount, the surrounding light levels, and degree of photomorphogenic growth, measured by the hypocotyl length, in a developing seedling correlate with each other. While HY5 has the ability to bind one third of all promoters in the *Arabidopsis thaliana* (Arabidopsis) genome, the lack of a transactivation domain (TAD) in its protein sequence raises the question how HY5 can regulate the transcription of its numerous potential target genes.

In this thesis I identified the B-Box (BBX) proteins BBX20, BBX21, and BBX22 as cofactors of HY5 that are required for HY5 to fulfil its role as a positive regulator of photomorphogenesis. For this purpose, it was shown that the triple mutant *bbx202122* genocopies the *hy5* mutant under monochromatic light conditions. This is supported by a transcriptome analysis, which showed that most of the BBX-regulated genes are similarly HY5-regulated. Importantly, no additive phenotypes nor transcriptional regulation of target genes were observed in a *bbx202122 hy5* mutant. In accordance with a proposed model in which HY5 binds its target promoters and the BBX proteins provide the transcriptional activation ability through their physical interaction with HY5, we could show that the interaction of BBX20 with the target promoters of *MYB12* and *F3H*, as well as its overexpression phenotypes, depend on the presence of HY5. In transient protoplast assays, transcriptional activation of a GUS-reporter under the control of the *MYB12* or *F3H* promoter was only achieved when HY5 was expressed together with either BBX20, BBX21 or BBX22.

It was previously observed that a dark stable HY5 protein (HY5ΔN77) could not induce photomorphogenesis when expressed in dark grown Arabidopsis seedlings. In line with these observations, we were able to show that HY5 and BBX21 together induce photomorphogenesis, when expressed under those conditions. This suggests that the molecular basis for the *constitutive photomorphogenic 1* (*cop1*) phenotype is the overaccumulation of HY5 and BBX proteins, which work interdependently to induce photomorphogenesis.

In the second part of this thesis, I investigated the role of BBX proteins in karrikin (KAR) signaling. As suggested by the strong transcriptional induction of *BBX20* in response to KAR treatment I found evidence that BBX20 and its closest homologue BBX21 are required for the induction of KAR-induced inhibition of hypocotyl elongation and induction of anthocyanin accumulation. Analysis of higher order mutants suggested that BBX20 and BBX21 act downstream of SUPPRESSOR OF MAX2 (SMAX1) and SMAX1-LIKE 2 (SMXL2), which are the main negative regulators of KAR signaling.

Whole transcriptome analysis showed that the induction of anthocyanin biosynthesis in *smax1 smxl2* is fully dependent on *BBX20* and *BBX21.* In contrast, the regulation of hypocotyl elongation requires other factors which are acting in parallel to the BBX proteins. Furthermore, I provide evidence that in the KAR signaling pathway, HY5 and BBX20 and BBX21 act interdependently to regulate hypocotyl elongation and anthocyanin biosynthesis.

The work of this thesis presents a mechanism of how HY5, as a master transcriptional regulator, can gain specificity by interacting with its cofactors BBX20, BBX21 and BBX22 to regulate photomorphogenesis and KAR responses.

Zusammenfassung

Wenn ein Keimling zum ersten Mal dem vollen Lichtspektrum ausgesetzt ist, wechselt er vom skotomorphogenetischen zum photomorphogenetischen Wachstum. Dieser Übergang ist von einer tiefgreifenden Reorganisation des Transkriptoms begleitet. Der bZIP Transkriptionsfaktor ELONGATED HYPOCOTYL 5 (HY5) ist ein wichtiger positiver Regulator der Photomorphogenese. HY5s Proteinmenge, die Lichtintensität in der Umgebung und der Grad an Photomorphogenese, gemessen anhand der Hypokotyl-Länge eines sich entwickelnden Keimlings, korrelieren miteinander. HY5 besitzt das Potenzial, ein Drittel aller Promotoren im *Arabidopsis thaliana* (Arabidopsis) Genom zu binden. Da HY5 allerdings keine Transaktivierungsdomäne (TAD) besitzt, ist es unklar, wie HY5 die Transkription dieser großen Anzahl an potenziellen Zielgenen reguliert.

In dieser Arbeit wurden die B-Box (BBX) Proteine BBX20, BBX21 und BBX22 als Kofaktoren von HY5 identifiziert. Diese sind unerlässlich, damit HY5 seine Rolle als positiver Regulator der Photomorphogenese erfüllen kann. Es wurde gezeigt, dass die Dreifachmutante *bbx202122* unter monochromatischen Lichtbedingungen denselben Phänotyp wie eine *hy5* Mutante aufweist. Eine Transkriptomanalyse zeigte, dass der Großteil der BBX-regulierten Gene in gleicher Weise HY5-reguliert ist. Insbesondere wurden in der *bbx202122 hy5* Mutante keine additiven Phänotypen oder verstärkte transkriptionelle Regulationen der BBX- und HY5-Zielgene beobachtet. Im Einklang mit der Hypothese, dass HY5 an die Promotoren der Zielgene bindet und die BBX Proteine die transkriptionelle Aktivierung durch die direkte Interaktion mit HY5 ermöglichen, wurde gezeigt, dass die Interaktion von BBX20 mit den Zielpromotoren von *MYB12* und *F3H*, sowie die BBX20 Überexpressionsphänotypen von der Anwesenheit von HY5 abhängig sind. In transienten Protoplastenassays wurde ein GUS-Reporter, der unter der Kontrolle des *MYB12* oder *F3H* Promotors stand, nur aktiviert, wenn HY5 zusammen mit BBX20, BBX21 oder BBX22 exprimiert wurde.

Eine im Dunkeln stabile Version des HY5 Proteins (HY5ΔN77) induziert keine Photomorphogenese in Arabidopsis Keimlingen, die im Dunkeln gewachsen sind. Werden allerdings HY5 und BBX21 zusammen unter diesen Bedingungen exprimiert, induzieren sie Photomorphogenese. Dies legt nahe, dass die Überakkumulation von HY5 und BBX Proteinen, welche die Photomorphogenese in Abhängigkeit voneinander regulieren, die molekulare Grundlage für den *constitutively photomorphogenic 1 (cop1*) Phänotyp bilden.

Im zweiten Teil dieser Arbeit wurde die Rolle von BBX Proteinen im Karrikin (KAR) Signalweg untersucht. Wie durch die starke transkriptionelle Induktion von *BBX20* durch KAR bereits impliziert wurde, wird BBX20 und sein nächstes Homolog BBX21 für die Inhibierung der Hypokotyl-Elongation sowie der Akkumulation von Anthocyanen durch KAR benötigt. Die Analyse von Mehrfachmutanten hat gezeigt, dass BBX20 und BBX21 den beiden Inhibitoren des KAR Signalwegs SUPPRESSOR OF MAX2 (SMAX1) und SMAX1-LIKE 2 (SMXL2), nachgeschaltet sind.

Transkriptomanalysen zeigten, dass die Induktion der Anthocyan-Biosynthese in der *smax1 smxl2* Doppelmutante vollständig von BBX20 und BBX21 abhängig ist. Im Gegensatz dazu, benötigt die Regulation der Hypokotyl-Elongation weitere Faktoren, die parallel zu den BBX Proteinen im KAR Signalweg wirken. Außerdem wurde gezeigt, dass im KAR Signalweg höchstwahrscheinlich HY5 zusammen mit BBX20 und BBX21 in Abhängigkeit voneinander Hypokotyl-Elongation und Anthocyan-Biosynthese regulieren.

Zusammenfassend stellen die Ergebnisse dieser Arbeit einen Mechanismus dar, wie HY5, als ein Master Transkriptionsregulator, Spezifizität durch die Interaktion mit den Kofaktoren BBX20, BBX21 und BBX22 erwerben kann, um Photomorphogenese und KAR Effekte zu regulieren.

List of publications

The work presented in this thesis is published as follows:

Bursch, K., Toledo-Ortiz, G., Pireyre, M., Lohr, M., Braatz, C. and Johansson, H. (2020), "Identification of BBX proteins as rate-limiting cofactors of HY5", *Nature Plants* (2020) 6, 921-928, Springer US. https://doi.org/10.1038/s41477-020-0725-0.

Bursch, K., Niemann, E.T., Nelson, D.C. and Johansson, H. (2021) "Karrikins control seedling photomorphogenesis and anthocyanin biosynthesis through a HY5-BBX transcriptional module." *The Plant Journal* (2021), 107, 1346-1362. https://doi.org/10.1111/tpj.15383.

Other published work, not included in this thesis

Job, N., Yadukrishnan, P., Bursch, K., Datta, S. and Johansson, H. (2018) Two B-box proteins regulate photomorphogenesis by oppositely modulating HY5 through their diverse C-terminal domains. *Plant Physiol.*, 176, 2963–2976. https://doi.org/10.1104/pp.17.00856

Yadukrishnan, P., Rahul, P.V., Ravindran, N., Bursch, K., Johansson, H. and Datta, S. (2020) CONSTITUTIVELY PHOTOMORPHOGENIC1 promotes ABA-mediated inhibition of post-germination seedling establishment. *Plant J.*, 103, 481–496. https://doi.org/10.1111/tpj.14844

Content

Figures

Abbreviations

3-AT	3-amino-1, 2,4-triazol
ABA	abscisic acid
Ala	Alanine
AP2	APETALA2
APA	active phyA-binding
APB	active phyB-binding
Arabidopsis	*Arabidopsis thaliana*
Asp	aspartate
B	Blue
BBX	B-BOX
BBX1	B-BOX DOMAIN PROTEIN 1
BBX20	B-BOX DOMAIN PROTEIN 20
BBX21	B-BOX DOMAIN PROTEIN 21
BBX22	B-BOX DOMAIN PROTEIN 22
BBX23	B-BOX DOMAIN PROTEIN 23
BBX24	B-BOX DOMAIN PROTEIN 24
BBX25	B-BOX DOMAIN PROTEIN 25
bHLH	basic helix-loop-helix
BIC	BLUE-LIGHT INHIBITOR OF CRYPTOCHROMES
bZIP	basic leucine zipper
BZS1	bzr1-1D SUPPRESSOR1
Cas9	CRISPR-associated protein 9
CCD7	CLEAVAGE DIOXYGENASE 7
CCD8	CLEAVAGE OXYGENASE 8
CCT	CONSTANS, CO-like, and TOC1
CIB	CRYPTOCHROME-INTERACTING BASIC-HELIX-LOOP-HELIX
CO	CONSTANS
Col-0	Columbia-0

COP1	CONSTITUTIVE PHOTOMORPHOGENIC 1
CRISPR	clustered regularly interspaced short palindromic repeats
CRY	Cryptochrome
CSU1	COP1 SUPPRESSOR 1
CUL4	CULLIN4
D14	DWARF14
D27	DWARF27
DEG	differentially expressed gene
DLK2	*DWARF14-LIKE2*
Est	17-β-estradiol
FAD	Flavin adenine dinucleotide
FAD^-	Reduced FAD
FAD°	Radical FAD
FADox	Oxidized FAD
FHL	FAR-RED-ELONGATED HYPOCOTYL1-LIKE
FHY1	FAR-RED ELONGATED HYPOCOTYL 1
FKF1	FLAVIN-BINDING, KELCH REPEAT, F BOX 1
FR	Far-red
FT	FLOWERING LOCUS T
GA	gibberellins
GARP	GOLDEN2, ARR-B, Psr1
GO	Gene ontology
HEC	HECATE1
HIR	High irradiance response
His	Histidine
Hsp100/ClpB	Heat shock protein 100 / Caseinolytic peptidase B
HY5	ELONGATED HYPOCTOYL 5
HYH	HY5-HOMOLOG
JA	jasmonate

KAI2	KARRIKIN INSENSITIVE 2
KAR	Karrikin
KL	KAI2 ligand
KUF1	*KARRIKIN UPREGULATED F-BOX1*
L*er*	Landsberg *erecta*
Leu	Leucine
LKP2	LOV KELCH PROTEIN 2
LUC	luciferase gene
LZF1	LIGHT-REGULATED ZINC FINGER PROTEIN 1
MAX2	MORE AXILLARY GROWTH 2
MIDA10	MISREGULATED IN DARK10
MUG	4-methylumbelliferyl ß-D-glucuronide
MUN	2′-(4-methylumbelliferyl)-α-d-*N*-acetylneuraminic acid
NLS	nuclear localization signal
ONPG	o-Nitrophenyl-β-D-galactopyranosid
PCH1	PHOTOPERIODIC CONTROL OF HYPOCOTYL 1
PCHL	PCH1-LIKE
Pfr	Phytochrome, far-red light absorbing form
PHOT	Phototropin
PHY	Phytochrome
PIF	PHY-INTERACTING FACTOR
pifQ	*pif1 pif3 pif4 pif5*
PIFQ	PIF quartet
PPK	PHOTOREGULATORY PROTEIN KINASE
Pr	Phytochrome, red light absorbing form
Ptotal	Total amount of phytochrome
R	Red
RBCC	RING, B-Box, Coiled-coil
RING	Really Interesting New Gene

RUP	REPRESSOR OF UV-B PHOTOMORPHOGENESIS
SL	strigolactone
smax	*suppressor of max2*
SPA	SUPPRESSOR OF PHYA-105
SRDX	EAR REPRESSION DOMAIN
STH	SALT TOLERANCE HOMOLOG
STH2	SALT TOLERANCE HOMOLOG 2
STH3	SALT TOLERANCE HOMOLOG 3
STH7	SALT TOLERANCE HOMOLOG 7
STO	SALT TOLERANCE
TAD	Transactivation domain
TOE	TARGET OF EAT
TRIM	tripartite motif
Trp	Tryptophan
Ura	Uracil
UVR8	UVB-RESISTANCE 8
VLFR	Very low fluence response
VP	Valine-proline
WRKY36	WRKY DNA-BINDING PROTEIN 36
WT	wildtype
Y2H	Yeast two-hybrid
ZTL	ZEITLUPE

1 Introduction

1.1 Light controls plant development

Throughout the whole life cycle of a plant the surrounding light conveys crucial information that is perceived, transduced, and interpreted by the plant. As sessile organisms, plants have a limited capacity to escape unfavorable conditions. However, the constantly changing light environment comprises various information for a plant to adapt its development and growth to complete a successful life cycle. This lifecycle begins with the onset of germination at the correct time of year to facilitate effective seedling development and transition to the vegetative growth phase. With the onset of flowering and prolific ripening newly developed seeds can be released, marking the successful completion of a plant's lifecycle (Figure 1.1).

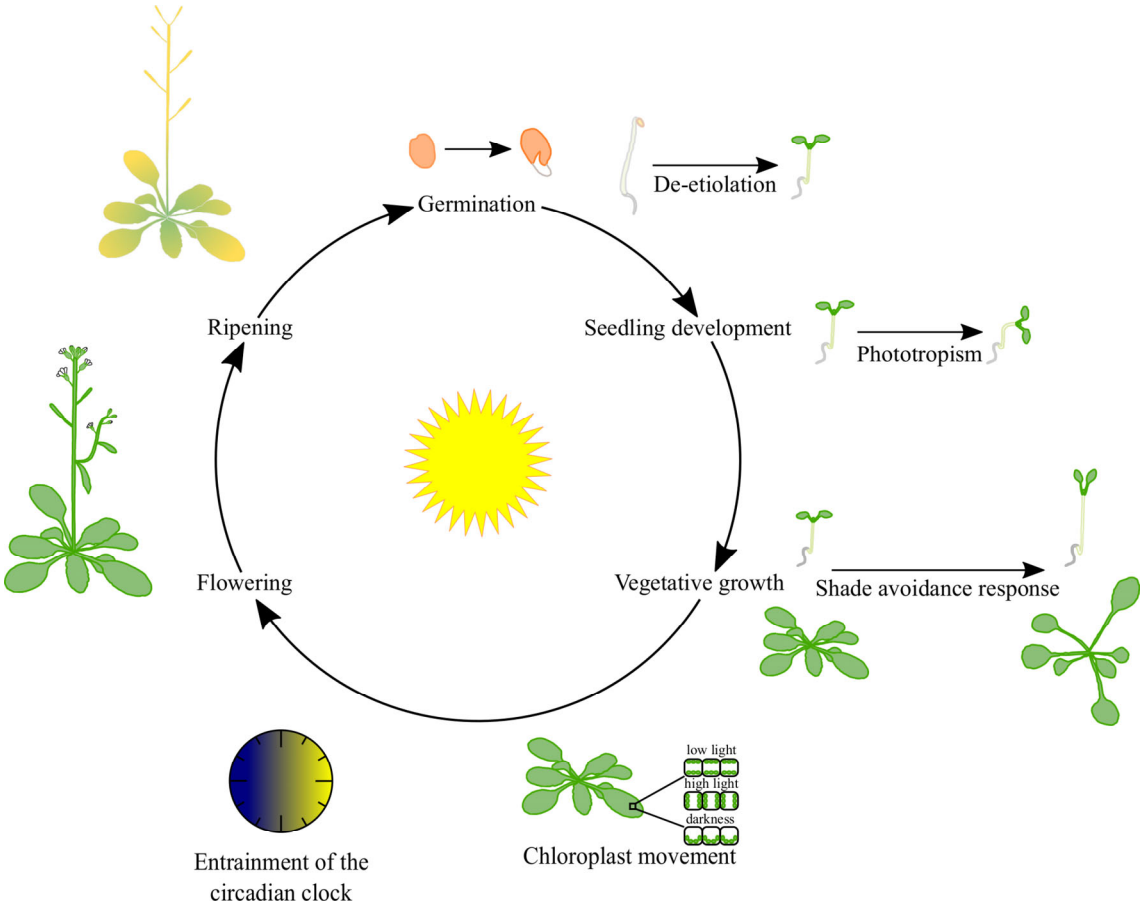

Figure 1.1: Light controlled processes throughout the lifecycle of a plant.

The lifecycle of a plant has to be tightly regulated to ensure its successful completion. Plants have evolved various strategies to perceive, transduce, and interpret the crucial information from the surrounding light which leads to numerous developmental adaptions that are controlled by light.

After the onset of germination, a process predominantly induced by light, seedlings in natural conditions are often buried under soil where light levels are low to absent (Sullivan and Deng, 2003). Under these conditions, seedlings follow the developmental program of skotomorphogenesis, meaning that the elongation of the hypocotyl is promoted, so that seedlings reach the soil surface. Furthermore, while growing through the soil they retain an apical hook and closed cotyledons to protect the shoot apical meristem. Once exposed to light, after emerging from the soil, plants switch from skotomorphogenic to photomorphogenic growth. This transition, called de-etiolation, is characterized by the inhibition of hypocotyl elongation, opening of the apical hook, and unfolding and greening of the cotyledons (Chory et al., 1996). As the sole source of energy for most plants, it is important that they optimize their ability to harvest light. That is why they adapt their aerial growth, in a process called phototropism, constantly towards incoming light (Liscum et al., 2014). But as full sunlight can also be harmful and cause severe damage, plants have developed several protective mechanisms, one of which is the chloroplast avoidance movement. This means that under high light conditions chloroplasts move from the cell surface to the side of the cells to prevent the photosystem from harm (Kasahara et al., 2002). Under natural conditions plants often grow under the shade of neighboring plants. These shade conditions are marked by a decreased ratio of red (R) to far-red (FR) light as well as overall reduced light intensity and lead to the promotion of elongation growth in the so-called shade avoidance response that enables plants to outcompete those neighbors (Franklin, 2008). Furthermore, light entrains the circadian clock and allows plants to measure the daylength. This information is used by a plant to regulate the induction of flowering and ensures the successful completion of a plants' lifecycle marked by ripening and release of a new generation of seeds at the appropriate time of year (Figure 1.1) (Devlin and Kay, 2001).

1.1.1 Light perception by plant photoreceptors

To correctly regulate the above-mentioned developmental processes in response to a constantly changing light environment, plants have evolved at least five classes of photoreceptors. In Arabidopsis, phytochromes (phyA-E) perceive R/FR light (600 – 750 nm), cryptochromes (CRY1, CRY2) phototropins (PHOT1, PHOT2) and F-box containing Flavin binding proteins (e.g. ZEITLUPE (ZTL), FLAVIN-BINDING, KELCH REPEAT, F BOX 1 (FKF1), LOV KELCH PROTEIN 2 (LKP2)) perceive blue

(B)/UV-A light (320 – 500 nm) while UVB-RESISTANCE 8 (UVR8) detects UV-B light (280 – 320 nm) (Figure 1.2) (Paik and Huq, 2019). The function of photoreceptors is to perceive light and integrate this signal to regulate the plants response. In general this function is achieved by interaction with, and inhibition of downstream signaling components, that are mainly negative regulators of light signaling (Paik and Huq, 2019).

In the following sections I will further discuss previous work related to the phytochromes, cryptochromes and UVR8, as the activity of these photoreceptors in the regulation of seedling development is most relevant for the work contained in this thesis.

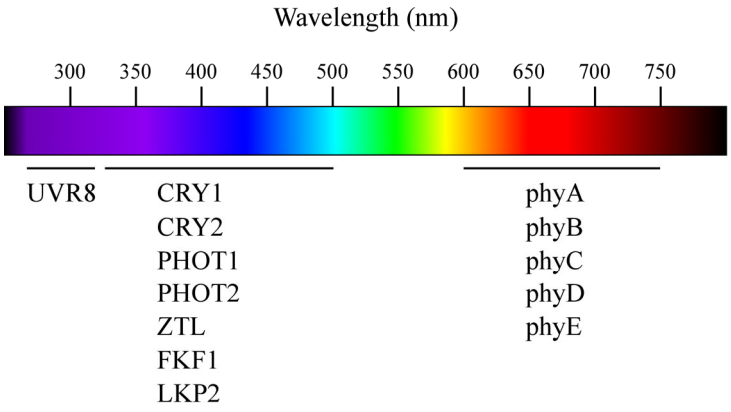

Figure 1.2: Absorption regions of plant photoreceptors.

UVR8 perceives UV-B light, while cryptochromes (CRY1,2), phototropins (PHOT1,2) and F-box containing Flavin binding proteins (ZTL, FKF1, LKP2) absorb light in the UV-A and B range of the spectrum. Phytochromes (phyA-phyE) act as R and FR light receptors.

1.1.1.1 Phytochromes control plant development in response to R/FR light

Phytochromes (phyA – phyE) are a protein family often titled molecular switches based on their distinct mode of action in sensing R and FR light. Phytochromes are synthesized as an apoprotein which becomes covalently linked to a linear tetrapyrrole bilin chromophore, forming the holoprotein which is able to perceive light (Rockwell et al., 2006; Terry et al., 1993). The inactive phytochromes are assembled in the cytoplasm, and while phyA remains exclusively in the cytoplasm in darkness, phyB to phyE are distributed in the cytosol and the nucleus (Terry, 1997). However, upon light perception phytochromes rapidly accumulate in the nucleus, where they form nuclear bodies with a yet unknown function (Cheng et al., 2021; Kircher et al., 2002; Klose et al., 2015; Yamaguchi et al., 1999).

In darkness, phytochromes occur in their inactive R light absorbing (660 nm) Pr form which is converted to the active, FR light absorbing (730 nm) Pfr form upon irradiation

with R light (Figure 1.3) (Butler et al., 1959; Quail, 1991; Sharrock, 2008). This conversion is reversible either by the absorption of FR light or by a light independent relaxation process termed thermal or dark reversion (Butler et al., 1963; Klose et al., 2020). Thermal reversion of phyB is a passive process influenced by temperature that allows phyB to integrate not only changes in the surrounding light, but also variations of the ambient temperature (Jung et al., 2016; Legris et al., 2016). Furthermore, the thermal reversion of phyB is also actively inhibited by interaction of phyB with PHOTOPERIODIC CONTROL OF HYPOCOTYL 1 (PCH1) and PCH1-LIKE (PCHL) (Figure 1.3) (Enderle et al., 2017).

The combination of photoconversion and thermal reversion leads to the establishment of a dynamic photoequilibrium Pfr/Ptotal which is highly dependent on the relative R and FR light levels. This gives plants the ability to sense and adapt to changes in the spectral composition, as can be observed in the shade avoidance response. Shade, as occurring under a larger, neighboring plant, leads to a lower R/FR ratio and lower overall light intensity and thereby induces various phenotypic changes, e.g. induction of elongation growth in the hypocotyl of seedlings or of the internode in adult plants, a strategy to outcompete neighbors (Ballaré and Pierik, 2017).

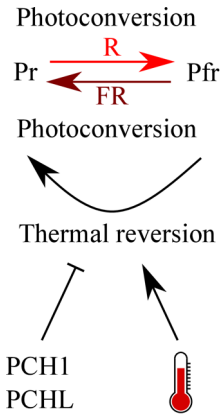

Figure 1.3: Photoequilibrium of phytochromes.

Phytochromes can convert from their inactive R light absorbing (Pr) form to the active FR light absorbing (Pfr) form and vice versa by the absorption of R and FR light, respectively. Additionally, the reconversion from Pfr to Pr can happen as a relaxation process (thermal reversion) which is accelerated with an increase in temperature or can be inhibited by PCH1 and PCHL.

Although phytochromes are found in some prokaryotes the canonical plant phytochromes evolved from an ancestor of streptophytes (Hughes et al., 1997; Li et al., 2015). Early in the evolution of angiosperms, phytochromes diverged into three major clades: phyA,

phyB and phyC and gene duplication events of phyB have led to the arising of phyE and phyD (Clack et al., 1994; Li et al., 2015; Mathews, 2010; Quail, 1991). Interestingly, despite only small differences in the absorption spectra of phytochromes are observed, they show immense differences in their action spectra (Eichenberg et al., 2000).

PhyA mediates responses to very low fluences of any wavelength of visible light (VLFR) and to strong continuous irradiation with FR light (HIR) which can naturally occur under a thin layer of soil or in deep shade conditions, respectively (Legris et al., 2019; Sheerin and Hiltbrunner, 2017). Under these conditions phyA can induce germination (Botto et al., 1996), regulate seedling development (Nagatani et al., 1993; Parks and Quail, 1993; Whitelam et al., 1993) and induce flowering (Reed et al., 1994; Sheerin and Hiltbrunner, 2017). Relative to phyB – E, phyA is more light labile (Bae and Choi, 2008; Hennig et al., 1999). Upon white light irradiation it is quickly degraded by the 26S proteasome, mediated predominantly through polyubiquitination by the E3 ubiquitin ligase complex CONSTITUTIVE PHOTOMORPHOGENIC 1 (COP1)/SUPRESSOR OF PHYA-105 (SPA) (Seo et al., 2004). Upon activation, phyA is transported to the nucleus through a shuttle mechanism mediated by the plant specific proteins FAR-RED ELONGATED HYPOCOTYL 1 (FHY1) and FAR-RED-ELONGATED HYPOCOTYL1-LIKE (FHL) (Genoud et al., 2008; Hiltbrunner et al., 2005, 2006; Rausenberger et al., 2011; Zeidler et al., 2004). It has been proposed that this shuttle mechanism causes the shift towards FR light in the action spectrum of phyA compared to its absorption spectrum (Rausenberger et al., 2011; Sheerin and Hiltbrunner, 2017). The dimeric phyA photoreceptor exclusively forms homodimers which can occur as PrPr, PrPfr or PfrPfr dimers (Brockmann et al., 1987; Jones and Quail, 1986; Liu and Sharrock, 2017).

PhyB – E are historically classified as light stable phytochromes and confer responses to low fluences of R light with phyB being the most abundant and most investigated member of this group (Legris et al., 2019; Sharrock and Clack, 2002). They form, like phyA, dimers, which can occur as homo- or heterodimers (Clack et al., 2009; Sharrock and Clack, 2004). The identification of mutants for each phytochrome has allowed investigations of each individual phytochrome in plant development (Aukerman et al., 1997; Devlin et al., 1998; Franklin and Quail, 2010; Koornneef et al., 1980; Monte et al., 2003; Nagatani et al., 1993; Parks and Quail, 1993; Reed et al., 1993; Sánchez-Lamas et al., 2016; Somers et al., 1991; Whitelam et al., 1993). A *phyA phyB phyC phyD phyE* quintuple mutant is largely insensitive to R light throughout plant development, with the

exception of chlorophyll synthesis (Strasser et al., 2010). While *phyA phyB phyC phyD phyE* mutant seeds are not able to germinate irrespective of the light condition, seedling de-etiolation can be induced by B light in this mutant through the activity of the cryptochromes (Strasser et al., 2010).

The process of de-etiolation, when a seedling is exposed to light for the first time upon emergence from soil, is accompanied by massive transcriptional changes (Ma et al., 2001; Tepperman et al., 2001, 2004). Phytochromes control this process in response to R and FR light via the interaction and deactivation of negative regulators of de-etiolation as well as the activation of positive regulators (Paik and Huq, 2019). This involves the inhibition of the COP1/SPA E3 ligase complex as well as interaction and degradation of the PHYTOCHROME INTERACTING FACTORs (PIFs) basic helix-loop-helix (bHLH) transcription factors (see section 1.1.2).

1.1.1.2 Cryptochromes are B light receptors

In Arabidopsis there are three photolyase-like cryptochromes identified (CRY1 – CRY3). While CRY1 and CRY2 serve as B light receptors, the chloroplast localized CRY3 is potentially involved in repair of UV-induced DNA damage (Ahmad and Cashmore, 1993; Kleine et al., 2003; Lin et al., 1998; Pokorny et al., 2008). Among the various B light induced responses mediated by CRY1 and CRY2 in Arabidopsis, regulation of seedling photomorphogenesis and induction of flowering are perhaps most well studied (Yang et al., 2017).

To perceive blue light, the chromophore utilized by cryptochromes is a flavin adenine dinucleotide (FAD) molecule and in its resting state *in vivo* it occurs in an oxidized FADox form (Giovani et al., 2003; Lin et al., 1995; Malhotra et al., 1995). Upon B light illumination the chromophore is reduced via electron transfer to radical FAD° and FAD° is further reduced to flavin FAD^- via the so-called photoactivation. Reoxidation can occur spontaneous in darkness (Figure 1.4) (Ahmad, 2016; Giovani et al., 2003). The mechanism by which the cryptochrome apoprotein supports the photoactivation of the chromophore is still under debate. It has been hypothesized that the reduction of FAD is mediated by electron transfer from three conserved tryptophan (Trp) residues, but as a *cry2* mutant altered in these Trp residues retains biological activity, alternative pathways for the photoreduction likely exist (Ahmad, 2016; Wang and Lin, 2020).

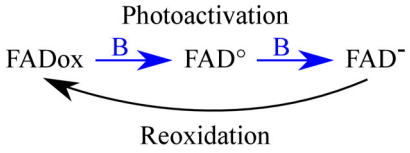

Figure 1.4: Photoactivation of the cryptochrome chromophore FAD.

In its resting state FAD occurs in its oxidized form (FADox). Upon B light illumination the chromophore is oxidized to its radical (FAD°) and reduced (FAD^-) form which can reoxidize in darkness.

Nevertheless, while the exact mechanism of photoactivation of cryptochromes is not clear, it has been shown that B light illumination triggers a cascade beginning with conformational changes, leading to homodimerization and phosphorylation to activate the cryptochromes (Figure 1.5) (Sang et al., 2005; Shalitin et al., 2002, 2003; Shao et al., 2020). Activation of the cryptochromes leads to interaction with downstream signaling components to regulate a variety of developmental processes e.g. photo- and thermomorphogenesis as well as flowering (Figure 1.5).

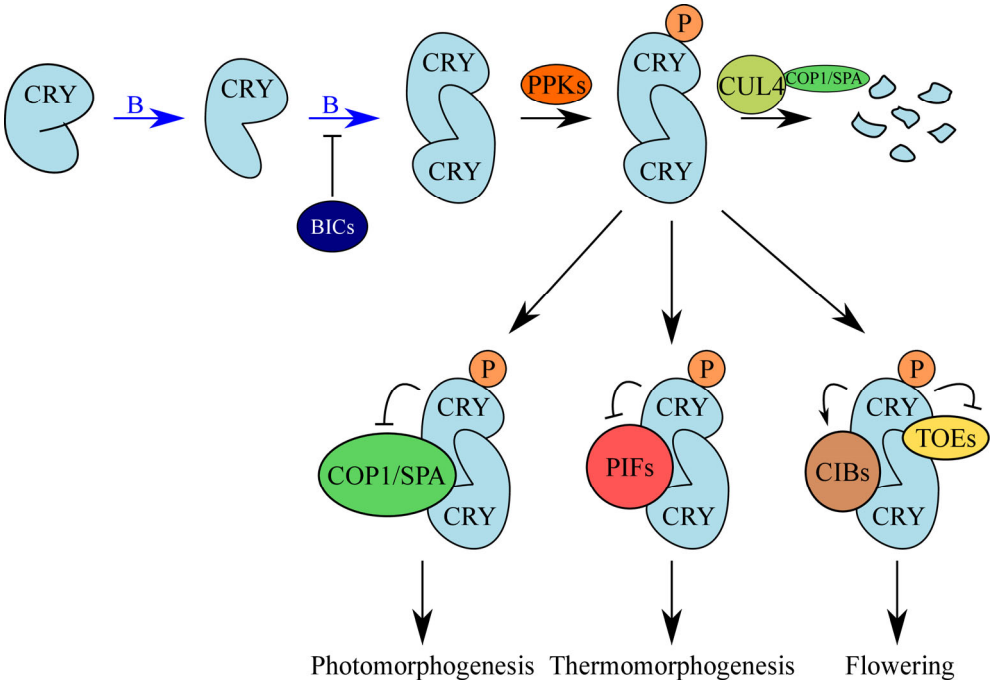

Figure 1.5: B light perception by the cryptochromes.

B light induces conformational changes in the cryptochromes: These conformational changes lead to the dimerization of cryptochromes, a process inhibited by BICs. Phosphorylation of the cryptochromes is mediated by the PPKs and can lead to the degradation by the $CUL4^{COP1/SPA}$ complex or the interaction with downstream signaling factors to induce photomorphogenesis, thermomorphogenesis, or flowering.

For the constantly nuclear localized CRY2, the activation is accompanied by the formation of nuclear photobodies (Kleiner et al., 1999; Mas et al., 2000). In contrast,

CRY1 is distributed in the nucleus and cytoplasm, where it confers responses to B light, depending on its localization (Cashmore et al., 1999; Guo et al., 1999; Wu and Spalding, 2007). The nuclear localized CRY1 regulates B light-induced inhibition of hypocotyl and petiole elongation as well as anthocyanin accumulation (Wu and Spalding, 2007). Interestingly, primary root growth and cotyledon expansion are induced by cytoplasmic CRY1 but inhibited by nuclear CRY1 (Wu and Spalding, 2007).

To enhance the cryptochrome activity, the dimerized cryptochromes are phosphorylated which has been shown to be mediated by four PHOTOREGULATORY PROTEIN KINASES (PPK1 – 4) in case of CRY2 (Figure 1.5) (Liu et al., 2017; Shalitin et al., 2002, 2003). In addition, the phosphorylation of CRY2 leads to polyubiquitination via interaction with the CULLIN4 (CUL4)$^{COP1/SPA}$ complex and other E3 ubiquitin ligases. This finally leads to degradation of CRY2 through the 26S proteasome (Figure 1.5) (Lin et al., 1998; Liu et al., 2016; Weidler, Oven-Krockhaus, et al., 2012; Yu et al., 2007). In line with its rapid degradation, CRY2 mediates mainly responses to low fluencies of B light (Lin et al., 1998). To further regulate the activity of cryptochromes plants establish a negative feedback loop involving BLUE-LIGHT INHIBITOR OF CRYPTOCHROMES (BIC) proteins. Light induces the expression of BIC proteins (BIC1 and BIC2) which act to inhibit the dimerization of cryptochromes (Figure 1.5) (Wang et al., 2016; Wang, Wang, Han, et al., 2017).

Although shown to have multiple roles in regulating B light dependent plant development in addition to photomorphogenesis, the probably most prominent role of cryptochromes is the induction of flowering (Wang, Wang, Nguyen, et al., 2017). The regulation of flowering is accomplished by the cryptochromes through the interaction with APETALA2 (AP2)-like transcriptional factors TARGET OF EAT (TOE1 and TOE2) or through the interaction with a B light specifically induced class of bHLH transcription factors CRYPTOCHROME-INTERACTING BASIC-HELIX-LOOP-HELIX (CIBs, CIB1 – 5) (Figure 1.5) (Du et al., 2020; Liu et al., 2008, 2013).

Similar to the phytochromes, cryptochromes can interact with the COP1/SPA complex to inhibit its activity and promote photomorphogenesis (Figure 1.5) (Lian et al., 2011; Wang et al., 2001; Yang et al., 2001; Zuo et al., 2011). In addition, the interaction with PIFs (namely PIF3, PIF4 and PIF5) allow cryptochromes to not only integrate information about the surrounding light but also about ambient temperature (Figure 1.5) (see section 1.1.2) (Ma et al., 2016; Pedmale et al., 2016).

1.1.1.3 UVR8 is the UV-B receptor in Arabidopsis

Although UV-B light is only a minor component of the sunlight, it can have a high impact on plant development and growth (Jenkins, 2017). As an abiotic stressor, high UV-B irradiation can cause severe damage. However, plants have evolved means to tolerate and acclimate to UV-B irradiation, so that under natural conditions plants rarely show UV-B-induced damage (Jenkins, 2017). The most recently identified photoreceptor, UVR8, is responsible for sensing and transducing the UV-B signal (Rizzini et al., 2011). UVR8 is not only important for the acclimation to UV-B light which is displayed by reduced UV-B tolerance of a *uvr8* mutant (Kliebenstein et al., 2002). Among other processes, UVR8 has also been shown to play a role in UV-B-induced photomorphogenesis, entrainment of the circadian clock, thermomorphogenesis, shade avoidance response and regulation of the onset of flowering (Arongaus et al., 2018; Dotto et al., 2018; Favory et al., 2009; Fehér et al., 2011; Hayes et al., 2014, 2017; Yin and Ulm, 2017).

In contrast to other photoreceptors, UVR8 does not utilize an extragenic chromophore but instead employs intrinsic Trp residues for UV-B perception (Christie et al., 2012; Rizzini et al., 2011; Di Wu et al., 2012). In its inactive ground state UVR8 is a dimeric protein, stabilized by a network of salt bridges between those Trp residues (Christie et al., 2012; Di Wu et al., 2012). Upon irradiation with UV-B, UVR8 dissociates into active monomers which accumulate in the nucleus and induce numerous signaling cascades (Figure 1.6) (Kaiserli and Jenkins, 2007; Rizzini et al., 2011). The nuclear accumulation of the UVR8 monomers is mediated by a mechanism dependent on COP1 (Figure 1.6) (Qian et al., 2016; Yin et al., 2016). The active UVR8 monomers can redimerize *in vivo*, a process promoted via direct interaction with REPRESSOR OF UV-B PHOTOMORPHOGENESIS 1 (RUP1) and RUP2 which allows for the establishment of a photoequilibrium between monomeric and dimeric UVR8 under natural conditions (Figure 1.6) (Findlay and Jenkins, 2016; Gruber et al., 2010; Heijde and Ulm, 2013; Podolec et al., 2021).

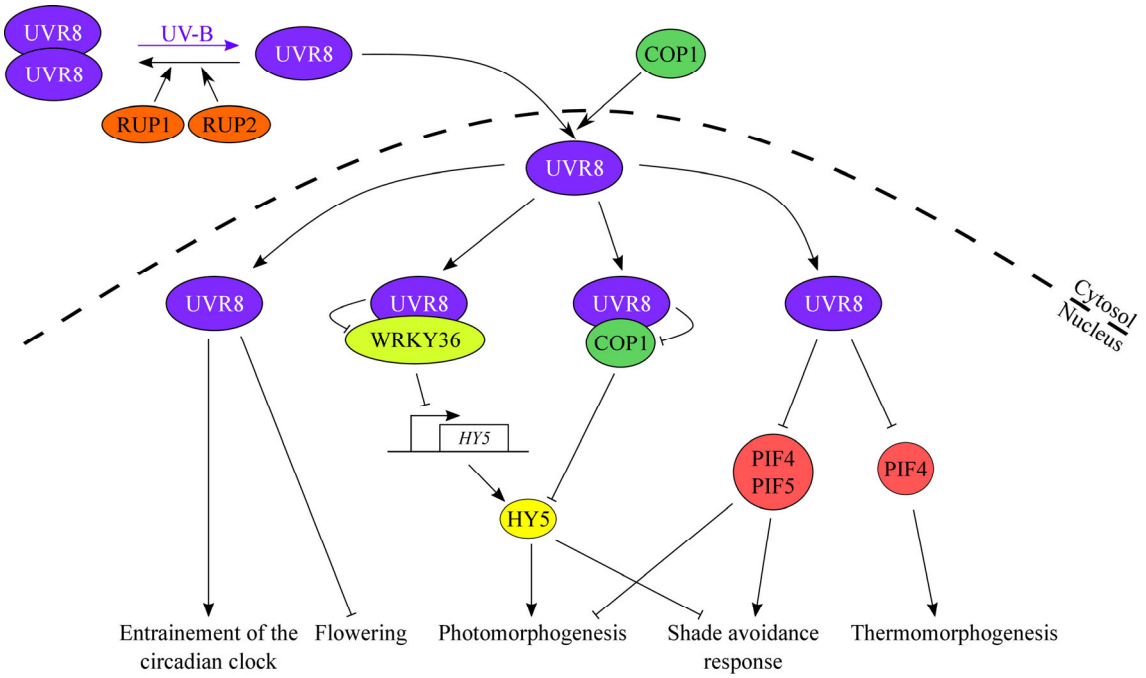

Figure 1.6: Schematic depiction of UV-B signaling.

The dimeric UV-B receptor reversibly monomerizes upon activation by UV-B irradiation. Redimerization is regulated by RUP1 and RUP2. Active UVR8 accumulates in the nucleus in a COP1-dependent manner. The activated UVR8 regulates entrainment of the circadian clock and flowering. By inhibiting PIFs it also regulates photomorphogenesis, shade avoidance response and thermomorphogenesis. In parallel *HY5* is transcriptionally induced by the inhibition of the transcription factor WRKY36 and post-transcriptionally stabilized by the inhibition of COP1 to induce photomorphogenesis.

Like other photoreceptors UVR8 inhibits the activity of PIFs to promote UV-B-induced photomorphogenesis, but also to regulate shade avoidance response and thermomorphogenesis (Figure 1.6) (Hayes et al., 2014, 2017; Tavridou et al., 2020).

Furthermore, the activated UVR8 photoreceptor interacts with the E3 ubiquitin ligase COP1 (Cloix et al., 2012; Favory et al., 2009). This interaction competes for COP1 interaction with its major target ELONGATED HYPOCOTYL (HY5) and reduces the COP1/SPA-mediated degradation of HY5 resulting in the accumulation of HY5 protein to promote UV-B-induced photomorphogenesis (Figure 1.6) (Lau et al., 2019; Osterlund et al., 2000). In addition, UVR8 promotes the transcriptional induction of *HY5* by UV-B light through interaction with the transcriptional repressor WRKY DNA-BINDING PROTEIN 36 (WRKY36) (Ulm et al., 2004; Yang et al., 2018). This interaction interferes with the association of WRKY36 to the *HY5* promoter and ultimately leads to the transcriptional induction of *HY5* (Figure 1.6) (Yang et al., 2018).

1.1.2 Signaling networks downstream of the photoreceptors

Although recent evidence suggests that phyA and phyB are able to directly interact with DNA and data under discussion suggests that UVR8 might be able to bind DNA, the main function of these photoreceptors is likely mediated by the interaction with downstream signaling components (Figure 1.7) (Binkert et al., 2016; Brown et al., 2005; Chen et al., 2014; Cloix and Jenkins, 2008; Jung et al., 2016; Wang and Lin, 2020; Yin and Ulm, 2017). Interestingly, these components are mainly negative regulators of light signaling whose function is inhibited by the interaction with the activated photoreceptors (Paik and Huq, 2019).

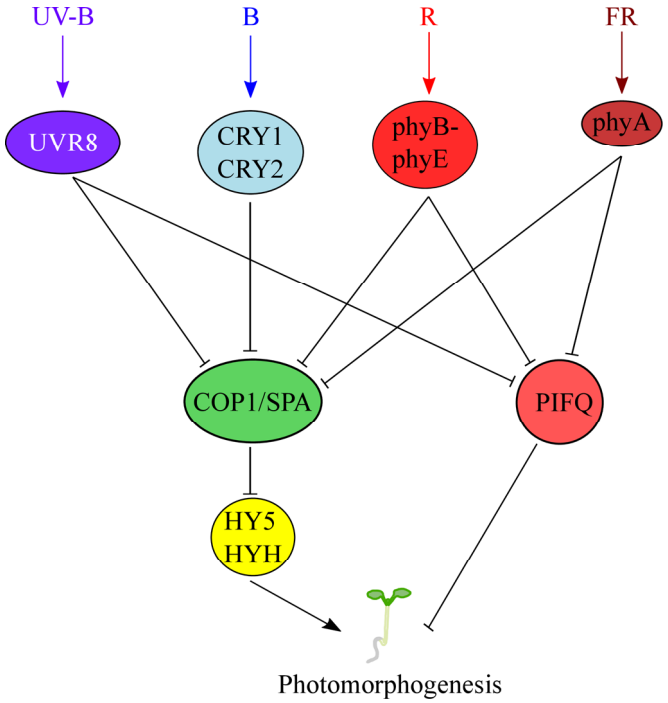

Figure 1.7: Genetic networks that control seedling photomorphogenesis.

The photoreceptors UVR8, cryptochromes and phytochromes are active in UV-B, B, R and FR light, respectively. The activated photoreceptors inhibit the activity of the COP1/SPA complex which leads to the accumulation of HY5 and HYH, positive regulators of photomorphogenesis. In parallel the PIF quartet (PIFQ) members (PIF1, PIF3, PIF4, PIF5), promoters of skotomorphogenesis in darkness, are inhibited by the photoreceptors.

1.1.2.1 PIFs promote skotomorphogenesis

Upon activation by light, phytochromes have been found to interact with a group of bHLH transcription factors collectively called the PIFs. Within the large protein family of bHLH transcription factors in Arabidopsis the PIFs belong to subfamily 15 (Toledo-Ortiz et al., 2003). The first member of this group was PIF3, which was identified through a yeast two-hybrid (Y2H) screen using the C-terminal domain of phyB as bait (Ni et al., 1998).

Since then, a total of eight PIFs (PIF1 - PIF8) have been found to directly interact with the light activated phyB, through a conserved active phyB-binding (APB) domain (Huq et al., 2004; Huq and Quail, 2002; Khanna et al., 2004; Leivar, Monte, Al-Sady, et al., 2008; Luo et al., 2014; Ni et al., 1999; Oh et al., 2004, 2020). PIF1 and PIF3 additionally interact with phyA through an active phyA-binding (APA) domain, which is not conserved between the two proteins (Al-Sady et al., 2006; Shen et al., 2008).

As transcription factors, most of the PIFs (PIF1, PIF3, PIF4, PIF5 and PIF7) have been shown to interact with DNA through a G-box (CACGTG) motif or a variant of an E-box, designated PBE (CACATG) motif (Hornitschek et al., 2009, 2012; Huq et al., 2004; Huq and Quail, 2002; Kim et al., 2008; Leivar, Monte, Al-Sady, et al., 2008; Martínez-García et al., 2000; Moon et al., 2008; Toledo-Ortiz et al., 2003; Zhang, Mayba, et al., 2013).

The less characterized PIFs PIF2, PIF7, and PIF8 are more abundant in light, and PIF2 and PIF8 have been shown to be degraded through the 26S proteasome in a COP1-dependent manner in darkness (Leivar, Monte, Al-Sady, et al., 2008; Luo et al., 2014; Oh et al., 2020). In contrast, the PIF quartet (PIFQ) members (PIF1, PIF3, PIF4 and PIF5) are phosphorylated, ubiquitinated and rapidly degraded upon light illumination supporting their role as promotors of skotomorphogenesis in darkness (Al-Sady et al., 2006; Bauer et al., 2004; Lorrain et al., 2007; Monte et al., 2004; Nozue et al., 2007; Oh et al., 2006; Park et al., 2004; Shen et al., 2005, 2008; Shen, Khanna, et al., 2007). Consequently a *pif1 pif3 pif4 pif5* (*pifQ*) mutant shows a constitutively photomorphogenic phenotype in darkness and transcriptome analysis showed that the dark grown *pifQ* mutant resembles R light grown wildtype (WT) (Figure 1.7) (Leivar, Monte, Oka, et al., 2008; Shin et al., 2009).

Although many PIFs appear to have overlapping functions they also have distinct roles in a variety of developmental processes and integrate not only light but several other abiotic and biotic signals (Balcerowicz, 2020; Leivar and Monte, 2014; Shin et al., 2009). Until this day, PIF1 is the only described negative regulator of phytochrome-induced seed germination most likely due to its unique high expression levels in imbibed seeds (Jeong and Choi, 2013; Oh et al., 2004). In the regulation of thermomorphogenesis, PIF4 is the key player while minor roles have been described for both PIF5 and PIF7 (Balcerowicz, 2020; Fiorucci et al., 2020; Koini et al., 2009; Quint et al., 2016; Stavang et al., 2009). Interestingly, in the control of the shade avoidance response these roles are changed, and PIF7 is the key player to induce the shade avoidance response. However, only a *pif4 pif5*

pif7 triple mutant is completely insensitive for low R:FR-induced hypocotyl elongation (Li et al., 2012; Lorrain et al., 2007; de Wit et al., 2016).

1.1.2.2 The COP1/SPA complex inhibits photomorphogenesis

One of the main inhibitors of photomorphogenesis acting in darkness is the E3 ubiquitin ligase complex COP1/SPA. The active tetrameric complex consists of two COP1 proteins and two SPA (SPA1 – SPA4) proteins (Zhu et al., 2008). Interestingly, although the SPA proteins are required for the *in vivo* E3 ubiquitin ligase activity of COP1 only a *cop1* null mutant is seedling lethal (Laubinger et al., 2004; McNellis et al., 1994; Ordoñez-Herrera et al., 2015). In contrast, the *spa1234* null mutant is viable but shows an extreme dwarf phenotype in light and constitutive photomorphogenic development in darkness similar to knockdown mutants of *cop1* (Deng et al., 1991; Laubinger et al., 2004; McNellis et al., 1994; Ordoñez-Herrera et al., 2015).

As an E3 ubiquitin ligase, the COP1/SPA complex ubiquitinates its targets and thereby marks them for degradation through the 26S proteasome (Hoecker, 2017; Soo Seo et al., 2003). Among the numerous targets of COP1/SPA, the first identified was the basic leucine zipper (bZIP) transcription factor HY5, which functions as a key positive regulator of photomorphogenesis (Osterlund et al., 2000; Saijo et al., 2003).

The activity of the COP1/SPA complex has been observed to be regulated in numerous manners (Podolec and Ulm, 2018; Ponnu and Hoecker, 2021). Early observations suggested that COP1 is excluded from the nucleus upon illumination with light, indicating that its activity is inhibited by a physical separation from its nuclear localized targets (von Arnim and Deng, 1994). Although at first observed as a rather slow process, the nuclear exclusion of COP1 was later shown to be relatively fast (von Arnim and Deng, 1994; Pacín et al., 2014). The nuclear exclusion of COP1 negatively correlates with the accumulation of the COP1 target HY5 supporting the importance of nuclear exclusion of COP1 as a regulatory mechanism for COP1/SPA activity (Pacín et al., 2014).

Regardless, the activity of the COP1/SPA complex is also regulated through the direct interaction with active phytochromes, cryptochromes and UVR8 through several mechanisms (Figure 1.7). For example, the interaction of phyA, phyB, and CRY1 with COP1/SPA can lead to the inhibition of the COP1/SPA activity by disruption of the complex (Lian et al., 2011; Liu et al., 2011; Lu et al., 2015; Sheerin et al., 2015).

Additionally, CRY1, CRY2 and UVR8 have been shown to compete for COP1 binding with its targets. A higher affinity of COP1 to the photoreceptors mediated by a conserved valine-proline (VP) motif protects other COP1 targets from degradation (Lau et al., 2019; Ponnu et al., 2019).

On the other hand, the interactions of the phytochromes and cryptochromes with the COP1/SPA complex also lead to the degradation of the photoreceptors, providing a negative feedback mechanism in the light signaling networks (Debrieux et al., 2013; Jang et al., 2010; Seo et al., 2004; Shalitin et al., 2002; Weidler, Heunemann, et al., 2012).

1.2 HY5, a master regulator of plant development

The central positive regulator of photomorphogenesis, HY5, is a bZIP transcription factor (Oyama et al., 1997). Interestingly, the crystal structure of the C-terminal leucine zipper domain revealed an α-helical coiled coil structure supporting homodimerization of the HY5 protein (Yoon et al., 2007). Its N-terminal domain is intrinsically unstructured and might fold upon the interaction with protein partners (Yoon et al., 2006).

As a transcription factor HY5 has been shown to bind DNA through a variety of motifs, including the ACE-element (CACGT) containing G-box (CACGTG), hybrid C/G-box (GACGTG) and T/G-box (CACGTT), the E-box (CAATG), GATA-box (GATGATA), Z-box (ATACGTGT), C-Box (GACGTC), and C/A-box (GACGTA) (Abbas et al., 2014; Lee et al., 2007; Shi et al., 2011; Shin et al., 2013; Song et al., 2008; Toledo-Ortiz et al., 2014; Yadav et al., 2002; Zhang et al., 2011). In accordance with its ability to bind multiple DNA motifs HY5 has been shown to bind over one third of the promoters in the Arabidopsis genome (Hajdu et al., 2018; Lee et al., 2007; Zhang et al., 2011).

HY5 shares redundant functions with its close homologue HY5-HOMOLOG (HYH), with HYH showing limited importance, mainly in B light (Holm et al., 2002). In line with HY5's role as a positive regulator of photomorphogenesis, a *hy5* mutant has an elongated hypocotyl under both white light, and monochromatic R, FR or B light as well as under white light supplemented with UV-B, suggesting that HY5 acts downstream of the phytochromes, cryptochromes and UVR8 (Figure 1.7) (Koornneef et al., 1980; Oravecz et al., 2006).

Although the transcript levels of *HY5* have been shown to be induced by light (Oyama et al., 1997) its post-translational regulation through the COP1/SPA complex is more

important for the regulation of photomorphogenesis (Osterlund et al., 2000; Saijo et al., 2003; Zhu et al., 2008). HY5 interacts through its N-terminal domain with COP1 via a conserved VP motif and this interaction leads to HY5's ubiquitination and degradation through the 26S proteasome in darkness (Figure 1.7) (Ang et al., 1998; Holm et al., 2001; Osterlund et al., 2000). Accordingly a mutated version of HY5 in which the 77 N-terminal amino acids are deleted (HY5ΔN77) is stable in darkness (Osterlund et al., 2000). Interestingly, the expression of this dark stable version of HY5 does not lead to the induction of photomorphogenesis in darkness (Ang et al., 1998). This result, together with the observation that HY5 lacks any apparent transactivation domain (TAD) and cannot induce expression by itself when expressed in yeast led to the conclusion that HY5 requires interacting protein cofactors to regulate photomorphogenesis (Ang et al., 1998).

An additional layer of regulation of the HY5 activity was discovered when it was observed that HY5 can be phosphorylated *in vivo* (Hardtke et al., 2000). This phosphorylation, mediated by the SPAs, leads to stronger interaction with COP1 and preferred degradation of HY5 in darkness but also to a stronger interaction with target promoters (Hardtke et al., 2000; Wang, Paik, et al., 2021). Hence, it has been concluded that in darkness a less active, but more stable pool of unphosphorylated HY5 is present, which than can be rapidly activated by dephosphorylation upon the exposure to light (Hardtke et al., 2000).

Besides its well described role in regulating photomorphogenesis, analyses of *hy5* mutants have revealed a variety of developmental processes in which HY5 plays an important role e.g. seed germination, root development, entrainment of the circadian clock or the regulation of flowering (Figure 1.8) (Andronis et al., 2008; Burko et al., 2020; Chen et al., 2008; Oyama et al., 1997). HY5 also serves to integrate a variety of hormonal signaling pathways and is required for the induction of responses to cytokinin, auxin, gibberellins (GA), abscisic acid (ABA), brassinosteroids, ethylene, jasmonate (JA) and karrikins (KARs) (Figure 1.8) (Alabadí et al., 2007; Chen et al., 2008; Cluis et al., 2004; Li and He, 2016; Nelson et al., 2010; Vandenbussche et al., 2007; Yi et al., 2020; Yu et al., 2013).

How exactly HY5 fulfils its multiple roles remains elusive, but it has been repeatedly suggested that HY5 requires partner proteins to allow for the transcriptional activation of its numerous target genes (Ang et al., 1998; Burko et al., 2020; Stracke et al., 2010).

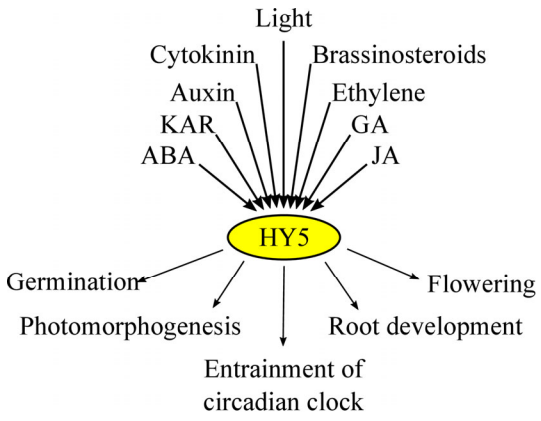

Figure 1.8: HY5 functions as a central integrator for light and hormone signaling to regulate a variety of developmental processes.

The bZIP transcription factor HY5 has been shown to be involved in the signal transduction of light and hormone signals by the inability of a *hy5* mutant to respond to these external cues (ABA, KAR, Auxin, Cytokinin, Light, Brassinosteroids, Ethylene, GA, JA). The developmental processes regulated by HY5 include germination, photomorphogenesis, entrainment of the circadian clock, root development and flowering.

1.3 The transcription factor family of BBX proteins

Zinc binding B-Box domains can be found in numerous proteins and a variety of organisms, emphasized by the fact, that in the SMART's genomes database 13494 B-Box domains in 10059 proteins are found in a variety of eukaryotic organisms (EMBL, 2020). Originally, the B-Box domain was identified in the *Xenopus* nuclear factor 7 (*xnf7*) from *Xenopus laevis*. This B-Box domain is a zinc-finger domain in which two zinc ions are coordinated by a cysteine/histidine-rich motif (Reddy et al., 1991; Reddy and Etkin, 1991; Torok and Etkin, 2001).

In mammals, B-Box domains are mostly found in so-called tripartite motif (TRIM) proteins which are characterized by the N-terminal RING (Really Interesting New Gene, formerly A-Box) domain followed by one or two B-Box domains and a coiled-coil region (Lovering et al., 1993; Torok and Etkin, 2001). The arrangement of these domains (RBCC) is widely conserved and these proteins are proposed to form a new class of E3 RING-type ligases in which the B-Box domains contribute to substrate targeting and ligase activity enhancement (Anthony Massiah, 2019; Short and Cox, 2006).

In plants however, B-Box domains are found in proteins without a RING or coiled-coil domain and form a family of transcription factors called B-BOX DOMAIN (BBX) proteins (Khanna et al., 2009). In Arabidopsis this protein family counts 32 members which are structurally classified in five groups (Khanna et al., 2009). The proteins in

structural group I and II contain two N-terminal located B-Box domains (B-Box1 and B-Box2) and a C-terminal CONSTANS, CO-like, and TOC1 (CCT) domain. The proteins in structural group III contain only one B-Box domain and a CCT domain. The BBX proteins in group IV and V lack the CCT domain and are distinguishable by the occurrence of two (IV) or one (V) B-Box domain, respectively (Figure 1.9) (Khanna et al., 2009).

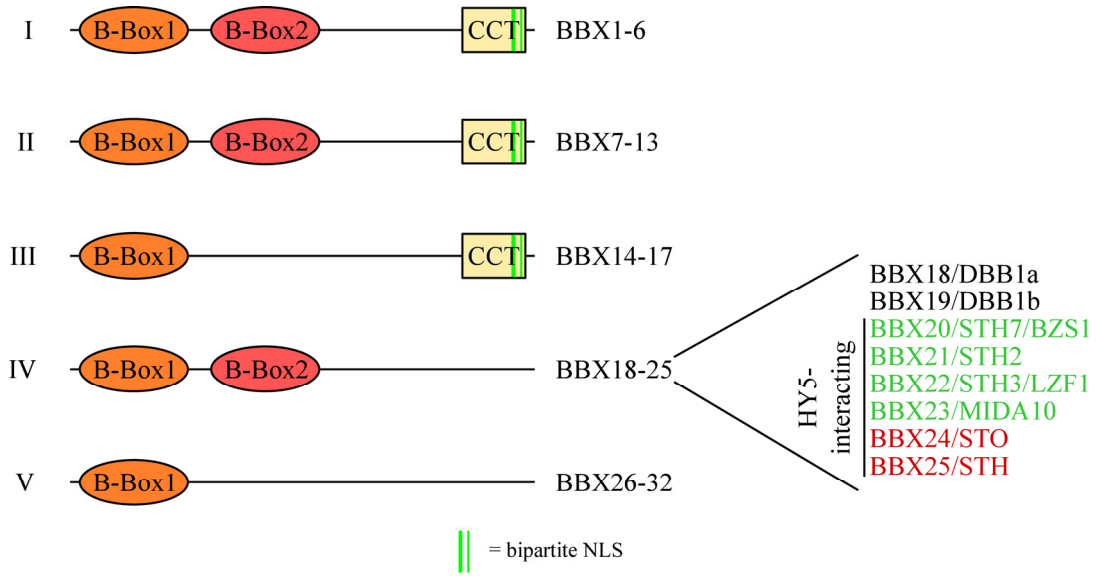

Figure 1.9: The BBX transcription factor family in Arabidopsis.

In Arabidopsis, the BBX transcription factor family contains 32 members that are divided in five structural groups based on their B-Box domains and the occurrence of a CCT domain. In structural group IV six HY5-interacting BBX proteins (BBX20-BBX25) have been identified. Those BBX proteins can be divided in positive (depicted in green) and negative (depicted in red) regulators of photomorphogenesis.

Bioinformatic analyses revealed that the CCT domain contains a bipartite nuclear localization signal (NLS) with the consensus sequence R-K-X11-R (Figure 1.9) (Crocco and Botto, 2013). Although the experimental validation of this NLS is currently lacking it has been shown that CONSTANS (CO)/ B-BOX DOMAIN PROTEIN 1 (BBX1), BBX4 and BBX5 are indeed nuclear localized. Furthermore, the nuclear localization of the CO protein is dependent on the CCT domain (Crocco and Botto, 2013; Datta et al., 2006; Robson et al., 2001; Steinbach, 2019). The CCT domain also confers DNA binding and is important for certain protein-protein interactions (Gendron et al., 2012; Laubinger et al., 2006; Tiwari et al., 2010). Also the B-Box domains have been identified as required for conferring protein-protein interactions, as well as protein-DNA interaction (Datta et al., 2007, 2008; Heng et al., 2020; Wang et al., 2014; Wang, Khoshhal Sarmast, et al., 2015; Xu et al., 2018). It should be noted however, that some of these studies rely on the

analysis of point mutations in conserved aspartate (Asp) amino acids involved in the binding of zinc. The loss of zinc coordination in the B-Box domain has been show to lead to complete unfolding of the protein structure of a human TRIM protein (Anthony Massiah, 2019; Wright et al., 2014). Hence, from those studies it is difficult to conclude if the disruption of zinc binding in the B-Box domain exclusively affects this domain or impacts the overall protein structure.

1.3.1 Regulation of plant development by BBX proteins

The first identified, and arguably most investigated BBX protein is CO, which has been shown to promote flowering in Arabidopsis by regulating the expression of the florigen *FLOWERING LOCUS T* (*FT*) (Putterill et al., 1995; Tiwari et al., 2010). The regulation of CO in turn serves as an integration point for a variety of signals leading to the induction or inhibition of flowering (Shim et al., 2017). Although CO is a central regulator of flowering, multiple other BBX proteins have been shown to impact flowering as well (Cheng and Wang, 2005; Datta et al., 2006; Liu et al., 2020; Song, Bian, et al., 2020; Steinbach, 2019; Wang et al., 2014).

Recent advances have also shown that numerous BBX proteins are important for the regulation of photomorphogenesis in seedlings (Song, Bian, et al., 2020). The analysis of mutants and overexpression lines of BBX proteins has led to the identification of both positive and negative regulators of photomorphogenesis. Structural group V contains mainly negative regulators of photomorphogenesis (BBX28 - BBX31) (Heng et al., 2019; Lin et al., 2018; Song, Yan, et al., 2020) whereas structural group IV consists of a mixture of positive (BBX20 – BBX23) and negative regulators of photomorphogenesis (BBX18, BBX19, BBX24, BBX25) (Chang et al., 2008; Datta et al., 2007, 2008; Fan et al., 2012; Gangappa, Crocco, et al., 2013; Indorf et al., 2007; Wang, Khoshhal Sarmast, et al., 2015; Wang et al., 2011; Zhang et al., 2017).

Interestingly, an interplay between positive and negative regulators of photomorphogenesis within the BBX protein family has been reported (Job et al., 2018; Song, Yan, et al., 2020). This interplay might involve direct physical interaction as it was reported e.g. for BBX32 and BBX21/SALT TOLERANCE HOMOLOG 2 (STH2), or BBX24/SALT TOLERANCE (STO) and BBX21 (Holtan et al., 2011; Wei et al., 2016).

Although all BBX proteins from structural group IV (BBX18 – BBX25) have been shown to regulate photomorphogenesis, BBX20 - BBX25 form a subgroup by their ability to interact with the bZIP transcription factor HY5 (Figure 1.9) (Datta et al., 2007, 2008; Gangappa, Crocco, et al., 2013; Gangappa, Holm, et al., 2013; Wei et al., 2016; Zhang et al., 2017). This subgroup can be further divided in positive (BBX20 - BBX23) and negative (BBX24 – BBX25) regulators of photomorphogenesis and genetic analyses suggest that the function of these BBX proteins depends on HY5 (Figure 1.9) (Chang et al., 2008; Datta et al., 2007, 2008; Fan et al., 2012; Gangappa, Crocco, et al., 2013; Indorf et al., 2007; Zhang et al., 2017).

BBX20 – BBX25 have also been shown to interact with the COP1/SPA complex and are consequently targeted for degradation through the 26S proteasome in darkness (Chang et al., 2011; Datta et al., 2008; Fan et al., 2012; Gangappa, Crocco, et al., 2013; Holm et al., 2001; Wei et al., 2016; Xu, Jiang, et al., 2016; Yan et al., 2011; Zhang et al., 2017).

Interestingly, bioinformatic analysis led to the identification of a conserved monopartite NLS in BBX21, BBX22/SALT TOLERANCE HOMOLOG 3 (STH3)/LIGHT-REGULATED ZINC FINGER PROTEIN 1 (LZF1), BBX24, and BBX25/SALT TOLERANCE HOMOLOG (STH) (Crocco and Botto, 2013). Consistently, GFP-fusion proteins of BBX21 and BBX24 proteins have been shown to mainly localize in the nucleus in Arabidopsis seedlings and BBX22 and BBX25 showed nuclear localization in transient expression assays in onion cells (Datta et al., 2008; Gangappa, Crocco, et al., 2013; Indorf et al., 2007; Job et al., 2018; Xu et al., 2017; Yan et al., 2011). In contrast, BBX20/SALT TOLERANCE HOMOLOG 7 (STH7)/bzr1-1D SUPPRESSOR1 (BZS1) and BBX23/MISREGULATED IN DARK10 (MIDA10) appear to be both nuclear and cytosolic localized in Arabidopsis seedlings (Fan et al., 2012; Zhang et al., 2017).

Mutant and overexpression analysis of *BBX21*, *BBX22* and *BBX23* clearly shows their role as positive regulators of photomorphogenesis by an elongated or shortened hypocotyl in the mutants or overexpression lines respectively under white light as well as monochromatic B, R or FR light (Chang et al., 2008; Datta et al., 2007, 2008; Xu et al., 2018; Zhang et al., 2017). Furthermore, in line with their role as positive regulators of light signaling, anthocyanin accumulation is suppressed in the mutants of *BBX21* and *BBX22* (Datta et al., 2007, 2008). Double mutant analysis suggests functional redundancy between BBX21 and BBX22 as well as between BBX22 and BBX23 (Datta et al., 2008; Zhang et al., 2017).

However, because of the lack of available T-DNA insertion lines, the analysis of *BBX20* has been limited to the analysis of transgenic lines overexpressing the native BBX20 protein or a BBX20-EAR REPRESSION DOMAIN (SRDX) fusion protein, causing dominant-negative transcriptional repression, which all support its role as a positive regulator of photomorphogenesis (Fan et al., 2012; Thussagunpanit et al., 2017; Wei et al., 2016). In accordance with their role as negative regulators of photomorphogenesis, mutants of *BBX24* and *BBX25* show a short hypocotyl and enhanced anthocyanin accumulation under white and monochromatic light and double mutant analysis suggests functional redundancy between these two BBX proteins (Gangappa, Crocco, et al., 2013; Indorf et al., 2007; Yan et al., 2011).

Hence, since the discovery of CO as a master regulator of flowering, recent work on BBX proteins suggests that many of them regulate light-dependent plant development.

1.4 Karrikin a germination stimulant from smoke

In 1990 it was discovered that a water-soluble chemical compound, derived from burning plant material, induces germination in plant species which are known to germinate in nature only after bushfires. By forcing smoke from burning plant material to bubble through water, so-called smoke water was created. Watering areas with this smoke water induced germination of *Audouinia capitata* (de Lange and Boucher, 1990). The effect of smoke water is reported in a variety of plant species and its interaction with other cues like light, temperature and other plant hormones is reviewed in Brown and Van Staden (1997). Nearly ten years later, extensive research had led to the identification of the active compound from smoke, via bioassay guided fractionation as the butenolide derivative, 3-methyl-2H-furo[2,3-c]pyran-2-one (Flematti et al., 2004; Van Staden et al., 2004) and further proven by chemical synthesis (Flematti et al., 2005). Up to now, there are 6 alkyl-substituted 3-methyl-2H-furo[2,3-c]pyran-2-ones (KAR_1 – KAR_6) (Figure 1.10) identified occurring in smoke with the ability to induce germination (Flematti et al., 2009). The name KARs comes from the Noongar word “karrik” meaning “smoke”(Dixon et al., 2009). Structurally, KARs are similar to the plant hormones strigolactones (SLs) which consist of a tricyclic lactone (ABC ring) and a butenolide (D-ring) (Figure 1.10) (Gomez-Roldan et al., 2008; Umehara et al., 2008; Xie et al., 2010). The structural similarity of the two classes of molecules has caused problems, as the most commonly used SL-analogue GR24 is often used as a racemic mixture. The enantiomer $GR24^{5DS}$ has

been shown to mainly mimic the effect of natural SLs, whereas GR24$^{ent\text{-}5DS}$ mainly mimics the effect of KAR treatment (Scaffidi et al., 2014). Hence, some responses attributed to SL treatment in the literature might in fact be caused by KAR.

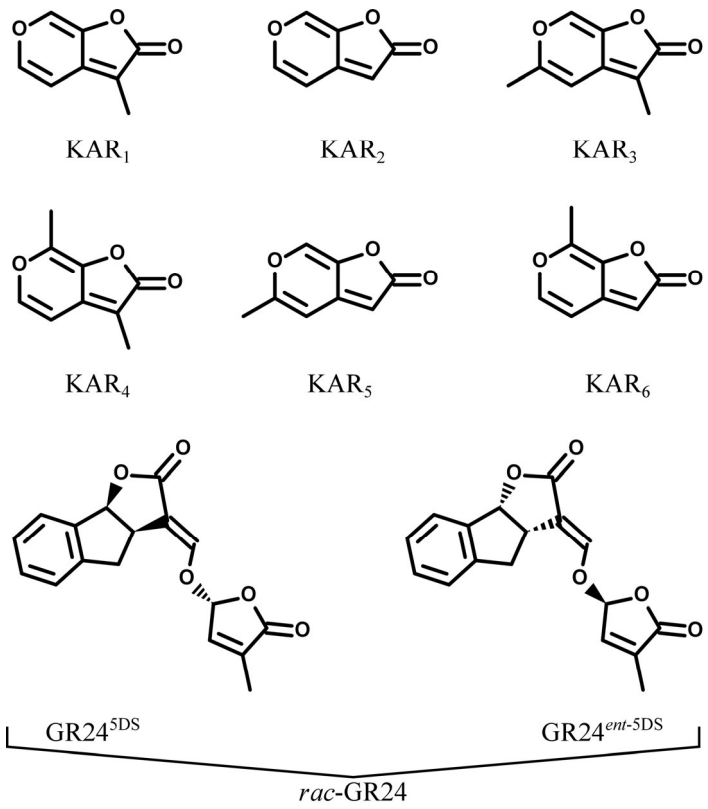

Figure 1.10: Structures of KAR_1 – KAR_6 and *rac*-GR24.

Although structurally similar molecules, karrikins (KARs) and strigolactones (SLs) are two separate classes of bio-active molecules. Nevertheless, the commonly used SL-analogue *rac*-GR24 consists of two enantiomers that can activate the SL and KAR signaling pathway, respectively.

1.4.1 Karrikin in Arabidopsis

Interestingly, a germination inducing effect of KAR has not only been observed in fire-following plant species (reviewed in Light et al., (2009) and Dixon et al., (2009).

A key finding that accelerated the understanding of the mechanism of the KAR mode of action was that also the model plant Arabidopsis (not fire-following species) responded to treatment with KAR_1 with the induction of germination. Testing of different KARs has revealed that KAR_2 is the most active germination stimulant in Arabidopsis (Nelson et al., 2009).

1.4.1.1 The Karrikin signaling pathway

The KAR signal is perceived by the receptor KARRIKIN INSENSITIVE 2 (KAI2) (Waters et al., 2012). The crystal structure of KAI2, that was solved by four individual research groups, shows that KAI2 is an α/β hydrolase consisting of an α/β hydrolase domain formed by a seven stranded ß-sheet surrounded by seven helices and a four helix cap domain displaying a double layer V-shaped helical fold. The active site consists of a serine hydrolase catalytic triad (Ser95 – His246 – Asp217) and seems to be located at the bottom of a largely hydrophobic pocket (Bythell-Douglas et al., 2013; Guo et al., 2013; Kagiyama et al., 2013; Zhao et al., 2013). Via isothermal titration calorimetry binding of KAR_1 to KAI2 could be shown, but the structure of the KAI2-KAR_1 cocrystal revealed that KAR_1 is bound distal to the catalytic triad not likely getting hydrolyzed by KAI2 (Kagiyama et al., 2013). Instead, binding of KAR_1 seems to induce a conformational change that possibly allows for the interaction with other proteins (Guo et al., 2013). Upon KAR perception KAI2 forms a complex with MORE AXILLARY GROWTH 2 (MAX2) (Toh et al., 2014; Wang et al., 2020). MAX2 is an F-box leucine rich repeat protein (Stirnberg et al., 2002) which is part of an SCF complex that might confer substrate specificity leading to ubiquitination and degradation of further signaling components (Stirnberg et al., 2007). To identify downstream signaling components a genetic screen for *suppressor of max2 (smax)* mutants was conducted leading to the identification of SUPPRESSOR OF MAX2 1 (SMAX1) (Stanga et al., 2013). SMAX1 belongs to a family of eight genes which show structural similarity to Heat shock protein 100 / Caseinolytic peptidase B (Hsp100/ClpB) proteins (Stanga et al., 2013). In the KAR signaling pathway SMAX1 and its closest homolog SMAX1-LIKE 2 (SMXL2) act mainly redundantly as negative regulators of the pathway (Stanga et al., 2016). The activation of the pathway leads to interaction of KAI2 with SMAX1 and SMXL2 which is believed to result in a multicomplex of KAI2 – MAX2 – SMAX1/SMXL2 (Khosla et al., 2020; Wang et al., 2020). Finally this interaction results in the degradation of SMAX1 and SMXL2, which has been shown for SMAX2 to be preceded by ubiquitination leading to the activation of the KAR response (Figure 1.11) (Khosla et al., 2020; Wallner et al., 2017; Wang et al., 2020).

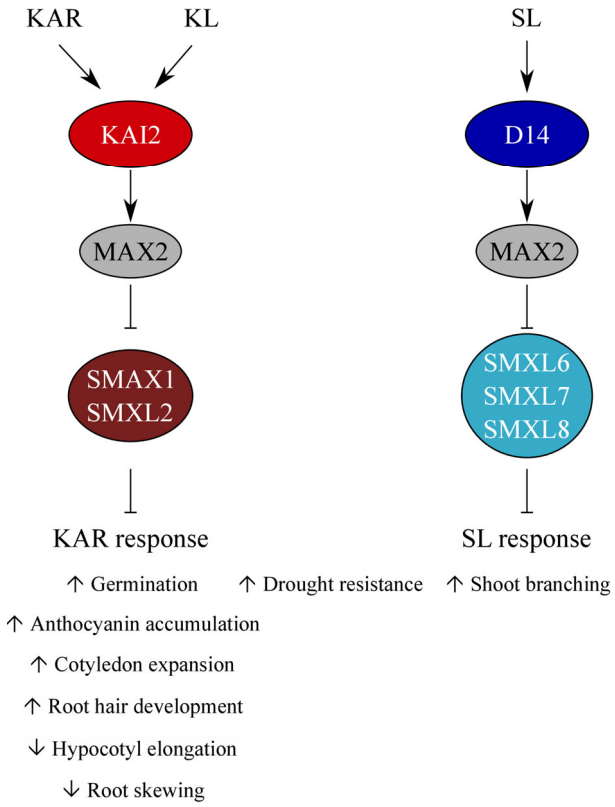

Figure 1.11: The KAR and SL signaling pathways in Arabidopsis.

Schematic depiction of the KAR and SL signaling pathways as described in the text. The KAR or KL signal is perceived by the receptor KAI2 which leads to the activation of MAX2, resulting in the degradation/inhibition of SMAX1 and SMXL2 and subsequently the activation of the KAR response. SLs are perceived by the receptor D14 and thereby activates MAX2. The activation of this pathway leads to the degradation/inhibition of SMXL6, SMXL7 and SMXL8 and thereby induction of the SL response. The SL response consists of, but is not limited to, the induction of shoot branching. An upward arrow before the components of the KAR or SL response represents induction of the process by the respective pathway, while a downward arrow represents inhibition. Drought resistance is regulated by both KAR and SL signaling.

1.4.1.2 The effect of Karrikin, more than a germination stimulant

Interestingly, the KAR response has been shown to not only include the induction of germination, but to also include a variety of phenotypic changes. Mostly, it was observed that the KAR signaling mutants show respective treatment-independent mutant phenotypes. The dormancy breaking effect of the KAR treatment, for example, is accompanied by increased primary dormancy in the signaling mutants *kai2* and *max2* (Nelson et al., 2011; Waters et al., 2012). In contrast, mutants of the negative regulators of KAR signaling, *smax1* and *smxl2*, which can be considered mutants with a constitutively active KAR signaling, show a reduction in primary dormancy (Stanga et al., 2013, 2016).

In seedlings, KAR treatment induces photomorphogenesis, measurable by the inhibition of hypocotyl elongation (Nelson et al., 2010). Consequently *kai2, max2* and *smax1 smxl2* mutants show hypophotomorphogenic and hyperphotomorphogenic phenotypes, respectively, under monochromatic R light (Nelson et al., 2011; Stanga et al., 2013, 2016; Waters et al., 2012). Further photomorphogenic responses, like cotyledon expansion, or chlorophyll and anthocyanin accumulation are induced by treatment with KAR (Nelson et al., 2010; Thussagunpanit et al., 2017). Correspondingly, *kai2* and *max2* mutants have smaller cotyledons, and the *kai2* mutant accumulates less chlorophyll and anthocyanin compared to WT (Shen, Luong, et al., 2007; Sun and Ni, 2011).

On the transcriptional level, KAR treatment leads to the strong induction of *BBX20*, *KARRIKIN UPREGULATED F-BOX1* (*KUF1)* and *DWARF14-LIKE2* (*DLK2*) (Nelson et al., 2010; Waters et al., 2012). While this differential expression is confirmed by the downregulation of those genes in *kai2* and/or *max2* and a strong induction of *KUF1* and *DLK2* in *smax1* and *smxl2* mutants, the roles of *BBX20*, *DLK2*, and *KUF1* in KAR signaling remain elusive (Nelson et al., 2011; Stanga et al., 2013, 2016; Waters et al., 2012).

Also root development is influenced by KAR. The *kai2* and *max2* mutants show an enhanced root skewing phenotype which can be suppressed by the mutation of *SMAX1* and *SMXL2* (Swarbreck et al., 2019). Furthermore, the treatment with KAR_2 leads to an increase in root hair density and length. This observation is accompanied by a decrease in root hair density and length in the *kai2* and *max2* mutant which can be suppressed by the mutation of *SMAX1* and *SMXL2* (Villaécija-Aguilar et al., 2019).

Under mild osmotic stress, KAR seems to play a protective role as KAR_2 treatment leads to the inhibition of germination under these conditions, accompanied by enhanced induction of osmotic stress marker genes. Furthermore, the *kai2* mutant is more sensitive to osmotic stress in germination assays (Wang et al., 2018). In adult plants the *kai2* mutant shows a higher sensitivity to drought stress caused by impaired ABA-mediated stomatal closure, lower anthocyanin levels and faster water loss caused by cuticular defects (Li, Nguyen, et al., 2017).

1.4.1.3 Karrikin, mirroring an endogenous KAI2 ligand?

The discovery that also Arabidopsis responds to KAR treatment has raised the question of why non-fire following species have a perception system for a signal that they may never perceive. The identification of KAR signaling mutants in Arabidopsis and the connected phenotypes that are independent of exogenous applied KAR (e.g. elongated hypocotyl of *kai2* and *max2*) led to the hypothesis that KAR is mirroring an endogenous not yet identified KAI2 ligand (KL) (Nelson et al., 2011; Waters et al., 2012).

Because of the structural similarity between KAR and SL it has also been hypothesized that KAR mirrors new and not yet identified forms of SLs (Waters et al., 2014). Contradicting this hypothesis, it is believed that all SLs derive from the precursor carlactone by the subsequent action of CLEAVAGE DIOXYGENASE 7 (CCD7), CLEAVAGE OXYGENASE 8 (CCD8) and DWARF27 (D27) (Alder et al., 2012; Seto et al., 2014). But it has been shown that the treatment with carlactone cannot overcome seed dormancy like KAR (Scaffidi et al., 2013). In support of a clear distinction between KARs and SLs as two different classes of butenolide signaling molecules, the receptors of KAR and SL (KAI2 and DWARF14 (D14), respectively) are not interchangeable. Expression of one receptor under the control of the promotor of the other does not rescue the respective mutant phenotypes (Waters et al., 2015).

Phylogenetic analyses have shown, that the SL signaling pathway has evolved by neo-functionalization after gene duplication events of the KAR signaling pathway (Bythell-Douglas et al., 2017). In the course of phylogenetic analyses, KAI2 paralogs from *Striga hermonthica* and *Phelipanche aegyptiaca,* that can rescue the *kai2* phenotype in Arabidopsis, were identified. However, these did not confer responses to exogenously added KAR or SL, further supporting the hypothesis that KAI2 from Arabidopsis (and its paralogs) recognize an endogenous signal (Conn et al., 2015; Conn and Nelson, 2016).

Direct evidence for the existence of KL was obtained by creating a *DLK2:LUC* reporter construct consisting of the *DLK2* promoter and the firefly luciferase gene (*LUC*). *DLK2* is one of the strong and specific KAR target genes (see section 1.4.1.2) (Waters et al., 2012). When this reporter construct is stably expressed in Arabidopsis it is specifically activated by KAR through the KAI2, MAX2, SMAX1, SMXL2 signaling pathway but not by SL treatment. Strikingly, this reporter can also be activated when transgenic reporter seeds are treated with leaf extracts from Arabidopsis WT leaves. Importantly, this response is abolished when the leaf extract is applied to transgenic reporter seeds

with a *kai2* mutant background. This suggests, that WT leaves contain an endogenous signal with the ability to activate the KAI2, MAX2, SMAX1, SMXL2 signaling pathway (Sun et al., 2016).

1.4.2 Comparison of KAR/KL and SL signaling pathways

SLs were originally identified in root exudates from cotton plants with the ability to induce germination of witchweed (*Striga lutea Lour*.), hence the first SL was named strigol (Cook et al., 1966). As parasitic plants, witchweed depend on the presence of a host root, from which they obtain water and nutrients which can cause severe damage in the host plant and lead to severe yield losses when crop plants are infested (Hu et al., 2020; Jamil et al., 2021). Besides the harmful induction of germination of root parasitic weeds, SLs were also identified in root exudates from *Lotus japonicus*. Here they induce hyphal branching in the arbuscular mycorrhizal fungus *Gigaspora margarita* supporting the establishment of the fungus – plant symbiosis (Akiyama et al., 2005).

Further research has led to the discovery that SLs are endogenous plant hormones inhibiting shoot branching (Gomez-Roldan et al., 2008; Umehara et al., 2008). As mentioned above (see section 1.4) the SLs show strong similarities to the KAR molecules. These similarities proceed with the components of the SL signaling pathway. SLs are bound by the receptor D14, a homologue of KAI2 (Arite et al., 2009; Waters et al., 2012). The activation of D14 leads to hydrolyzation of the SL molecule and the interaction of D14 and MAX2 (Zhao et al., 2013). Hence, MAX2 functions as a central signaling component for both the KAR and SL pathway and the *max2* mutant phenotypes are a combination of the *kai2* and *d14* single mutant phenotypes (Waters et al., 2012). Finally, the activation of the SL pathway leads to the degradation of SMXL6,7,8, homologues of SMAX1, SMXL2 (Figure 1.11) (Soundappan et al., 2015; Wang, Wang, et al., 2015).

While the major impact of KAR is observed in seeds or at the seedling stage, the best-investigated effect of SLs is the regulation of shoot branching in adult plants (Morffy et al., 2016). Nevertheless, also overlapping functions between KAR and SLs can be observed. For instance, both have been described as positive regulators of drought resistance. But mutant analyses of the receptors *kai2* and *d14* showed that the mediated drought resistance is achieved through different mechanisms (Li et al., 2020; Li, Nguyen, et al., 2017). Recently, it was shown that also crosstalk between the two signaling

pathways can occur. Exogenous applied SL can induce the degradation of SMXL2 and thereby lead to the inhibition of hypocotyl elongation, a response that is attributed to the KAR signaling pathway (Wang et al., 2020). But as a *d14* mutant does not show any treatment-independent hypocotyl phenotypes the significance of this crosstalk remains elusive (Scaffidi et al., 2013).

1.5 Research objectives

In this thesis I aimed to extend the understanding of HY5's function as a master transcriptional regulator of photomorphogenesis by focusing on the role of HY5-interacting BBX proteins from structural group IV.

The inability of HY5 alone to promote photomorphogenesis in darkness and the lack of a TAD has led to the development of a model, in which HY5 interacts with a cofactor that is rate-limiting for its function (Ang et al., 1998; Oyama et al., 1997). Based on this model, predictions about the properties that a potential cofactor should fulfil could be made, which led to the hypothesis that BBX20, BBX21, and BBX22 could act as those cofactors. To test this hypothesis, the CRISPR/Cas9 technology was deployed to create a *bbx20-1* null mutant, which allowed the required analysis of higher order mutants and overexpression lines on the phenotypic and molecular level.

In the second part of this thesis, I aimed to investigate the role of BBX proteins in KAR signaling. Previous results showed strong transcriptional induction of *BBX20* in response to KAR treatment (Nelson et al., 2010). I performed extensive single and higher order mutant analysis on the phenotypic and transcriptomic level to elucidate how the KAR and light signaling pathways interact.

2 Identification of BBX proteins as rate-limiting cofactors of HY5

This is a post-peer-review, pre-copyedit version of an article published in *Nature Plants.* The final authenticated version is available online at: https://doi.org/10.1038/s41477-020-0725-0.

Bursch, K., Toledo-Ortiz, G., Pireyre, M., Lohr, M., Braatz, C. and Johansson, H. (2020), "Identification of BBX proteins as rate-limiting cofactors of HY5", *Nature Plants*, (2020) 6, 921-928, Springer US. https://doi.org/10.1038/s41477-020-0725-0.

2.1 Abstract

As a source of both energy and environmental information, monitoring the incoming light is crucial for plants to optimize growth throughout development (Sullivan and Deng, 2003). Concordantly, the light signalling pathways in plants are highly integrated with numerous other regulatory pathways (Lau and Deng, 2010; Paik et al., 2017). One of these signal integrators is the bZIP transcription factor HY5 which holds a key role as a positive regulator of light signalling in plants (Gangappa and Botto, 2016; Koornneef et al., 1980). Although HY5 is thought to act as a DNA-binding transcriptional regulator (Chattopadhyay et al., 1998; Zhang et al., 2011), the lack of any apparent transactivation domain (Oyama et al., 1997) makes it unclear how HY5 is able to accomplish its many functions. Here, we describe the identification of three B-box containing proteins (BBX20, 21 and 22) as essential partners for HY5 dependent modulation of hypocotyl elongation, anthocyanin accumulation and transcriptional regulation. The *bbx202122* triple mutant mimics the phenotypes of *hy5* in the light and its ability to suppress the *cop1* mutant phenotype in darkness. Furthermore, 84% of genes that exhibit differential expression in *bbx202122* are also HY5 regulated, and we provide evidence that HY5 requires the B-box proteins for transcriptional regulation. Lastly, expression of a truncated dark stable version of HY5 (HY5ΔN77) together with BBX21 mutated in its VP-motif, strongly promoted de-etiolation in dark grown seedlings evidencing the functional interdependence of these factors. Taken together, this work clarifies long standing questions regarding HY5 action and provides an example of how a master regulator might gain both specificity and dynamicity by the obligate dependence of cofactors.

2.2 Main text

Light perception by the cryptochromes, phytochromes and UVR8 in plants results in the inhibition of the COP1/SPA E3 ubiquitin ligase complex that generally targets positive regulators of photomorphogenesis for degradation (Galvão and Fankhauser, 2015; Podolec and Ulm, 2018). Exposure to light consequently results in the accumulation of several COP1/SPA targets that ultimately promote de-etiolation. Consequently, mutants of *cop1* exhibit photomorphogenic development when grown in darkness (Deng et al., 1992). Out of the several targets of COP1 mediated protein degradation, the bZIP transcription factor HY5 plays the most prominent role in light-induced photomorphogenesis as a modulator of hypocotyl elongation, anthocyanin and chlorophyll accumulation, in addition to integrating numerous external and internal signalling pathways (Gangappa and Botto, 2016; Osterlund et al., 2000). Genetically, mutants of *hy5* are largely epistatic to weaker alleles of *cop1* in darkness (Ang Lay Hong and Deng Xing Wang, 1994), suggesting that accumulation of HY5 is partly causing the *constitutively photomorphogenic (cop)* phenotype. This supports a model where light inhibition of COP1 results in HY5 accumulation followed by activation of transcriptional cascades that promote de-etiolation and photomorphogenesis (Figure 2.1a). Accordingly, HY5 protein levels progressively accumulate with increasing light intensities and correlate with a gradually stronger photomorphogenic phenotype in seedlings (Osterlund et al., 2000).

Interestingly, early reports showed that overexpression of *HY5* does not result in the expected strong photomorphogenic phenotypes (Ang et al., 1998). In addition, *in planta* expression of a dark stable HY5 construct (*HY5ΔN77*) does not promote de-etiolation in darkness (Ang et al., 1998). These observations together with the apparent lack of a transactivation domain in the HY5 protein (Oyama et al., 1997), prompted an expansion of the linear COP1-HY5 model to include an unknown factor X, that is negatively regulated by COP1 and is both required and rate-limiting for HY5 to function (Figure 2.1a) (Ang et al., 1998; Burko et al., 2020). The model predicts the properties of factor X as being negatively regulated by COP1 and functionally dependent on HY5. Furthermore, the *x* mutant would phenotypically mimic *hy5*, while overexpression should result in hyper-photomorphogenic phenotypes expected (but not seen) by overexpression of *HY5* (Figure 2.1a).

Like HY5, the B-box Zinc finger transcription factors BBX20, BBX21 and BBX22 have been described as positive regulators of photomorphogenesis (Chang et al., 2008; Datta et al., 2007; Fan et al., 2012). Overexpression of these factors results in seedlings strongly hypersensitive to light, and all are negatively regulated by COP1 at a post-transcriptional level (Chang et al., 2011; Fan et al., 2012; Xu, Jiang, et al., 2016). In addition, these three factors directly interact with HY5 *in planta*, and HY5 appears to be largely required for their function (Datta et al., 2007, 2008; Wei et al., 2016). Thus, as these BBX proteins fulfil many of the predicted properties of factor X, we hypothesised that these BBX proteins have a functional role in modulating the transcriptional capacity of the master regulator HY5 (Figure 2.1a).

To genetically test the hypothesis, we first evaluated the phenotype of a *bbx20-1* null mutant generated by CRISPR/Cas9 editing (Supplemental Figure 5.1.1a, b). The *bbx20-1* mutant displayed a long hypocotyl phenotype that co-segregated with the genotype and which could be restored by complementation using a genomic *BBX20* construct (Supplemental Figure 5.1.1c-e). In contrast to the suppressed hypocotyl elongation observed in two transgenic lines overexpressing *GFP-BBX20* ~20- and ~40-fold, the *bbx20-1* mutant showed a long hypocotyl phenotype in monochromatic red, blue and far-red light (Supplemental Figure 5.1.2a, b) to which *hy5* appeared largely epistatic (Supplemental Figure 5.1.2c). Furthermore, while the BBX20 overexpressing lines showed a small phenotype in darkness as previously reported (Fan et al., 2012), the *bbx20-1* monogenic mutant behaved like WT (Supplemental Figure 5.1.2b, c). However, *bbx20-1* partially suppressed the dark phenotype of *cop1* mutants, consistent with BBX20 being targeted by COP1 for degradation (Supplemental Figure 5.1.2d) (Fan et al., 2012). To investigate redundancy, the *bbx20-1* mutant was then crossed with *bbx21-1 bbx22-1* to generate the *bbx202122* triple mutant. Indeed, redundancy was evident as an incremental increase in hypocotyl length was observed for single, double and triple mutants when grown in red light, while no significant differences was observed in darkness (Figure 2.1b). Furthermore, as postulated by the model, the *bbx202122* mutant largely mimicked both the strong hypocotyl phenotype and reduced anthocyanin accumulation of *hy5* and no additive phenotypes were observed in the *bbx202122 hy5* mutant, consistent with the view that these factors are operating in the same pathway (Figure 2.1c, d).

To further test this hypothesis, we investigated transcriptomic changes in *bbx202122 vs WT* through RNA-seq analysis of 4-day-old seedlings grown in monochromatic red light. GO analysis of the 142 differentially expressed genes (DEGs) in *bbx202122* (Supplemental Data 5.1.1) revealed biological processes related to cell wall organization, hydrogen peroxide, flavonoids, UV-B, red light and auxin (Figure 2.1e), largely consistent with the observed phenotypes. Reassuringly, we found that 119 (~84%) of *bbx202122* DEGs were also miss-regulated in the *hy5* mutant grown under the same conditions (Figure 2.1f and Supplemental Data 5.1.1). In this overlap, all but one gene were co-regulated between the two mutants whereas 64% were co-down regulated, indicating that HY5 and these B-box proteins primarily act to promote transcription of their common targets (Figure 2.1g). Based on the three most highly enriched GO-terms (Figure 2.1e), we further analysed *XTH12*/*13*/*26, PRX7*/*26*/*44*, *MYB12*, *F3H* and *FLS1* by qPCR and found that these genes were similarly down-regulated in both *bbx202122* and *hy5* compared to WT (Figure 2.1h-j). In addition, we observed comparable elevation of transcript abundance of *XTH18*, *PRX53* and *IAA6* in *bbx202122* and *hy5* (Supplemental Figure 5.1.3), verifying the RNA-seq results. Importantly, no additional miss-regulation was observed in the *bbx202122 hy5* mutant (Figure 2.1h-j, Supplemental Figure 5.1.3), consistent with a model where BBX20-22 and HY5 work largely interdependently to regulate these transcripts. Overall, comparing the phenotypic and transcriptional analyses with the model predictions, the B-box proteins match the requirements for factor X (Figure 2.1a), as key modulators of HY5 function.

Both BBX20 and BBX21 have previously been shown to promote the transcript levels of *HY5* (Wei et al., 2016; Xu, Jiang, et al., 2016). In our conditions, *bbx202122* showed a ~35% reduction in *HY5* transcript levels which was ~4 and ~10 fold over-compensated in two independent transgenic *bbx202122* lines overexpressing *HY5* (Supplemental Figure 5.1.4a). Further corroborating the functional interdependence of HY5 and BBX20-22, these two lines were not phenotypically different from *bbx202122* when grown in red light or darkness (Supplemental Figure 5.1.4b), rejecting the possibility that the observed *bbx202122* mutant phenotype is due to a reduction of *HY5* levels.

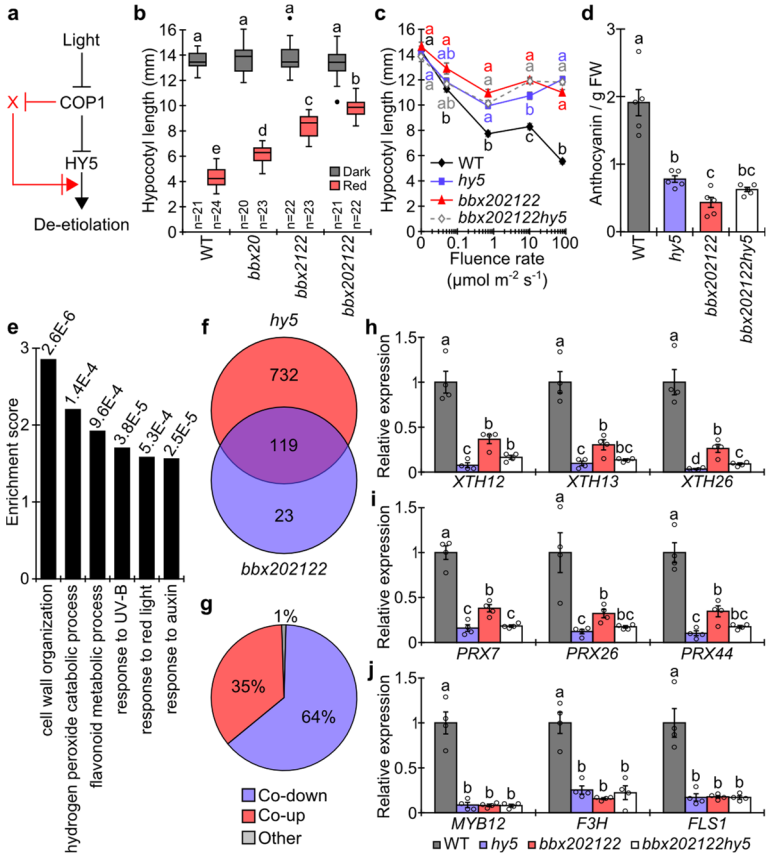

Figure 2.1: BBX20-22 and HY5 are interdependently promoting photomorphogenesis.

a) Model of the linear COP1-HY5 pathway (black) and the HY5-X module extension (red) regulating de-etiolation. Adapted from Ang *et al.* 1998. **b)** Hypocotyl measurements of 5-day-old seedlings grown in constant darkness or 80 µmol m^{-2} s^{-1} red light. Box plots represent medians and interquartile ranges with whiskers extending to the largest/smallest value and outliers are shown as dots. **c)** Hypocotyl measurements of indicated mutant seedlings grown for 5 days at different fluence rates of red light. Data represents means ± SE. n= 27, 34, 33, 31, 39 for WT, 28, 28, 34, 34, 31 for *hy5*, 26, 27, 30, 34, 32 for *bbx202122*, 27, 31, 33, 30, 29 for *bbx202122 hy5* from left to right. Statistical tests were performed within each treatment. **d)** Anthocyanin measurements of indicated seedlings grown as in (b). Data represents means ± SE. n=5 independent biological replicates. **e)** Gene Ontology analysis of *bbx202122* DEGs, from 4-day-old seedlings grown in 80 µmol m^{-2} s^{-1} of red light, as determined by DAVID 6.8. **f)** Venn diagram showing overlap between *bbx202122* and *hy5* DEGs. **g)** Pie-chart indicating percentages of co-regulation from the *bbx202122* and *hy5* overlap in (f). **h-j)** Analysis of *XTH12*, *XTH13*, *XTH26* (h) *PRX7*, *PRX26*, *PRX44* (i) *MYB12*, *F3H* and *FLS1* (j) transcript abundance relative to the *GADPH* and *TFIID* reference genes in 4-day-old seedlings grown in 80 µmol m^{-2} s^{-1} of red light. n=4 independent biological replicates. Data represents means and error bars represent SE. Different letters denote statistical significant differences ($p<0.05$) as determined by one-way (c-d, h-j) or two-way (b) ANOVA followed by Tukey's Post Hoc test. Open circles indicate single biological measurements.

To investigate the functional interdependence of HY5 and the B-box proteins at the post-transcriptional level, we performed transient expression assays using *bbx202122 hy5 hyh* mutant protoplasts. Two reporter constructs were created (*pMYB12*$^{-588}$*::GUS* and *pF3H*$^{-398}$*::GUS*) containing the promoter sequence known to be directly bound and regulated by HY5 (Figure 2a, b) (Hajdu et al., 2018; Shin et al., 2007; Stracke et al., 2010). Consistent with the requirement of a cofactor to activate transcription, HY5 had little to

no effect on the expression of the *pMYB12*$^{-588}$ and *pF3H*$^{-398}$ reporters when expressed alone (Figure 2.2c-e). However, when co-expressed together with BBX20-22, HY5 strongly activated the *pMYB12*$^{-588}$*::GUS* reporter, while co-expression of BBX21-22 (but not BBX20) resulted in strong activation of *pF3H*$^{-398}$*::GUS* (Figure 2.2c-e). Quantification of HY5-YFP in single protoplasts expressed alone or together with CFP-BBX21 revealed no difference in HY5 accumulation (Supplemental Figure 5.1.4c). Taken together, this suggests that HY5 is dependent on the B-Box proteins for transcriptional regulation. Interestingly, yeast two-hybrid (Y2H) experiments probing the interaction between HY5 and BBX21-22 has previously been performed without the addition of an activation domain to the BBX bait (Datta et al., 2007, 2008). Including BBX20, we show that all of these B-box proteins have the capability to activate transcription when bound to HY5 in a heterologous yeast system (Supplemental Figure 5.1.5a). Consistently, we identified a predicted transactivation domain (TAD) in both BBX20 and BBX21 (Supplemental Figure 5.1.5b) and found that a 33aa fragment of BBX21 containing the predicted 9aaTAD was sufficient to strongly activate transcription in yeast (Supplemental Figure 5.1.5c, d). To investigate the possible importance of this TAD, we first generated a full length BBX21$_{mTAD}$ construct in which 5 amino acids within the TAD were exchanged to alanine (Supplemental Figure 5.1.5b). While, BBX21$_{mTAD}$ retained its ability to interact with HY5 in yeast (Supplemental Figure 5.1.5e), the combined ability of HY5 and BBX21$_{mTAD}$ to activate the *pF3H*$^{-398}$*::GUS* reporter in protoplasts was severely reduced, suggesting a functional role of the predicted TAD (Figure 2.2f). Reassuringly, fusing the transactivation domain of VP16 to the C-terminal end of BBX21$_{mTAD}$ restored its ability to activate transcription together with HY5 (Figure 2.2f). Taken together, these results are supporting a mechanism where HY5 binds to promoter regions and the B-box proteins associate with DNA-bound HY5 to allow transcriptional regulation. To further test this hypothesis, we performed ChIP-qPCR experiments for BBX20 and BBX21, where the GFP-tagged BBX proteins were immunoprecipitated in a WT or in a *hy5* mutant background. Targeting the *MYB12* and *F3H* promoter regions previously shown to be immunoprecipitated by HY5 (Figure 2.2a, b) (Hajdu et al., 2018), we observed BBX specific enrichment for both promoters in the WT genetic background (Figure 2.2g, h and Supplemental Figure 5.1.6a-d). However, this enrichment was reduced in the *hy5* mutant, suggesting that HY5 is partly required for BBX-DNA association (Figure 2.2g, h and Supplemental Figure 5.1.6a-d). Interestingly, although some DNA association was still present in the *hy5* mutant, the promotion of

MYB12 and *F3H* transcript levels observed in *35S::GFP-BBX20* was completely dependent on HY5 (Figure 2.2i), similar to the short hypocotyl phenotype and high anthocyanin accumulation seen in this line (Figure 2.2j-k). To investigate if the BBX proteins are required for HY5 to associate with promoter regions, we performed ChIP-qPCR experiments using a native HY5 antibody on WT, *hy5*, *bbx202122* and *35S::GFP-BBX20* seedling samples. Interestingly, this analysis revealed decreased and increased HY5 binding to the *MYB12* promoter in *bbx202122* and *35S::GFP-BBX20*, respectively (Supplemental Figure 5.1.7a). However, while immunoblotting using the HY5 antibody did not detect any specific signal in our red light conditions, the reduced and increased *HY5* transcript levels in *bbx202122* and *35S::GFP-BBX20* are consistent with the B-box proteins affecting HY5 abundance rather than HY5-DNA association (Supplemental Figure 5.1.7b).

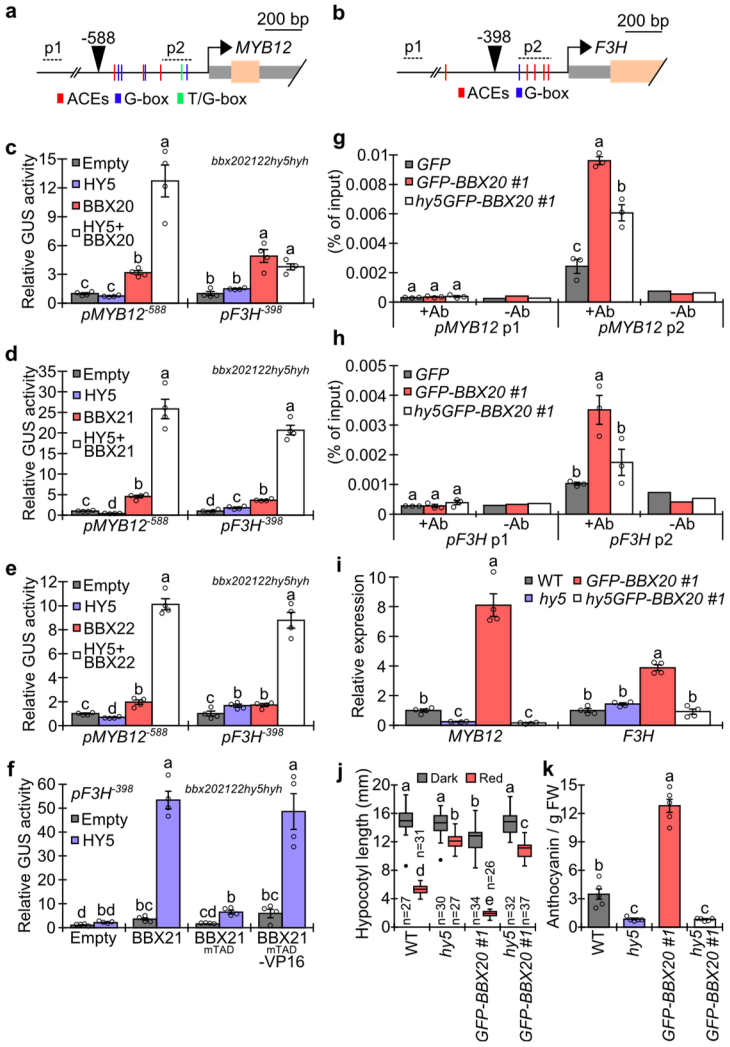

Figure 2.2: HY5 requires BBX proteins for transcriptional regulation.

a-b) Schematic of the *MYB12* and *F3H* promoter region. Gray indicates 5' UTR and introns, beige indicates exon, respectively. Dotted line indicates sequence amplified for ChIP-qPCR where the non-binding control (p1) is located 1216-1493 and 742-945 bp upstream of the *MYB12* and *F3H* transcriptional start site, respectively. Arrowhead indicates the first base of the *pMYB12*$^{-588}$*::GUS* and *pF3H*$^{-398}$*::GUS* reporter constructs relative to the transcriptional start site. **c-e)** Transient expression of BBX20, BBX21, BBX22 and HY5 in *Arabidopsis bbx202122 hy5 hyh* protoplasts using the *pMYB12*$^{-588}$*::GUS* or *pF3H*$^{-398}$*::GUS* reporter constructs. n=4 biological replicates. **f)** Transient expression of HY5, BBX21, BBX21$_{mTAD}$ and BBX21$_{mTAD}$-VP16 in *Arabidopsis bbx202122 hy5 hyh* protoplasts using the *pF3H*$^{-398}$*::GUS* reporter construct. n=4 biological replicates. **g-h)** Chromatin immunoprecipitation using no antibody (-Ab) or an anti-GFP antibody (+Ab) on samples harvested from 4-day-old *35S::GFP*, *35S::GFP-BBX20 #1* and *hy5 35S::GFP-BBX20 #1* transgenic seedlings grown in 80 µmol m^{-2} s^{-1} of red light. p1 and p2 denotes primer pairs amplifying a non-binding control region and HY5 binding region, respectively. n=3 biological replicates for +Ab samples and a single sample for -Ab**. i)** Transcript analysis of *MYB12* and *F3H* shown as relative to the reference genes *GADPH* and *TFIID* in 4-day-old seedlings grown in 80 µmol m^{-2} s^{-1} of red light. n=4 biological replicates. **j)** Hypocotyl measurements of 5-day-old seedlings grown in darkness or 80 µmol m^{-2} s^{-1} of red light. Box plots represent medians and interquartile ranges with whiskers extending to the largest/smallest value and outliers are shown as dots. **k)** Anthocyanin measurements of seedlings grown as in (j). n=5 biological replicates. Bar graphs represent means ± SE and different letters represent statistical significant differences ($p<0.05$) as determined by one-way (c-i, k) or two-way (j) ANOVA followed by Tukey's Post Hoc test. Open circles indicate single biological measurements.

In darkness, our working model (Figure 2.1a) suggests that the *cop1* mutant seedling phenotype results from the accumulation of both HY5 and factor X and predicts that *bbx202122* should be equally epistatic to *cop1* mutant alleles as *hy5*. To test this prediction, we generated the *cop1-4 bbx202122* mutant and observed a suppression of the short *cop1-4* hypocotyl phenotype similar to *cop1-4 hy5* (Figure 2.3a). Likewise, using the temperature sensitive *cop1-6* background (Ma et al., 2002), no difference in hypocotyl elongation was observed between *bbx202122* and *hy5* (Figure 2.3b, c). In line with the proposed interdependency of these factors, *cop1-4 bbx202122 hy5* did not show any significant additional elongation phenotype compared to the respective double and quadruple mutants (Figure 2.3a). Intriguingly, additional elevation of BBX20 protein levels in the *cop1-4* mutant by overexpression resulted in a *fusca*-like phenotype (Supplemental Figure 5.1.8a). This phenotype was also dependent on the presence of HY5 (Supplemental Figure 5.1.8a), suggesting that the BBX-HY5 module is functional at multiple developmental stages and might contribute to the reported *fusca* phenotype of seedling-lethal *cop1* null mutants (Miséra et al., 1994). Collectively, these results suggest that accumulation of HY5 together with the three B-box proteins under study, are largely responsible for the *cop1* phenotype. In addition, the reported lack of a *cop* phenotype in seedlings expressing the dark stable HY5ΔN77 construct (Ang et al., 1998) may result from COP1 dependent degradation of the B-box proteins (Chang et al., 2011; Fan et al., 2012; Xu, Jiang, et al., 2016). To test this hypothesis, we first identified a potential VP-motif in BBX21, showing similarity to the VP-motifs of HY5, BBX24 and BBX25, which are required for their interaction with COP1 (Supplemental Figure 5.1.8b) (Holm et al., 2001; Lau et al., 2019). We mutated the Val-Pro pair to Ala-Ala to create BBX21$_{VP\text{-}AA}$ and expressed this construct in *Arabidopsis* under the control of the 35S promoter and fused with an N-terminal GFP. Consistent with increased stability in darkness, this construct accumulated to a higher degree than GFP-BBX21 in the dark, although expressed to a lower extent (Supplemental Figure 5.1.8c, d). Next, we expressed BBX21$_{VP\text{-}AA}$ under the control of XVE in *Arabidopsis*, allowing for transcriptional induction by the addition of 17-β-estradiol (Est) (Supplemental Figure 5.1.8e). The *XVE::BBX21$_{VP\text{-}AA}$* transgenic line was then crossed to *hy5 35S::HY5ΔN77* in addition to the relevant controls, to analyse hypocotyl elongation in the F_1 generation when grown in darkness with or without the addition of Est. In line with the proposed model, no phenotypes were observed when only one side of the module was expressed (Figure 2.3d, e). However, as predicted, co-expression of BBX21$_{VP\text{-}AA}$ (induced by the addition of Est)

and HY5ΔN77 resulted in a partly de-etiolated seedling, resembling a *cop* seedling (Figure 2.3d, e).

Transcript analysis of the four crosses grown on Est showed a ~70-90 and ~7-9 fold overexpression of *HY5ΔN77* and *BBX21$_{VP\text{-}AA}$*, respectively (Supplemental Figure 5.1.8f). Furthermore, analysis of *XTH12*/*13*/*26*, *PRX7*/*26*/*44*, *MYB12*, *F3H* and *FLS1* revealed that BBX21$_{VP\text{-}AA}$ together with HY5ΔN77 strongly promotes the accumulation of these transcripts in darkness, while little effect was observed when expressed alone (Supplemental Figure 5.1.8g-i). These results that mirror the transcriptional analysis of the *bbx202122 hy5* mutant (Figure 2.1h-j), further support the required presence of B-box proteins for HY5's capacity to act as a transcriptional regulator. As recently reported (Burko et al., 2020), in agreement with the model and a mechanism where the BBX proteins provide transcriptional capability to HY5, seedlings harbouring a *35S::VP16HY5ΔN77* construct exhibited phenotypes similar to the combined expression of *BBX21$_{VP\text{-}AA}$* and *HY5ΔN77* when grown in darkness, suggesting that the requirement of BBX proteins for HY5 to promote de-etiolation can be bypassed by the addition of a TAD (Figure 2.3f and Supplemental Figure 5.1.8j).

In summary, the presented genetic and molecular data strongly suggests that BBX20-22 are acting as essential cofactors of HY5, surprisingly compatible with a working model proposed over two decades ago postulating that HY5 requires additional cofactors to function (Ang et al., 1998). In light of these results, the model explains the observation that HY5ΔN77 does not cause a COP phenotype when expressed in darkness and further illuminates the molecular network underlying the *cop1* phenotype. Although our data supports a role for these B-box proteins in HY5 dependent regulation of hypocotyl elongation and anthocyanin accumulation, the fact that *bbx202122* only affected ~15% of *hy5*-regulated genes indicate the presence of additional cofactors (Figure 2.1f). Hence, the ability of HY5 to specifically and dynamically modulate various responses throughout plant development might depend on the specific temporal and spatial regulation of its cofactors, as described for master regulators in other biological systems (Spiegelman and Heinrich, 2004).

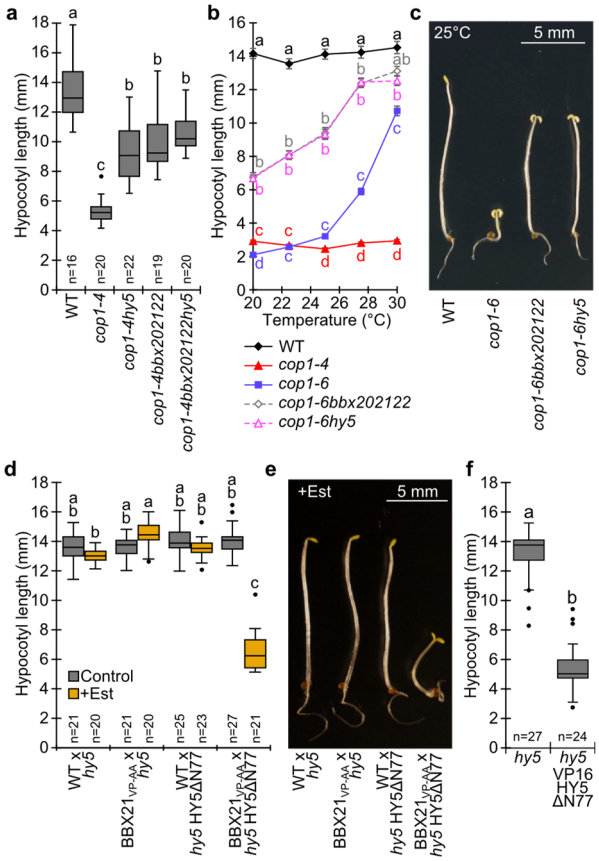

Figure 2.3: COP1 suppression of the HY5-BBX module inhibits de-etiolation in darkness.

a) Hypocotyl measurements of 5-day-old seedlings grown in darkness. One-way ANOVA, Tukey's Post Hoc test. **b)** Hypocotyl measurements of seedlings grown for 1 day at 20°C and 4 additional days at the indicated temperature in darkness. Data represents means ± SE. n= 30, 31, 31, 32, 28 for WT, 30, 34, 35, 35, 34 for *cop1-4*, 29, 33, 35, 35, 34 for *cop1-6*, 34, 36, 33, 35, 28 for *cop1-6 bbx202122*, 34, 36, 36, 36, 25 for *cop1-6 hy5* from left to right and statistical tests were performed within each temperature treatment. **c)** Representative seedlings from (b) grown at 25 °C. **d)** Hypocotyl measurements of 5-day-old F_1 crosses between WT, *hy5*, *XVE::BBX21$_{VP-AA}$* and *hy5 35S::HA-HY5ΔN77* grown with 20 µM of 17-β-estradiol (+Est) or 0.1% ethanol (v/v) (Control). **e)** Representative seedlings from (d) grown on Est. **f)** Hypocotyl measurements of 5-day-old dark grown T_1 *hy5* mutant seedlings transformed with *35S::VP16HY5ΔN77* and non-transformed *hy5* siblings. The pFAST-G02 vector used allowed for selection of primary transformed seeds in the T_1 generation. Different letters represent statistically significant differences ($p<0.05$) as determined by one-way (a, b) or two-way (d) ANOVA followed by Tukey's Post Hoc test or Mann-Whitney-U-Test (f). Box plots represent medians and interquartile ranges with whiskers extending to the largest/smallest value and outliers are shown as dots.

2.3 Material and methods

2.3.1 Plant material and growth conditions

All plant material used in this study originates from the *Arabidopsis* Col-0 accession. The *bbx21-1*, *bbx22-1*, *hy5-215*, *hyh*, *cop1-4*, *cop1-6* have been described previously (Datta et al., 2007, 2008; McNellis et al., 1994; Oyama et al., 1997; Toledo-Ortiz et al., 2014). The *bbx20-1* point mutation was created using a CRISPR/Cas9 system. A gRNA targeting the first exon (Supplemental Figure 5.1.1a) was inserted in to the pEN-Chimera vector and shuttled to the pDE-CAS9 vector (Fauser et al., 2014) using the Gateway LR reaction. This vector was transformed into Col-0 and the mutants were identified by the loss of the HindIII recognition site of a PCR product in T_2 plants that had lost the Cas9 cassette. Higher order mutants were obtained by sequential crosses genotyped by PCR or by phenotype in the case of *cop1-4* and *cop1-6*.

Unless stated otherwise, surface sterilized seeds were sown on ½ MS-media, 0.05% (w/v) MES, pH 5.7, 1% agar (w/v), stratified for 3 days at 4°C in darkness followed by a 2-hour white light pulse (90 µmol m^{-2} s^{-1}) and returned to darkness for 22 hours at 22°C before moved to the indicated experimental conditions.

2.3.1.1 Generation of plant material

To generate *35S::GFP-BBX20* lines, the full length *BBX20* CDS was amplified from cDNA using the BBX20_LB_attB1 and BBX20_RBws_attB2 primers and inserted into the pDONR221 vector through the Gateway BP reaction. *BBX20* was then shuttled to the pB7WGF2 vector (Karimi et al., 2002) to be transformed into *Arabidopsis* by floral dip to generate GFP-BBX20 expressing lines under the control of the 35S promoter.

For complementation analysis of the *bbx20-1* mutant a genomic fragment including 1 Kb promoter region of *BBX20* was amplified from genomic DNA using the primers gBBX20_F and gBBX20_R. The PCR fragment was then inserted into pDONR221 and shuttled into the pFAST-G01 vector (Shimada et al., 2010). The *bbx20-1* mutant was then transformed with this construct, and hypocotyl lengths were measured in the T_1 generation utilizing the seed specific GFP selection marker.

To generate the BBX21$_{VP\text{-}AA}$ constructs, *BBX21* CDS was first amplified by PCR using the BBX21_LB_attB1 and BBX21_RP_VP-AA primers, followed by a consecutive PCR reaction using the BBX21_LB_attB1 and BBX21_RBws_attB2 primers. This fragment was inserted into the pDONR221 vector and shuttled to the pB7WGF2 and pMDC7 (Zuo

et al., 2000) vectors. The BBX21$_{VP\text{-}AA}$ containing vectors were then transformed into *Arabidopsis* Col-0 to generate *35S::GFP-BBX21$_{VP\text{-}AA}$* and *XVE::BBX21$_{VP\text{-}AA}$*.

The HY5_DN77_LB_attB1 and HY5RBws_attB2 primer were used to amplify the *HY5ΔN77* fragment from cDNA, which was inserted into the pDONR221 vector and shuttled to the pGWB15 (Nakagawa et al., 2007) using Gateway technology and later transformed into the *hy5-215* mutant to generate the *hy5 35S:: HY5ΔN77* transgenic lines. The pGWB15-HY5 vector has been described previously (Job et al., 2018) and was transformed into the *bbx202122* mutant to generate the *bbx202122 35S::HY5* lines. To generate *hy5 35S::VP16HY5ΔN77* the VP16 sequence was amplified from the pMDC7 plasmid using the VP16attB1 and VP16DN77_rev primer, and the *HY5ΔN77* fragment was amplified from cDNA using the VP16DN77_fw and HY5RBws_attB2 primers. The two fragments were then fused by PCR using the VP16attB1 and HY5RBws_attB2 primers to generate *VP16HY5ΔN77*. This construct was then inserted into the pDONR221 vector and shuttled to the pFAST-G02 vector (Shimada et al., 2010) which was transformed into the *hy5-215* mutant using the floral dip method. All primers used for cloning are listed in Supplemental Table 5.1.1.

2.3.2 Phenotypic analysis

For hypocotyl measurements, 5-day-old seedlings were flattened on the growth medium and photographed before measurements were performed using the ImageJ software (https://imagej.nih.gov/ij/). To measure anthocyanin levels, seedlings were collected, weighed and frozen in liquid nitrogen before ground to a powder. 600 µl of extraction buffer (1% HCl (v/v) in methanol) was added to the samples followed by an overnight incubation in darkness at 4°C. After the addition of 650 µl chloroform and 200 µl dH_2O the samples were vortexed and centrifuged at 14000g for 5 min. Anthocyanin levels were estimated by spectrophotometric measurement of the upper liquid phase (A_{530} and A_{657}) and calculated by the formula (A_{530}-0.33*A_{657})/(tissue weight in gram). With the exception of T_1 seedling analysis and segregation analysis (Figure 2.3f and Supplemental Figure 5.1.1c-d), all experiments measuring hypocotyls lengths and anthocyanin levels were repeated three times with similar results.

2.3.3 Transcript analysis

For total RNA isolation, samples were stratified for 2 days at 4 °C before given a 2-hour white light pulse (~90 μmol m^{-2} s^{-1}). The samples were then kept in darkness for 22 hours before moved to the experimental conditions or kept in darkness. After 3 additional days, the seedlings were harvested and frozen in liquid nitrogen. Four biological replicates were analysed for each experiment. Total RNA was extracted using RNeasy Plant Mini Kit (Qiagen) according to the manufacturer's instructions, including an on-column DNAse treatment. cDNA was synthesised using Superscript III Reverse Transcriptase (Invitrogen) with random N9 and dT25 primers following the manufacturer's instructions. The primer pairs used for qPCR reactions are listed in Supplementary Table 5.1.1 and the qPCR was performed using the CFX96 Real-Time System (Bio-Rad). *GADPH* and *TFIID* were used as reference genes unless stated otherwise. Transcript levels relative to the control was calculated as previously described (Vandesompele et al., 2002).

For RNA-sequencing, total RNA was extracted from Col-0, *hy5* and *bbx202122* seedlings that were grown as above. Three independent biological replicates were sent to BGI (Hong Kong, China) for RNA quality and integrity control, library synthesis, high-throughput sequencing and bioinformatic analysis. In short, Agilent 2100 Bio analyzer was used to measure RNA concentration, RIN value, 28S/18S and fragment length distribution. The mRNA was enriched by using oligo (dT) magnetic beads and double-stranded cDNA was synthesized with random hexamer primers. After end repair the cDNA was 3' adenylated and adaptors were ligated to the adenylated cDNA. The ligation products were purified and enriched via PCR amplification, followed by denaturation and cyclization. The library products were sequenced via the BGISEQ-500 platform. The raw sequencing reads (> 23 million) were filtered, by removing reads with adaptors, reads with unknown bases and low quality reads to obtain clean reads (approximately 23 million) which were stored in FASTQ format (Cock et al., 2009). The clean reads were mapped to TAIR10 using Bowtie2 (Langmead and Salzberg, 2012) and gene expression level was calculated with RSEM (Li and Dewey, 2011). Differentially expressed genes were identified with the Deseq2 (Love et al., 2014) method with the following criteria: fold-change ≥ 2 and Bonferroni adjusted p-value ≤ 0.05. The RNA-seq data are deposited in NCBI's Gene Expression Omnibus (GSE137147). Gene Ontology analysis was

performed by DAVID 6.8 (Huang et al., 2009a, 2009b) using GOTERM_BP_FAT and medium classification stringency.

2.3.4 Yeast assays

β-galactosidase activity assay was performed following the protocol outlined in the Yeast Protocols Handbook (Clonetech). In short, 6 individual primary transformed colonies were grown for each vector combination in liquid –Leu –Trp medium. After protein extraction, β-galactosidase activity was measured using o-Nitrophenyl-β-D-galactopyranosid (ONPG) as substrate. The activity was calculated relative to the amount of cells (OD_{600}) and presented as relative to the empty vector control. Alternatively, yeast was dropped on –Leu –Trp medium, or –Leu –Trp –Ura –His medium with the addition of 1 mM 3-amino-1, 2,4-triazol (3-AT), and growth was recorded after 4 days at 30°C.

2.3.4.1 Construction of vectors for yeast assays

For expression of BBX20-22 in yeast without the addition of an activation domain, the CDS of *BBX20-22* were inserted into the pXP522 vector (Fang et al., 2011). In short, BBX20, BBX21 and BBX22 CDS were amplified by PCR using the primers XbaI_BBX20f and XhoI_BBX20r, XbaI_BBX21f and XhoI_BBX21r, XbaI_BBX22f and XhoI_BBX22r, respectively, followed by XbaI and XhoI digestion and ligation into SpeI and XhoI digested pXP522 vector. Construction of the bait vector pBTM116-HY5 has previously been described (Job et al., 2018). For generating the BBX21 fragments, 21A-21D, with an N-terminal LexA-DBD fusion, the primers BBX21DN133_attB1 and BBX21_RBws_attB2, BBX21-TAD_attB1 and BBX21_RBws_attB2, BBX21DN133_attB1 and BBX21-TAD_attB2, BBX21-TAD_attB1 and BBX21-TAD_attB2 were used to amplify 21A, 21B, 21C and 21D, respectively. The PCR fragments were used for a BP reaction into the pDONR221 vector, followed by LR shuttling into the pBTM116 vector.

A 9aaTAD prediction tool (Piskacek et al., 2007) (https://www.med.muni.cz/9aaTAD) was used to identify the transactivation domain in the BBX20 and BBX21 protein sequences. To generate the $BBX21_{mTAD}$ construct, *BBX21* CDS was first amplified by PCR using the BBX21_LB_attB1, mTAD_f and mTAD_r, BBX21_RBws_attB2 primer pairs, followed by a consecutive PCR reaction using the BBX21_LB_attB1 and

BBX21_RBws_attB2 primer. This fragment was inserted into the pDONR221 vector and shuttled to pGAD42 vector to generate AD-BBX21$_{mTAD}$. Construction of the pGAD42-BBX21 vector has been described previously (Job et al., 2018).

2.3.5 Immunoblotting

Etiolated seedlings grown for 4 days in darkness were flash frozen in liquid nitrogen and ground to a fine powder. Total protein extraction, SDS-PAGE separation and transfer to PVDF membrane was performed as previously described (Job et al., 2018). Anti-GFP (Takara Bio Clontech, #632380) and anti-ACT (Sigma, #A0480) was used at a 1:2000 and 1:10000 dilutions, respectively, followed by the secondary anti-mouse-HRP (Thermo Scientific, #31431) at a dilution of 1:10000. Complete scans of the membranes are online available as Source Data.

2.3.6 Protoplast assays

For generating protoplasts, seeds of the *hy5 hyh bbx202122* mutant were sown on soil and stratified in darkness for 2 days at 4 °C. The plants were then grown for 4 – 6 weeks in short day conditions (8 h light, 16 h dark) with 100 µmol m^{-2} s^{-1} white light at 21 °C. To isolate and transform the protoplasts, an adapted version of a previously described protocol was used (Yoo et al., 2007). In short, leaves were cut with a scalpel and the protoplasts were extracted by incubation in enzyme solution containing Cellulase "Onozuka" R-10 (Yakult Honsha Co., Ltd., Japan) and Macerozyme R-10 (Yakult Honsha Co., Ltd., Japan) (without vacuum) over night at 21 °C in the dark. The protoplasts were then filtered through a 60 µm nylon filter and washed twice with W5 solution before resuspended in MMG solution to a concentration of 2 x 10^5 ml^{-1} and stored on ice for 3 h - 24 h. 40000 protoplasts were then transformed with a mixture of expression vector, reporter construct and transformation control by DNA-PEG-calcium-induced transfection. For each experiment, the protoplasts were transformed with a reporter construct (*pMYB12*$^{-588}$*::GUS* or *pF3H*$^{-398}$*::GUS*), two effector constructs (HY5, BBX20, BBX21, BBX22 or pB2GW7-empty) and the 35S::NAN control construct. In total the protoplasts were transformed with 12.5 µg (for the BBX20 and BBX21$_{mTAD}$ experiments (Fig. 2c, f)) or 25 µg (for the BBX21 and BBX22 experiments) of total DNA, with a ratio of 2:1:1:1 (reporter:effector:effector:control). Each transformation was

performed in four biological replicates. After removing the PEG solution the protoplasts were incubated overnight (16 – 18 h) in W1 solution with 70 µmol m^{-2} s^{-1} red light. Samples were harvested in liquid nitrogen. GUS and NAN activity was measured as described before (Kirby and Kavanagh, 2002) with 4-methylumbelliferyl ß-D-glucuronide (MUG) and 2′-(4-methylumbelliferyl)-α-d-*N*-acetylneuraminic acid (MUN) as substrates. The results are given as GUS activity relative to the NAN activity and all experiments were independently repeated three times.

For confocal laser scanning microscopy of Protoplasts, the full length CDS of *BBX21* was shuttled from pDONR221-BBX21 into the pB7WGC2 (Karimi et al., 2002) vector via Gateway LR reaction. The full length CDS of *HY5* was amplified without the stop codon using the HY5LB_attB1 and HY5RBns_attB2 primer pair and the resulting fragment was inserted into the pDONR221 vector by the Gateway BP reaction and shuttled by LR reaction into the pB7YWG2 (Karimi et al., 2002) vector. Protoplasts were generated and transformed with 5 µg of pB7YWG2-HY5 and 5 µg of either pB7WGC2-BBX21 or pB7WGC2-empty as described above. The protoplasts were incubated overnight (16 – 18 h) in 70 µmol m^{-2} s^{-1} red light followed by analysis with confocal laser scanning microscopy (Leica TCS SP5). Imaging was done with identical excitation intensity and detection sensitivity. YFP was excited at 514 nm and fluorescence was detected at 520 – 580 nm. The fluorescence intensity of YFP was measured using the ImageJ software by defining the nucleus as ROI and measuring the “integrated density” of this region. The experiment was performed two times with similar results.

2.3.6.1 Construction of vectors for protoplast assays

To generate pDONR221-BBX21$_{mTAD}$-VP16, the primer pair BBX21_LB_attB1, BBX21_r_C-VP16 was used on pDONR221-BBX21$_{mTAD}$ template and BBX21_f_C-VP16, VP16_r_attB2 was used to amplify the VP16 domain from the pMDC7 vector. The two PCR fragments were fused by a consecutive PCR reaction using the BBX21_LB_attB1, VP16_r_attB2 primer pair and the generated BBX21$_{mTAD}$-VP16 fragment was inserted into the pDONR221 vector through the Gateway BP reaction. The full length *BBX22* CDS was amplified from cDNA using the B22LB_attB1 and B22RBws_attB2 primers and inserted into the pDONR221 vector. To express HY5, BBX20, BBX21, BBX22, BBX21$_{mTAD}$ and BBX21$_{mTAD}$-VP16 under the 35S promotor the full length CDS were shuttled from the respective pDONR221 vector (pDONR221-

HY5 (Job et al., 2018), pDONR221-BBX20, pDONR221-BBX21 (Job et al., 2018), pDONR221-BBX22, pDONR221-BBX21$_{mTAD}$, pDONR221-BBX21$_{mTAD}$-VP16) to the pB2GW7 vector (Karimi et al., 2002). To generate the *pMYB12*$^{-588}$*::GUS* reporter construct, a fragment containing 700 bp upstream of the *MYB12* ATG start codon (588 bp upstream of the TSS) was amplified from genomic DNA using the pMYB12_fwd_HindIII and pMYB12_rev_EcoRI primers. The fragment was then digested with HindIII and EcoRI and ligated into the pBT10-GUS vector (Sprenger-Haussels and Weisshaar, 2000). A 615 bp fragment upstream of the *F3H* ATG start codon (398 bp upstream of the TSS) was amplified using the pF3H_fwd_BamHI and pF3H_rev_EcoRI primers. After BamHI and EcoRI digestion, the fragment was inserted into the pBT10-GUS vector to generate the *pF3H*$^{-398}$*::GUS* reporter construct. All primers used for the cloning are listed in Supplemental Table 5.1.1. As transformation control a plasmid containing the synthetic NAN gene (Kirby and Kavanagh, 2002) under the control of the 35S promotor was used.

2.3.7 Chromatin immunoprecipitation

For experiments with BBX20 and BBX21, seedlings were sown on ½ MS-media, 0.05% (w/v) MES, pH 5.7, 1% agar (w/v) and stratified in darkness at 4 °C for 48 h before treated for 2 h with a white light pulse (100 µmol m^{-2} s^{-1}). The seedlings were then kept in darkness at 20 °C for 22 h before moving them to red light (80 µmol m^{-2} s^{-1}) for 72 h before harvesting. ChIP assays were conducted following the protocol reported previously (Martín et al., 2018) with the following modifications. For immunoprecipitation, Anti-GFP mAb-Magnetic Beads from MBL (Cat. #D153-11) or Protein A-Dynabeads (Invitrogen, Cat. #10001D) were used overnight at 4°C for +Ab and -Ab controls, respectively. Three biological replicates were performed for all the "+Ab" samples, and one for the "-Ab" control. RT-PCR was conducted according to standard protocol in three technical replicates. Primers were designed to target a known HY5 binding region "p2" (p2_MYB12_F, p2_MYB12_R and p2_F3H_F, p2_F3H_R) of the *MYB12* and *F3H* promoter regions, or a sequence further upstream "p1" (p1_MYB12_F, p1_MYB12_R and p1_F3H_F, p1_F3H_R) with no predicted HY5 binding, as negative control (Figure 2.2a, b and Supplemental Table 5.1.1). Calculations were based on the percent input method.

For experiments with HY5, ChIP was processed as described previously (Binkert et al., 2014). Shortly, 1 g of fresh material was harvested and processed for crosslinking in PBS 3 % formaldehyde under vacuum for 2 x 10 minutes. The crosslinking reaction was quenched by adding Glycine to 0.2 M. After nuclei extraction and sonication, the chromatin was immune-precipitated with antibodies against HY5 (Oravecz et al., 2006). qPCR data was obtained using PowerUp SYBR Green Master Mix reagents and QuantStudio 5 real-time PCR system (Applied Biosystem) with the p2_MYB12_F and p2_MYB12_R primer pair for the *MYB12* promoter region and ip_ACT_F and ip_ACT_R for the *ACT2* negative control region. The qPCR data were analysed according to the percentage of input method. To account for variation across the three experimental replicates, IPs were normalized to the WT-IP for the *MYB12* p2 for each replicate.

2.3.8 Data analysis

Statistical analysis was performed using Prism7.03 (GraphPad Software, La Jolla, USA). The data was tested for normality using Shapiro-Wilk normality test and equal variance using Brown-Forsythe test. Log transformed or non-transformed data was then analysed by one-way or two-way ANOVA followed by Tukey's Post Hoc test or two-tailed Mann-Whitney-U-Test as indicated. Statistically significant groups ($p<0.05$) are indicated by different letters. P values for all comparisons can be found with the Source Data. Box-plots were generated with the ggplot2 (package version 3.2.0) (Wickham, 2009) in RStudio (version 1.1.453) (http://www.rstudio.com), where outliers are defined as greater than 1.5*interquartile ranges.

2.4 Acknowledgements

We thank Prof. Karen Halliday for proof-reading the manuscript. This project was supported by Deutsche Forschungsgemeinschaft (DFG grant JO 1409/1-1 to H.J and JO 1409/2-1 to K.B) and a Royal Society Grant (RG150711 to G.T.O). Work in Geneva was supported by the Swiss National Science Foundation grant 31003A_175774 to Roman Ulm.

2.5 Author contributions

H.J conceived, designed and directed the project. G.T.O and M.P performed ChIP-qPCR experiments while M.L created *bbx20-1* and higher order mutants. K.B and C.B performed the protoplast assays while H.J and K.B performed all other experiments. H.J and K.B analysed the data. H.J, K.B and G.T.O wrote the manuscript and all authors revised the manuscript.

2.6 Data Availability

The RNA-seq data is deposited at NCBI's Gene Expression Omnibus under the accession number GSE137147 at:

https://www.ncbi.nlm.nih.gov/geo/query/acc.cgi?acc=GSE137147.

3 Karrikins control seedling photomorphogenesis and anthocyanin biosynthesis through a HY5-BBX transcriptional module

This chapter was published as follows:

Bursch, K., Niemann, E.T., Nelson, D.C. and Johansson, H. (2021) "Karrikins control seedling photomorphogenesis and anthocyanin biosynthesis through a HY5-BBX transcriptional module." *The Plant Journal* (2021), 107, 1346-1362. https://doi.org/10.1111/tpj.15383.

3.1 Summary

The butenolide molecule, karrikin (KAR), emerging in smoke of burned plant material, enhances light responses like germination, inhibition of hypocotyl elongation, and anthocyanin accumulation in Arabidopsis. The KAR signaling pathway consists of KARRIKIN INSENSITIVE 2 (KAI2) and MORE AXILLARY GROWTH 2 (MAX2), which upon activation act in an SCF E3 ubiquitin ligase complex to target the downstream signaling components SUPPRESSOR OF MAX2 1 (SMAX1) and SMAX1-LIKE 2 (SMXL2) for degradation. How degradation of SMAX1 and SMXL2 is translated into growth responses remains unknown. Although light clearly influences the activity of KAR, the molecular connection between the two pathways is still poorly understood. Here we demonstrate that the KAR signaling pathway promotes the activity of a transcriptional module consisting of ELONGATED HYPOCOTYL 5 (HY5), B-BOX DOMAIN PROTEIN 20 (BBX20), and BBX21. The *bbx20 bbx21* mutant is largely insensitive to treatment with KAR_2, like a *hy5* mutant, with regards to inhibition of hypocotyl elongation and anthocyanin accumulation. Detailed analysis of higher order mutants in combination with RNA-seq analysis revealed that anthocyanin accumulation downstream of SMAX1 and SMXL2 is fully dependent on the HY5-BBX module. However, the promotion of hypocotyl elongation by SMAX1 and SMXL2 is, in contrast to KAR_2 treatment, only partially dependent on BBX20, BBX21, and HY5. Taken together, these results suggest that light- and KAR-dependent signaling intersect at the HY5-BBX transcriptional module.

3.2 Introduction

Karrikins (KARs) are a class of butenolide molecules found in the smoke of burned plant material that can induce germination of many plant species that emerge after fire (Dixon et al., 2009; Flematti et al., 2004; Nelson et al., 2012). Intriguingly, KAR perception is widely conserved and not limited to fire-followers (Merritt et al., 2006; Nelson et al., 2012). For example, germination of dormant *Arabidopsis thaliana* seeds can be stimulated by KARs (Nelson et al., 2009). Additionally, KAR treatment enhances responses of seedlings to light. These responses include inhibition of hypocotyl elongation, enhancement of cotyledon expansion, and transcriptional upregulation of light-responsive genes not only in Arabidopsis but also in *Brassica tournefortii* (Nelson et al., 2010; Sun et al., 2020). Six KARs have been detected in smoke extracts (KAR_1 – KAR_6) (Flematti et al., 2009; Hrdlička et al., 2019) with KAR_2 being most potent in Arabidopsis, inducing responses at the nanomolar to micromolar range (Nelson et al., 2009, 2010).

Many studies have sought to understand how KARs affect plant growth by using Arabidopsis as a model system. KAR signaling is mediated by the α/β-hydrolase KARRIKIN INSENSITIVE 2 (KAI2)/HYPOSENSITIVE TO LIGHT (HTL), which acts as a receptor (Guo et al., 2013; Sun and Ni, 2011; Waters et al., 2012). Activation of KAI2 promotes its interaction with the F-box protein MORE AXILLARY GROWTH 2 (MAX2) (Toh et al., 2014; Wang et al., 2020). Both KAI2 and MAX2 are essential for KAR signaling. Arabidopsis *kai2* and *max2* mutants share many phenotypes, including increased primary seed dormancy (Nelson et al., 2011; Waters et al., 2012), an elongated hypocotyl (Nelson et al., 2011; Waters et al., 2012), reduced cotyledon size (Shen, Luong, et al., 2007; Sun and Ni, 2011), enhanced root skewing (Swarbreck et al., 2019) and impaired root hair development (Villaécija-Aguilar et al., 2019). In rice, KAI2/DWARF14-LIKE (D14L) inhibits elongation of dark-grown mesocotyls (Zheng et al., 2020) and is required for symbiosis with arbuscular mycorrhizal fungi (Choi et al., 2020; Gutjahr et al., 2015). The many developmental defects of KAR signaling mutants in the absence of KAR and the lack of evidence for KARs in living plants have led to the hypothesis that KAR mimics an endogenous signal named KAI2 ligand (KL) (Bythell-Douglas et al., 2017; Conn and Nelson, 2016; Sun et al., 2016; Waters et al., 2012). As an F-box protein, MAX2 functions within an SCF (Skp1, Cullin, F-box) E3 ubiquitin ligase complex to polyubiquitinate specific proteins, targeting them for proteolysis

(Stirnberg et al., 2007). Mutations in the downstream signaling components *SUPPRESSOR OF MAX2 1* (*SMAX1*) and *SMAX1-LIKE 2* (*SMXL2*) completely suppress *max2* phenotypes at germination and early seedling stages, suggesting that they are the main inhibitors of KAR responses (Stanga et al., 2013, 2016). Upon activation, the KAI2-SCF^{MAX2} complex targets SMAX1 and SMXL2 for degradation (Khosla et al., 2020; Wang et al., 2020).

The plant hormones auxin, jasmonate, and gibberellic acid also signal through SCF-mediated mechanisms. In auxin and jasmonate signaling, the Aux/IAA and JAZ proteins that are targeted for degradation act in complexes with transcription factors and TOPLESS (TPL)/TOPLESS-RELATED (TPR) transcriptional corepressors. Thus, hormone perception leads to a loss of transcriptional repression (Blázquez et al., 2020). SMAX1 and SMXL2 may act similarly, as they are nuclear-localized proteins that share a conserved EAR motif that recruits TPL/TPRs (Bennett and Leyser, 2014; Khosla et al., 2020; Soundappan et al., 2015; Wang et al., 2020). The direct transcriptional targets of SMAX1 and SMXL2 and the identity of any transcription factor partner proteins remain unknown, however. Nonetheless, a number of genes that are transcriptionally regulated by KARs have been identified. The transcript levels of *DWARF14-LIKE2* (*DLK2*), *KARRIKIN UPREGULATED F-BOX1* (*KUF1*), and *B-BOX DOMAIN PROTEIN 20* (*BBX20*)/*SALT TOLERANCE HOMOLOG 7* (*STH7*)/*bzr1-1D SUPPRESSOR1* (*BZS1*) are particularly strongly and consistently up-regulated by KARs and are often used as marker genes for KAR signaling (Nelson et al., 2010, 2011; Scaffidi et al., 2013; Waters et al., 2012; Waters and Smith, 2013; Yao et al., 2018). Consequently, the transcript levels of these genes are downregulated in the *kai2* and *max2* mutants (Nelson et al., 2011; Waters et al., 2012) and at least *DLK2* and *KUF1* are highly upregulated in the *smax1 smxl2* mutant (Stanga et al., 2016).

Intriguingly, the KAR signaling pathway strongly resembles that of the most recently identified plant hormone, strigolactone (SL) (Gomez-Roldan et al., 2008; Umehara et al., 2008). Also being butenolide-containing compounds, SLs are perceived by the α/β-hydrolase DWARF 14 (D14), a homologue of KAI2 (Waters et al., 2012). Upon SL perception, D14 interacts with SCF^{MAX2} and targets SMXL6, SMXL7 and SMXL8 (orthologs of DWARF53 in rice) for degradation (Jiang et al., 2013; Soundappan et al., 2015; Wang, Wang, et al., 2015; Yao et al., 2016; Zhou et al., 2013). Hence, KAR and SL signal through MAX2-dependent pathways that use homologous receptor proteins to

target different sets of homologous target proteins. Although the KAR downstream signaling component SMXL2 can be targeted by SL signaling (Wang et al., 2020), these are two largely distinct pathways (Soundappan et al., 2015; Waters et al., 2015). It is important to note that many studies investigating the SL signaling pathway have relied on the use of the synthetic SL-analogue GR24 as a racemic mixture (*rac*-GR24). The two enantiomers that compose *rac*-GR24, GR24^{5DS} and GR24$^{ent\text{-}5DS}$, primarily activate D14- and KAI2-dependent signaling, respectively (Scaffidi et al., 2014). Hence, it is likely that some effects of *rac*-GR24 that have been attributed as SL pathway responses in the literature are in fact mediated by the KAR pathway.

Interestingly, *KAI2* was first identified as *HYPOSENSITIVE TO LIGHT* (*HTL*) due to the elongated hypocotyl phenotype of the *htl* mutant (Sun and Ni, 2011). Mutants of *MAX2* display a similar phenotype, while the *smax1 smxl2* double mutant shows strong suppression of hypocotyl elongation. This suggests a close connection between KAR and light signaling (Nelson et al., 2011; Shen, Luong, et al., 2007; Stanga et al., 2013, 2016). Indeed there is significant overlap between KAR-induced genes and light-responsive transcripts (Nelson et al., 2010). In addition, a mutant of the bZIP transcription factor HY5, a key positive regulator of photomorphogenesis, shows a strongly reduced inhibition of hypocotyl elongation when treated with KAR. This suggests that HY5 activity is important for this response (Nelson et al., 2010). Furthermore, KAR-induced inhibition of hypocotyl elongation is dependent on the presence of light (Nelson et al., 2010). This light requirement can be overcome by mutation of the E3 ubiquitin ligase CONSTITUTIVELY PHOTOMORPHOGENIC 1 (COP1) (Jia et al., 2014). However, light and HY5 are not essential for KAR perception or many KAR-induced transcriptional responses (Nelson et al., 2010; Waters and Smith, 2013), suggesting that HY5 represents a downstream point of convergence between light and KAR signaling.

As a major positive regulator of photomorphogenesis in Arabidopsis, HY5 is negatively regulated by the COP1/SUPPRESSOR OF PHYA-105 (SPA) E3 ubiquitin ligase complex in darkness and accumulates in correlation with the surrounding light intensity (Osterlund et al., 2000). Its function as a DNA-binding transcriptional regulator without any apparent transactivation domain (TAD) suggests that HY5 requires partner proteins to induce transcription of its direct targets (Ang et al., 1998; Burko et al., 2020; Oyama et al., 1997). Within the Arabidopsis B-box (BBX) zinc finger family of transcription factors, BBX20 to BBX23 belong to structural group IV. These proteins form a unique

cluster within group IV that interact with HY5 and positively regulate photomorphogenesis (Chang et al., 2008; Datta et al., 2008; Fan et al., 2012; Khanna et al., 2009; Zhang et al., 2017). Similar to HY5, these BBX proteins are negatively regulated by the COP1/SPA complex in darkness and hence accumulate in response to light (Chang et al., 2011; Fan et al., 2012; Xu, Jiang, et al., 2016; Zhang et al., 2017). Recent work suggests that BBX20 to BBX23 fulfill the role of cofactors of HY5, allowing for HY5-dependent transcriptional regulation, induction of photomorphogenic growth, and anthocyanin accumulation (Bursch et al., 2020; Zhang et al., 2017). The strong transcriptional induction of *BBX20* in response to KAR (Nelson et al., 2010) suggests that BBX20 could also play a role in KAR responses. In fact, transgenic lines overexpressing a BBX20-SRDX fusion protein, which causes dominant-negative transcriptional repression, are hyposensitive to KAR_1 and *rac*-GR24 treatment (Thussagunpanit et al., 2017; Wei et al., 2016). It is difficult to attribute the specific role of *BBX20* versus its homologues in these responses, however, based on experiments that have used dominant-negative fusion proteins or overexpression.

Although the core KAR signaling mechanism, consisting of KAI2-SCF^{MAX2}-mediated degradation of SMAX1 and SMXL2, is well described, it is not known how SMXL degradation leads to downstream growth responses. In this study, we analyse the role of BBX20 in the KAR signaling pathway through both chemical and genetic approaches using knock-out mutants. We find that BBX20 and its close homologue BBX21 are essential for KAR-induced inhibition of hypocotyl elongation and anthocyanin accumulation. Our detailed genetic analysis suggests that BBX20 and BBX21 act in a HY5-dependent transcriptional module downstream of SMAX1 and SMXL2. RNA-seq analysis reveals large-scale transcriptional changes in the *smax1 smxl2* mutant, and we show that BBX20 and BBX21 are required for a subset of SMAX1/SMXL2-dependent transcriptional regulation. Overall, our data imply that the KAR signaling pathway promotes the activity of the HY5-BBX module and that this module represents a point of convergence between KAR and light signaling.

3.3 Results

3.3.1 *BBX20* expression is inhibited by SMAX1 and SMXL2

BBX20/STH7/BZS1 is frequently used as a transcriptional reporter for KAR-induced signaling as *BBX20* transcript levels are promoted by KAR_1 or KAR_2 treatment in both seeds and young seedlings (Nelson et al., 2010; Scaffidi et al., 2013; Waters et al., 2012; Waters and Smith, 2013; Yao et al., 2018). Accordingly, *BBX20* transcript levels are reduced in *kai2* and *max2* mutants, which are unable to perceive KARs or putatively KL (Nelson et al., 2011; Waters et al., 2012). Similar to these previous reports, we observed a 1.5-fold increase in *BBX20* transcript levels in Arabidopsis seedlings grown for 4 days in constant red light on medium supplemented with 1 µm KAR_2 compared to seedlings grown on medium containing 0.1 % (v/v) acetone (control) (Figure 3.1a). Correspondingly, we observed a two-fold reduction of *BBX20* transcript levels in the *kai2* and *max2* mutants as previously described (Figure 3.1b) (Nelson et al., 2011; Waters et al., 2012). By contrast, *BBX20* transcript levels were upregulated more than three-fold in the *smax1 smxl2* mutant (Figure 3.1b). This is consistent with the proposed role of *SMAX1* and *SMXL2* as inhibitors of KAR/KL responses that are targeted for degradation by KAI2-SCF^{MAX2} (Khosla et al., 2020; Stanga et al., 2016; Wang et al., 2020).

To examine tissue-specific changes of *BBX20* expression in response to KAR_2 treatment, we created two independent *pBBX20::GUS-GFP* transcriptional reporter lines in *Arabidopsis thaliana*. We analyzed GUS expression in seedlings from these lines grown in red light for 24, 48 and 96 h after the induction of germination on medium with or without 1 µM KAR_2 (Figure 3.1c-t). Under control conditions, the promoter activity of *BBX20* was most strongly observed in the roots of seedlings at all timepoints (Figure 3.1c,d,f). This was consistent with previous observations of *BZS1::GUS* activity in the roots of light- and dark-grown seedlings (Fan et al., 2012). More specifically, the promoter of *BBX20* was active in the differentiation zone of developing seedlings (Figure 3.1e,h). At 96 h, GUS expression was also evident in the shoot apical meristematic region (Figure 1g). In line with the results from the qRT-PCR analysis (Figure 3.1a), treatment with KAR_2 enhanced the activity of the transcriptional reporter (Figure 3.1i-n). Next, we introgressed the reporter transgene into the *smax1 smxl2* background. This also resulted in increased *BBX20* promoter activity in the roots and the shoot apical meristem (Figure 3.1o-t). Additionally, GUS expression was increased in the cotyledons and the hypocotyl of KAR_2-treated seedlings and *smax1 smxl2* seedlings by 24 h (Figure 3.1i,o). A second

transgenic line produced similar results, although with lower GUS expression overall (Supplemental Figure 5.2.1a-l). Although these experiments did not reveal any GUS staining of the hypocotyl and cotyledons in 4-day old seedlings, further analysis of *BBX20* transcript levels via qRT-PCR in dissected cotyledons and hypocotyls revealed that *BBX20* is also induced by KAR_2 in these tissues after 96 h (Supplemental Figure 5.2.1m). Regardless, although the activity of the *BBX20* promoter was increased in response to KAR_2 treatment or loss of *SMAX1* and *SMXL2*, it remained restricted to the same tissues. This implies that the spatial distribution of *BBX20* expression in seedlings is not limited by the KAR/KL pathway.

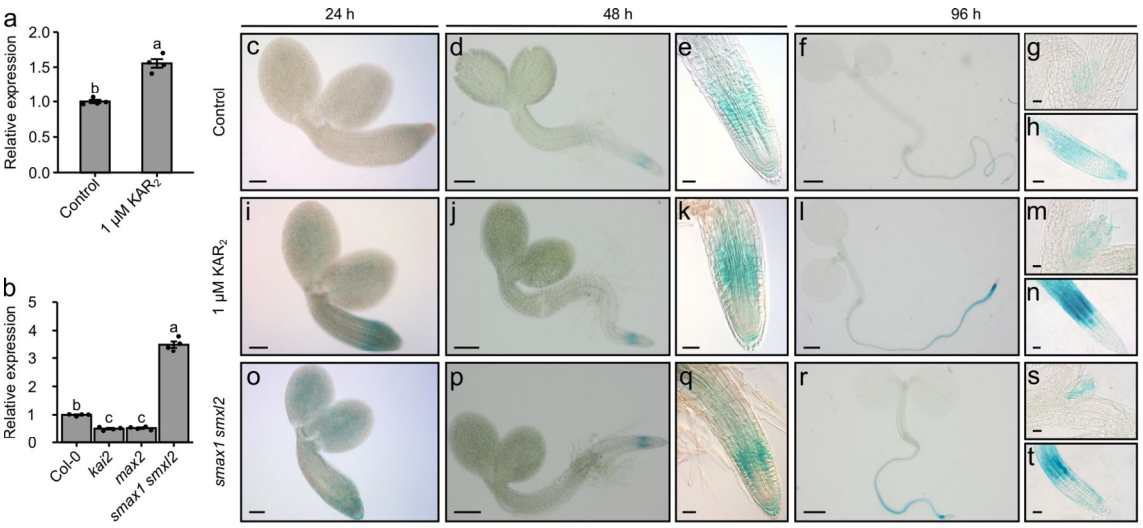

Figure 3.1: *BBX20* expression is promoted by KAR downstream of SMAX1 and SMXL2.

a-b Transcript abundance of *BBX20* relative to *GADPH* and *TFIID* reference genes in 4-day old seedlings grown in 80 µmol m^{-2} s^{-1} red light treated with 0.1 % Acetone (Control) or 1 µM Kar_2 (a) or without supplements (b). n = 4 independent biological replicates represented by black dots. Bars represent the mean and error bars represent SE. Different letters denote statistically significant differences as determined by two-sample t-test ($p<0.05$) (a) or one-way ANOVA followed by Tukey's post hoc test ($p<0.05$) (b). **c – t** GUS-staining of *pBBX20::GUS-GFP* line #1 grown for 24 h, 48 h or 96 h in 80 µmol m^{-2} s^{-1} red light. In (c – h and o - t) the seeds were grown on control medium (containing 0.1 % Acetone). In (j – o) the seeds were grown on medium containing 1 µM KAR_2. Scale bars represent 50 µm (c, e, g, h, i, j, k, m, n, o, q, s, t), 200 µm (d, j, p) and 500 µm (f, l, r).

3.3.2 BBX20 is partially required for KAR-induced inhibition of hypocotyl elongation

Although the positive regulation of *BBX20* transcript levels by KAR treatment has long been known (Nelson et al., 2010), a lack of available T-DNA insertion mutant alleles for *BBX20* has limited genetic evaluations of its potential physiological role in KAR signaling. As we had recently generated a loss-of-function allele of *BBX20* with clustered regularly interspaced short palindromic repeats (CRISPR)-CRISPR-associated protein 9

(Cas9) (Bursch et al., 2020), we set out to investigate whether KAR signaling is impaired in this mutant. In line with previous observations, increasing concentrations of KAR_2 resulted in progressively stronger inhibition of hypocotyl elongation in wildtype (WT) Col-0 seedlings grown in constant red light (Supplemental Figure 5.2.2a, Figure 3.2b) (Nelson et al., 2010). The *bbx20-1* mutant, which has an elongated hypocotyl compared to WT (Bursch et al., 2020), also showed inhibition of hypocotyl elongation in response to KAR_2 treatment (Supplemental Figure 5.2.2a). However, analysis of the effect of KAR_2 treatment relative to control conditions for each genotype revealed that the *bbx20-1* mutant is partially insensitive to the KAR_2 treatment (Figure 3.2a,b). We investigated whether the different effects of KAR_2 on WT and *bbx20-1* seedling growth are due to different germination rates in our conditions. No significant difference was observed between the two genotypes or treatments in the first three days of growth, suggesting that KAR_2 has minimal effects on germination in these conditions (Supplemental Figure 5.2.2c). In order to verify the reduced KAR_2 sensitivity of *bbx20*, we additionally created a *bbx20-2* mutant in the Landsberg *erecta* ecotype (L*er*), using CRISPR-Cas9 as described before (Bursch et al., 2020). We identified a frameshift allele with the same 1 bp deletion as in the Col-0 background (*bbx20-1*) resulting in an early stop codon (Bursch et al., 2020). Like *bbx20-1*, *bbx20-2* seedlings had elongated hypocotyls compared to WT (L*er*) and reduced sensitivity to KAR_2 (Supplemental Figure 5.2.2b; Figure 3.2c,d). These data suggest that the transcriptional induction of *BBX20* by KAR is a component of growth responses to KAR in seedlings.

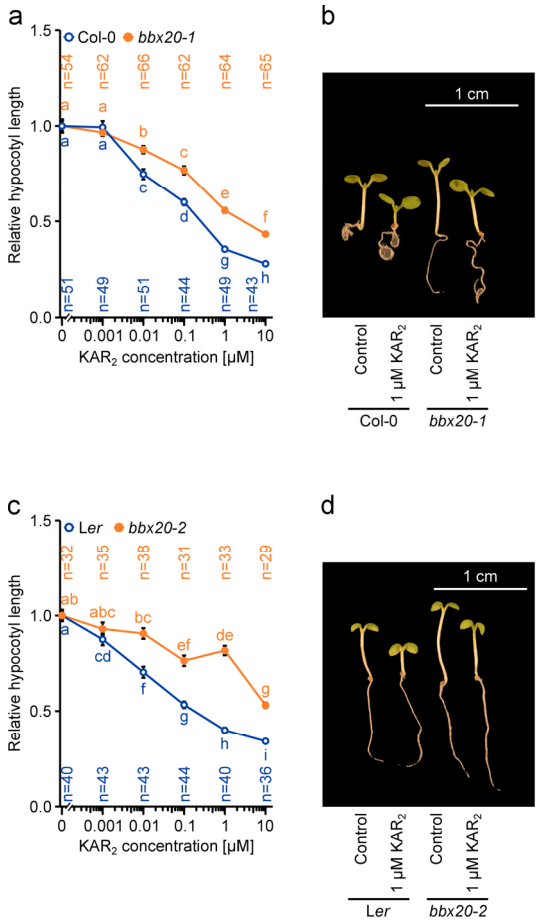

Figure 3.2: The *bbx20* mutant is hyposensitive to KAR_2 treatment.

a Hypocotyl measurements of Col-0 and *bbx20-1* mutant seedlings grown for 5 days on ½ MS medium supplemented with different concentrations of KAR_2 in 70 µmol m^{-2} s^{-1} red light. The data is shown as relative to Control (0 µM KAR_2) within each genotype. **b** Representative picture of seedlings grown as in (a). **c** Hypocotyl measurements of L*er* and *bbx20-2* mutant seedlings grown and analyzed as in (a). For (a) and (c) error bars represent SE and different letters denote statistically significant differences as determined by Pairwise Wilcoxon Rank Sum Test ($p<0.05$). **d** Representative picture of seedlings grown as in (c).

3.3.3 BBX20 and BBX21 act redundantly to inhibit hypocotyl elongation in response to KAR

BBX20 belongs to structural group IV of the Arabidopsis BBX proteins, showing the highest sequence homology to BBX21/STH2, BBX22/LZF1/STH3, and BBX23 (Khanna et al., 2009), which all positively regulate photomorphogenesis (Datta et al., 2007, 2008; Zhang et al., 2017). Previous studies have indicated that these factors can act redundantly (Bursch et al., 2020; Datta et al., 2008; Zhang et al., 2017). Therefore, we investigated whether other BBX proteins are involved in KAR-induced inhibition of hypocotyl elongation by testing the *bbx20-1 (bbx20)*, *bbx21-1 (bbx21)*, *bbx22-1 (bbx22)* and *bbx23-1 (bbx23)* single mutants. Analysis of the average KAR_2 response of three independent experiments revealed that, in addition to the *bbx20* mutant, *bbx21* showed a small

reduction of the KAR_2 response (29% and 44% inhibition of hypocotyl elongation, respectively, vs. 57% for WT) (Figure 3.3a,d). In contrast, the *bbx22* and *bbx23* mutants showed a response to KAR_2 that was similar to WT, with 50% and 53% growth inhibition, respectively. This suggests that *BBX22* and *BBX23* do not play a role in KAR responses. However, as functional redundancy might mask the role of individual BBX proteins, we tested higher order mutants. Strikingly, we observed a strongly reduced KAR_2 response in the *bbx20-1 bbx21-1* (*bbx2021*) double mutant (Figure 3.3b,e). To verify these results, we created a *bbx20-2 bbx21-2* double mutant in the L*er* background. We observed a similar reduction in KAR_2 response in this independent double mutant (Supplemental Figure 5.2.3). This suggests that *BBX20* and *BBX21* have essential, partially redundant roles in mediating inhibition of hypocotyl elongation in response to KAR_2.

Functional redundancy in the regulation of hypocotyl elongation has also been shown for *BBX22* and *BBX23* (Zhang et al., 2017). However, although we used the same mutant alleles as previously studied, in our conditions the *bbx22-1 bbx23-1* (*bbx2223*) double mutant showed a similar hypocotyl length and response to KAR_2 treatment as WT (Figure 3.3c,f). Additionally, we observed little difference in the KAR_2 response of *bbx20-1 bbx21-1 bbx22-1 bbx23-1* (*bbx20212223*) seedlings compared to *bbx2021* (Figure 3.3c,f). This comprehensive genetic analysis of single and higher order *bbx* mutants suggests that *BBX22* and *BBX23* do not contribute to KAR_2-dependent growth responses in light-grown seedlings.

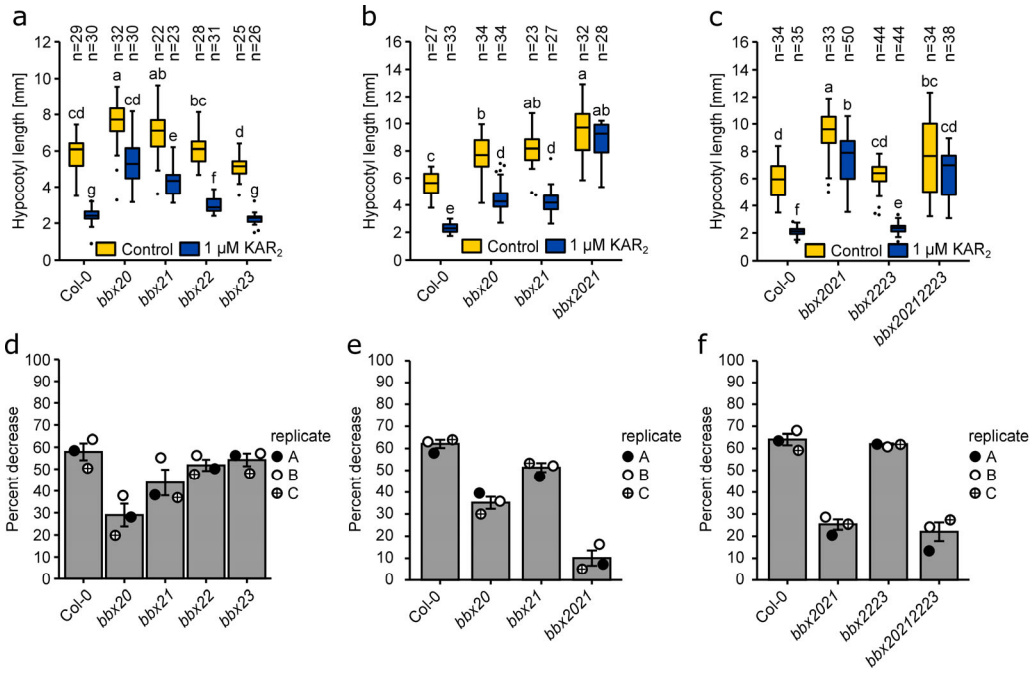

Figure 3.3: *BBX20* acts together with *BBX21* to inhibit hypocotyl elongation in response to KAR.

a - c Hypocotyl measurements of seedlings grown for 5 days on ½ MS medium containing 0.1 % Acetone (Control) or 1 µM Kar_2 in 70 µol m^{-2} s^{-1} red light. Box plots represent medians and interquartile ranges with whiskers extending to the largest/smallest value within 1.5*interquartile range and outliers are shown as dots. Different letters denote statistically significant differences as determined by Two way ANOVA followed by Tukey test (a,b) or Wilcoxon rank sum test (c) ($p<0.05$). **d-f** Average percent decrease of hypocotyl length in response to KAR treatment in three individual experiments corresponding to a - c. Bars represent the mean and error bars represent SE. Replicate A corresponds to the data shown in a-c.

3.3.4 *bbx20* and *bbx21* partially suppress the *smax1 smxl2* mutant phenotype in seedlings

BBX20 transcript levels have an inverse relationship with the hypocotyl length of the *kai2*, *max2* and *smax1 smxl2* mutants (Figure 3.1b) (Nelson et al., 2011; Stanga et al., 2016; Waters et al., 2012). Our data also suggest that *BBX20* and *BBX21* are essential for KAR-induced inhibition of hypocotyl elongation. Therefore, we hypothesized that altered BBX activity could account for at least some phenotypes of KAR pathway mutants. To test this, we first analyzed the genetic relationship between *bbx2021* and the *smax1 smxl2* double mutant. The *smax1 smxl2* double mutant has strongly reduced hypocotyl elongation compared to WT in accordance with a constitutively active KAR/KL signaling pathway (Figure 3.4a,b) (Stanga et al., 2016). Under the proposed hypothesis, the short hypocotyl phenotype of *smax1 smxl2* could be due to increased BBX20/21 activity. We observed a hypocotyl elongation phenotype for the *smax1 smxl2 bbx2021* quadruple mutant that was between the extremes of *smax1 smxl2* and *bbx2021* (Figure 3.4a,b). A conservative interpretation of this result is that SMAX1/SMXL2 and BBX20/21 affect

hypocotyl elongation through independent pathways that have additive effects. Alternatively, it may signify a partial epistatic interaction due to functional redundancy, e.g. BBX20 and BBX21 are not the only proteins that act downstream of SMAX1 and SMXL2 to control hypocotyl elongation. In fact, the relative phenotype of the *bbx2021* mutant was enhanced in the *smax1 smxl2* mutant background (~60% and ~320% longer compared to WT and *smax1 smxl2*, respectively) (Figure 3.4a,b). Also considering the transcriptional regulation of *BBX20* by KAR/KL signaling and the reduced response to KAR in *bbx2021*, we favor the interpretation that BBX20 and BBX21 are acting downstream of SMAX1 and SMXL2. In line with the stronger phenotype of *bbx20* compared to *bbx21* when treated with KAR_2 (Figure 3.3a,b), the *smax1 smxl2* phenotype was more strongly suppressed by *bbx20* than by *bbx21* (Figure 3.4a,b).

Next, we analyzed the genetic relationship between *bbx2021*, *kai2*, and *max2*, respectively. Consistent with previous studies, *kai2* and *max2* showed a long hypocotyl phenotype when grown in constant red light for five days (Shen, Luong, et al., 2007; Sun and Ni, 2011) (Supplemental Figure 5.2.4a,b). Analysis of the *kai2 bbx2021* and the *max2 bbx2021* triple mutants revealed significantly longer hypocotyls than either *kai2*, *max2*, or *bbx2021*. This additive phenotype further suggests that that if BBX20 and BBX21 regulate hypocotyl growth downstream of SMAX1 and SMXL2, they are not the only proteins to do so.

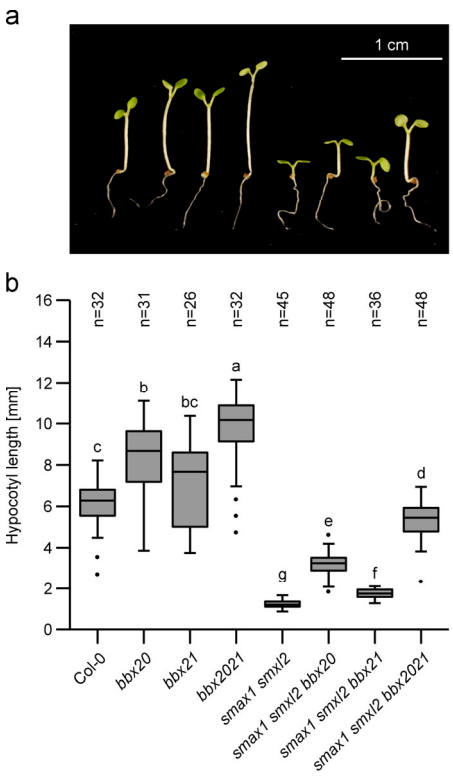

Figure 3.4: *bbx20* and *bbx21* partially suppress the *smax1 smxl2* mutant phenotype.

a Representative picture of 5-day old seedlings grown in 70 µmol m^{-2} s^{-1} red light. **b** Hypocotyl measurements of seedlings grown as in (a). Box plots represent medians and interquartile ranges with whiskers extending to the largest/smallest value within 1.5*interquartile range and outliers are shown as dots. Different letters denote statistically significant differences as determined by Welch test followed by Wilcoxon test ($p<0.05$).

3.3.5 *BBX20* and *BBX21* promote anthocyanin biosynthesis downstream of *SMAX1* and *SMXL2*

To further investigate the genetic interaction of *BBX20/21* and *SMAX1/SMXL2*, we performed an RNA-seq analysis of *bbx2021* and *smax1 smxl2* seedlings grown for four days in red light. We defined differentially expressed genes (DEGs) as those with an absolute fold change of 1.5-fold or more in the mutant compared to WT, with a Bonferroni adjusted p-value of 0.05 or less. We identified 2,635 genes that were differentially expressed in the *smax1 smxl2* mutant. In contrast, only 111 genes were misregulated in the *bbx2021* mutant compared to WT (Supplemental Data 5.2.1). A comparison of both sets of DEGs showed a statistically significant overlap of 48 genes (Fisher's exact test, $p<0.05$) (Figure 3.5a, Supplemental Table 5.2.1). Consistent with the opposing roles of these factors in the regulation of hypocotyl elongation, ~90% of these overlapping DEGs were oppositely regulated in *bbx2021* and *smax1 smxl2* (Figure 3.5b). GO-term analysis of these overlapping genes revealed an enrichment in genes known to be involved in the

flavonoid biosynthetic process and glucosinolate catabolic process, as well as genes known to be regulated in response to UV-B and karrikin (Figure 3.5c). qRT-PCR analysis of two genes classified as “responsive to karrikin” (*BIC1* and *ABCI20*) confirmed that their transcript levels were reduced in *bbx2021* and elevated in *smax1 smxl2*. Furthermore, the elevated expression of *BIC1* and *ABCI20* in the *smax1 smxl2* mutant was completely suppressed by *bbx2021* in the *smax1 smxl2 bbx2021* quadruple mutant (Figure 3.5d,e). This suggests that the KAR-induced regulation of these transcripts is fully dependent on BBX20 and BBX21.

The GO-term analysis revealed “flavonoid biosynthetic process” as the most enriched GO-term in the overlap of DEGs from *bbx2021* and *smax1 smxl2* (Figure 3.5c). qRT-PCR analysis of genes from this GO-term confirmed the low and high transcript levels of *FLS1*, *F3H*, *MYB12* and *CHS* in *bbx2021* and *smax1 smxl2*, respectively. Similar to the regulation of *BIC1* and *ABCI20*, analysis of the *smax1 smxl2 bbx2021* quadruple mutant showed that *bbx2021* is epistatic to *smax1 smxl2* in the regulation of these genes (Figure 3.5f-i). This suggests that BBX20 and BBX21 act downstream of SMAX1 and SMXL2 to promote flavonoid biosynthesis and led us to test whether the induction of anthocyanin accumulation by KAR is dependent on BBX20 and BBX21. KAR treatment has previously been shown to induce anthocyanin accumulation in WT seedlings associated with a *KAI2*-dependent transcriptional induction of the flavonoid biosynthesis gene *CHS* (Thussagunpanit et al., 2017; Waters and Smith, 2013). In line with these reports, we observed increased anthocyanin accumulation in WT seedlings after a 1 µM KAR_2 treatment that was dependent on KAI2 (Figure 3.5j). Consistent with earlier reports, *bbx2021* seedlings accumulated less anthocyanin under control conditions than WT (Figure 3.5j) (Bursch et al., 2020; Datta et al., 2007). Strikingly however, the *bbx2021* seedlings did not accumulate higher levels of anthocyanins in response to the KAR_2 treatment, suggesting that BBX20 and BBX21 are important regulators of KAR-induced anthocyanin accumulation that act downstream of SMAX1 and SMXL2 (Figure 3.5j). Supporting this idea, we observed that anthocyanin levels were increased more than 2.5-fold in *smax1 smxl2* seedlings (Figure 3.5k). This phenotype was completely suppressed by *bbx2021* in the *smax1 smxl2 bbx2021* quadruple mutant (Figure 3.5k).

We observed that mutation of *SMAX1* and *SMXL2* had led to widespread changes in transcript abundance (Figure 3.5a). GO-term analysis of the 2,635 DEGs revealed that, besides the impact on known KAR-responsive genes that had been identified in seeds,

smax1 smxl2 DEGs were enriched for genes involved in processes related to photosynthesis and translation (Supplemental Figure 5.2.5a). To identify new genes that are most likely to be regulated by the KAR signaling pathway, we compared our *smax1 smxl2* data with publicly available transcriptome datasets from *kai2* and *max2* mutants (Ha et al., 2014; Li, Nguyen, et al., 2017). Although these studies used different experimental conditions, we found an overlap of 41 genes among the three datasets (Supplemental Figure 5.2.5b, Supplemental Table 5.2.2). In line with the antagonistic roles of KAI2 or MAX2 and SMAX1/SMXL2, 38 of those genes had opposite differential expression patterns in *smax1 smxl2* compared to *kai2* and *max2* (Supplemental Figure 5.2.5c). These putative KAR target genes included the often-used marker genes *KUF1*, *DLK2*, and *BBX20*. Interestingly, we identified a set of auxin-responsive genes that are suppressed by the KAR signaling pathway (Supplemental Figure 5.2.5c). This list also contained *SMXL2*, suggesting that its transcript levels are suppressed by KAR signaling, but the elevated expression of *SMXL2* in the *smax1 smxl2* mutant is likely an effect of the T-DNA insertion in *smxl2* as previously described (Stanga et al., 2016). It is notable that although BBX20 and BBX21 regulate a subset of the putative SMAX1/SMXL2 target genes, the majority of the genes seem to be regulated independently of BBX20/BBX21. Accordingly, qRT-PCR showed that expression of *KUF1*, *DLK2*, and *AT3G60290* was unaffected in *bbx2021* seedlings and was not significantly different from *smax1 smxl2* in the *smax1 smxl2 bbx2021* quadruple mutant (Supplemental Figure 5.2.5d-f).

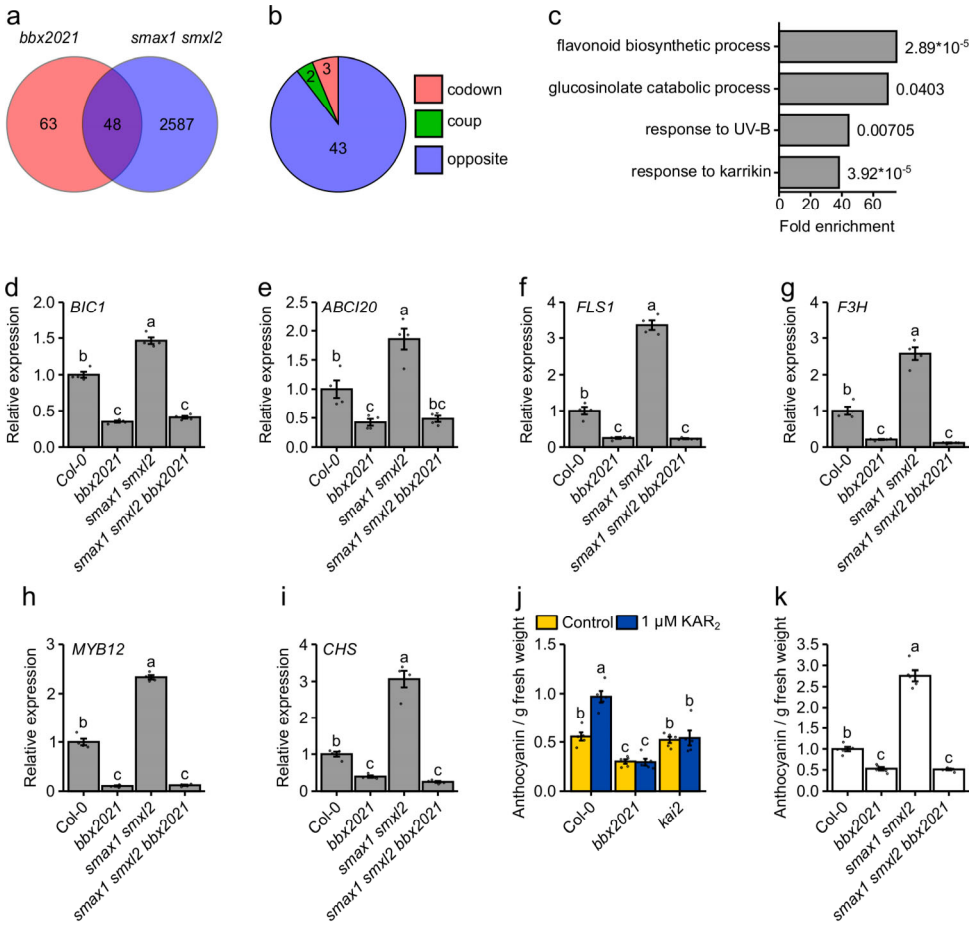

Figure 3.5: *BBX20* and *BBX21* promote anthocyanin biosynthesis downstream of *SMAX1* and *SMXL2*.

a Venn diagram showing the overlap between DEGs in *bbx2021* and *smax1 smxl2* from 4-day old seedlings grown in 80 µmol m^{-2} s^{-1} of red light. **b** Pie chart indicating coregulation of genes between the *bbx2021* and *smax1 smxl2* mutants. **c** Gene ontology analysis of the DEGs from the *bbx2021* and *smax1 smxl2* overlap in a. **d – i** Transcript abundance of *BIC1* (d), *ABCI20* (e), *FLS1* (f), *F3H* (g), *MYB12* (h) *and CHS* (i) relative to *GADPH* and *TFIID* reference genes in 4-day old seedlings grown in 80 µmol m^{-2} s^{-1} red light. n = 4 independent biological replicates indicated by black dots. Bars represent the mean and error bars represent SE. Different letters denote statistically significant differences as determined by one-way ANOVA followed by Tukey's post hoc test ($p<0.05$). **j-k** Anthocyanin measurements of 4-day old seedlings grown in 80 µmol m^{-2} s^{-1} red light on medium containing 0.1 % acetone (control) or 1 µM KAR_2 (j) or without supplements (k). n = 5 independent biological replicates represented by black dots. Bars represent the mean and error bars represent SE and different letters denote statistically significant differences as determined by Welch test followed by Wilcoxon test ($p<0.05$) (j) or by one-way ANOVA followed by Tukey's post hoc test ($p<0.05$) (k).

3.3.6 BBX20/21 and HY5 act together in KAR-induced inhibition of hypocotyl elongation

Similar to *bbx2021*, the inhibition of hypocotyl elongation by KAR is highly reduced in a *hy5* mutant (Nelson et al., 2010; Waters and Smith, 2013). Although *HY5* expression was not changed in the *smax1 smxl2* mutant under our conditions (Supplemental Data 5.2.1), the transcript levels of *HY5* have previously been shown to be elevated in response

to KAR (Nelson et al., 2010). Furthermore, *rac*-GR24 has been shown to promote HY5 protein stability in a MAX2-dependent manner (Tsuchiya et al., 2010). We recently demonstrated that BBX20 and BBX21, together with BBX22, act as essential cofactors of HY5 in promoting photomorphogenesis (Bursch et al., 2020). Therefore, we questioned if HY5, BBX20, and BBX21 act together to regulate the hypocotyl elongation response to KAR. Alternatively, as the *bbx2021* mutant did not fully suppress the *smax1 smxl2* short hypocotyl phenotype (Figure 3.4b), HY5 might represent a second pathway that regulates hypocotyl elongation downstream of SMAX1 and SMXL2 in parallel to BBX20 and BBX21. To distinguish these possibilities, we first analyzed the KAR-induced inhibition of hypocotyl elongation of *bbx2021*, *hy5,* and the *hy5 bbx2021* triple mutant (Figure 3.6a). Like the *bbx202122* triple mutant, *bbx2021* displayed a long hypocotyl phenotype similar to *hy5* when grown under control conditions (Bursch et al., 2020) and the *hy5 bbx2021* triple mutant showed no additional phenotype compared to *bbx2021* and *hy5* (Figure 3.6a). All of these mutants were largely insensitive to the KAR_2 treatment (Figure 3.6a), consistent with the hypothesis that BBX proteins and HY5 act together in regulating hypocotyl elongation. However, it does not rule out the possibility of parallel pathways, as a further reduction of the KAR response would be difficult to observe.

In order to resolve this genetic relationship, we created *smax1 smxl2 hy5* and *smax1 smxl2 hy5 bbx2021* mutants. Although *hy5* counteracted the short hypocotyl phenotype of *smax1 smxl2*, the *smax1 smxl2 hy5* triple mutant was not as long as *hy5*. However, mutation of *hy5* in WT led to an increase in hypocotyl length by 110%, whereas in *smax1 smxl2* the hypocotyl length was increased by 470% (Figure 3.6b). This suggests enhanced HY5 activity makes an important contribution to the phenotype of *smax1 smxl2*. In addition, hypocotyl elongation of *smax1 smxl2 hy5* was not further increased by the addition of *bbx2021* (Figure 3.6b). This result is consistent with a functional HY5-BBX20/BBX21 module acting downstream of SMAX1 and SMXL2 to partially suppress hypocotyl elongation. However, the *hy5* mutation had a stronger counteracting effect on *smax1 smxl2* hypocotyl elongation than *bbx2021*, implying that HY5 may rely on cofactors in addition to BBX20 and BBX21 to regulate hypocotyl elongation under these conditions. Hence, we hypothesized that there might be a role for BBX22 and BBX23 in the KAR signaling pathway as partners of HY5 that we were not able to detect with the chemical approach (Figure 3.3a,c). However, a *smax1 smxl2 bbx202122223* mutant did

not show additional suppression of the *smax1 smxl2* phenotype compared to *smax1 smxl2 bbx2021* (Figure 3.6c). This supports our earlier conclusion that BBX20 and BBX21, but not BBX22 and BBX23, are involved in KAR-induced inhibition of hypocotyl elongation.

We noted that while *hy5* strongly counteracted the *smax1 smxl2* phenotype, it was not complete suppression. This suggests that factors additional to HY5 act downstream of SMAX1 and SMXL2 to inhibit hypocotyl elongation. We reasoned that HY5-HOMOLOG (HYH), which can function redundantly with *HY5* in regulating hypocotyl elongation (Holm et al., 2002), might also regulate hypocotyl elongation downstream of SMAX1 and SMXL2. To test this hypothesis, we created and analyzed the *smax1 smxl2 hy5 hyh* mutant. Interestingly, the addition of *hyh* resulted in further suppression of the *smax1 smxl2 hy5* phenotype (Figure 3.6d), suggesting that HYH also plays a role in suppressing hypocotyl elongation after activation of the KAR signaling pathway. However, the hypocotyl length of the quadruple mutant was still shorter than that of *hy5 hyh*, so other players may yet be found. Taken together, these data indicate that HY5 and HYH, together with BBX20 and BBX21, in part, regulate hypocotyl elongation downstream of SMAX1 and SMXL2.

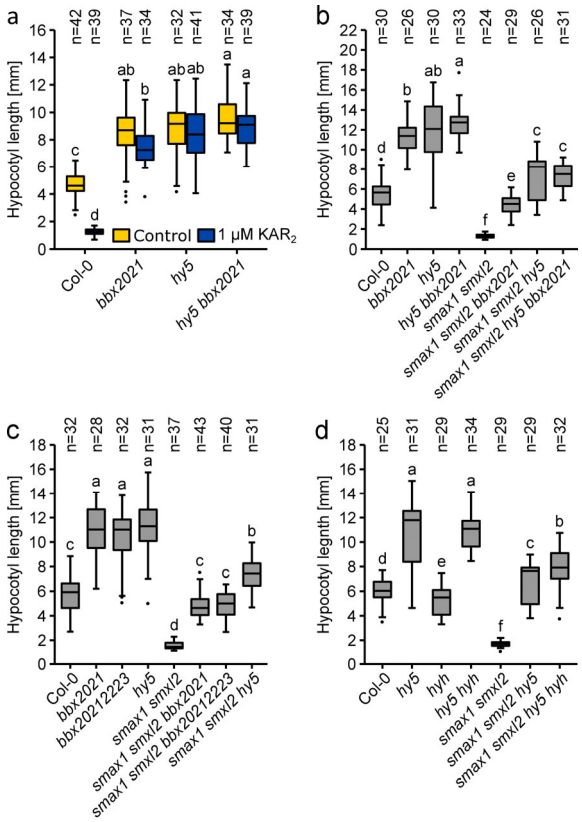

Figure 3.6: *bbx2021* dependent suppression of the *smax1 smxl2* phenotype requires *HY5*.

a –d Hypocotyl measurements of 5-day old seedlings grown in 70 µmol m^{-2} s^{-1} red light. The seedlings were grown on medium containing 0.1 % Acetone (Control) or 1 µM KAR_2 (a) or on medium without supplements (b-d). Box plots represent medians and interquartile ranges with whiskers extending to the largest/smallest value within 1.5*interquartile range and outliers are shown as dots. Different letters denote statistically significant differences as determined by one-way ANOVA followed by Tukey test (a + c) or as determined by Welch test followed by Wilcoxon test (b + d) ($p<0.05$).

3.3.7 The HY5-BBX20/21 module promotes anthocyanin accumulation downstream of SMAX1 and SMXL2

Consistent with the functional interdependence of HY5 and BBX20, BBX21, and BBX22 in the regulation of gene expression (Bursch et al., 2020), evidence for HY5 regulation of most of the 44 genes coregulated by BBX20/21 and SMAX1/SMXL2 (Figure 3.5a) can be found in publicly available transcriptomic datasets (Supplemental Table 5.2.1) (Bursch et al., 2020; Zhao et al., 2019). We observed similarly reduced expression of *BIC1*, *ABCI20*, *FLS1*, *F3H*, *MYB12* and *CHS* in the *hy5* mutant as in *bbx2021*, and no additional changes in expression were observed for these genes in *hy5 bbx2021* (Figure 3.7a-f). Furthermore, *hy5* suppressed the elevated expression of these genes in the *smax1 smxl2* mutant to a similar degree as *bbx2021*. The *smax1 smxl2 hy5 bbx2021* quintuple mutant did not show further inhibition of expression compared to *smax1 smxl2 hy5* and *smax1 smxl2 bbx2021* (Figure 3.7a-f). These results further support the notion that HY5 and

BBX20/21 are functioning together downstream of the KAR signaling pathway to regulate gene expression. Consistently, *hy5* and *hy5 bbx2021* also suppressed the high levels of anthocyanin accumulation in *smax1 smxl2* to similar levels (Figure 3.7g). This suggests that the HY5-BBX20/21 module promotes anthocyanin accumulation downstream of SMAX1/SMXL2 through transcriptional activation of anthocyanin biosynthesis genes.

In contrast, but similar to what we observed in *bbx2021* seedlings, we did not find evidence for transcriptional regulation of *KUF1*, *DLK2* or *AT3G60290* by HY5 or the HY5-BBX module (Supplemental Figure 5.2.6a-c). Therefore, the HY5-BBX20/BBX21 module is responsible for regulating a subset of the transcriptional responses downstream of SMAX1 and SMXL2.

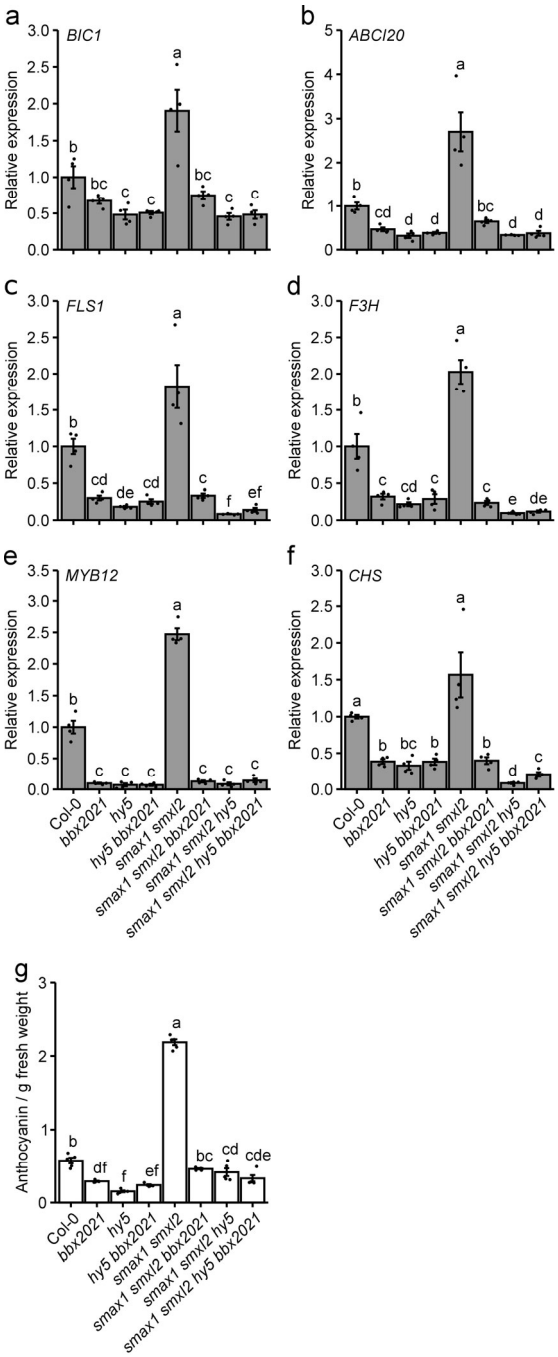

Figure 3.7:The HY5 – BBX20/BBX21 module promotes anthocyanin biosynthesis downstream of SMAX1 and SMXL2.

a - f Transcript abundance of *BIC1* (a), *ABCI20* (b), *FLS1* (c), *F3H* (d), *MYB12* (e) *and CHS* (f) relative to *GADPH* and *TFIID* reference genes in 4-day old seedlings grown in 80 µmol m^{-2} s^{-1} red light. **g** Anthocyanin measurements of seedlings grown as in (a-f). n = 4 (a-f) and n = 5 (g) independent biological replicates are indicated by black dots. Bars represent the mean and error bars represent SE and different letters denote statistically significant differences as determined by one-way ANOVA followed by Tukey's post hoc test ($p<0.05$).

3.3.8 BBX20 is post-transcriptionally stabilized by KAI2

Our data suggest that a functional HY5-BBX20/BBX21 module is required for accumulation of anthocyanins in response to KAR_2 or in the *smax1 smxl2* mutant. While the transcriptional promotion of *BBX20* by the KAR signaling pathway is consistent with the observed increase in BBX20 activity, little is known about the post-transcriptional regulation of BBX20 by KAR. To investigate possible effects on BBX20 protein levels, we treated 3-day old Col-0 and *kai2* seedlings expressing *GFP-BBX20* with 10 µM KAR_2 for 6 hours. The *GFP-BBX20* transgene was expressed under the control of a constitutive 35S promoter to bypass transcriptional regulation of *BBX20* expression by KAR. These experiments revealed a significant KAI2-dependent accumulation of GFP-BBX20 protein in response to KAR_2 treatment (Figure 3.8a,b). Furthermore, the levels of GFP-BBX20 protein in the absence of KAR treatment were markedly lower in the *kai2* mutant compared to Col-0 (Figure 3.8a-d). We confirmed that the decreased abundance of GFP-BBX20 in *kai2* is not caused by differential expression of the transgene (Supplemental Figure 5.2.7c). Therefore, KAI2 activity may stabilize BBX20. We observed that treatment with the proteasomal inhibitor MG132 resulted in stabilization of GPF-BBX20 protein in the *kai2* mutant, suggesting that BBX20 turnover is mediated by the 26S proteasome (Figure 3.8e,f).

Following these results, and as we could not detect any transcriptional regulation of BBX21 or HY5 by KAR signaling components (Supplemental Figure 5.2.7a,b), we hypothesized that KAI2 may also affect the stability of BBX21 and HY5. To test this, we crossed lines overexpressing GFP-BBX21 and HY5-GFP with the *kai2* mutant to compare the respective protein levels between the WT and mutant background. Introgression of these transgenes into the *kai2* mutant did not significantly alter their expression (Supplemental Figure 5.2.7d,e). In contrast to GFP-BBX20, *kai2* did not affect GFP-BBX21 or HY5-GFP protein levels (Supplemental Figure 5.2.8a-d).

Overall, these results indicate that KAR/KL signaling mediated by KAI2 promotes the accumulation of BBX20 transcripts and proteins. Both modes of regulation are likely to enhance BBX20 activity.

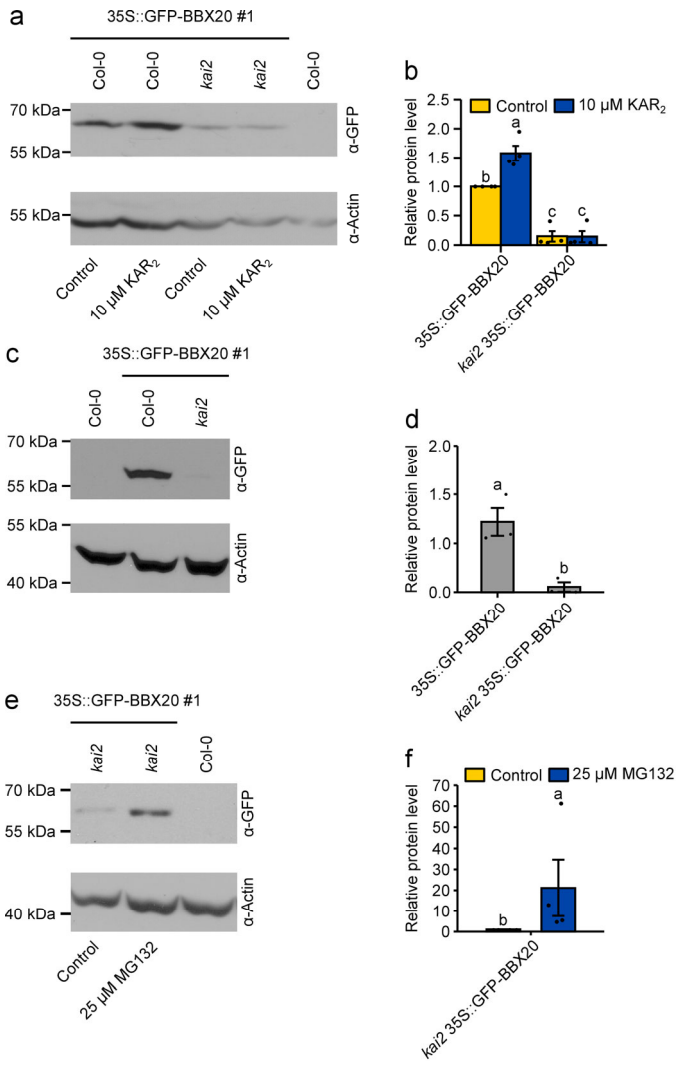

Figure 3.8: BBX20 accumulates in response to KAR_2 and is destabilized in the *kai2* mutant.

a, c, e Immunoblot analysis of total protein samples collected from Col-0 or *kai2* transgenic seedlings expressing GFP-BBX20 grown in 80 µmol m^{-2} s^{-1} red light. Seedlings were grown for 3 days and treated with 0.1% Acetone (Control) or 10 µM KAR_2 for 6h (a), grown for 5 days (c) or grown for 4 days and treated with 0.1 % DMSO (Control) or 25 µM MG132 for 24 h (e). Anti-GFP and anti-Actin antibodies were used to detect the recombinant proteins and the Actin loading control, respectively. A representative replicate of 3 independent biological replicates is shown. **b, d, f** Relative protein levels of BBX20 relative to Actin, quantified from the immunoblot analysis in a, c and e. Bars represent the mean and error bars represent SE and different letters denote statistically significant differences as determined by Wilcoxon rank sum test (b) or by two sample t-test (d, f) ($p<0.05$).

3.4 Discussion

The ability of KARs to promote a variety of light-dependent responses including germination, inhibition of hypocotyl elongation, cotyledon expansion, anthocyanin accumulation, and chlorophyll accumulation (Nelson et al., 2009, 2010; Thussagunpanit et al., 2017) makes it abundantly clear that the KAR signaling pathway is closely connected to the light signaling networks. Concordantly, a mutant of *HY5* was found to

display severely reduced inhibition of hypocotyl elongation in response to KAR treatment, suggesting a requirement of the HY5 protein for this KAR response (Nelson et al., 2010). However, while the KAR signaling pathway has been reported to elevate *HY5* transcript levels in Arabidopsis seeds (Nelson et al., 2010), regulation of *HY5* levels is unlikely to be the complete mechanism by which KAR promotes HY5 activity as HY5 appears to lack the ability to activate transcription on its own (Burko et al., 2020; Oyama et al., 1997). Several recent studies suggest that BBX20, BBX21, BBX22, and BBX23 act as transcriptional cofactors of HY5 to regulate a subset of HY5 target genes (An et al., 2019; Bai, Tao, Yin, et al., 2019; Bursch et al., 2020; Fang et al., 2019; Zhang et al., 2017). In this study, we have characterized the role of these BBX proteins in KAR signaling through detailed genetic analysis and found that BBX20, BBX21, and HY5 act together to promote KAR-induced anthocyanin accumulation and inhibition of hypocotyl elongation downstream of SMAX1 and SMXL2.

3.4.1 The HY5-BBX transcriptional module regulates seedling responses to KAR

Because *bbx20* knockout lines were unavailable, the potential role of the BBX20 protein in KAR and SL signaling has previously been analyzed using transgenic lines overexpressing *BBX20* fused with an EAR repression domain (SRDX) that recruits TPL/TPR proteins (Thussagunpanit et al., 2017; Wei et al., 2016). While these lines had reduced photomorphogenic development and a reduced response to KAR and *rac*-GR24, the relative contributions of BBX20 and its homologues to these processes may be confounded by the antimorphic nature of the fusion protein. With a CRISPR-Cas9 knockout mutant we demonstrate that BBX20 indeed plays an important role in KAR-induced inhibition of hypocotyl elongation (Figure 3.2). Furthermore, we observed that *bbx2021* was largely insensitive to KAR_2 treatment with regards to the inhibition of hypocotyl elongation and induction of anthocyanin accumulation (Figure 3.3b, 3.5j). Considering that mutants of *hy5* display a similar insensitivity to KAR treatment (Figure 3.6a) (Nelson et al., 2010; Waters and Smith, 2013) and that the BBX proteins can act as cofactors for transcriptional regulation by HY5 (Bursch et al., 2020), these results are consistent with KAR signaling acting through the HY5-BBX transcriptional module. This conclusion was also supported by analysis of higher order mutants. First, *hy5* and *bbx2021* fully suppressed the elevated anthocyanin levels of the *smax1 smxl2* mutant, and no additional phenotype was observed in the *smax1 smxl2 hy5 bbx2021* quintuple mutant

(Figure 3.7g). Second, both *hy5* and *bbx2021* were epistatic to *smax1 smxl2* in the regulation of *BIC1*, *ABCI20*, *FLS1*, *F3H*, *MYB12*, and *CHS* while no additional suppression was observed in the quintuple mutant (Figure 3.7a-f). Overall, these results support a simple pathway in which KAR treatment, or mutation of *SMAX1* and *SMXL2*, partially mimicking the effect of KL, promotes BBX20 and BBX21 activity. In turn, the HY5-BBX20/BBX21 transcriptional module promotes anthocyanin accumulation (Figure 3.9).

However, the detailed genetic analysis between the *bbx* mutants and *hy5* with the *smax1 smxl2* mutant revealed a more complex pathway when measuring the effects on hypocotyl elongation. First, while *bbx20*, *bbx21*, and *hy5* suppressed the short *smax1 smxl2* hypocotyl phenotype, suggesting increased activity of the HY5-BBX module in the *smax1 smxl2* mutant, this suppression was not complete (Figure 3.6b). Hence, these results show that SMAX1 and SMXL2 are partially promoting hypocotyl elongation independent of the BBX proteins, HY5, or the HY5-BBX module (Figure 3.9). Furthermore, as the *hy5* mutant suppressed the *smax1 smxl2* mutant phenotype more strongly than *bbx2021* or *bbx20212223* (Figure 3.6c), HY5 also appears to have functions independent of the BBX proteins in the context of KAR signaling (Figure 3.9). We have previously seen that BBX20, BBX21, and BBX22 in their role as transcriptional cofactors of HY5 only account for ~15% of HY5-regulated genes (Bursch et al., 2020). Hence the BBX-independent function of HY5 in regulating hypocotyl elongation downstream of SMAX1 and SMXL2 could indicate the presence of unknown partners to HY5 acting in the KAR signaling pathway (Figure 3.9). Furthermore, although the *bbx2021* mutant, like *hy5*, showed a strongly reduced response to KAR_2 treatment (Figure 3.3b; Supplemental Figure 5.2.3), little evidence for a genetic interaction was observed when analyzing the *bbx2021 kai2* or *bbx2021 max2* mutant (Supplemental Figure 5.2.4). Others have concluded that HY5 works largely in a parallel pathway to KAI2 and MAX2 to inhibit hypocotyl elongation (Waters and Smith, 2013). Hence, these observations highlight the fact that the core KAR signaling pathway, consisting of KAI2, MAX2, SMAX1 and SMXL2, has functions independent of the HY5-BBX module and suggest that removal of KAI2 or MAX2 might specifically promote the HY5-BBX independent pathway by which SMAX1 and SMXL2 promote hypocotyl elongation (Figure 3.9).

In contrast to *kai2*, neither SL-insensitive *d14* nor SL-deficient *max* mutants show defects in the inhibition of hypocotyl elongation (Nelson et al., 2011; Scaffidi et al., 2013).

However, application of exogenous SL or GR24 inhibits hypocotyl elongation. This response is mediated by D14-dependent destabilization of SMXL2 (Wang et al., 2020). Hence, our genetic analysis of higher order mutants using *smax1 smxl2* might also be applicable to the effects of exogenously added SLs on photomorphogenic development (Figure 3.9). This notion is supported by the fact that both HY5 and BBX20 have been implicated in GR24-dependent inhibition of hypocotyl elongation (Jia et al., 2014; Wei et al., 2016).

3.4.2 Transcriptional regulation downstream of SMAX1 and SMXL2

The comparison of transcriptomic changes between *bbx2021* and *smax1 smxl2* revealed a subset of genes that are regulated by SMAX1 and SMXL2 through the HY5-BBX transcriptional module. However, most misregulated genes in *smax1 smxl2* do not depend on HY5-BBX (Figure 3.5, Supplemental Figure 5.2.5). Interestingly, the list of DEGs in the *smax1 smxl2* mutant was enriched for genes involved in photosynthesis and translation. These results are in line with the early proteome responses observed in Arabidopsis seedlings after short term KAR treatment (Baldrianová et al., 2015). Furthermore, as our transcriptomic analysis of the *smax1 smxl2* mutant represented the first analysis of a constitutive KAR signaling mutant, we further compared our dataset with previously published transcriptome datasets for the KAR-insensitive *kai2* and *max2* mutants. Despite the very distinct experimental conditions, we were able to identify a list of high-confidence KAR target genes that are oppositely regulated in *kai2* and *max2* versus *smax1 smxl2* (Supplemental Figure 5.2.5). Reassuringly, this list contained the often-used marker genes *KUF1*, *DLK2* and *BBX20*, which have homologues in *Brassica tournefortii* that are also strongly promoted by KAR treatment (Sun et al., 2020). The suggestion that SMAX1 and SMXL2 function in a transcriptional repressor complex (Soundappan et al., 2015) led us to the hypothesis that these genes, among the other genes from this list upregulated in *smax1 smxl2*, might represent a core set of possible direct targets of SMAX1 and SMXL2.

Interestingly, the list of high-confidence KAR response genes contains a number of auxin-responsive genes that are downregulated in *smax1 smxl2* but upregulated in *kai2* and *max2* (Supplemental Figure 5.2.5C). Treatment of the *max2* mutant with the auxin transport inhibitor NPA suggested that enhanced auxin transport contributes to the

elongated hypocotyl phenotype of *max2* (Shen et al., 2012). Similarly, the *kai2* mutant phenotypes were recently shown to be suppressed by both NPA and the auxin efflux carrier triple mutant *pin3 pin4 pin7*. Consistently, KAI2 was shown to modulate the abundance of several PIN proteins, likely contributing to the *kai2* phenotype (Hamon-Josse et al., 2021). While the effect of SMAX1 and SMXL2 on auxin transport is less clear, the SL pathway targets SMXL6, SMXL7, and SMXL8 promote auxin transport, likely by promoting accumulation of PIN1 at the basal plasma membrane (Soundappan et al., 2015). Hence, the downregulation of the auxin response genes in *smax1 smxl2* may be a consequence of altered auxin transport, which might also contribute to the shortened hypocotyl phenotype of *smax1 smxl2*.

3.4.3 The HY5-BBX module as a point of convergence of light and KAR/SL signaling

As targets of COP1/SPA-dependent degradation, HY5 and the BBX proteins accumulate in response to light but not in darkness (Fan et al., 2012; Osterlund et al., 2000; Xu, Jiang, et al., 2016). Hence, the reported inability of KAR to modulate hypocotyl elongation in etiolated Arabidopsis seedlings (Nelson et al., 2010) is consistent with a lack of the HY5-BBX module components in these conditions. Similarly, photoreceptor mutants have been shown to be hyposensitive to KAR and *rac*-GR24 when grown in light (Jia et al., 2014; Nelson et al., 2010), while mutants of *COP1* show hypocotyl elongation responses to KAR and *rac*-GR24 when grown in darkness (Jia et al., 2014; Lee et al., 2019). These observations are all consistent with KAR signaling requiring an activated light signaling pathway, including COP1 inactivation and accumulation of HY5 and the BBX proteins, to generate a robust developmental response in seedlings. Interestingly, high levels of *rac*-GR24 have been shown to promote de-etiolation in dark-grown seedlings. This response was attributed to reduced nuclear levels of COP1 resulting in increased HY5 accumulation in darkness (Toh et al., 2014). However, under high levels of *rac*-GR24, inhibition of hypocotyl elongation in darkness is largely independent of MAX2 or SMAX1 and SMXL2 (Jia et al., 2014; Stanga et al., 2016; Tsuchiya et al., 2010). In contrast, HY5 was also shown to undergo COP1-independent accumulation in response to more moderate levels of 10 µM *rac*-GR24, dependent on MAX2, suggesting a separate pathway for HY5 stabilization (Tsuchiya et al., 2010). Similarly, BBX20 has been shown to accumulate in response to moderate levels of *rac*-GR24, which might be dependent on

either D14 or KAI2 activation by *rac*-GR24 (Wei et al., 2016). In line with these observations, we observed accumulation of BBX20 in response to KAR_2 and destabilization of BBX20 in the *kai2* background, suggesting that the activity of the HY5-BBX module is regulated at the transcriptional and post-transcriptional levels (Figure 3.8a-d).

In contrast to the studies showing *rac*-GR24-dependent accumulation of HY5, we did not observe any influence of *kai2* on HY5 protein levels (Figure 3.8e). However, promotion of photomorphogenesis by the HY5-BBX module is mainly dependent on the rate-limiting, TAD-containing BBX proteins, while overexpression of HY5 has little effect (Ang et al., 1998; Burko et al., 2020; Bursch et al., 2020). Consequently, while the *hy5* mutant lacks a functional HY5-BBX transcriptional module, KAI2 dependent stabilization of HY5 would not be expected to strongly contribute to the observed phenotypes. Nevertheless, in contrast to BBX20, we did not observe any regulation of BBX21 by KAR signaling at the transcriptional or post-transcriptional level (Figure 3.8d, Supplemental Figure 5.2.8). This can on the one hand suggest that regulation of BBX21 is not necessary, as HY5, BBX20, and BBX21 could work in a protein complex for which the regulation of one component is already sufficient to enhance the complex activity. On the other hand, our genetic analysis clearly shows that *bbx20* has a greater impact on the *smax1 smxl2* phenotype than *bbx21* (Figure 3.4b), compatible with the less-pronounced regulation of BBX21 by the KAR pathway.

In summary, our data suggest that light and KAR signaling intersect at the HY5-BBX module to promote accumulation of anthocyanins and partially inhibit hypocotyl elongation in response to KAR/KL. BBX20 activity is positively regulated by KAI2-dependent signaling through transcriptional upregulation and increased protein stability. BBX20 acts together with BBX21 and HY5 to control the expression of a subset of SMAX1- and SMXL2-regulated genes.

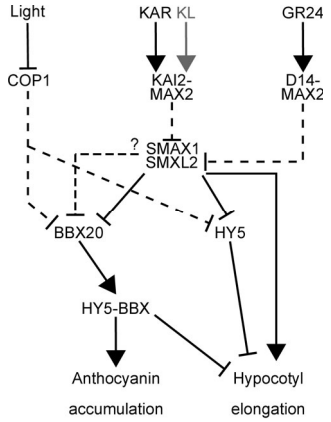

Figure 3.9: Model of SMAX1 and SMXL2 dependent regulation of photomorphogenesis.

Karrikin (KAR) or a putative KAI2 ligand (KL) promotes the interaction of KAI2 and MAX2 which act as a complex targeting SMAX1 and SMXL2 for degradation. Similarly, application of the synthetic SL-analogue GR24 promotes the formation of a D14-MAX2 complex which targets SMXL2. BBX20 and HY5 accumulate in response to light dependent inactivation of COP1, while *BBX20* is transcriptionally suppressed by SMAX1 and SMXL2. BBX20 is also post-transcriptionally stabilized by KAR, dependent on KAI2 and most likely SMAX1 and SMXL2. HY5 and the BBX proteins act as a transcriptional module promoting gene expression resulting in increased accumulation of anthocyanins. Hence, light and SMAX1/SMXL2 dependent signaling intersects on HY5 and the BBX proteins. However, HY5 partially inhibits hypocotyl elongation downstream of SMAX1 and SMXL2 independently of the BBX proteins, and SMAX1 and SMXL2 can partially promote elongation independently of HY5. Dashed lines indicate post-transcriptional regulation.

3.5 Experimental procedures

3.5.1 Plant material and growth conditions

The *bbx20-1*, *bbx21-1*, *bbx22-1*, *bbx23-1*, *hy5-215*, *hyh*, *kai2* (*htl-3*), *max2-1*, and *smax1-2 smxl2-1* mutants originate from Arabidopsis Col-0 accession and have been described previously (Bursch et al., 2020; Datta et al., 2007, 2008; Oyama et al., 1997; Sentandreu et al., 2011; Stanga et al., 2016; Stirnberg et al., 2002; Toh et al., 2014; Zoulias et al., 2020). The *bbx21-2* (GT_5_101627) mutant originates from Arabidopsis L*er* accession and was described previously (Datta et al., 2007). The *bbx20-2* was created using CRISPR-Cas9 as described previously for *bbx20-1* (Bursch et al., 2020) but in the L*er* background and was backcrossed to the wildtype background two times. Removal of the CRISPR-Cas9 cassette was confirmed by PCR. All higher order mutants were obtained by genetic crossing and subsequent PCR-based genotyping or by phenotype in the case of *max2-1*. The primers used for genotyping are listed in Table S3. 35S::GFP-BBX20 #1 and 35S::GFP-BBX21 #2 were described previously (Bursch et al., 2020). To create 35S::HY5-GFP, the coding sequence of *HY5* lacking the stop codon was shuttled from pDONR221-HY5_ns (Bursch et al., 2020) via Gateway LR reaction into pK7FWG2

(Karimi et al., 2002) and transformed into *hy5-215* via the *Agrobacterium* floral dip method. To create the pBBX20::GUS-GFP transgenic lines, a 2-kb fragment of the *BBX20* promoter was amplified with the primers pBBX20_F and pBBX20_R and shuttled into pDONR221 via Gateway BP reaction. The fragment was subsequently shuttled via Gateway LR reaction into pKGWFS7 (Karimi et al., 2002) and transformed into Arabidopsis Col-0 via the floral dip method. Primers used for cloning are listed in Supplemental Table 5.2.3. Two independent transgenic lines were then crossed with the *smax1 smxl2* mutant.

Seeds were surface-sterilized and sown on ½ MS medium (0.05% (w/v) MES, pH 5.7, 1% (w/v) agar). To analyze the effect of KAR_2 treatment the medium was supplemented with 0.1% (v/v) acetone (Control) or various concentrations of KAR_2 as indicated in the figure legends. Seeds were stratified for 2–3 days at 4 °C in darkness, followed by 4 or 5 days growth in red light (70 µmol m^{-2} s^{-1}).

3.5.2 Phenotypic analysis

For hypocotyl measurements, 5-day old seedlings were flattened on the growth medium and photographed before measurements were performed using the ImageJ software (https://imagej.nih.gov/ij/).

For anthocyanin measurements, 4-day old seedlings grown on ½ MS medium with sucrose (0.05% (w/v) MES, pH 5.7, 1% (w/v) sucrose, 1% (w/v) agar) were harvested, weighed, and flash-frozen in liquid nitrogen. After grinding the frozen material to a powder, 600 µl of anthocyanin extraction buffer (1% (v/v) HCl in methanol) was added and the samples were incubated in darkness at 4 °C overnight. 650 µl chloroform and 200 µl of H_2O were added to each sample and vortexed before being centrifuged for 10 minutes at 16,000 x g. Anthocyanin levels were estimated by spectrophotometric measurement of the absorbance (A) of the upper liquid phase (A_{530} and A_{657}) and calculated by the formula ($A_{530} – 0.33 * A_{657}$)/(tissue weight in gram).

All phenotypic analyses were performed three times with similar results.

3.5.3 Germination assay

To determine germination rates ~100 seeds per biological replicate were sown on ½ MS medium containing 0.1 % Acetone or 1 µM KAR_2. The seeds were stratified for 3 days

at 4 °C and germination was counted 24 h, 48 h and 72 h after incubation in constant red light (~80 µmol m^{-2} s^{-1}).

3.5.4 Analysis of transcript levels

For total RNA isolation, samples were stratified for 2-3 days at 4 °C before incubation in red light (~80 µmol m^{-2} s^{-1}) for 4 days. The seedlings were then harvested and frozen in liquid nitrogen. Four biological replicates were analyzed for each genotype. To analyze tissue-specific transcriptional changes in response to KAR treatment the seedlings were harvested in RNA*later* solution (Thermo Scientific) prior to the dissection of cotyledons and hypocotyls followed by RNA extraction.

Total RNA was extracted using RNeasy Plant Mini Kit (Qiagen) according to the manufacturer's instructions, including on-column DNAse treatment. A two-step qRT-PCR analysis was performed. First, cDNA was synthesized using Superscript III Reverse Transcriptase (Invitrogen) with random N9 and dT_{25} primers following the manufacturer's instructions. The primer pairs used for qPCR reactions on cDNA templates are listed in Supplemental Table 5.2.3. The qPCR was performed using the CFX96 Real-Time System (Bio-Rad). *GADPH* and *TFIID* or *UBC21* and *PP2A* were used as reference genes as indicated in the figure legend and transcript levels relative to the controls were calculated as previously described (Vandesompele et al., 2002).

For RNA-sequencing, total RNA was extracted from Col-0, *bbx2021* and *smax1 smxl2* seedlings that were grown as described above. RNA was extracted according to (Sokolovsky et al., 1990). In short, samples were flash-frozen in liquid nitrogen and ground to a powder. The powder was dissolved in 750 µl extraction buffer (0.6 M NaCl, 10 mM EDTA, 4 % (w/v) SDS, 0.1 M Tris-HCl pH 7.5) and 750 µl of phenol/chloroform/isoamyl alcohol solution (25:24:1). After shaking the samples for 10 minutes they were centrifuged at 16,000 x g for 5 minutes. The supernatant was mixed 1:1 with chloroform/isoamyl alcohol (24:1) solution. After centrifugation for 3 min at maximum speed, the supernatant was mixed with 340 µl of 8 M LiCl. After incubation on ice for 30 minutes followed by centrifugation of 15 min at 4 °C the pellet was dissolved in RNase-free water, mixed with 30 µl of 3 M sodium acetate, pH 5.2 and 700 µl of absolute ethanol. After incubation at -80 °C for 30 minutes and centrifugation, the pellet was washed with 70% ethanol (v/v) and the RNA was dissolved in RNase-free water. RNA was cleaned up and on-column DNAse treatment was performed with the RNeasy

Plant Mini Kit (Quiagen), according to the manufacturer's protocol. Three independent biological replicates were sent to BGI (Hong Kong, China) for RNA quality and integrity control, library synthesis, high-throughput sequencing and bioinformatic analysis. In short, Agilent 2100 Bioanalyzer was used to measure RNA concentration, RIN value, 28S/18S, and fragment length distribution. NanoDrop™ was used to identify the purity of RNA samples. The mRNA was enriched by using oligo (dT) magnetic beads and double-stranded cDNA was synthesized with random hexamer primers. After end-repair the cDNA was 3' adenylated and adaptors were ligated to the adenylated cDNA. The ligation products were purified and enriched via PCR amplification, followed by denaturation and cyclization. The library products were sequenced via the BGISEQ-500 platform. The raw sequencing reads (> 26 million per sample) were filtered by removing reads with adaptors, reads with unknown bases, and low quality reads. Clean reads (approximately 26 million per sample) were stored in FASTQ format (Cock et al., 2009). The clean reads were mapped to TAIR10 using Bowtie2 (Langmead and Salzberg, 2012) and gene expression level was calculated with RSEM (Li and Dewey, 2011). Differentially expressed genes were identified with the Deseq2 (Love et al., 2014) method with the following criteria: fold-change ≥ 1.5 and Bonferroni adjusted p-value ≤ 0.05.

3.5.5 GO-term analysis

GO-term analysis was performed with the "PANTHER Overrepresentation Test" using GO Ontology database (doi: 10.5281/zenodo.4081749, released 2020-10-09) as described before (Mi et al., 2019) utilizing the "GO biological process complete" annotation data set.

3.5.6 GUS staining

For the GUS staining, seeds were sown on ½ MS containing 0.1 % acetone (v/v) (control) or 1 µM KAR_2, stratified for 2 days, and then incubated in red light (~80 µmol m^{-2} s^{-1}) for 24, 48 or 96 h. The GUS staining (Hemerly et al., 1993) and subsequent clearing (Malamy and Benfey, 1997) was performed as described previously. After the harvest, seedlings were incubated in 90 % acetone at -20 °C for 1 hour. The samples were washed twice with a 50 mM sodium phosphate buffer (pH 7.0) and then incubated in the staining solution [10 mM potassium ferricyanide, 10 mM potassium ferrocyanide, 1 mM 5-bromo-4-chloro-3-indolyl β-D-glucuronic acid, 0.2% (v/v) Triton X-100 in 50 mM sodium phosphate buffer (pH 7.0) at 37 °C overnight. To clear the tissue, seedlings were incubated in a solution of 0.24 N HCl in 20% ethanol at 57 °C for 15 minutes. The solution

was replaced with a solution of 7% NaOH (w/v) in 60% Ethanol and the samples were incubated for 15 minutes at room temperature. After stepwise rehydration in 40%, 20% and 10% ethanol the samples were incubated in a solution of 25 % glycerine in 5% ethanol for 15 min at room temperature. Pictures were taken with a stereomicroscope (SZX12; Olympus, Shinjuku, Japan) or a microscope (Axioskop 2 plus; Zeiss, Jena, Germany) equipped with an Olympus C-4040ZOOM camera.

3.5.7 Immunoblotting

For analyzing protein levels in response to KAR_2, seedlings were grown in red light (80 µmol m^{-2} s^{-1}) for 3 days before treatment with liquid ½ MS supplemented with 0.1 % Acetone (Control) or 10 µM KAR_2 for 6 h before harvest. For MG132 experiments, 4-day old seedlings were incubated with liquid ½ MS supplemented 0.1 % DMSO (Control) or 25 µM MG132 for 24 h and harvested on day 5. Seedlings without treatment were grown for 5 days. After harvest, seedlings were flash-frozen in liquid nitrogen and ground to a fine powder using a tissue lyser. Extraction buffer [50 mM Tris-HCl pH 7.5, 150 mM NaCl, 1 % (w/v) sodium deoxycholate, 0.5 % Triton X-100, 1 mM DTT, 50 µM MG132, 50 µM MG115, 1 x COMPLETE protease inhibitor cocktail (EDTA-free, Roche)] was added and the samples were centrifuged for 10 min with 16,000 x g at 4°C. The total protein sample, collected from the supernatant, was then separated on a 10% SDS-PAGE and transferred to a PVDF membrane. After blocking with 6% (w/v) skim milk powder in PBS-T, anti-GFP (Takara Bio Clontech, #632380) and anti-ACT (Sigma, #A0480) were used at a 1:2,000 and 1:10,000 dilutions, respectively, followed by the secondary anti-mouse-HRP (Thermo Scientific, #31431) at a dilution of 1:10,000 in blocking solution. For protein detection, the membrane was incubated with SuperSignal West Pico Chemiluminescent Substrate (Thermo Scientific) according to the manufacturer's protocol using CL-Xposure Films (Thermo Scientific). Quantification of the immunoblots was done using ImageJ software (https://imagej.nih.gov/ij/).

3.5.8 Statistical Analysis

Statistical analysis was performed with Rstudio (version 1.2.1335) (http://www.rstudio.com). The data was tested for equal variances using Brown-Forsythe test (car package version 3.0-6) and for normal distribution by Shapiro-Wilk test. Log transformed or non-transformed data was then analysed by one-way or two-way ANOVA followed by Tukey's Post Hoc test or Wilcoxon Rank Sum test (stats package version 4.0.2). Statistically significant differences ($p<0.05$) are indicated by different letters.

Boxplots were generated with ggplot2 (version 3.2.1), where outliers are defined as greater than 1.5*interquartile ranges.

3.6 Data availability statement

The RNA-seq data were deposited in the NCBI Gene Expression Omnibus (GSE166857).

3.7 Acknowledgements

We thank Cordula Braatz for technical assistance. This project was funded by the Deutsche Forschungsgemeinschaft (DFG, German Research Foundation) – Project numbers 409212330; 320656366 to H.J. and by National Science Foundation IOS-1856741 to D.C.N.

3.8 Author contributions

H.J., and K.B. designed the research with input from D.C.N.; K.B. performed all experiments; K.B. and H.J. analyzed the data; E.T.N. generated *bbx20-2* and higher order mutants and performed preliminary experiments; H.J., K.B. and D.C.N. wrote the manuscript.

4 Discussion

Four decades ago a mutant of the major positive regulator of photomorphogenesis, *HY5*, was found in a genetic screen for mutants with an elongated hypocotyl in white light as well as in monochromatic B, R and FR light (Koornneef et al., 1980). Analysis of the protein sequence revealed that HY5 is a bZIP transcription factor that lacks any recognizable TAD (Ang et al., 1998). In accordance with this observation HY5, could not activate transcription on its own when expressed in a yeast system (Ang et al., 1998). The *hy5* mutant was also shown to largely suppress the phenotype of weak *cop1* mutant alleles in darkness, which led to the conclusion that HY5 acts downstream of COP1 to induce photomorphogenesis (Ang Lay Hong and Deng Xing Wang, 1994). As a target of the COP1/SPA complex, HY5 is degraded in darkness. Accordingly, its protein levels correlate with the surrounding light levels and the degree of photomorphogenic growth (Osterlund et al., 2000). However, it was reported that a dark stable version of HY5 (HY5ΔN77) did not induce photomorphogenesis when expressed in dark grown Arabidopsis seedlings (Ang et al., 1998). Together with the lack of a TAD these results prompted the hypothesis that HY5 requires cofactors to fulfil its role as a transcriptional activator to regulate photomorphogenesis (Ang et al., 1998; Burko et al., 2020).

In the work presented in this thesis, I have shown that the BBX proteins BBX20, BBX21 and BBX22 act as cofactors for HY5 in the regulation of photomorphogenesis (chapter 2). Furthermore, I could show that a part of this HY5-BBX module is required for KAR-induced regulation of seedling development (chapter 3).

4.1 Conservation of the HY5-BBX module

Within the last years, it has become evident that the HY5-BBX transcriptional module, identified in Arabidopsis, also is conserved in various crop plants.

A recent study suggests that in poplar (*Populus trichocarpa*), the HY5-BBX module is conserved and induces anthocyanin and proanthocyanidin biosynthesis by the transcriptional regulation of biosynthesis genes, a possible protection mechanism against high light stress (Li et al., 2021). In pear (*Pyrus pyrifolia*) it was observed that the light signaling pathway consisting of a photoreceptor (cryptochrome), that inhibits the E3 ubiquitin ligase COP1, leading to the accumulation of the transcription factor HY5 to induce anthocyanin accumulation is conserved (Tao et al., 2018). However, similar to its

homologue from Arabidopsis, the pear HY5 protein (PpHY5) lacks a TAD and could not induce transcription of target genes on its own (Ang et al., 1998; Tao et al., 2018). Strikingly, Bai and colleagues could show that only when PpHY5 was transiently expressed in tobacco leaves together with PpBBX16 or PpBBX18, homologues of Arabidopsis BBX22 and BBX21 respectively, the complex showed transcriptional activation activity, similar to the results from my protoplast assays (Figure 2.2) (Bai, Tao, Tang, et al., 2019; Bai, Tao, Yin, et al., 2019). The overexpression of the BBX proteins alone or the whole HY5-BBX module in pear fruits induced anthocyanin accumulation (Bai, Tao, Tang, et al., 2019; Bai, Tao, Yin, et al., 2019). This promoted the red coloration of the fruit peel which could make pears more appealing to consumers (Zhang, Qian, et al., 2013). The red skin coloration is also an important trait in apple (*Malus x domestica*) fruits, which appears to also be under the control of a homologous HY5-BBX transcriptional module as the one identified in Arabidopsis (chapter 2) (Fang et al., 2019). In addition to their effect on the appearance of fruits, anthocyanins are also beneficial for human health (Khoo et al., 2017; de Pascual-Teresa et al., 2010). Hence, the induction of anthocyanin biosynthesis, specifically in fruits, is a promising approach to create more nutritional food. In tomato (*Solanum lycopersicum*), which mainly accumulates anthocyanins in its vegetative tissues but not in the widely consumed fruits, successful attempts have been made to increase anthocyanin levels in the fruits (Gonzali et al., 2009; Gonzali and Perata, 2020; Mes et al., 2008). Recent evidence suggests that homologues of the Arabidopsis HY5 and BBX20 can also be found in tomato and both play a role in the regulation of carotenoid and anthocyanin biosynthesis, opening a new leverage point to increase the nutritional value of tomatoes (Luo et al., 2021; Wang, Wang, et al., 2021; Xiong et al., 2019). Based on our results showing that HY5 and BBX proteins work interdependently to induce anthocyanin biosynthesis together with their wide conservation in dicotyledonous crop plants, it would be interesting to see if increased expression levels of both HY5 and BBX proteins in fruits could increase their nutritional value.

Although the knowledge about the light signaling pathways is more limited in monocotyledonous plants, homologues of COP1 and HY5 were identified in maize (*Zea mays*) which can functionally replace their homologues in Arabidopsis (Huai et al., 2020). Also the BBX protein family is conserved in maize which contains a homologue of BBX20, suggesting that the HY5-BBX module is conserved in maize (Li, Wang, et al.,

2017). In rice (*Oryza sativa*) six HY5 homologues have been found (Bai, Lu, et al., 2019; Burman et al., 2018). One of these has been shown to complement the Arabidopsis *hy5* mutant phenotypes (Burman et al., 2018). Furthermore, OsBBX14, a homologue of Arabidopsis BBX22, promotes photomorphogenesis in rice (Bai, Lu, et al., 2019). Overall, these multiple reports suggest that the HY5-BBX transcriptional module is likely conserved also in monocotyledonous crop plants. Hence, similar to the recent work in dicotyledonous plants it is possible that the nutritional value of monocotyledons could be increased through the modulation of the activity of the HY5-BBX transcriptional module.

4.2 BBX23, a fourth co-factor for transcriptional activation by HY5?

When the work for this thesis was initiated, only limited information regarding BBX23 was available. It belongs to structural group IV of Arabidopsis BBX proteins and is the closest homologue of BBX22 (Khanna et al., 2009). Some evidence suggested that BBX23 may act as a repressor of hook unfolding that is specifically transcriptionally induced by PIF3 in darkness (Sarmiento, 2013; Sentandreu et al., 2011). As this *bbx23* mutant phenotype suggested a negative role of BBX23 in the regulation of photomorphogenesis, BBX23 was initially disregarded as a potential co-factor of HY5 during this work. Instead we focused on BBX20, BBX21, and BBX22, that had been described to play a positive role in the regulation of photomorphogenesis (Chang et al., 2008; Datta et al., 2007, 2008; Fan et al., 2012). However, BBX23 was later shown to clearly act as a positive regulator of photomorphogenesis. But as an elongated hypocotyl was only detected in a double mutant of *bbx22* and *bbx23*, the importance of BBX23 is likely relatively minor (Zhang et al., 2017). Nevertheless, BBX23 was shown to be degraded in a COP1-dependent fashion in darkness, similar to BBX20 – BBX22, fulfilling one of the requirements we had established for a potential transcriptional cofactor of HY5 (chapter 2) (Zhang et al., 2017).

Consequently, as BBX23 now is known to positively regulate photomorphogenesis, physically interact with HY5, be recruited to target promoters by HY5 and induce transcription when expressed in Arabidopsis protoplasts together with HY5 (Zhang et al., 2017), it is reasonable to consider BBX23 as a fourth cofactor for HY5-induced photomorphogenesis. However, under the conditions used in this thesis, BBX23 seems to have only limited function, as we did not observe a mutant phenotype (Figure 3.3). A more prominent role for BBX23 was recently observed in the induction of

thermomorphogenesis, where BBX23 heterodimerizes with BBX18 to promote hypocotyl elongation in response to an elevation of the ambient temperature (Ding et al., 2018).

4.3 Individual roles for individual BBX proteins?

Although proteins share redundant functions, it is commonly observed that they also fulfil individual roles. In the light signaling networks the PIF quartet shares redundant function to promote skotomorphogenesis, while the four SPAs act together to inhibit photomorphogenesis (Laubinger et al., 2004; Leivar, Monte, Oka, et al., 2008). Nevertheless, only PIF1 plays a role in the regulation of germination, whereas PIF4, PIF5, and PIF7 regulate thermomorphogenesis (Balcerowicz, 2020; Oh et al., 2004). Evidence suggests, that SPA3 and SPA4 play a major role in the regulation of adult plant growth, while all of the four SPAs are important for seedling development (Laubinger et al., 2004). For the BBX proteins investigated in this thesis evidence can be found that, despite their shared redundant functions in the regulation of light-induced inhibition of hypocotyl elongation and accumulation of anthocyanin, also individual functions exist. For example, in the analysis of BBX proteins in the KAR signaling pathway we observed that both BBX20 and BBX21 have a function as cofactors of HY5, with BBX20 appearing to be more important than BBX21 (Figure 3.2, 3.4). In contrast neither BBX22 nor BBX23 seem to play a role in KAR signaling (Figure 3.3). Furthermore, of these two BBX proteins, only BBX21 has been reported to regulate root development (Datta et al., 2007). Possibly, more distinct roles for each BBX protein in the regulation of plant development can be found by careful comparative analysis of *bbx* single mutants. The data presented in this thesis, and that of others, support this view where BBX20, BBX21 and BBX22 share redundant function in the regulation of photomorphogenesis but also have individual functions in regulating plant development. This raises the question of how the individual functions of these quite similar BBX proteins can be accomplished.

One explanation could be variations in their expression patterns. While BBX20 and BBX21 both are required for KAR-induced inhibition of hypocotyl elongation only *BBX20* was transcriptionally regulated by the KAR signaling pathway (Figure 3.1, Supplemental Figure 5.2.7). In line with this observation, we found that BBX20 plays a more important role in KAR signaling than BBX21 (Figure 3.3, 3.4). Similar to these

observations, BBX21 or BBX22 could be specifically induced by other stimuli to fulfil individual roles in the stimulated response.

It is also possible that the BBX proteins are expressed in different cell types, where they fulfil individual functions. So far, only the promoter activity of *BBX20* has been analysed, suggesting that the *BBX20* promoter is mainly active in the roots of seedlings (Figure 3.1) (Fan et al., 2012). In the future it will be interesting to see, if *BBX21* has a similar expression pattern, or if, based on its unique function as a negative regulator of lateral root emergence (Datta et al., 2007), it has a more pronounced expression in lateral root primordia. Regardless, to test if functional differences between BBX20 and BBX21 are solely dependent on potential differences in expression patterns, promoter swap experiments could be performed where *BBX20* is expressed under the control of the *BBX21* promoter in *bbx21* mutant and vice versa to test if those constructs can rescue respective mutant phenotypes.

On the other hand, the different functions of individual BBX proteins could also be caused by differences in their amino acid sequences. The strongest similarities between the BBX proteins from structural group IV are observed in their N-terminal B-Box domains (Khanna et al., 2009). Accordingly, the interaction with HY5, a feature shared by BBX20-BBX25, has been largely attributed to the N-terminal B-box domains of these proteins (Datta et al., 2007, 2008; Gangappa, Crocco, et al., 2013; Gangappa, Holm, et al., 2013; Wei et al., 2016; Zhang et al., 2017). In contrast, we have shown that the less conserved C-terminal regions of BBX21 and BBX24 determine their function as a positive or negative regulator of photomorphogenesis, respectively (Job et al., 2018). However, not much is known about structural differences between the BBX proteins, that were focused on in this thesis. The 9 aa TAD we identified could only be found in BBX20 and BBX21, but not in BBX22 (Supplemental Figure 5.1.5). Interestingly, that TAD partially overlaps with a motif of unknown function (M6) that was identified by sequence comparison between numerous BBX proteins from multiple organisms (Crocco and Botto, 2013). Further research is required to determine if there is a function for this novel motif. As we could only detect a TAD in BBX20 and BBX21 it remains elusive how BBX22 and BBX23 activate transcription in concert with HY5. Considering the minor phenotypes of *bbx22* and *bbx23* mutants it is possible that they require BBX20 and BBX21 and function in multimeric protein complexes (Figure 3.3) (Zhang et al., 2017). However, BBX22 has been shown to activate transcription in yeast and activates transcription in

bbx202122 hy5 hyh protoplasts when expressed together with HY5 (Figure 2.2) (Datta et al., 2008). Hence, it is possible that BBX22 and BBX23 carry a TAD that significantly differs from the ones in BBX20 and BBX21 which could not be detected with the 9 aa TAD prediction tool used in chapter 2 (Piskacek et al., 2007).

4.4 HY5, a basis for additional transcriptional modules?

HY5 has been shown to play a role in multiple pathways and integrates a variety of biotic and abiotic signals into a plant's lifecycle (Gangappa and Botto, 2016). Additionally, multiple studies have shown that HY5 can associate with up to one third of the promoters in the Arabidopsis genome, raising the potential of a high number of direct transcriptional target genes (Hajdu et al., 2018; Lee et al., 2007; Zhang et al., 2011). This raises the question how HY5 gains its specificity to regulate a specific gene, at the correct timepoint and tissue to induce an appropriate response to a variety of stimuli.

The RNA-seq experiment, comparing the *bbx202122* mutant with a *hy5* mutant showed that most of the DEGs of *bbx202122* were also deregulated in the *hy5* mutant (Figure 2.1). However, the *hy5* mutant showed a plethora of DEGs that were regulated seemingly independent of the BBX proteins (Figure 2.1). As mentioned above, BBX23 might constitute a fourth co-factor of HY5, and therefore this experiment would have been more appropriate with a *bbx20212223* quadruple mutant. However, as BBX23 only has limited function in the regulation of photomorphogenesis (Zhang et al., 2017) this alternative experimental design is not expected to resolve the discrepancy in total DEG numbers between *bbx202122* and *hy5*.

All in all, these results support the possibility that HY5 is dependent on a variety of cofactors that specifically allow for HY5 to fulfil its multiple roles. Hence, it will be of special interest to identify novel cofactors in the future, to better understand how a master transcriptional regulator like HY5 gains transcriptional specificity while it has the potential to associate with one third of all promoters in Arabidopsis (Hajdu et al., 2018; Lee et al., 2007; Zhang et al., 2011).

Based on the model established in chapter 2 (Figure 1.1), we were able to predict the properties that a cofactor of HY5 has to fulfil to function interdependently to regulate photomorphogenesis. This allowed the identification of BBX20, BBX21 and BBX22 as these cofactors. It is possible that the same model could be used to identify new cofactors

of HY5. As a first step, the literature could be screened for potential candidates of new HY5 cofactors to test in future experiments.

A new cofactor, that acts together with HY5 in signaling pathways other than light signaling, does not necessarily have to be post-transcriptionally regulated by COP1. This prediction was based on the observation that the dark stable HY5ΔN77, that does not interact with COP1, was unable to induce photomorphogenesis in dark grown seedlings (Ang et al., 1998). However, if investigating responses in which *hy5* is epistatic to *cop1* in darkness, and where expression of HY5ΔN77 is unable to regulate the response, the potential novel cofactor is likely to be a target of COP1/SPA-mediated degradation.

According to our model for the activity of the HY5-BBX transcriptional module, HY5 confers the DNA binding to the protein complex, whereas the cofactors contribute the transcriptional activation activity. Consequently, the DNA binding and overexpression phenotype of BBX20 has been shown to be dependent on the presence of HY5 (Figure 2.2). Similar to these observations, overexpression phenotypes of new cofactors are expected to be dependent on the presence of HY5. Furthermore, a recent publication suggested that HY5 acts mainly to positively regulate its direct targets by HY5 and its required cofactors (Burko et al., 2020). As HY5 itself does not have a TAD and does not induce transcription on its own, it is also expected that the potential cofactor has the ability to induce transcription (Ang et al., 1998). This could mean, that a potential novel cofactor should either have an identifiable TAD, or at least should be shown to have the potential to activate transcription by other means as it was the case for BBX22 (Figure 2.2) (Datta et al., 2008). Regardless, the most likely feature of a new co-factor of HY5 is the physical interaction between the two proteins. The BioGRID database currently lists 46 interactors of HY5 where evidence for a physical interaction can be found, providing a reasonable starting point to identify candidate proteins for new HY5 cofactors (Stark et al., 2006). Experimentally this question could be targeted by an interactor screen using HY5 as the bait, potentially allowing for the identification of new HY5-interacting proteins under specific conditions *in planta*.

A mutant of the potential cofactor should show a similar phenotype like a *hy5* mutant under the conditions in which it is required for the HY5 activity. Such a phenotype could be an insensitivity to hormone treatment or the inability to respond to abiotic stress.

In the context of KAR signaling the strong transcriptional induction of *BBX20* led us to investigate its potential role in KAR signaling, which led to the discovery that a HY5-

BBX transcriptional module is active in KAR signaling (Figure 3.6, 3.7). In a similar fashion a potential new co-factor could be transcriptionally induced by conditions in which HY5 has been shown to be important but does not seem to be strongly regulated itself.

A HY5-regulated process in which the BBX proteins have not yet been reported to play a role is light-induced chlorophyll accumulation. Chlorophyll accumulation is impaired in a *hy5* mutant, whereas a *cop1* mutant accumulates enhanced levels of chlorophyll (Oyama et al., 1997; Usami et al., 2004). The GOLDEN2, ARR-B, Psr1 (GARP) family transcription factors GOLDEN2-LIKE (GLK) 1 and 2 have been shown to play an essential role in the induction of chlorophyll accumulation in Arabidopsis (Fitter et al., 2002; Waters et al., 2008). Moreover it was shown that enhanced chlorophyll accumulation of GLK-overexpression lines is dependent on the presence of HY5 (Kobayashi et al., 2012). Hence, the GLKs represent possible new cofactors of HY5, which could be further investigated provided that a HY5-GLK complex can be observed in *planta*.

In strawberry (*Fragaria vesca*) FvbHLH9 physically interacts with FvHY5 to induce anthocyanin biosynthesis by cooperative transcriptional activation of anthocyanin biosynthesis genes (Yang et al., 2020). FvbHLH9 is a homologue of the Arabidopsis bHLH transcription factor HECATE1 (HEC1) that has two more closely related genes *HEC2* and *HEC3* (Gremski et al., 2007; Hollender et al., 2014). In Arabidopsis the *HEC* genes are involved in the regulation of photomorphogenesis and HEC2 has been shown to be negatively regulated by the COP1/SPA complex (Kathare et al., 2020). Interestingly, the HEC transcription factors have been shown to regulate a variety of developmental processes besides the regulation of photomorphogenesis, including flowering transition or gynoecium development (Gaillochet et al., 2018; Gremski et al., 2007). It remains to be tested if HY5 and HEC proteins from Arabidopsis physically interact and form a transcriptional module that can act in parallel to the HY5-BBX module to regulate photomorphogenesis. Alternatively, the HEC proteins can act as cofactors for HY5 in the regulation of other developmental processes.

4.5 HY5 a transcriptional activator, repressor, or both?

Before this work was conducted it was unclear how the bZIP transcription factor HY5 regulates transcription of its target genes. Although it was shown that the HY5 protein itself neither has a TAD nor a repressor domain, HY5 has been defined as an activator or repressor of transcription, or both (Ang et al., 1998; Delker et al., 2014; Gangappa and Kumar, 2017; Lee et al., 2007; Nawkar et al., 2017; Norén et al., 2016; Ruckle et al., 2007; Xu, Chi, et al., 2016; Zhang et al., 2017).

In the RNA-seq experiment comparing a *hy5* and a *bbx202122* mutant we found more genes that were upregulated in the *hy5* mutant than downregulated (591 vs 259) (Figure 2.1). Consistently the overlap of *hy5* and *bbx202122* DEGs contained more co-downregulated genes (Figure 2.1). These results suggest that in the context of regulating photomorphogenesis the HY5-BBX module works as a transcriptional activator rather than a repressor. In line with this hypothesis the HY5-BBX complex could activate gene expression when expressed in Arabidopsis protoplasts (Figure 2.2).

These results are supported by a recent study where chimeric activator (HY5-VP16) and repressor (HY5-SRDX) fusion proteins of HY5 were expressed in Arabidopsis seedlings (Burko et al., 2020). Comprehensive analysis of these stable transgenic lines showed that the expression of HY5-SRDX enhanced the *hy5* mutant phenotype. In contrast the expression of HY5-VP16 led to opposite phenotypes, similar to those expected, but not always observed in HY5 overexpression lines (Burko et al., 2020). These results were consistently observed with regards to measurements of hypocotyl length, cotyledon area, chlorophyll and anthocyanin content, shade avoidance response, seedling root length as well as flowering time in fully grown plants (Burko et al., 2020). Collectively, these results suggest that under these conditions HY5 primarily acts as a transcriptional activator of its direct targets. Consequently, previously identified target genes that showed negative regulation by HY5 might rather represent indirect targets.

Nevertheless, as discussed above the BBX proteins are most likely not the only cofactors that are essential for HY5 function. Under specific conditions where the role of HY5 has been described as a repressor of gene expression it is still possible that the cofactor under these conditions provides repressive activity. To fully understand the various mechanisms by which HY5 regulates plant development it will be crucial to identify and characterize additional HY5 cofactors.

Furthermore, HY5 activity has been shown to be regulated through modifications of its ability to bind DNA. The bHLH transcription factors PIFs have been shown to compete with HY5 for DNA binding to specific motifs to antagonistically regulate gene expression (Toledo-Ortiz et al., 2014). Interestingly, within the structural group IV of HY5-interacting BBX proteins, BBX24 and BBX25 have been shown to share redundant function to negatively regulate photomorphogenesis (Gangappa, Crocco, et al., 2013; Indorf et al., 2007). We have shown that BBX24 accomplishes this function, by interfering with HY5's ability to bind to target promoters (Job et al., 2018). It will be interesting to test if BBX24 and BBX25 work as specific antagonists of the HY5-BBX transcriptional module identified in this work (chapter 2). This would allow for fine-tuning of HY5 activity and could be a common mechanism for future cofactors.

In summary, the data in this thesis provides a mechanism by which HY5, as a master transcriptional regulator, can gain specificity by interacting with its cofactors BBX20, BBX21 and BBX22. Nevertheless, as the BBX proteins are seemingly not the only cofactors of HY5 this work represents a framework for future research to fully understand how HY5 regulates plant development.

References

Abbas, N., Maurya, J.P., Senapati, D., Gangappa, S.N. and Chattopadhyay, S. (2014), "Arabidopsis CAM7 and HY5 Physically Interact and Directly Bind to the HY5 Promoter to Regulate Its Expression and Thereby Promote Photomorphogenesis", *The Plant Cell*, Vol. 26 No. 3, pp. 1036–1052.

Ahmad, M. (2016), "Photocycle and signaling mechanisms of plant cryptochromes", *Current Opinion in Plant Biology*, Elsevier Ltd, Vol. 33, pp. 108–115.

Ahmad, M. and Cashmore, A.R. (1993), "HY4 gene of A. thaliana encodes a protein with characteristics of a blue-light photoreceptor", *Nature*, Vol. 366 No. 6451, pp. 162–166.

Akiyama, K., Matsuzaki, K. and Hayashi, H. (2005), "Plant sesquiterpenes induce hyphal branching in arbuscular mycorrhizal fungi", *Nature*, Vol. 435 No. 7043, pp. 824–827.

Al-Sady, B., Ni, W., Kircher, S., Schäfer, E. and Quail, P.H. (2006), "Photoactivated Phytochrome Induces Rapid PIF3 Phosphorylation Prior to Proteasome-Mediated Degradation", *Molecular Cell*, Vol. 23 No. 3, pp. 439–446.

Alabadí, D., Gallego-Bartolomé, J., Orlando, L., García-Cárcel, L., Rubio, V., Martínez, C., Frigerio, M., et al. (2007), "Gibberellins modulate light signaling pathways to prevent Arabidopsis seedling de-etiolation in darkness", *The Plant Journal*, Vol. 53 No. 2, pp. 324–335.

Alder, A., Jamil, M., Marzorati, M., Bruno, M., Vermathen, M., Bigler, P., Ghisla, S., et al. (2012), "The Path from -Carotene to Carlactone, a Strigolactone-Like Plant Hormone", *Science*, Vol. 335 No. 6074, pp. 1348–1351.

An, J.P., Wang, X.F., Zhang, X.W., Bi, S.Q., You, C.X. and Hao, Y.J. (2019), "MdBBX22 regulates UV-B-induced anthocyanin biosynthesis through regulating the function of MdHY5 and is targeted by MdBT2 for 26S proteasome-mediated degradation", *Plant Biotechnology Journal*, Vol. 17 No. 12, pp. 2231–2233.

Andronis, C., Barak, S., Knowles, S.M., Sugano, S. and Tobin, E.M. (2008), "The clock protein CCA1 and the bZIP transcription factor HY5 physically interact to regulate gene expression in Arabidopsis", *Molecular Plant*, The Authors 2007. All rights reserved., Vol. 1 No. 1, pp. 58–67.

Ang, L.H., Chattopadhyay, S., Wei, N., Oyama, T., Okada, K., Batschauer, A. and Deng, X.W. (1998), "Molecular interaction between COP1 and HY5 defines a regulatory switch for light control of Arabidopsis development", *Molecular Cell*, Vol. 1 No. 2, pp. 213–222.

Ang Lay Hong and Deng Xing Wang. (1994), "Regulatory hierarchy of photomorphogenic loci: Allele-specific and light-dependent interaction between the HY5 and COP1 loci", *Plant Cell*, Vol. 6 No. 5, pp. 613–628.

Anthony Massiah, M. (2019), "Zinc-Binding B-Box Domains with RING Folds Serve Critical Roles in the Protein Ubiquitination Pathways in Plants and Animals", *Ubiquitin Proteasome System - Current Insights into Mechanism Cellular Regulation and Disease*, IntechOpen, pp. 1–29.

Arite, T., Umehara, M., Ishikawa, S., Hanada, A., Maekawa, M., Yamaguchi, S. and Kyozuka, J. (2009), "D14, a strigolactone-Insensitive mutant of rice, shows an accelerated outgrowth of tillers", *Plant and Cell Physiology*, Vol. 50 No. 8, pp. 1416–1424.

von Arnim, A.G. and Deng, X.W. (1994), "Light inactivation of arabidopsis photomorphogenic repressor COP1 involves a cell-specific regulation of its nucleocytoplasmic partitioning", *Cell*, Vol. 79 No. 6, pp. 1035–1045.

Arongaus, A.B., Chen, S., Pireyre, M., Glöckner, N., Galvão, V.C., Albert, A., Winkler, J.B., et al. (2018), "Arabidopsis RUP2 represses UVR8-mediated flowering in noninductive photoperiods", *Genes and Development*, Vol. 32 No. 19–20, pp. 1332–1343.

Aukerman, M.J., Hirschfeld, M., Wester, L., Weaver, M., Clack, T., Amasino, R.M. and Sharrock, R.A. (1997), "A deletion in the PHYD gene of the Arabidopsis Wassilewskija ecotype defines a role for phytochrome D in red/far-red light sensing.", *The Plant Cell*, Vol. 9 No. 8, pp. 1317–1326.

Bae, G. and Choi, G. (2008), "Decoding of light signals by plant phytochromes and their interacting proteins", *Annual Review of Plant Biology*, Vol. 59, pp. 281–311.

Bai, B., Lu, N., Li, Y., Guo, S., Yin, H., He, Y., Sun, W., et al. (2019), "OsBBX14 promotes photomorphogenesis in rice by activating OsHY5L1 expression under blue light conditions", *Plant Science*, Elsevier, Vol. 284 No. April, pp. 192–202.

Bai, S., Tao, R., Tang, Y., Yin, L., Ma, Y., Ni, J., Yan, X., et al. (2019), "BBX16, a B-box protein, positively regulates light-induced anthocyanin accumulation by activating MYB10 in red pear", *Plant Biotechnology Journal*, Vol. 17 No. 10, pp. 1985–1997.

Bai, S., Tao, R., Yin, L., Ni, J., Yang, Q., Yan, X., Yang, F., et al. (2019), "Two B-box proteins, PpBBX18 and PpBBX21, antagonistically regulate anthocyanin biosynthesis via competitive association with Pyrus pyrifolia ELONGATED HYPOCOTYL 5 in the peel of pear fruit", *Plant Journal*, Vol. 100 No. 6, pp. 1208–1223.

Balcerowicz, M. (2020), "PHYTOCHROME-INTERACTING FACTORS at the interface of light and temperature signalling", *Physiologia Plantarum*, Vol. 169 No. 3, pp. 347–356.

Baldrianová, J., Černý, M., Novák, J., Jedelský, P.L., Divíšková, E. and Brzobohatý, B. (2015), "Arabidopsis proteome responses to the smoke-derived growth regulator karrikin", *Journal of Proteomics*, Vol. 120, pp. 7–20.

Ballaré, C.L. and Pierik, R. (2017), "The shade-avoidance syndrome: Multiple signals and ecological consequences", *Plant Cell and Environment*, Vol. 40 No. 11, pp. 2530–2543.

Bauer, D., Viczián, A., Kircher, S., Nobis, T., Nitschke, R., Kunkel, T., Panigrahi, K.C.S., et al. (2004), "Constitutive Photomorphogenesis 1 and Multiple Photoreceptors Control Degradation of Phytochrome Interacting Factor 3, a Transcription Factor Required for Light Signaling in Arabidopsis", *The Plant Cell*, Vol. 16 No. 6, pp. 1433–1445.

Bennett, T. and Leyser, O. (2014), "Strigolactone signalling: Standing on the shoulders of DWARFs", *Current Opinion in Plant Biology*, Elsevier Ltd, Vol. 22, pp. 7–13.

Binkert, M., Crocco, C.D., Ekundayo, B., Lau, K., Raffelberg, S., Tilbrook, K., Yin, R., et al. (2016), "Revisiting chromatin binding of the Arabidopsis UV-B photoreceptor UVR8", *BMC Plant Biology*, BMC Plant Biology, Vol. 16 No. 1, pp. 1–11.

Binkert, M., Kozma-Bognár, L., Terecskei, K., De Veylder, L., Nagy, F. and Ulm, R. (2014), "UV-B-Responsive association of the Arabidopsis bZIP transcription factor ELONGATED HYPOCOTYL5 with target genes, including its own promoter", *Plant Cell*, Vol. 26 No. 10, pp. 4200–4213.

Blázquez, M.A., Nelson, D.C. and Weijers, D. (2020), "Evolution of Plant Hormone Response Pathways", *Annual Review of Plant Biology*, Vol. 71 No. 1, pp. 327–353.

Botto, J.F., Sanchez, R.A., Whitelam, G.C. and Casal, J.J. (1996), "Phytochrome A Mediates the Promotion of Seed Germination by Very Low Fluences of Light and Canopy Shade Light in Arabidopsis", *Plant Physiology*, Vol. 110 No. 2, pp. 439–444.

Brockmann, J., Rieble, S., Kazarinova-Fukshansky, N., Seyfried, M. and Schafer, E. (1987), "Phytochrome behaves as a dimer in vivo.", *Plant, Cell and Environment*, Vol. 10 No. 2, pp. 105–111.

Brown, B.A., Cloix, C., Jiang, G.H., Kaiserli, E., Herzyk, P., Kliebenstein, D.J. and Jenkins, G.I. (2005), "A UV-B-specific signaling component orchestrates plant UV protection", *Proceedings of the National Academy of Sciences of the United States of America*, Vol. 102 No. 50, pp. 18225–18230.

Brown, N.A.C. and Van Staden, J. (1997), "Smoke as a germination cue: A review", *Plant Growth Regulation*, Vol. 22 No. 2, pp. 115–124.

Burko, Y., Seluzicki, A., Zander, M., Pedmale, U. V., Ecker, J.R. and Chory, J. (2020), "Chimeric activators and repressors define HY5 activity and reveal a light-regulated feedback mechanism", *Plant Cell*, Vol. 32 No. 4, pp. 967–983.

Burman, N., Bhatnagar, A. and Khurana, J.P. (2018), "OsbZIP48, a HY5 transcription factor Ortholog, exerts pleiotropic effects in light-regulated development", *Plant Physiology*, Vol. 176 No. 2, pp. 1262–1285.

Bursch, K., Toledo-Ortiz, G., Pireyre, M., Lohr, M., Braatz, C. and Johansson, H. (2020), "Identification of BBX proteins as rate-limiting cofactors of HY5", *Nature Plants*, Springer US, available at:https://doi.org/10.1038/s41477-020-0725-0.

Butler, W.L., Lane, H.C. and Siegelman, H.W. (1963), "Nonphotochemical Transformations of Phytochrome in Vivo", *Plant Physiology*, Vol. 38 No. 5, pp. 514–519.

Butler, W.L., Norris, K.H., Siegelman, H.W. and Hendricks, S.B. (1959), "DETECTION, ASSAY, AND PRELIMINARY PURIFICATION OF THE PIGMENT CONTROLLING PHOTORESPONSIVE DEVELOPMENT OF PLANTS", *Proceedings of the National Academy of Sciences*, Vol. 45 No. 12, pp. 1703–1708.

Bythell-Douglas, R., Rothfels, C.J., Stevenson, D.W.D., Graham, S.W., Wong, G.K.S., Nelson, D.C. and Bennett, T. (2017), "Evolution of strigolactone receptors by gradual neo-functionalization of KAI2 paralogues", *BMC Biology*, BMC Biology,

Vol. 15 No. 1, pp. 1–21.

Bythell-Douglas, R., Waters, M.T., Scaffidi, A., Flematti, G.R., Smith, S.M. and Bond, C.S. (2013), "The Structure of the Karrikin-Insensitive Protein (KAI2) in Arabidopsis thaliana", edited by Newcomb, R.D.*PLoS ONE*, Vol. 8 No. 1, p. e54758.

Cashmore, A.R., Jarillo, J.A., Wu, Y.J. and Liu, D. (1999), "Cryptochromes: Blue light receptors for plants and animals", *Science*, Vol. 284 No. 5415, pp. 760–765.

Chang, C.S.J., Li, Y.H., Chen, L.T., Chen, W.C., Hsieh, W.P., Shin, J., Jane, W.N., et al. (2008), "LZF1, a HY5-regulated transcriptional factor, functions in Arabidopsis de-etiolation", *Plant Journal*, Vol. 54 No. 2, pp. 205–219.

Chang, C.S.J., Maloof, J.N. and Wu, S.H. (2011), "COP1-mediated degradation of BBX22/LZF1 optimizes seedling development in arabidopsis", *Plant Physiology*, Vol. 156 No. 1, pp. 228–239.

Chattopadhyay, S., Ang, L.H., Puente, P., Deng, X.W. and Wei, N. (1998), "Arabidopsis bZIP protein HY5 directly interacts with light-responsive promoters in mediating light control of gene expression", *Plant Cell*, Vol. 10 No. 5, pp. 673–683.

Chen, F., Li, B., Li, G., Charron, J.B., Dai, M., Shi, X. and Deng, X.W. (2014), "Arabidopsis phytochrome a directly targets numerous promoters for individualized modulation of genes in a wide range of pathways", *Plant Cell*, Vol. 26 No. 5, pp. 1949–1966.

Chen, H., Zhang, J., Neff, M.M., Hong, S.W., Zhang, H., Deng, X.W. and Xiong, L. (2008), "Integration of light and abscisic acid signaling during seed germination and early seedling development", *Proceedings of the National Academy of Sciences of the United States of America*, Vol. 105 No. 11, pp. 4495–4500.

Cheng, M.-C., Kathare, P.K., Paik, I. and Huq, E. (2021), "Phytochrome Signaling Networks.", *Annual Review of Plant Biology*, Vol. 72 No. 1, pp. 217–244.

Cheng, X.F. and Wang, Z.Y. (2005), "Overexpression of COL9, a CONSTANS-LIKE gene, delays flowering by reducing expression of CO and FT in Arabidopsis thaliana", *Plant Journal*, Vol. 43 No. 5, pp. 758–768.

Choi, J., Lee, T., Cho, J., Servante, E.K., Pucker, B., Summers, W., Bowden, S., et al. (2020), "The negative regulator SMAX1 controls mycorrhizal symbiosis and strigolactone biosynthesis in rice", *Nature Communications*, Springer US, Vol. 11 No. 1, p. 2114.

Chory, J., Chatterjee, M., Cook, R.K., Elich, T., Fankhauser, C., Li, J., Nagpal, P., et al. (1996), "From seed germination to flowering, light controls plant development via the pigment phytochrome", *Proceedings of the National Academy of Sciences of the United States of America*, Vol. 93 No. 22, pp. 12066–12071.

Christie, J.M., Arvai, A.S., Baxter, K.J., Heilmann, M., Pratt, A.J., Hara, A.O., Kelly, S.M., et al. (2012), "Plant UVR8 Photoreceptor Senses Disruption of Cross-Dimer Salt Bridges", *Science*, Vol. 335 No. March, pp. 1492–1497.

Clack, T., Mathews, S. and Sharrock, R.A. (1994), "The phytochrome apoprotein family in Arabidopsis is encoded by five genes: the sequences and expression of PHYD and PHYE", *Plant Molecular Biology*, Vol. 25 No. 3, pp. 413–427.

Clack, T., Shokry, A., Moffet, M., Liu, P., Faul, M. and Sharrock, R.A. (2009), "Obligate heterodimerization of Arabidopsis phytochromes C and e and interaction with the PIF3 basic helix-loop-helix transcription factor", *Plant Cell*, Vol. 21 No. 3, pp. 786–799.

Cloix, C. and Jenkins, G.I. (2008), "Interaction of the Arabidopsis UV-B-specific signaling component UVR8 with chromatin", *Molecular Plant*, The Authors 2007. All rights reserved., Vol. 1 No. 1, pp. 118–128.

Cloix, C., Kaiserli, E., Heilmann, M., Baxter, K.J., Brown, B.A., O'Hara, A., Smith, B.O., et al. (2012), "C-terminal region of the UV-B photoreceptor UVR8 initiates signaling through interaction with the COP1 protein", *Proceedings of the National Academy of Sciences of the United States of America*, Vol. 109 No. 40, pp. 16366–16370.

Cluis, C.P., Mouchel, C.F. and Hardtke, C.S. (2004), "The Arabidopsis transcription factor HY5 integrates light and hormone signaling pathways", *Plant Journal*, Vol. 38 No. 2, pp. 332–347.

Cock, P.J.A., Fields, C.J., Goto, N., Heuer, M.L. and Rice, P.M. (2009), "The Sanger FASTQ file format for sequences with quality scores, and the Solexa/Illumina FASTQ variants", *Nucleic Acids Research*, Vol. 38 No. 6, pp. 1767–1771.

Conn, C.E., Bythell-Douglas, R., Neumann, D., Yoshida, S., Whittington, B., Westwood, J.H., Shirasu, K., et al. (2015), "Convergent evolution of strigolactone perception enabled host detection in parasitic plants", *Science*, Vol. 349 No. 6247, pp. 540–543.

Conn, C.E. and Nelson, D.C. (2016), "Evidence that KARRIKIN-INSENSITIVE2 (KAI2) receptors may perceive an unknown signal that is not karrikin or strigolactone", *Frontiers in Plant Science*, Vol. 6 No. JAN2016, pp. 1–7.

Cook, C.E., Whichard, L.P., Turner, B., Wall, M.E. and Egley, G.H. (1966), "Germination of Witchweed (Striga lutea Lour.): Isolation and Properties of a Potent Stimulant", *Science*, Vol. 154 No. 3753, pp. 1189–1190.

Crocco, C.D. and Botto, J.F. (2013), "BBX proteins in green plants: Insights into their evolution, structure, feature and functional diversification", *Gene*, Elsevier B.V., Vol. 531 No. 1, pp. 44–52.

Datta, S., Hettiarachchi, C., Johansson, H. and Holm, M. (2007), "Salt Tolerance Homolog2, a B-box protein in Arabidopsis that activates transcription and positively regulates light-mediated development", *Plant Cell*, Vol. 19 No. 10, pp. 3242–3255.

Datta, S., Hettiarachchi, G.H.C.M., Deng, X.W. and Holm, M. (2006), "Arabidopsis CONSTANS-LIKE3 is a positive regulator of red light signaling and root growth", *Plant Cell*, Vol. 18 No. 1, pp. 70–84.

Datta, S., Johansson, H., Hettiarachchi, C., Irigoyen, M.L., Desai, M., Rubio, V. and Holm, M. (2008), "LZF1/salt tolerance HOMOLOG3, an Arabidopsis B-box protein involved in light-dependent development and gene expression, undergoes COP1-mediated ubiquitination", *Plant Cell*, Vol. 20 No. 9, pp. 2324–2338.

Debrieux, D., Trevisan, M. and Fankhauser, C. (2013), "Conditional Involvement of CONSTITUTIVE PHOTOMORPHOGENIC1 in the Degradation of Phytochrome A", *Plant Physiology*, Vol. 161 No. 4, pp. 2136–2145.

Delker, C., Sonntag, L., James, G.V., Janitza, P., Ibañez, C., Ziermann, H., Peterson, T., et al. (2014), "The DET1-COP1-HY5 Pathway Constitutes a Multipurpose Signaling Module Regulating Plant Photomorphogenesis and Thermomorphogenesis", *Cell Reports*, Vol. 9 No. 6, pp. 1983–1989.

Deng, X.W., Caspar, T. and Quail, P.H. (1991), "cop1: A regulatory locus involved in light-controlled development and gene expression in Arabidopsis", *Genes and Development*, Vol. 5 No. 7, pp. 1172–1182.

Deng, X.W., Matsui, M., Wei, N., Wagner, D., Chu, A.M., Feldmann, K.A. and Quail, P.H. (1992), "COP1, an arabidopsis regulatory gene, encodes a protein with both a zinc-binding motif and a Gβ homologous domain", *Cell*, Vol. 71 No. 5, pp. 791–801.

Devlin, P.F. and Kay, S.A. (2001), "Circadian photoperception.", *Annual Review of Physiology*, Vol. 63, pp. 677–94.

Devlin, P.F., Patel, S.R. and Whitelam, G.C. (1998), "Phytochrome E Influences Internode Elongation and Flowering Time in Arabidopsis", *The Plant Cell*, Vol. 10 No. 9, pp. 1479–1487.

Ding, L., Wang, S., Song, Z.T., Jiang, Y., Han, J.J., Lu, S.J., Li, L., et al. (2018), "Two B-Box Domain Proteins, BBX18 and BBX23, Interact with ELF3 and Regulate Thermomorphogenesis in Arabidopsis", *Cell Reports*, ElsevierCompany., Vol. 25 No. 7, pp. 1718-1728.e4.

Dixon, K.W., Merritt, D.J., Flematti, G.R. and Ghisalberti, E.L. (2009), "Karrikinolide - A phytoreactive compound derived from smoke with applications in horticulture, ecological restoration and agriculture", *Acta Horticulturae*, Vol. 813 No. March, pp. 155–170.

Dotto, M., Gómez, M.S., Soto, M.S. and Casati, P. (2018), "UV-B radiation delays flowering time through changes in the PRC2 complex activity and miR156 levels in Arabidopsis thaliana", *Plant Cell and Environment*, Vol. 41 No. 6, pp. 1394–1406.

Du, S.-S., Li, L., Li, L., Wei, X., Xu, F., Xu, P.-B., Wang, W., et al. (2020), "Photoexcited Cryptochrome 2 Interacts Directly with TOE1 and TOE2 in Flowering Regulation", *Plant Physiology*, p. pp.00486.2020.

Eichenberg, K., Bäurle, I., Paulo, N., Sharrock, R.A., Rüdiger, W. and Schäfer, E. (2000), "Arabidopsis phytochromes C and E have different spectral characteristics from those of phytochromes A and B", *FEBS Letters*, Vol. 470 No. 2, pp. 107–112.

EMBL, Letunic, I., Khedkar, S. and Bork, P. (2020), "SMART (Simple Modular Architecture Research Tool) - BBOX - B-Box-type zinc finger", available at: http://smart.embl.de/smart/do_annotation.pl?DOMAIN=SM00336 (accessed 30 April 2021).

Enderle, B., Sheerin, D.J., Paik, I., Kathare, P.K., Schwenk, P., Klose, C., Ulbrich, M.H., et al. (2017), "PCH1 and PCHL promote photomorphogenesis in plants by controlling phytochrome B dark reversion", *Nature Communications*, Springer US, Vol. 8 No. 1, available at:https://doi.org/10.1038/s41467-017-02311-8.

Fan, X.Y., Sun, Y., Cao, D.M., Bai, M.Y., Luo, X.M., Yang, H.J., Wei, C.Q., et al. (2012), "BZS1, a B-box protein, promotes photomorphogenesis downstream of both

brassinosteroid and light signaling pathways", *Molecular Plant*, © The Authors. All rights reserved., Vol. 5 No. 3, pp. 591–600.

Fang, F., Salmon, K., Shen, M.W.Y., Aeling, K.A., Ito, E., Irwin, B., Tran, U.P.C., et al. (2011), "A vector set for systematic metabolic engineering in Saccharomyces cerevisiae", *Yeast*, Vol. 28 No. 2, pp. 123–136.

Fang, H., Dong, Y., Yue, X., Hu, J., Jiang, S., Xu, H., Wang, Y., et al. (2019), "The B-box zinc finger protein MdBBX20 integrates anthocyanin accumulation in response to ultraviolet radiation and low temperature", *Plant Cell and Environment*, Vol. 42 No. 7, pp. 2090–2104.

Fauser, F., Schiml, S. and Puchta, H. (2014), "Both CRISPR/Cas-based nucleases and nickases can be used efficiently for genome engineering in Arabidopsis thaliana", *Plant Journal*, Vol. 79 No. 2, pp. 348–359.

Favory, J.J., Stec, A., Gruber, H., Rizzini, L., Oravecz, A., Funk, M., Albert, A., et al. (2009), "Interaction of COP1 and UVR8 regulates UV-B-induced photomorphogenesis and stress acclimation in Arabidopsis", *EMBO Journal*, Vol. 28 No. 5, pp. 591–601.

Fehér, B., Kozma-Bognár, L., Kevei, É., Hajdu, A., Binkert, M., Davis, S.J., Schäfer, E., et al. (2011), "Functional interaction of the circadian clock and UV RESISTANCE LOCUS 8-controlled UV-B signaling pathways in Arabidopsis thaliana", *Plant Journal*, Vol. 67 No. 1, pp. 37–48.

Findlay, K.M.W. and Jenkins, G.I. (2016), "Regulation of UVR8 photoreceptor dimer/monomer photo-equilibrium in Arabidopsis plants grown under photoperiodic conditions", *Plant Cell and Environment*, Vol. 39 No. 8, pp. 1706–1714.

Fiorucci, A.S., Galvão, V.C., Ince, Y.Ç., Boccaccini, A., Goyal, A., Allenbach Petrolati, L., Trevisan, M., et al. (2020), "PHYTOCHROME INTERACTING FACTOR 7 is important for early responses to elevated temperature in Arabidopsis seedlings", *New Phytologist*, Vol. 226 No. 1, pp. 50–58.

Fitter, D.W., Martin, D.J., Copley, M.J., Scotland, R.W. and Langdale, J.A. (2002), "GLK gene pairs regulate chloroplast development in diverse plant species", *Plant Journal*, Vol. 31 No. 6, pp. 713–727.

Flematti, G.R., Ghisalberti, E.L., Dixon, K.W. and Trengove, R.D. (2004), "A compound from smoke that promotes seed germination", *Science*, Vol. 305 No. 5686, p. 977.

Flematti, G.R., Ghisalberti, E.L., Dixon, K.W. and Trengove, R.D. (2005), "Synthesis of the seed germination stimulant 3-methyl-2H-furo[2,3-c]pyran-2- one", *Tetrahedron Letters*, Vol. 46 No. 34, pp. 5719–5721.

Flematti, G.R., Ghisalberti, E.L., Dixon, K.W. and Trengove, R.D. (2009), "Identification of alkyl substituted 2H-furo[2,3-c]pyran-2-ones as germination stimulants present in smoke", *Journal of Agricultural and Food Chemistry*, Vol. 57 No. 20, pp. 9475–9480.

Franklin, K.A. (2008), "Shade avoidance", *New Phytologist*, Vol. 179 No. 4, pp. 930–944.

Franklin, K.A. and Quail, P.H. (2010), "Phytochrome functions in Arabidopsis development", *Journal of Experimental Botany*, Vol. 61 No. 1, pp. 11–24.

Gaillochet, C., Jamge, S., van der Wal, F., Angenent, G., Immink, R. and Lohmann, J.U. (2018), "A molecular network for functional versatility of HECATE transcription factors", *Plant Journal*, Vol. 95 No. 1, pp. 57–70.

Galvão, V.C. and Fankhauser, C. (2015), "Sensing the light environment in plants: Photoreceptors and early signaling steps", *Current Opinion in Neurobiology*, Vol. 34 No. Figure 1, pp. 46–53.

Gangappa, S.N. and Botto, J.F. (2016), "The Multifaceted Roles of HY5 in Plant Growth and Development", *Molecular Plant*, Elsevier Ltd, Vol. 9 No. 10, pp. 1353–1365.

Gangappa, S.N., Crocco, C.D., Johansson, H., Datta, S., Hettiarachchi, C., Holm, M. and Botto, J.F. (2013), "The Arabidopsis B-BOX protein BBX25 interacts with HY5, negatively regulating BBX22 expression to suppress seedling photomorphogenesis", *Plant Cell*, Vol. 25 No. 4, pp. 1243–1257.

Gangappa, S.N., Holm, M. and Botto, J.F. (2013), "Molecular interactions of BBX24 and BBX25 with HYH, HY5 HOMOLOG, to modulate Arabidopsis seedling development", *Plant Signaling and Behavior*, Vol. 8 No. 8, pp. 24–28.

Gangappa, S.N. and Kumar, S.V. (2017), "DET1 and HY5 Control PIF4-Mediated Thermosensory Elongation Growth through Distinct Mechanisms", *Cell Reports*, ElsevierCompany., Vol. 18 No. 2, pp. 344–351.

Gendron, J.M., Pruneda-Paz, J.L., Doherty, C.J., Gross, A.M., Kang, S.E. and Kay, S.A. (2012), "Arabidopsis circadian clock protein, TOC1,is a DNA-binding transcription factor", *Proceedings of the National Academy of Sciences of the United States of America*, Vol. 109 No. 8, pp. 3167–3172.

Genoud, T., Schweizer, F., Tscheuschler, A., Debrieux, D., Casal, J.J., Schäfer, E., Hiltbrunner, A., et al. (2008), "FHY1 mediates nuclear import of the light-activated phytochrome A photoreceptor", *PLoS Genetics*, Vol. 4 No. 8, available at:https://doi.org/10.1371/journal.pgen.1000143.

Giovani, B., Byrdin, M., Ahmad, M. and Brettel, K. (2003), "Light-induced electron transfer in a cryptochrome blue-light photoreceptor", *Nature Structural Biology*, Vol. 10 No. 6, pp. 489–490.

Gomez-Roldan, V., Fermas, S., Brewer, P.B., Puech-Pagès, V., Dun, E.A., Pillot, J.-P., Letisse, F., et al. (2008), "Strigolactone inhibition of shoot branching", *Nature*, Vol. 455 No. 7210, pp. 189–194.

Gonzali, S., Mazzucato, A. and Perata, P. (2009), "Purple as a tomato: towards high anthocyanin tomatoes", *Trends in Plant Science*, Vol. 14 No. 5, pp. 237–241.

Gonzali, S. and Perata, P. (2020), "Anthocyanins from purple tomatoes as novel antioxidants to promote human health", *Antioxidants*, Vol. 9 No. 10, pp. 1–17.

Gremski, K., Ditta, G. and Yanofsky, M.F. (2007), "The HECATE genes regulate female reproductive tract development in Arabidopsis thaliana", *Development*, Vol. 134 No. 20, pp. 3593–3601.

Gruber, H., Heijde, M., Heller, W., Albert, A., Seidlitz, H.K. and Ulm, R. (2010), "Negative feedback regulation of UV-B-induced photomorphogenesis and stress acclimation in Arabidopsis", *Proceedings of the National Academy of Sciences of the United States of America*, Vol. 107 No. 46, pp. 20132–20137.

Guo, H., Duong, H., Ma, N. and Lin, C. (1999), "The Arabidopsis blue light receptor cryptochrome 2 is a nuclear protein regulated by a blue light-dependent post-transcriptional mechanism", *Plant Journal*, Vol. 19 No. 3, pp. 279–287.

Guo, Y., Zheng, Z., La Clair, J.J., Chory, J. and Noel, J.P. (2013), "Smoke-derived karrikin perception by the / -hydrolase KAI2 from Arabidopsis", *Proceedings of the National Academy of Sciences*, Vol. 110 No. 20, pp. 8284–8289.

Gutjahr, C., Gobbato, E., Choi, J., Riemann, M., Johnston, M.G., Summers, W., Carbonnel, S., et al. (2015), "Rice perception of symbiotic arbuscular mycorrhizal fungi requires the karrikin receptor complex", *Science*, Vol. 350 No. 6267, pp. 1521–1524.

Ha, C. Van, Leyva-Gonzalez, M.A., Osakabe, Y., Tran, U.T., Nishiyama, R., Watanabe, Y., Tanaka, M., et al. (2014), "Positive regulatory role of strigolactone in plant responses to drought and salt stress", *Proceedings of the National Academy of Sciences of the United States of America*, Vol. 111 No. 2, pp. 851–856.

Hajdu, A., Dobos, O., Domijan, M., Bálint, B., Nagy, I., Nagy, F. and Kozma-Bognár, L. (2018), "ELONGATED HYPOCOTYL 5 mediates blue light signalling to the Arabidopsis circadian clock", *Plant Journal*, Vol. 96 No. 6, pp. 1242–1254.

Hamon-Josse, M., Villaecija-Aguilar, J.A., Ljung, K., Leyser, O., Gutjahr, C. and Bennett, T. (2021), "KAI2 regulates seedling development by mediating light-induced remodelling of auxin transport", *BioRxiv*, p. 2021.05.06.443001.

Hardtke, C.S., Gohda, K., Osterlund, M.T., Oyama, T., Okada, K. and Deng, X.W. (2000), "HY5 stability and activity in Arabidopsis is regulated by phosphorylation in its COP1 binding domain", *EMBO Journal*, Vol. 19 No. 18, pp. 4997–5006.

Hayes, S., Sharma, A., Fraser, D.P., Trevisan, M., Cragg-Barber, C.K., Tavridou, E., Fankhauser, C., et al. (2017), "UV-B Perceived by the UVR8 Photoreceptor Inhibits Plant Thermomorphogenesis", *Current Biology*, Elsevier Ltd., Vol. 27 No. 1, pp. 120–127.

Hayes, S., Velanis, C.N., Jenkins, G.I. and Franklin, K.A. (2014), "UV-B detected by the UVR8 photoreceptor antagonizes auxin signaling and plant shade avoidance", *Proceedings of the National Academy of Sciences of the United States of America*, Vol. 111 No. 32, pp. 11894–11899.

Heijde, M. and Ulm, R. (2013), "Reversion of the Arabidopsis UV-B photoreceptor UVR8 to the homodimeric ground state", *Proceedings of the National Academy of Sciences of the United States of America*, Vol. 110 No. 3, pp. 1113–1118.

Hemerly, A.S., Ferreira, P., de Almeida Engler, J., Van Montagu, M., Engler, G. and Inze, D. (1993), "cdc2a expression in Arabidopsis is linked with competence for cell division", *Plant Cell*, Vol. 5 No. 12, pp. 1711–1723.

Heng, Y., Jiang, Y., Zhao, X., Zhou, H., Wang, X., Deng, X.W. and Xu, D. (2020), "Erratum: BBX4, a phyB-interacting and modulated regulator, directly interacts with PIF3 to fine tune red lightmediated photomorphogenesis (Proceedings of the National Academy of Sciences of the United States of America (2019) 116 (26049–26056) DOI: 10.107", *Proceedings of the National Academy of Sciences of the United States of America*, Vol. 117 No. 8, pp. 4429–4430.

Heng, Y., Lin, F., Jiang, Y., Ding, M., Yan, T., Lan, H., Zhou, H., et al. (2019), "B-Box Containing Proteins BBX30 and BBX31, Acting Downstream of HY5, Negatively Regulate Photomorphogenesis in Arabidopsis", *Plant Physiology*, Vol. 180 No. 1, pp. 497–508.

Hennig, L., Büche, C., Eichenberg, K. and Schäfer, E. (1999), "Dynamic properties of endogenous phytochrome A in Arabidopsis seedlings", *Plant Physiology*, Vol. 121 No. 2, pp. 571–577.

Hiltbrunner, A., Tscheuschler, A., Viczián, A., Kunkel, T., Kircher, S. and Schäfer, E. (2006), "FHY1 and FHL act together to mediate nuclear accumulation of the phytochrome A photoreceptor", *Plant and Cell Physiology*, Vol. 47 No. 8, pp. 1023–1034.

Hiltbrunner, A., Viczián, A., Bury, E., Tscheuschler, A., Kircher, S., Tóth, R., Honsberger, A., et al. (2005), "Nuclear accumulation of the phytochrome A photoreceptor requires FHY1", *Current Biology*, Vol. 15 No. 23, pp. 2125–2130.

Hoecker, U. (2017), "The activities of the E3 ubiquitin ligase COP1/SPA, a key repressor in light signaling", *Current Opinion in Plant Biology*, Elsevier Ltd, Vol. 37, pp. 63–69.

Hollender, C.A., Kang, C., Darwish, O., Geretz, A., Matthews, B.F., Slovin, J., Alkharouf, N., et al. (2014), "Floral transcriptomes in woodland strawberry uncover developing receptacle and anther gene networks", *Plant Physiology*, Vol. 165 No. 3, pp. 1062–1075.

Holm, M., Hardtke, C.S., Gaudet, R. and Deng, X.W. (2001), "Identification of a structural motif that confers specific interaction with the WD40 repeat domain of Arabidopsis COP1", *EMBO Journal*, Vol. 20 No. 1–2, pp. 118–127.

Holm, M., Ma, L.-G., Qu, L.-J. and Deng, X.-W. (2002), "Two interacting bZIP proteins are direct targets of COP1-mediated control of light-dependent gene expression in Arabidopsis.", *Genes & Development*, Vol. 16 No. 10, pp. 1247–59.

Holtan, H.E., Bandong, S., Marion, C.M., Adam, L., Tiwari, S., Shen, Y., Maloof, J.N., et al. (2011), "BBX32, an Arabidopsis B-Box Protein, Functions in Light Signaling by Suppressing HY5-Regulated Gene Expression and Interacting with STH2/BBX21", *Plant Physiology*, Vol. 156 No. 4, pp. 2109–2123.

Hornitschek, P., Kohnen, M. V., Lorrain, S., Rougemont, J., Ljung, K., López-Vidriero, I., Franco-Zorrilla, J.M., et al. (2012), "Phytochrome interacting factors 4 and 5 control seedling growth in changing light conditions by directly controlling auxin signaling", *The Plant Journal*, Vol. 71 No. 5, pp. 699–711.

Hornitschek, P., Lorrain, S., Zoete, V., Michielin, O. and Fankhauser, C. (2009), "Inhibition of the shade avoidance response by formation of non-DNA binding bHLH heterodimers.", *The EMBO Journal*, Vol. 28 No. 24, pp. 3893–902.

Hrdlička, J., Gucký, T., Novák, O., Kulkarni, M., Gupta, S., Van Staden, J. and Doležal, K. (2019), "Quantification of karrikins in smoke water using ultra-high performance liquid chromatography-tandem mass spectrometry", *Plant Methods*, BioMed Central, Vol. 15 No. 1, pp. 1–12.

Hu, L., Wang, J., Yang, C., Islam, F., Bouwmeester, H.J., Muños, S. and Zhou, W. (2020),

"The effect of virulence and resistance mechanisms on the interactions between parasitic plants and their hosts", *International Journal of Molecular Sciences*, Vol. 21 No. 23, pp. 1–27.

Huai, J., Jing, Y. and Lin, R. (2020), "Functional analysis of ZmCOP1 and ZmHY5 reveals conserved light signaling mechanism in maize and Arabidopsis", *Physiologia Plantarum*, Vol. 169 No. 3, pp. 369–379.

Huang, D.W., Sherman, B.T. and Lempicki, R.A. (2009a), "Bioinformatics enrichment tools: Paths toward the comprehensive functional analysis of large gene lists", *Nucleic Acids Research*, Vol. 37 No. 1, pp. 1–13.

Huang, D.W., Sherman, B.T. and Lempicki, R.A. (2009b), "Systematic and integrative analysis of large gene lists using DAVID bioinformatics resources", *Nature Protocols*, Vol. 4 No. 1, pp. 44–57.

Hughes, J., Lamparter, T., Mittmann, F., Hartmann, E., Gärtner, W., Wilde, A. and Börner, T. (1997), "A prokaryotic phytochrome", *Nature*, Vol. 386 No. 6626, pp. 663–663.

Huq, E., Al-Sady, B., Hudson, M., Kim, C., Apel, K. and Quail, P.H. (2004), "Phytochrome-interacting factor 1 is a critical bHLH regulator of chlorophyll biosynthesis.", *Science (New York, N.Y.)*, Vol. 305 No. 5692, pp. 1937–41.

Huq, E. and Quail, P.H. (2002), "PIF4, a phytochrome-interacting bHLH factor, functions as a negative regulator of phytochrome B signaling in Arabidopsis.", *The EMBO Journal*, Vol. 21 No. 10, pp. 2441–50.

Indorf, M., Cordero, J., Neuhaus, G. and Rodríguez-Franco, M. (2007), "Salt tolerance (STO), a stress-related protein, has a major role in light signalling", *Plant Journal*, Vol. 51 No. 4, pp. 563–574.

Jamil, M., Kountche, B.A. and Al-Babili, S. (2021), "Current progress in Striga management", *Plant Physiology*, Vol. 185 No. 4, pp. 1339–1352.

Jang, I., Henriques, R., Seo, H.S., Nagatani, A. and Chua, N. (2010), "Arabidopsis PHYTOCHROME INTERACTING FACTOR Proteins Promote Phytochrome B Polyubiquitination by COP1 E3 Ligase in the Nucleus", *The Plant Cell*, Vol. 22 No. 7, pp. 2370–2383.

Jenkins, G.I. (2017), "Photomorphogenic responses to ultraviolet-B light", *Plant Cell and Environment*, pp. 2544–2557.

Jeong, J. and Choi, G. (2013), "Phytochrome-Interacting Factors Have Both Shared and Distinct Biological Roles", pp. 371–380.

Jia, K.P., Luo, Q., He, S.B., Lu, X.D. and Yang, H.Q. (2014), "Strigolactone-regulated hypocotyl elongation is dependent on cryptochrome and phytochrome signaling pathways in arabidopsis", *Molecular Plant*, Â© The Authors. All rights reserved., Vol. 7 No. 3, pp. 528–540.

Jiang, L., Liu, X., Xiong, G., Liu, H., Chen, F., Wang, L., Meng, X., et al. (2013), "DWARF 53 acts as a repressor of strigolactone signalling in rice", *Nature*, Nature Publishing Group, Vol. 504 No. 7480, pp. 401–405.

Job, N., Yadukrishnan, P., Bursch, K., Datta, S. and Johansson, H. (2018), "Two B-box

proteins regulate photomorphogenesis by oppositely modulating HY5 through their diverse C-terminal domains", *Plant Physiology*, Vol. 176 No. 4, pp. 2963–2976.

Jones, A.M. and Quail, P.H. (1986), "Quaternary Structure of 124-Kilodalton Phytochrome from Avena sativa L.", *Biochemistry*, Vol. 25 No. 10, pp. 2987–2995.

Jung, J.H., Domijan, M., Klose, C., Biswas, S., Ezer, D., Gao, M., Khattak, A.K., et al. (2016), "Phytochromes function as thermosensors in Arabidopsis", *Science*, Vol. 354 No. 6314, pp. 886–889.

Kagiyama, M., Hirano, Y., Mori, T., Kim, S.Y., Kyozuka, J., Seto, Y., Yamaguchi, S., et al. (2013), "Structures of D14 and D14L in the strigolactone and karrikin signaling pathways", *Genes to Cells*, Vol. 18 No. 2, pp. 147–160.

Kaiserli, E. and Jenkins, G.I. (2007), "UV-B promotes rapid nuclear translocation of the Arabidopsis UV-B-specific signaling component UVR8 and activates its function in the nucleus", *Plant Cell*, Vol. 19 No. 8, pp. 2662–2673.

Karimi, M., Inzé, D. and Depicker, A. (2002), "GATEWAY^{TM} vectors for Agrobacterium-mediated plant transformation", *Trends in Plant Science*, Vol. 7 No. 5, pp. 193–195.

Kasahara, M., Kagawa, T., Oikawa, K., Suetsugu, N., Miyao, M. and Wada, M. (2002), "Chloroplast avoidance movement reduces photodamage in plants", *Nature*, Vol. 420 No. 6917, pp. 829–832.

Kathare, P.K., Xu, X., Nguyen, A. and Huq, E. (2020), "A COP1-PIF-HEC regulatory module fine-tunes photomorphogenesis in Arabidopsis", *Plant Journal*, Vol. 104 No. 1, pp. 113–123.

Khanna, R., Huq, E., Kikis, E.A., Al-Sady, B., Lanzatella, C. and Quail, P.H. (2004), "A Novel Molecular Recognition Motif Necessary for Targeting Photoactivated Phytochrome Signaling to Specific Basic Helix-Loop-Helix Transcription Factors", *The Plant Cell*, Vol. 16 No. 11, pp. 3033–3044.

Khanna, R., Kronmiller, B., Maszle, D.R., Coupland, G., Holm, M., Mizuno, T. and Wu, S.H. (2009), "The arabidopsis B-Box zinc finger family", *Plant Cell*, Vol. 21 No. 11, pp. 3416–3420.

Khoo, H.E., Azlan, A., Tang, S.T. and Lim, S.M. (2017), "Anthocyanidins and anthocyanins: Colored pigments as food, pharmaceutical ingredients, and the potential health benefits", *Food and Nutrition Research*, Taylor & Francis, Vol. 61 No. 1, available at:https://doi.org/10.1080/16546628.2017.1361779.

Khosla, A., Morffy, N., Li, Q., Faure, L., Chang, S.H., Yao, J., Zheng, J., et al. (2020), "Structure–Function analysis of SMAX1 reveals domains that mediate its karrikin-induced proteolysis and interaction with the receptor KAI2", *Plant Cell*, Vol. 32 No. 8, pp. 2639–2659.

Kim, D.H., Yamaguchi, S., Lim, S., Oh, E., Park, J., Hanada, A., Kamiya, Y., et al. (2008), "SOMNUS, a CCCH-type zinc finger protein in Arabidopsis, negatively regulates light-dependent seed germination downstream of PIL5.", *The Plant Cell*, Vol. 20 No. 5, pp. 1260–77.

Kirby, J. and Kavanagh, T.A. (2002), "NAN fusions: A synthetic sialidase reporter gene as a sensitive and versatile partner for GUS", *Plant Journal*, Vol. 32 No. 3, pp. 391–

400.

Kircher, S., Gil, P., Kozma-Bognár, L., Fejes, E., Speth, V., Husselstein-Muller, T., Bauer, D., et al. (2002), "Nucleocytoplasmic partitioning of the plant photoreceptors phytochrome A, B, C, D, and E is regulated differentially by light and exhibits a diurnal rhythm", *Plant Cell*, Vol. 14 No. 7, pp. 1541–1555.

Kleine, T., Lockhart, P. and Batschauer, A. (2003), "An Arabidopsis protein closely related to Synechocystis cryptochrome is targeted to organelles", *Plant Journal*, Vol. 35 No. 1, pp. 93–103.

Kleiner, O., Kircher, S., Harter, K. and Batschauer, A. (1999), "Nuclear localization of the Arabidopsis blue light receptor cryptochrome 2", *Plant Journal*, Vol. 19 No. 3, pp. 289–296.

Kliebenstein, D.J., Lim, J.E., Landry, L.G. and Last, R.L. (2002), "Arabidopsis UVR8 regulates ultraviolet-B signal transduction and tolerance and contains sequence similarity to human Regulator of Chromatin Condensation 1", *Plant Physiology*, Vol. 130 No. 1, pp. 234–243.

Klose, C., Nagy, F. and Schäfer, E. (2020), "Thermal Reversion of Plant Phytochromes", *Molecular Plant*, Chinese Society for Plant Biology, Vol. 13 No. 3, pp. 386–397.

Klose, C., Viczián, A., Kircher, S., Schäfer, E. and Nagy, F. (2015), "Molecular mechanisms for mediating light-dependent nucleo/cytoplasmic partitioning of phytochrome photoreceptors", *New Phytologist*, Vol. 206 No. 3, pp. 965–971.

Kobayashi, K., Baba, S., Obayashi, T., Sato, M., Toyooka, K., Keränen, M., Aro, E.M., et al. (2012), "Regulation of root greening by light and auxin/cytokinin signaling in Arabidopsis", *Plant Cell*, Vol. 24 No. 3, pp. 1081–1095.

Koini, M.A., Alvey, L., Allen, T., Tilley, C.A., Harberd, N.P., Whitelam, G.C. and Franklin, K.A. (2009), "High Temperature-Mediated Adaptations in Plant Architecture Require the bHLH Transcription Factor PIF4", *Current Biology*, Elsevier Ltd, Vol. 19 No. 5, pp. 408–413.

Koornneef, M., Rolff, E. and Spruit, C.J.P. (1980), "Genetic Control of Light-inhibited Hypocotyl Elongation in Arabidopsis thaliana (L.) Heynh", *Zeitschrift Für Pflanzenphysiologie*, Gustav Fischer Verlag Stuttgart, Vol. 100 No. 2, pp. 147–160.

de Lange, J.H. and Boucher, C. (1990), "Plant derived smoke as a seed germination cue", *South African Journal of Botany*, Elsevier Masson SAS, Vol. 56 No. 6, pp. 700–703.

Langmead, B. and Salzberg, S.L. (2012), "Fast gapped-read alignment with Bowtie 2", *Nature Methods*, Vol. 9 No. 4, pp. 357–359.

Lau, K., Podolec, R., Chappuis, R., Ulm, R. and Hothorn, M. (2019), " Plant photoreceptors and their signaling components compete for COP 1 binding via VP peptide motifs ", *The EMBO Journal*, Vol. 38 No. 18, pp. 1–18.

Lau, O.S. and Deng, X.W. (2010), "Plant hormone signaling lightens up: integrators of light and hormones", *Current Opinion in Plant Biology*, Elsevier Ltd, Vol. 13 No. 5, pp. 571–577.

Laubinger, S., Fittinghoff, K. and Hoecker, U. (2004), "The SPA quartet: A family of WD-repeat proteins with a central role in suppression of photomorphogenesis in

Arabidopsis", *Plant Cell*, Vol. 16 No. 9, pp. 2293–2306.

Laubinger, S., Marchal, V., Le Gourrierec, J., Wenkel, S., Andrian, J., Jang, S., Kulajta, C., et al. (2006), "Arabidopsis SPA proteins regulate photoperiodic flowering and interact with the floral inducer CONSTANS to regulate its stability", *Development*, Vol. 133 No. 22, pp. 4608–4608.

Lee, I., Choi, S., Lee, S. and Soh, M.S. (2019), "KAI2-KL signaling intersects with light-signaling for photomorphogenesis", *Plant Signaling and Behavior*, Taylor & Francis, Vol. 14 No. 4, pp. 1–4.

Lee, J., He, K., Stolc, V., Lee, H., Figueroa, P., Gao, Y., Tongprasit, W., et al. (2007), "Analysis of transcription factor HY5 genomic binding sites revealed its hierarchical role in light regulation of development", *Plant Cell*, Vol. 19 No. 3, pp. 731–749.

Legris, M., Ince, Y.Ç. and Fankhauser, C. (2019), "Molecular mechanisms underlying phytochrome-controlled morphogenesis in plants", *Nature Communications*, Springer US, Vol. 10 No. 1, available at:https://doi.org/10.1038/s41467-019-13045-0.

Legris, M., Klose, C., Burgie, E.S., Rojas, C.C., Neme, M., Hiltbrunner, A., Wigge, P.A., et al. (2016), "Phytochrome B integrates light and temperature signals in Arabidopsis", *Science*, Vol. 354 No. 6314, pp. 897–900.

Leivar, P. and Monte, E. (2014), "PIFs: Systems integrators in plant development", *Plant Cell*, Vol. 26 No. 1, pp. 56–78.

Leivar, P., Monte, E., Al-Sady, B., Carle, C., Storer, A., Alonso, J.M., Ecker, J.R., et al. (2008), "The Arabidopsis Phytochrome-Interacting Factor PIF7, Together with PIF3 and PIF4, Regulates Responses to Prolonged Red Light by Modulating phyB Levels", *The Plant Cell*, Vol. 20 No. 2, pp. 337–352.

Leivar, P., Monte, E., Oka, Y., Liu, T., Carle, C., Castillon, A., Huq, E., et al. (2008), "Multiple Phytochrome-Interacting bHLH Transcription Factors Repress Premature Seedling Photomorphogenesis in Darkness", *Current Biology*, Vol. 18 No. 23, pp. 1815–1823.

Li, B. and Dewey, C.N. (2011), "RSEM: accurate transcript quantification from RNA-Seq data with or without a reference genome", edited by Liu, Y.*BMC Bioinformatics*, Apple Academic Press, Vol. 12 No. 1, p. 323.

Li, C., Pei, J., Yan, X., Cui, X., Tsuruta, M., Liu, Y. and Lian, C. (2021), "A poplar B-box protein PtrBBX23 modulates the accumulation of anthocyanins and proanthocyanidins in response to high light", *Plant, Cell & Environment*, p. pce.14127.

Li, F.W., Melkonian, M., Rothfels, C.J., Villarreal, J.C., Stevenson, D.W., Graham, S.W., Wong, G.K.S., et al. (2015), "Phytochrome diversity in green plants and the origin of canonical plant phytochromes", *Nature Communications*, Nature Publishing Group, Vol. 6, pp. 1–12.

Li, L., Ljung, K., Breton, G., Schmitz, R.J., Pruneda-Paz, J., Cowing-Zitron, C., Cole, B.J., et al. (2012), "Linking photoreceptor excitation to changes in plant architecture", *Genes and Development*, Vol. 26 No. 8, pp. 785–790.

Li, Q.F. and He, J.X. (2016), "BZR1 Interacts with HY5 to Mediate Brassinosteroid- and

Light-Regulated Cotyledon Opening in Arabidopsis in Darkness", *Molecular Plant*, Elsevier, Vol. 9 No. 1, pp. 113–125.

Li, W., Nguyen, K.H., Chu, H.D., Ha, C. Van, Watanabe, Y., Osakabe, Y., Leyva-González, M.A., et al. (2017), "The karrikin receptor KAI2 promotes drought resistance in Arabidopsis thaliana", *PLoS Genetics*, Vol. 13 No. 11, pp. 1–23.

Li, W., Nguyen, K.H., Chu, H.D., Watanabe, Y., Osakabe, Y., Sato, M., Toyooka, K., et al. (2020), "Comparative functional analyses of DWARF14 and KARRIKIN INSENSITIVE 2 in drought adaptation of Arabidopsis thaliana", *Plant Journal*, Vol. 103 No. 1, pp. 111–127.

Li, W., Wang, J., Sun, Q., Li, W., Yu, Y., Zhao, M. and Meng, Z. (2017), "Expression analysis of genes encoding double B-box zinc finger proteins in maize", *Functional and Integrative Genomics*, Functional & Integrative Genomics, Vol. 17 No. 6, pp. 653–666.

Lian, H.L., He, S.B., Zhang, Y.C., Zhu, D.M., Zhang, J.Y., Jia, K.P., Sun, S.X., et al. (2011), "Blue-light-dependent interaction of cryptochrome 1 with SPA1 defines a dynamic signaling mechanism", *Genes and Development*, Vol. 25 No. 10, pp. 1023–1028.

Light, M.E., Daws, M.I. and Van Staden, J. (2009), "Smoke-derived butenolide: Towards understanding its biological effects", *South African Journal of Botany*, SAAB, Vol. 75 No. 1, pp. 1–7.

Lin, C., Robertson, D.E., Ahmad, M., Raibekas, A.A., Jorns, M.S., Dutton, P.L. and Cashmore, A.R. (1995), "Association of flavin adenine dinucleotide with the Arabidopsis blue light receptor CRY1", *Science*, Vol. 269 No. 5226, pp. 968–970.

Lin, C., Yang, H., Guo, H., Mockler, T., Chen, J. and Cashmore, A.R. (1998), "Enhancement of blue-light sensitivity of Arabidopsis seedlings by a blue light receptor cryptochrome 2", *Proceedings of the National Academy of Sciences of the United States of America*, Vol. 95 No. 5, pp. 2686–2690.

Lin, F., Jiang, Y., Li, J., Yan, T., Fan, L., Liang, J., Chen, Z.J., et al. (2018), "B-BOX DOMAIN PROTEIN28 negatively regulates photomorphogenesis by repressing the activity of transcription factor hy5 and undergoes COP1-mediated degradation", *Plant Cell*, Vol. 30 No. 9, pp. 2006–2019.

Liscum, E., Askinosie, S.K., Leuchtman, D.L., Morrow, J., Willenburg, K.T. and Coats, D.R. (2014), "Phototropism: Growing towards an understanding of plant movement", *Plant Cell*, Vol. 26 No. 1, pp. 38–55.

Liu, B., Zuo, Z., Liu, H., Liu, X. and Lin, C. (2011), "Arabidopsis cryptochrome 1 interacts with SPA1 to suppress COP1 activity in response to blue light", *Genes and Development*, Vol. 25 No. 10, pp. 1029–1034.

Liu, H., Yu, X., Li, K., Klejnot, J., Yang, H., Lisiero, D. and Lin, C. (2008), "Photoexcited CRY2 Interacts with CIB1 to Regulate Transcription and Floral Initiation in Arabidopsis", *Science*, Vol. 322 No. 5907, pp. 1535–1539.

Liu, P. and Sharrock, R.A. (2017), "Biological activity and dimerization state of modified phytochrome A proteins", *PLoS ONE*, Vol. 12 No. 10, pp. 1–18.

Liu, Q., Wang, Q., Deng, W., Wang, X., Piao, M., Cai, D., Li, Y., et al. (2017), "Molecular

basis for blue light-dependent phosphorylation of Arabidopsis cryptochrome 2", *Nature Communications*, Nature Publishing Group, Vol. 8 No. May, pp. 1–12.

Liu, Q., Wang, Q., Liu, B., Wang, W., Wang, X., Park, J., Yang, Z., et al. (2016), "The Blue Light-Dependent Polyubiquitination and Degradation of Arabidopsis Cryptochrome2 Requires Multiple E3 Ubiquitin Ligases", *Plant and Cell Physiology*, Vol. 57 No. 10, pp. 2175–2186.

Liu, Y., Li, X., Li, K., Liu, H. and Lin, C. (2013), "Multiple bHLH Proteins form Heterodimers to Mediate CRY2-Dependent Regulation of Flowering-Time in Arabidopsis", *PLoS Genetics*, Vol. 9 No. 10, available at:https://doi.org/10.1371/journal.pgen.1003861.

Liu, Y., Lin, G., Yin, C. and Fang, Y. (2020), "B-box transcription factor 28 regulates flowering by interacting with constans", *Scientific Reports*, Nature Publishing Group UK, Vol. 10 No. 1, p. 17789.

Lorrain, S., Allen, T., Duek, P.D., Whitelam, G.C. and Fankhauser, C. (2007), "Phytochrome-mediated inhibition of shade avoidance involves degradation of growth-promoting bHLH transcription factors", *The Plant Journal*, Vol. 53 No. 2, pp. 312–323.

Love, M.I., Huber, W. and Anders, S. (2014), "Moderated estimation of fold change and dispersion for RNA-seq data with DESeq2", *Genome Biology*, Vol. 15 No. 12, pp. 1–21.

Lovering, R., Hanson, I.M., Borden, K.L.B., Martin, S., O'Reilly, N.J., Evan, G.I., Rahman, D., et al. (1993), "Identification and preliminary characterization of a protein motif related to the zinc finger", *Proceedings of the National Academy of Sciences of the United States of America*, Vol. 90 No. 6, pp. 2112–2116.

Lu, X.D., Zhou, C.M., Xu, P.B., Luo, Q., Lian, H.L. and Yang, H.Q. (2015), "Red-light-dependent interaction of phyB with SPA1 promotes COP1-SPA1 dissociation and photomorphogenic development in arabidopsis", *Molecular Plant*, Elsevier Ltd, Vol. 8 No. 3, pp. 467–478.

Luo, D., Xiong, C., Lin, A., Zhang, C., Sun, W., Zhang, J., Yang, C., et al. (2021), "SlBBX20 interacts with the COP9 signalosome subunit SlCSN5-2 to regulate anthocyanin biosynthesis by activating SlDFR expression in tomato", *Horticulture Research*, Springer US, Vol. 8 No. 1, p. 163.

Luo, Q., Lian, H., He, S., Li, L., Jia, K. and Yang, H. (2014), "COP1 and phyB Physically Interact with PIL1 to Regulate Its Stability and Photomorphogenic Development in Arabidopsis", *The Plant Cell*, Vol. 26 No. 6, pp. 2441–2456.

Ma, D., Li, X., Guo, Y., Chu, J., Fang, S., Yan, C., Noel, J.P., et al. (2016), "Cryptochrome 1 interacts with PIF4 to regulate high temperature-mediated hypocotyl elongation in response to blue light", *Proceedings of the National Academy of Sciences of the United States of America*, Vol. 113 No. 1, pp. 224–229.

Ma, L., Gao, Y., Qu, L., Chen, Z., Li, J., Zhao, H. and Deng, X.W. (2002), "Genomic evidence for COP1 as a repressor of light-regulated gene expression and development in Arabidopsis", *Plant Cell*, Vol. 14 No. 10, pp. 2383–2398.

Ma, L., Li, J., Qu, L., Hager, J., Chen, Z. and Zhao, H. (2001), "Light Control of

Arabidopsis Development Entails Coordinated", *Society*, Vol. 13 No. December, pp. 2589–2607.

Malamy, J.E. and Benfey, P.N. (1997), "Organization and cell differentiation in lateral roots of Arabidopsis thaliana", *Development*, Vol. 124 No. 1, pp. 33–44.

Malhotra, K., Kim, S.T., Batschauer, A., Dawut, L. and Sancar, A. (1995), "Putative Blue-Light Photoreceptors from Arabidopsis thaliana and Sinapis alba with a High Degree of Sequence Homology to DNA Photolyase Contain the Two Photolyase Cofactors but Lack DNA Repair Activity", *Biochemistry*, Vol. 34 No. 20, pp. 6892–6899.

Martín, G., Rovira, A., Veciana, N., Soy, J., Toledo-Ortiz, G., Gommers, C.M.M., Boix, M., et al. (2018), "Circadian Waves of Transcriptional Repression Shape PIF-Regulated Photoperiod-Responsive Growth in Arabidopsis", *Current Biology*, Vol. 28 No. 2, pp. 311-318.e5.

Martínez-García, J.F., Huq, E. and Quail, P.H. (2000), "Direct targeting of light signals to a promoter element-bound transcription factor.", *Science (New York, N.Y.)*, Vol. 288 No. 5467, pp. 859–63.

Mas, P., Devlin, P.F., Panda, S. and Kay, S.A. (2000), "Functional interaction of phytochrome B and cryptochrome 2", *Nature*, Vol. 408 No. 6809, pp. 207–211.

Mathews, S. (2010), "Evolutionary studies illuminate the structural-functional model of plant phytochromes", *Plant Cell*, Vol. 22 No. 1, pp. 4–16.

McNellis, T.W., von Arnim, A.G., Araki, T., Komeda, Y., Misera, S. and Deng Xing Wang. (1994), "Genetic and molecular analysis of an allelic series of cop1 mutants suggests functional roles for the multiple protein domains", *Plant Cell*, Vol. 6 No. 4, pp. 487–500.

Merritt, D.J., Kristiansen, M., Flematti, G.R., Turner, S.R., Ghisalberti, E.L., Trengove, R.D. and Dixon, K.W. (2006), "Effects of a butenolide present in smoke on light-mediated germination of Australian Asteraceae", *Seed Science Research*, Vol. 16 No. 1, pp. 29–35.

Mes, P.J., Boches, P., Myers, J.R. and Durst, R. (2008), "Characterization of tomatoes expressing anthocyanin in the fruit", *Journal of the American Society for Horticultural Science*, Vol. 133 No. 2, pp. 262–269.

Mi, H., Muruganujan, A., Huang, X., Ebert, D., Mills, C., Guo, X. and Thomas, P.D. (2019), "Protocol Update for large-scale genome and gene function analysis with the PANTHER classification system (v.14.0)", *Nature Protocols*, Springer US, Vol. 14 No. 3, pp. 703–721.

Miséra, S., Müller, A.J., Weiland-Heidecker, U. and Jürgens, G. (1994), "The FUSCA genes of Arabidopsis: negative regulators of light responses", *MGG Molecular & General Genetics*, Vol. 244 No. 3, pp. 242–252.

Monte, E., Alonso, J.M., Ecker, J.R., Zhang, Y., Li, X., Young, J., Austin-Phillips, S., et al. (2003), "Isolation and characterization of phyC mutants in Arabidopsis reveals complex crosstalk between phytochrome signaling pathways", *Plant Cell*, Vol. 15 No. 9, pp. 1962–1980.

Monte, E., Tepperman, J.M., Al-Sady, B., Kaczorowski, K.A., Alonso, J.M., Ecker, J.R.,

Li, X., et al. (2004), “The phytochrome-interacting transcription factor, PIF3, acts early, selectively, and positively in light-induced chloroplast development”, *Proceedings of the National Academy of Sciences*, Vol. 101 No. 46, pp. 16091–16098.

Moon, J., Zhu, L., Shen, H. and Huq, E. (2008), “PIF1 directly and indirectly regulates chlorophyll biosynthesis to optimize the greening process in Arabidopsis”, *Proceedings of the National Academy of Sciences of the United States of America*, Vol. 105 No. 27, pp. 9433–9438.

Morffy, N., Faure, L. and Nelson, D.C. (2016), “Smoke and Hormone Mirrors: Action and Evolution of Karrikin and Strigolactone Signaling”, *Trends in Genetics*, Elsevier Ltd, Vol. 32 No. 3, pp. 176–188.

Nagatani, A., Reed, J.W. and Chory, J. (1993), “Isolation and initial characterization of Arabidopsis mutants that are deficient in phytochrome A”, *Plant Physiology*, Vol. 102 No. 1, pp. 269–277.

Nakagawa, T., Kurose, T., Hino, T., Tanaka, K., Kawamukai, M., Niwa, Y., Toyooka, K., et al. (2007), “Development of series of gateway binary vectors, pGWBs, for realizing efficient construction of fusion genes for plant transformation”, *Journal of Bioscience and Bioengineering*, Vol. 104 No. 1, pp. 34–41.

Nawkar, G.M., Kang, C.H., Maibam, P., Park, J.H., Jung, Y.J., Chae, H.B., Chi, Y.H., et al. (2017), “HY5, a positive regulator of light signaling, negatively controls the unfolded protein response in Arabidopsis”, *Proceedings of the National Academy of Sciences of the United States of America*, Vol. 114 No. 8, pp. 2084–2089.

Nelson, D.C., Flematti, G.R., Ghisalberti, E.L., Dixon, K.W. and Smith, S.M. (2012), “Regulation of Seed Germination and Seedling Growth by Chemical Signals from Burning Vegetation”, *Annual Review of Plant Biology*, Vol. 63 No. 1, pp. 107–130.

Nelson, D.C., Flematti, G.R., Riseborough, J.A., Ghisalberti, E.L., Dixon, K.W. and Smitha, S.M. (2010), “Karrikins enhance light responses during germination and seedling development in Arabidopsis thaliana”, *Proceedings of the National Academy of Sciences of the United States of America*, Vol. 107 No. 15, pp. 7095–7100.

Nelson, D.C., Riseborough, J.A., Flematti, G.R., Stevens, J., Ghisalberti, E.L., Dixon, K.W. and Smith, S.M. (2009), “Karrikins discovered in smoke trigger arabidopsis seed germination by a mechanism requiring gibberellic acid synthesis and light”, *Plant Physiology*, Vol. 149 No. 2, pp. 863–873.

Nelson, D.C., Scaffidi, A., Dun, E.A., Waters, M.T., Flematti, G.R., Dixon, K.W., Beveridge, C.A., et al. (2011), “F-box protein MAX2 has dual roles in karrikin and strigolactone signaling in Arabidopsis thaliana”, *Proceedings of the National Academy of Sciences of the United States of America*, Vol. 108 No. 21, pp. 8897–8902.

Ni, M., Tepperman, J.M. and Quail, P.H. (1998), “PIF3, a Phytochrome-Interacting Factor Necessary for Normal Photoinduced Signal Transduction, Is a Novel Basic Helix-Loop-Helix Protein”, *Cell*, Vol. 95 No. 5, pp. 657–667.

Ni, M., Tepperman, J.M. and Quail, P.H. (1999), “Binding of phytochrome B to its nuclear signalling partner PIF3 is reversibly induced by light.”, *Nature*, Vol. 400 No.

6746, pp. 781–4.

Norén, L., Kindgren, P., Stachula, P., Rühl, M., Eriksson, M.E., Hurry, V. and Strand, Å. (2016), "Circadian and plastid signaling pathways are integrated to ensure correct expression of the CBF and COR genes during photoperiodic growth", *Plant Physiology*, Vol. 171 No. 2, pp. 1392–1406.

Nozue, K., Covington, M.F., Duek, P.D., Lorrain, S., Fankhauser, C., Harmer, S.L. and Maloof, J.N. (2007), "Rhythmic growth explained by coincidence between internal and external cues", *Nature*, Vol. 448 No. 7151, pp. 358–361.

Oh, E., Kim, J., Park, E., Kim, J., Kang, C. and Choi, G. (2004), "PIL5, a phytochrome-interacting basic helix-loop-helix protein, is a key negative regulator of seed germination in Arabidopsis thaliana.", *The Plant Cell*, Vol. 16 No. 11, pp. 3045–58.

Oh, E., Yamaguchi, S., Kamiya, Y., Bae, G., Chung, W. and Choi, G. (2006), "Light activates the degradation of PIL5 protein to promote seed germination through gibberellin in Arabidopsis", *The Plant Journal*, Vol. 47 No. 1, pp. 124–139.

Oh, J., Park, E., Song, K., Bae, G. and Choi, G. (2020), "PHYTOCHROME INTERACTING FACTOR8 Inhibits Phytochrome A-Mediated Far-Red Light Responses in Arabidopsis", *The Plant Cell*, Vol. 32 No. 1, pp. 186–205.

Oravecz, A., Baumann, A., Máté, Z., Brzezinska, A., Molinier, J., Oakeley, E.J., Ádám, É., et al. (2006), "CONSTITUTIVELY PHOTOMORPHOGENIC1 is required for the UV-B response in Arabidopsis", *Plant Cell*, Vol. 18 No. 8, pp. 1975–1990.

Ordoñez-Herrera, N., Fackendahl, P., Yu, X., Schaefer, S., Koncz, C. and Hoecker, U. (2015), "A cop1 spa mutant deficient in COP1 and SPA proteins reveals partial Co-action of COP1 and SPA during arabidopsis post-embryonic development and photomorphogenesis", *Molecular Plant*, Vol. 8 No. 3, pp. 479–481.

Osterlund, M.T., Hardtke, C.S., Wei, N. and Deng, X.W. (2000), "Targeted destabilization of HY5 during light-regulated development of Arabidopsis", *Nature*, Vol. 405 No. 6785, pp. 462–466.

Oyama, T., Shimura, Y. and Okada, K. (1997), "The Arabidopsis HY5 gene encodes a bZIP protein that regulates stimulus- induced development of root and hypocotyl", *Genes and Development*, Vol. 11 No. 22, pp. 2983–2995.

Pacín, M., Legris, M. and Casal, J.J. (2014), "Rapid decline in nuclear COSTITUTIVE PHOTOMORPHOGENESIS1 abundance anticipates the stabilization of its target ELONGATED HYPOCOTYL5 in the light", *Plant Physiology*, Vol. 164 No. 3, pp. 1134–1138.

Paik, I. and Huq, E. (2019), "Plant photoreceptors: Multi-functional sensory proteins and their signaling networks", *Seminars in Cell and Developmental Biology*, Elsevier, Vol. 92 No. April 2018, pp. 114–121.

Paik, I., Kathare, P.K., Kim, J.-I. and Huq, E. (2017), "Expanding Roles of PIFs in Signal Integration from Multiple Processes", *Molecular Plant*, Vol. 10 No. 8, pp. 1035–1046.

Park, E., Kim, J., Lee, Y., Shin, J., Oh, E., Chung, W., Liu, J.R., et al. (2004), "Degradation of phytochrome interacting factor 3 in phytochrome-mediated light signaling.", *Plant & Cell Physiology*, Vol. 45 No. 8, pp. 968–75.

Parks, B.M. and Quail, P.H. (1993), “hy8, a new class of arabidopsis long hypocotyl mutants deficient in functional phytochrome A.”, *The Plant Cell*, Vol. 5 No. 1, pp. 39–48.

de Pascual-Teresa, S., Moreno, D.A. and García-Viguera, C. (2010), “Flavanols and anthocyanins in cardiovascular health: A review of current evidence”, *International Journal of Molecular Sciences*, Vol. 11 No. 4, pp. 1679–1703.

Pedmale, U. V., Huang, S.S.C., Zander, M., Cole, B.J., Hetzel, J., Ljung, K., Reis, P.A.B., et al. (2016), “Cryptochromes Interact Directly with PIFs to Control Plant Growth in Limiting Blue Light”, *Cell*, Elsevier Inc., Vol. 164 No. 1–2, pp. 233–245.

Piskacek, S., Gregor, M., Nemethova, M., Grabner, M., Kovarik, P. and Piskacek, M. (2007), “Nine-amino-acid transactivation domain: Establishment and prediction utilities”, *Genomics*, Vol. 89 No. 6, pp. 756–768.

Podolec, R., Demarsy, E. and Ulm, R. (2021), “Perception and Signaling of Ultraviolet-B Radiation in Plants.”, *Annual Review of Plant Biology*, Vol. 72 No. 1, pp. 793–822.

Podolec, R. and Ulm, R. (2018), “Photoreceptor-mediated regulation of the COP1/SPA E3 ubiquitin ligase”, *Current Opinion in Plant Biology*, Elsevier Ltd, Vol. 45, pp. 18–25.

Pokorny, R., Klar, T., Hennecke, U., Carell, T., Batschauer, A. and Essen, L.O. (2008), “Recognition and repair of UV lesions in loop structures of duplex DNA by DASH-type cryptochrome”, *Proceedings of the National Academy of Sciences of the United States of America*, Vol. 105 No. 52, pp. 21023–21027.

Ponnu, J. and Hoecker, U. (2021), “Illuminating the COP1/SPA Ubiquitin Ligase: Fresh Insights Into Its Structure and Functions During Plant Photomorphogenesis”, *Frontiers in Plant Science*, Vol. 12 No. March, pp. 1–19.

Ponnu, J., Riedel, T., Penner, E., Schrader, A. and Hoecker, U. (2019), “Cryptochrome 2 competes with COP1 substrates to repress COP1 ubiquitin ligase activity during Arabidopsis photomorphogenesis”, *Proceedings of the National Academy of Sciences of the United States of America*, Vol. 116 No. 52, pp. 27133–27141.

Putterill, J., Robson, F., Lee, K., Simon, R. and Coupland, G. (1995), “The CONSTANS gene of Arabidopsis promotes flowering and encodes a protein showing similarities to zinc finger transcription factors”, *Cell*, Vol. 80 No. 6, pp. 847–857.

Qian, C., Mao, W., Liu, Y., Ren, H., Lau, O.S., Ouyang, X. and Huang, X. (2016), “Dual-Source Nuclear Monomers of UV-B Light Receptor Direct Photomorphogenesis in Arabidopsis”, *Molecular Plant*, Vol. 9 No. 12, pp. 1671–1674.

Quail, P. (1991), “Phytochrome: A Light-Activated Molecular Switch That Regulates Plant Gene Expression”, *Annual Review of Genetics*, Vol. 25 No. 1, pp. 389–409.

Quint, M., Delker, C., Franklin, K.A., Wigge, P.A., Halliday, K.J. and Van Zanten, M. (2016), “Molecular and genetic control of plant thermomorphogenesis”, *Nature Plants*, Macmillan Publishers Limited, Vol. 2 No. January, pp. 1–9.

Rausenberger, J., Tscheuschler, A., Nordmeier, W., Wüst, F., Timmer, J., Schäfer, E., Fleck, C., et al. (2011), “Photoconversion and Nuclear Trafficking Cycles Determine Phytochrome A’s Response Profile to Far-Red Light”, *Cell*, Vol. 146 No. 5, pp. 813–

825.

Reddy, B.A. and Etkin, L.D. (1991), “A unique bipartite cysteine-histidine motif defines a subfamily of potential zinc-finger proteins”, *Nucleic Acids Research*, Vol. 19 No. 22, p. 6330.

Reddy, B.A., Kloc, M. and Etkin, L. (1991), “The cloning and characterization of a maternally expressed novel zinc finger nuclear phosphoprotein (xnf7) in Xenopus laevis”, *Developmental Biology*, Vol. 148 No. 1, pp. 107–116.

Reed, J.W., Nagatani, A., Elich, T.D., Fagan, M. and Chory, J. (1994), “Phytochrome A and phytochrome B have overlapping but distinct functions in Arabidopsis development”, *Plant Physiology*, Vol. 104 No. 4, pp. 1139–1149.

Reed, J.W., Nagpal, P., Poole, D.S., Furuya, M. and Chory, J. (1993), “Mutations in the gene for the red/far-red light receptor phytochrome B alter cell elongation and physiological responses throughout arabidopsis development”, *Plant Cell*, Vol. 5 No. 2, pp. 147–157.

Rizzini, L., Favory, J.-J., Cloix, C., Faggionato, D., O’Hara, A., Kaiserli, E., Baumeister, R., et al. (2011), “Perception of UV-B by the Arabidopsis UVR8 protein.”, *Science (New York, N.Y.)*, Vol. 332 No. 6025, pp. 103–6.

Robson, F., Costa, M.M.R., Hepworth, S.R., Vizir, I., Piñeiro, M., Reeves, P.H., Putterill, J., et al. (2001), “Functional importance of conserved domains in the flowering-time gene CONSTANS demonstrated by analysis of mutant alleles and transgenic plants”, *Plant Journal*, Vol. 28 No. 6, pp. 619–631.

Rockwell, N.C., Su, Y.-S. and Lagarias, J.C. (2006), “Phytochrome structure and signaling mechanisms.”, *Annual Review of Plant Biology*, Vol. 57 No. 1, pp. 837–58.

Ruckle, M.E., DeMarco, S.M. and Larkin, R.M. (2007), “Plastid signals remodel light signaling networks and are essential for efficient chloroplast biogenesis in Arabidopsis”, *Plant Cell*, Vol. 19 No. 12, pp. 3944–3960.

Saijo, Y., Sullivan, J.A., Wang, H., Yang, J., Shen, Y., Rubio, V., Ma, L., et al. (2003), “The COP1-SPA1 interaction defines a critical step in phytochrome A-mediated regulation of HY5 activity”, *Genes and Development*, Vol. 17 No. 21, pp. 2642–2647.

Sánchez-Lamas, M., Lorenzo, C.D. and Cerdán, P.D. (2016), “Bottom-up Assembly of the Phytochrome Network”, *PLoS Genetics*, Vol. 12 No. 11, pp. 1–24.

Sang, Y., Li, Q.H., Rubio, V., Zhang, Y.C., Mao, J., Deng, X.W. and Yang, H.Q. (2005), “N-terminal domain-mediated homodimerization is required for photoreceptor activity of Arabidopsis Cryptochrome 1”, *Plant Cell*, Vol. 17 No. 5, pp. 1569–1584.

Sarmiento, F. (2013), “The BBX subfamily IV: Additional cogs and sprockets to fine-tune light-dependent development”, *Plant Signaling and Behavior*, Vol. 8 No. 4, available at:https://doi.org/10.4161/psb.23831.

Scaffidi, A., Waters, M.T., Ghisalberti, E.L., Dixon, K.W., Flematti, G.R. and Smith, S.M. (2013), “Carlactone-independent seedling morphogenesis in Arabidopsis”, *Plant Journal*, Vol. 76 No. 1, pp. 1–9.

Scaffidi, A., Waters, M.T., Sun, Y.K., Skelton, B.W., Dixon, K.W., Ghisalberti, E.L., Flematti, G.R., et al. (2014), "Strigolactone Hormones and Their Stereoisomers Signal through Two Related Receptor Proteins to Induce Different Physiological Responses in Arabidopsis", *Plant Physiology*, Vol. 165 No. 3, pp. 1221–1232.

Sentandreu, M., Martín, G., González-Schain, N., Leivar, P., Soy, J., Tepperman, J.M., Quail, P.H., et al. (2011), "Functional profiling identifies genes involved in organ-specific branches of the PIF3 regulatory network in Arabidopsis", *Plant Cell*, Vol. 23 No. 11, pp. 3974–3991.

Seo, H.S., Watanabe, E., Tokutomi, S., Nagatani, A. and Chua, N.H. (2004), "Photoreceptor ubiquitination by COP1 E3 ligase desensitizes phytochrome A signaling", *Genes and Development*, Vol. 18 No. 6, pp. 617–622.

Seto, Y., Sado, A., Asami, K., Hanada, A., Umehara, M., Akiyama, K. and Yamaguchi, S. (2014), "Carlactone is an endogenous biosynthetic precursor for strigolactones", *Proceedings of the National Academy of Sciences of the United States of America*, Vol. 111 No. 4, pp. 1640–1645.

Shalitin, D., Yang, H., Mockler, T.C., Maymon, M., Guo, H., Whitelam, G.C. and Lin, C. (2002), "Regulation of Arabidopsis cryptochrome 2 by blue-light-dependent phosphorylation", *Nature*, Vol. 417 No. 6890, pp. 763–767.

Shalitin, D., Yu, X., Maymon, M., Mockler, T. and Lin, C. (2003), "Blue Light-Dependent in Vivo and in Vitro Phosphorylation of Arabidopsis Cryptochrome 1", *Plant Cell*, Vol. 15 No. 10, pp. 2421–2429.

Shao, K., Zhang, X., Li, X., Hao, Y., Huang, X., Ma, M., Zhang, M., et al. (2020), "The oligomeric structures of plant cryptochromes", *Nature Structural and Molecular Biology*, Vol. 27 No. 5, pp. 480–488.

Sharrock, R.A. (2008), "The phytochrome red/far-red photoreceptor superfamily", *Genome Biology*, Vol. 9 No. 8, p. 230.

Sharrock, R.A. and Clack, T. (2002), "Patterns of Expression and Normalized Levels of the Five Arabidopsis Phytochromes", *Plant Physiology*, Vol. 130 No. 1, pp. 442–456.

Sharrock, R.A. and Clack, T. (2004), "Heterodimerization of type II phytochromes in Arabidopsis", *Proceedings of the National Academy of Sciences*, Vol. 101 No. 31, pp. 11500–11505.

Sheerin, D.J. and Hiltbrunner, A. (2017), "Molecular mechanisms and ecological function of far-red light signalling", *Plant Cell and Environment*, pp. 2509–2529.

Sheerin, D.J., Menon, C., zur Oven-Krockhaus, S., Enderle, B., Zhu, L., Johnen, P., Schleifenbaum, F., et al. (2015), "Light-Activated Phytochrome A and B Interact with Members of the SPA Family to Promote Photomorphogenesis in Arabidopsis by Reorganizing the COP1/SPA Complex", *The Plant Cell*, Vol. 27 No. 1, pp. 189–201.

Shen, H., Luong, P. and Huq, E. (2007), "The F-box protein MAX2 functions as a positive regulator of photomorphogenesis in Arabidopsis", *Plant Physiology*, Vol. 145 No. 4, pp. 1471–1483.

Shen, H., Moon, J. and Huq, E. (2005), "PIF1 is regulated by light-mediated degradation

through the ubiquitin-26S proteasome pathway to optimize photomorphogenesis of seedlings in Arabidopsis.", *The Plant Journal : For Cell and Molecular Biology*, Vol. 44 No. 6, pp. 1023–35.

Shen, H., Zhu, L., Bu, Q.Y. and Huq, E. (2012), "MAX2 affects multiple hormones to promote photomorphogenesis", *Molecular Plant*, © The Authors. All rights reserved., Vol. 5 No. 3, pp. 750–762.

Shen, H., Zhu, L., Castillon, A., Majee, M., Downie, B. and Huq, E. (2008), "Light-Induced Phosphorylation and Degradation of the Negative Regulator PHYTOCHROME-INTERACTING FACTOR1 from Arabidopsis Depend upon Its Direct Physical Interactions with Photoactivated Phytochromes", *The Plant Cell*, Vol. 20 No. 6, pp. 1586–1602.

Shen, Y., Khanna, R., Carle, C.M. and Quail, P.H. (2007), "Phytochrome induces rapid PIF5 phosphorylation and degradation in response to red-light activation.", *Plant Physiology*, Vol. 145 No. 3, pp. 1043–51.

Shi, Q.M., Yang, X., Song, L. and Xue, H.W. (2011), "Arabidopsis MSBP1 is activated by HY5 and HYH and is involved in photomorphogenesis and brassinosteroid sensitivity regulation", *Molecular Plant*, The Authors 2011. All rights reserved., Vol. 4 No. 6, pp. 1092–1104.

Shim, J.S., Kubota, A. and Imaizumi, T. (2017), "Circadian clock and photoperiodic flowering in arabidopsis: CONSTANS is a Hub for Signal integration", *Plant Physiology*, Vol. 173 No. 1, pp. 5–15.

Shimada, T.L., Shimada, T. and Hara-Nishimura, I. (2010), "A rapid and non-destructive screenable marker, FAST, for identifying transformed seeds of Arabidopsis thaliana: TECHNICAL ADVANCE", *Plant Journal*, Vol. 61 No. 3, pp. 519–528.

Shin, D.H., Choi, M., Kim, K., Bang, G., Cho, M., Choi, S.B., Choi, G., et al. (2013), "HY5 regulates anthocyanin biosynthesis by inducing the transcriptional activation of the MYB75/PAP1 transcription factor in Arabidopsis", *FEBS Letters*, Vol. 587 No. 10, pp. 1543–1547.

Shin, J., Kim, K., Kang, H., Zulfugarov, I.S., Bae, G., Lee, C.-H., Lee, D., et al. (2009), "Phytochromes promote seedling light responses by inhibiting four negatively-acting phytochrome-interacting factors", *Proceedings of the National Academy of Sciences*, Vol. 106 No. 18, pp. 7660–7665.

Shin, J., Park, E. and Choi, G. (2007), "PIF3 regulates anthocyanin biosynthesis in an HY5-dependent manner with both factors directly binding anthocyanin biosynthetic gene promoters in Arabidopsis", *Plant Journal*, Vol. 49 No. 6, pp. 981–994.

Short, K.M. and Cox, T.C. (2006), "Subclassification of the RBCC/TRIM superfamily reveals a novel motif necessary for microtubule binding", *Journal of Biological Chemistry*, © 2006 ASBMB. Currently published by Elsevier Inc; originally published by American Society for Biochemistry and Molecular Biology., Vol. 281 No. 13, pp. 8970–8980.

Sokolovsky, V., Kaldenhoff, R., Ricci, M. and Russo, V.E.A. (1990), "Fast and reliable mini-prep RNA extraction from Neurospora crassa", *Fungal Genetics Reports*, Vol. 37 No. 1, available at:https://doi.org/10.4148/1941-4765.1492.

Somers, D.E., Sharrock, R.A., Tepperman, J.M. and Quail, P.H. (1991), "The hy3 Long Hypocotyl Mutant of Arabidopsis Is Deficient in Phytochrome B", *The Plant Cell*, Vol. 3 No. 12, p. 1263.

Song, Y.H., Yoo, C.M., Hong, A.P., Kim, S.H., Jeong, H.J., Shin, S.Y., Kim, H.J., et al. (2008), "DNA-Binding Study Identifies C-Box and Hybrid C/G-Box or C/A-Box Motifs as High-Affinity Binding Sites for STF1 and LONG HYPOCOTYL5 Proteins", *Plant Physiology*, Vol. 146 No. 4, pp. 1862–1877.

Song, Z., Bian, Y., Liu, J., Sun, Y. and Xu, D. (2020), "B-box proteins: Pivotal players in light-mediated development in plants", *Journal of Integrative Plant Biology*, Vol. 62 No. 9, pp. 1293–1309.

Song, Z., Yan, T., Liu, J., Bian, Y., Heng, Y., Lin, F., Jiang, Y., et al. (2020), "BBX28/BBX29, HY5 and BBX30/31 form a feedback loop to fine-tune photomorphogenic development", *Plant Journal*, Vol. 104 No. 2, pp. 377–390.

Soo Seo, H., Yang, J.Y., Ishikawa, M., Bolle, C., Ballesteros, M.L. and Chua, N.H. (2003), "LAF1 ubiquitination by COP1 controls photomorphogenesis and is stimulated by SPA1", *Nature*, Vol. 423 No. 6943, pp. 995–999.

Soundappan, I., Bennett, T., Morffy, N., Liang, Y., Stanga, J.P., Abbas, A., Leyser, O., et al. (2015), "SMAX1-LIKE/D53 Family Members Enable Distinct MAX2-Dependent Responses to Strigolactones and Karrikins in Arabidopsis", *The Plant Cell*, Vol. 27 No. 11, pp. 3143–3159.

Spiegelman, B.M. and Heinrich, R. (2004), "Biological control through regulated transcriptional coactivators", *Cell*, Vol. 119 No. 2, pp. 157–167.

Sprenger-Haussels, M. and Weisshaar, B. (2000), "Transactivation properties of parsley proline-rich bZIP transcription factors", *Plant Journal*, Vol. 22 No. 1, pp. 1–8.

Van Staden, J., Jäger, A.K., Light, M.E. and Burger, B. V. (2004), "Isolation of the major germination cue from plant-derived smoke", *South African Journal of Botany*, Elsevier Masson SAS, Vol. 70 No. 4, pp. 654–659.

Stanga, J.P., Morffy, N. and Nelson, D.C. (2016), "Functional redundancy in the control of seedling growth by the karrikin signaling pathway", *Planta*, Springer Berlin Heidelberg, Vol. 243 No. 6, pp. 1397–1406.

Stanga, J.P., Smith, S.M., Briggs, W.R. and Nelson, D.C. (2013), "SUPPRESSOR OF MORE AXILLARY GROWTH2 1 controls seed germination and seedling development in Arabidopsis", *Plant Physiology*, Vol. 163 No. 1, pp. 318–330.

Stark, C., Breitkreutz, B.J., Reguly, T., Boucher, L., Breitkreutz, A. and Tyers, M. (2006), "BioGRID: a general repository for interaction datasets.", *Nucleic Acids Research*, Vol. 34 No. Database issue, pp. 535–539.

Stavang, J.A., Gallego-Bartolomé, J., Gómez, M.D., Yoshida, S., Asami, T., Olsen, J.E., García-Martínez, J.L., et al. (2009), "Hormonal regulation of temperature-induced growth in Arabidopsis", *Plant Journal*, Vol. 60 No. 4, pp. 589–601.

Steinbach, Y. (2019), "The Arabidopsis thaliana CONSTANS-LIKE 4 (COL4) – A modulator of flowering time", *Frontiers in Plant Science*, Vol. 10 No. May, pp. 1–13.

Stirnberg, P., Furner, I.J. and Ottoline Leyser, H.M. (2007), "MAX2 participates in an SCF complex which acts locally at the node to suppress shoot branching", *Plant Journal*, Vol. 50 No. 1, pp. 80–94.

Stirnberg, P., van de Sande, K. and Leyser, H.M.O. (2002), "MAX1 and MAX2 control shoot lateral branching in Arabidopsis", *Development*, Vol. 129 No. 5, pp. 1131–1141.

Stracke, R., Favory, J.J., Gruber, H., Bartelniewoehner, L., Bartels, S., Binkert, M., Funk, M., et al. (2010), "The Arabidopsis bZIP transcription factor HY5 regulates expression of the PFG1/MYB12 gene in response to light and ultraviolet-B radiation", *Plant, Cell and Environment*, Vol. 33 No. 1, pp. 88–103.

Strasser, B., Sánchez-Lamas, M., Yanovsky, M.J., Casal, J.J. and Cerdán, P.D. (2010), "Arabidopsis thaliana life without phytochromes", *Proceedings of the National Academy of Sciences of the United States of America*, Vol. 107 No. 10, pp. 4776–4781.

Sullivan, J.A. and Deng, X.W. (2003), "From seed to seed: The role of photoreceptors in Arabidopsis development", *Developmental Biology*, Vol. 260 No. 2, pp. 289–297.

Sun, X.D. and Ni, M. (2011), "HYPOSENSITIVE to LIGHT, an alpha/beta fold protein, acts downstream of ELONGATED HYPOCOTYL 5 to regulate seedling de-etiolation", *Molecular Plant*, The Authors 2011. All rights reserved., Vol. 4 No. 1, pp. 116–126.

Sun, Y.K., Flematti, G.R., Smith, S.M. and Waters, M.T. (2016), "Reporter Gene-Facilitated Detection of Compounds in Arabidopsis Leaf Extracts that Activate the Karrikin Signaling Pathway", *Frontiers in Plant Science*, Vol. 7 No. DECEMBER2016, pp. 1–9.

Sun, Y.K., Yao, J., Scaffidi, A., Melville, K.T., Davies, S.F., Bond, C.S., Smith, S.M., et al. (2020), "Divergent receptor proteins confer responses to different karrikins in two ephemeral weeds", *Nature Communications*, Vol. 11 No. 1, p. 1264.

Swarbreck, S.M., Guerringue, Y., Matthus, E., Jamieson, F.J.C. and Davies, J.M. (2019), "Impairment in karrikin but not strigolactone sensing enhances root skewing in Arabidopsis thaliana", *Plant Journal*, Vol. 98 No. 4, pp. 607–621.

Tao, R., Bai, S., Ni, J., Yang, Q., Zhao, Y. and Teng, Y. (2018), "The blue light signal transduction pathway is involved in anthocyanin accumulation in 'Red Zaosu' pear", *Planta*, Springer Berlin Heidelberg, Vol. 248 No. 1, pp. 37–48.

Tavridou, E., Pireyre, M. and Ulm, R. (2020), "Degradation of the transcription factors PIF4 and PIF5 under UV-B promotes UVR8-mediated inhibition of hypocotyl growth in Arabidopsis", *Plant Journal*, Vol. 101 No. 3, pp. 507–517.

Tepperman, J.M., Hudson, M.E., Khanna, R., Zhu, T., Chang, S.H., Wang, X. and Quail, P.H. (2004), "Expression profiling of phyB mutant demonstrates substantial contribution of other phytochromes to red-light-regulated gene expression during seedling de-etiolation", *Plant Journal*, Vol. 38 No. 5, pp. 725–739.

Tepperman, J.M., Zhu, T., Chang, H.S., Wang, X. and Quail, P.H. (2001), "Multiple transcription-factor genes are early targets of phytochrome A signaling", *Proceedings of the National Academy of Sciences of the United States of America*,

Vol. 98 No. 16, pp. 9437–9442.

Terry, M.J. (1997), "Phytochrome chromophore-deficient mutants", *Plant, Cell and Environment*, Vol. 20 No. 6, pp. 740–745.

Terry, M.J., Wahleithner, J.A. and Lagarias, J.C. (1993), "Biosynthesis of the Plant Photoreceptor Phytochrome", *Archives of Biochemistry and Biophysics*, Vol. 306 No. 1, pp. 1–15.

Thussagunpanit, J., Nagai, Y., Nagae, M., Mashiguchi, K., Mitsuda, N., Ohme-Takagi, M., Nakano, T., et al. (2017), "Involvement of STH7 in light-adapted development in Arabidopsis thaliana promoted by both strigolactone and karrikin", *Bioscience, Biotechnology and Biochemistry*, Taylor & Francis, Vol. 81 No. 2, pp. 292–301.

Tiwari, S.B., Shen, Y., Chang, H.C., Hou, Y., Harris, A., Ma, S.F., McPartland, M., et al. (2010), "The flowering time regulator CONSTANS is recruited to the FLOWERING LOCUS T promoter via a unique cis-element", *New Phytologist*, Vol. 187 No. 1, pp. 57–66.

Toh, S., Holbrook-Smith, D., Stokes, M.E., Tsuchiya, Y. and McCourt, P. (2014), "Detection of parasitic plant suicide germination compounds using a high-throughput Arabidopsis HTL/KAI2 strigolactone perception system", *Chemistry & Biology*, Elsevier Ltd, Vol. 21 No. 8, pp. 988–998.

Toledo-Ortiz, G., Huq, E. and Quail, P.H. (2003), "The Arabidopsis basic/helix-loop-helix transcription factor family.", *The Plant Cell*, Vol. 15 No. 8, pp. 1749–70.

Toledo-Ortiz, G., Johansson, H., Lee, K.P., Bou-Torrent, J., Stewart, K., Steel, G., Rodríguez-Concepción, M., et al. (2014), "The HY5-PIF Regulatory Module Coordinates Light and Temperature Control of Photosynthetic Gene Transcription", *PLoS Genetics*, Vol. 10 No. 6, available at:https://doi.org/10.1371/journal.pgen.1004416.

Torok, M. and Etkin, L.D. (2001), "Two B or not two B? Overview of the rapidly expanding B-box family of proteins", *Differentiation*, Vol. 67 No. 3, pp. 63–71.

Tsuchiya, Y., Vidaurre, D., Toh, S., Hanada, A., Nambara, E., Kamiya, Y., Yamaguchi, S., et al. (2010), "A small-molecule screen identifies new functions for the plant hormone strigolactone", *Nature Chemical Biology*, Vol. 6 No. 10, pp. 741–749.

Ulm, R., Baumann, A., Oravecz, A., Máté, Z., Ádám, É., Oakeley, E.J., Schäfer, E., et al. (2004), "Genome-wide analysis of gene expression reveals function of the bZIP transcription factor HY5 in the UV-B response of Arabidopsis", *Proceedings of the National Academy of Sciences of the United States of America*, Vol. 101 No. 5, pp. 1397–1402.

Umehara, M., Hanada, A., Yoshida, S., Akiyama, K., Arite, T., Takeda-Kamiya, N., Magome, H., et al. (2008), "Inhibition of shoot branching by new terpenoid plant hormones", *Nature*, Vol. 455 No. 7210, pp. 195–200.

Usami, T., Mochizuki, N., Kondo, M., Nishimura, M. and Nagatani, A. (2004), "Cryptochromes and phytochromes synergistically regulate Arabidopsis root greening under blue light", *Plant and Cell Physiology*, Vol. 45 No. 12, pp. 1798–1808.

Vandenbussche, F., Habricot, Y., Condiff, A.S., Maldiney, R., Van Der Straeten, D. and

Ahmad, M. (2007), “HY5 is a point of convergence between cryptochrome and cytokinin signalling pathways in Arabidopsis thaliana”, *Plant Journal*, Vol. 49 No. 3, pp. 428–441.

Vandesompele, J., De Preter, K., Pattyn, F., Poppe, B., Van Roy, N., De Paepe, A. and Speleman, F. (2002), “Accurate normalization of real-time quantitative RT-PCR data by geometric averaging of multiple internal control genes.”, *Genome Biology*, Vol. 3 No. 7, p. RESEARCH0034.

Villaécija-Aguilar, J.A., Hamon-Josse, M., Carbonnel, S., Kretschmar, A., Schmidt, C., Dawid, C., Bennett, T., et al. (2019), “SMAX1/SMXL2 regulate root and root hair development downstream of KAI2-mediated signalling in Arabidopsis”, *PLoS Genetics*, Vol. 15 No. 8, pp. 1–27.

Wallner, E.S., López-Salmerón, V., Belevich, I., Poschet, G., Jung, I., Grünwald, K., Sevilem, I., et al. (2017), “Strigolactone- and Karrikin-Independent SMXL Proteins Are Central Regulators of Phloem Formation”, *Current Biology*, Vol. 27 No. 8, pp. 1241–1247.

Wang, C.Q., Guthrie, C., Sarmast, M.K. and Dehesh, K. (2014), “BBX19 interacts with CONSTANS to repress FLOWERING LOCUS T transcription, defining a flowering time checkpoint in Arabidopsis”, *Plant Cell*, Vol. 26 No. 9, pp. 3589–3602.

Wang, C.Q., Khoshhal Sarmast, M., Jiang, J. and Dehesh, K. (2015), “The transcriptional regulator BBX19 promotes hypocotyl growth by facilitating COP1-mediated EARLY FLOWERING3 degradation in arabidopsis”, *Plant Cell*, Vol. 27 No. 4, pp. 1128–1139.

Wang, H., Ma, L.G., Li, J.M., Zhao, H.Y. and Xing Wang Deng. (2001), “Direct interaction of Arabidopsis cryptochromes with COP1 in light control development”, *Science*, Vol. 294 No. 5540, pp. 154–158.

Wang, L., Wang, B., Jiang, L., Liu, X., Li, X., Lu, Z., Meng, X., et al. (2015), “Strigolactone signaling in Arabidopsis regulates shoot development by targeting D53-like SMXL repressor proteins for ubiquitination and degradation”, *Plant Cell*, Vol. 27 No. 11, pp. 3128–3142.

Wang, L., Waters, M.T. and Smith, S.M. (2018), “Karrikin-KAI2 signalling provides Arabidopsis seeds with tolerance to abiotic stress and inhibits germination under conditions unfavourable to seedling establishment”, *New Phytologist*, Vol. 219 No. 2, pp. 605–618.

Wang, L., Xu, Q., Yu, H., Ma, H., Li, X., Yang, J., Chu, J., et al. (2020), “Strigolactone and Karrikin Signaling Pathways Elicit Ubiquitination and Proteolysis of SMXL2 to Regulate Hypocotyl Elongation in Arabidopsis thaliana”, *The Plant Cell*, Vol. 2, p. tpc.00140.2020.

Wang, Q. and Lin, C. (2020), “Mechanisms of Cryptochrome-Mediated Photoresponses in Plants”, *Annual Review of Plant Biology*, Vol. 71, pp. 103–129.

Wang, Q., Zeng, J., Deng, K., Tu, X., Zhao, X., Tang, D. and Liu, X. (2011), “DBB1a, involved in gibberellin homeostasis, functions as a negative regulator of blue light-mediated hypocotyl elongation in Arabidopsis”, *Planta*, Vol. 233 No. 1, pp. 13–23.

Wang, Q., Zuo, Z., Wang, X., Gu, L., Yoshizumi, T., Yang, Z., Yang, L., et al. (2016),

"Photoactivation and inactivation of Arabidopsis cryptochrome 2", *Science*, Vol. 354 No. 6310, pp. 343–347.

Wang, W., Paik, I., Kim, J., Hou, X., Sung, S. and Huq, E. (2021), "Direct phosphorylation of HY5 by SPA kinases to regulate photomorphogenesis in Arabidopsis", *New Phytologist*, pp. 2311–2326.

Wang, W., Wang, P., Li, X., Wang, Y., Tian, S. and Qin, G. (2021), "The transcription factor SlHY5 regulates the ripening of tomato fruit at both the transcriptional and translational levels", *Horticulture Research*, Springer US, Vol. 8 No. 1, pp. 1–15.

Wang, X., Wang, Q., Han, Y.J., Liu, Q., Gu, L., Yang, Z., Su, J., et al. (2017), "A CRY–BIC negative-feedback circuitry regulating blue light sensitivity of Arabidopsis", *Plant Journal*, Vol. 92 No. 3, pp. 426–436.

Wang, X., Wang, Q., Nguyen, P. and Lin, C. (2017), "Cryptochrome-mediated light responses in plants.", *The Enzymes*, Vol. 35 No. 5, pp. 167–89.

Waters, M.T., Moylan, E.C. and Langdale, J.A. (2008), "GLK transcription factors regulate chloroplast development in a cell-autonomous manner", *Plant Journal*, Vol. 56 No. 3, pp. 432–444.

Waters, M.T., Nelson, D.C., Scaffidi, A., Flematti, G.R., Sun, Y.K., Dixon, K.W. and Smith, S.M. (2012), "Specialisation within the DWARF14 protein family confers distinct responses to karrikins and strigolactones in Arabidopsis", *Development*, Vol. 139 No. 7, pp. 1285–1295.

Waters, M.T., Scaffidi, A., Moulin, S.L.Y., Sun, Y.K., Flematti, G.R. and Smith, S.M. (2015), "A Selaginella moellendorffii Ortholog of KARRIKIN INSENSITIVE2 Functions in Arabidopsis Development but Cannot Mediate Responses to Karrikins or Strigolactones", *The Plant Cell*, Vol. 27 No. 7, pp. 1925–1944.

Waters, M.T., Scaffidi, A., Sun, Y.K., Flematti, G.R. and Smith, S.M. (2014), "The karrikin response system of Arabidopsis", *Plant Journal*, Vol. 79 No. 4, pp. 623–631.

Waters, M.T. and Smith, S.M. (2013), "KAI2- and MAX2-Mediated Responses to Karrikins and Strigolactones Are Largely Independent of HY5 in Arabidopsis Seedlings", *Molecular Plant*, Â© The Authors. All rights reserved., Vol. 6 No. 1, pp. 63–75.

Wei, C.-Q., Chien, C.-W., Ai, L.-F., Zhao, J., Zhang, Z., Li, K.H., Burlingame, A.L., et al. (2016), "The Arabidopsis B-box protein BZS1/BBX20 interacts with HY5 and mediates strigolactone regulation of photomorphogenesis", *Journal of Genetics and Genomics*, Vol. 43 No. 9, pp. 555–563.

Weidler, G., Heunemann, M., Orth, C., Schleifenbaum, F., Harter, K., Hoecker, U. and Batschauer, A. (2012), "Degradation of Arabidopsis CRY2 Is Regulated by SPA Proteins and Phytochrome A", Vol. 24 No. June, pp. 2610–2623.

Weidler, G., Oven-Krockhaus, S. Zur, Heunemann, M., Orth, C., Schleifenbaum, F., Harter, K., Hoecker, U., et al. (2012), "Degradation of Arabidopsis CRY2 is regulated by SPA proteins and phytochrome A", *Plant Cell*, Vol. 24 No. 6, pp. 2610–2623.

Whitelam, G.C., Johnson, E., Peng, J., Carol, P., Anderson, M.L., Cowl, J.S. and Harberd,

N.P. (1993), “Phytochrome A null mutants of Arabidopsis display a wild-type phenotype in white light.”, *The Plant Cell*, Vol. 5 No. 7, pp. 757–768.

Wickham, H. (2009), *Ggplot2: Elegant Graphics for Data Analysis*, Springer New York, New York, NY, available at:https://doi.org/10.1007/978-0-387-98141-3.

de Wit, M., Keuskamp, D.H., Bongers, F.J., Hornitschek, P., Gommers, C.M.M., Reinen, E., Martínez-Cerón, C., et al. (2016), “Integration of Phytochrome and Cryptochrome Signals Determines Plant Growth during Competition for Light”, *Current Biology*, Vol. 26 No. 24, pp. 3320–3326.

Wright, K.M., Wu, K., Babatunde, O., Du, H. and Massiah, M.A. (2014), “XLOS-observed mutations of MID1 Bbox1 domain cause domain unfolding”, *PLoS ONE*, Vol. 9 No. 9, pp. 1–9.

Di Wu, Hu, Q., Yan, Z., Chen, W., Yan, C., Huang, X., Zhang, J., et al. (2012), “Structural basis of ultraviolet-B perception by UVR8”, *Nature*, Vol. 484 No. 7393, pp. 214–219.

Wu, G. and Spalding, E.P. (2007), “Separate functions for nuclear and cytoplasmic cryptochrome 1 during photomorphogenesis of Arabidopsis seedlings”, *Proceedings of the National Academy of Sciences of the United States of America*, Vol. 104 No. 47, pp. 18813–18818.

Xie, X., Yoneyama, K. and Yoneyama, K. (2010), “The strigolactone story.”, *Annual Review of Phytopathology*, Vol. 48, pp. 93–117.

Xiong, C., Luo, D., Lin, A., Zhang, C., Shan, L., He, P., Li, B., et al. (2019), “A tomato B-box protein SlBBX20 modulates carotenoid biosynthesis by directly activating PHYTOENE SYNTHASE 1, and is targeted for 26S proteasome-mediated degradation”, *New Phytologist*, Vol. 221 No. 1, pp. 279–294.

Xu, D. bei, Gao, S. qing, Ma, Y. nan, Wang, X. ting, Feng, L., Li, L. cheng, Xu, Z. shi, et al. (2017), “The G-Protein β Subunit AGB1 Promotes Hypocotyl Elongation through Inhibiting Transcription Activation Function of BBX21 in Arabidopsis”, *Molecular Plant*, Elsevier Ltd, Vol. 10 No. 9, pp. 1206–1223.

Xu, D., Jiang, Y., Li, J., Holm, M. and Deng, X.W. (2018), “The B-box domain protein BBX21 promotes photomorphogenesis”, *Plant Physiology*, Vol. 176 No. 3, pp. 2365–2375.

Xu, D., Jiang, Y., Li, J., Lin, F., Holm, M. and Deng, X.W. (2016), “BBX21, an Arabidopsis B-box protein, directly activates HY5 and is targeted by COP1 for 26S proteasome-mediated degradation”, *Proceedings of the National Academy of Sciences of the United States of America*, Vol. 113 No. 27, pp. 7655–7660.

Xu, X., Chi, W., Sun, X., Feng, P., Guo, H., Li, J., Lin, R., et al. (2016), “Convergence of light and chloroplast signals for de-etiolation through ABI4-HY5 and COP1”, *Nature Plants*, Nature Publishing Group, Vol. 2 No. 6, pp. 1–7.

Yadav, V., Kundu, S., Chattopadhyay, D., Negi, P., Wei, N., Deng, X.W. and Chattopadhyay, S. (2002), “Light regulated modulation of Z-box containing promoters by photoreceptors and downstream regulatory components, COP1 and HY5, in Arabidopsis”, *Plant Journal*, Vol. 31 No. 6, pp. 741–753.

Yamaguchi, R., Nakamura, M., Mochizuki, N., Kay, S. a and Nagatani, A. (1999), “Light-

dependent translocation of a phytochrome B-GFP fusion protein to the nucleus in transgenic Arabidopsis.", *The Journal of Cell Biology*, Vol. 145 No. 3, pp. 437–45.

Yan, H., Marquardt, K., Indorf, M., Jutt, D., Kircher, S., Neuhaus, G. and Rodríguez-Franco, M. (2011), "Nuclear localization and interaction with COP1 are required for STO/BBX24 function during Photomorphogenesis", *Plant Physiology*, Vol. 156 No. 4, pp. 1772–1782.

Yang, H.Q., Tang, R.H. and Cashmore, A.R. (2001), "The signaling mechanism of Arabidopsis CRY1 involves direct interaction with COP1", *Plant Cell*, Vol. 13 No. 12, pp. 2573–2587.

Yang, L., Pengbo, X., Chen, G., Wu, J., Liu, Z. and Lian, H. (2020), "FvbHLH9 Functions as a Positive Regulator of Anthocyanin Biosynthesis by Forming a HY5-bHLH9 Transcription Complex in Strawberry Fruits", *Plant and Cell Physiology*, Vol. 61 No. 4, pp. 826–837.

Yang, Y., Liang, T., Zhang, L., Shao, K., Gu, X., Shang, R., Shi, N., et al. (2018), "UVR8 interacts with WRKY36 to regulate HY5 transcription and hypocotyl elongation in Arabidopsis", *Nature Plants*, Vol. 4 No. 2, pp. 98–107.

Yang, Z., Liu, B., Su, J., Liao, J., Lin, C. and Oka, Y. (2017), "Cryptochromes Orchestrate Transcription Regulation of Diverse Blue Light Responses in Plants", *Photochemistry and Photobiology*, Vol. 93 No. 1, pp. 112–127.

Yao, J., Mashiguchi, K., Scaffidi, A., Akatsu, T., Melville, K.T., Morita, R., Morimoto, Y., et al. (2018), "An allelic series at the KARRIKIN INSENSITIVE 2 locus of Arabidopsis thaliana decouples ligand hydrolysis and receptor degradation from downstream signalling", *Plant Journal*, Vol. 96 No. 1, pp. 75–89.

Yao, R., Ming, Z., Yan, L., Li, S., Wang, F., Ma, S., Yu, C., et al. (2016), "DWARF14 is a non-canonical hormone receptor for strigolactone", *Nature*, Nature Publishing Group, Vol. 536 No. 7617, pp. 469–473.

Yi, R., Yan, J. and Xie, D. (2020), "Light promotes jasmonate biosynthesis to regulate photomorphogenesis in Arabidopsis", *Science China Life Sciences*, Vol. 63 No. 7, pp. 943–952.

Yin, R., Skvortsova, M.Y., Loubéry, S. and Ulm, R. (2016), "COP1 is required for UV-B-induced nuclear accumulation of the UVR8 photoreceptor", *Proceedings of the National Academy of Sciences of the United States of America*, Vol. 113 No. 30, pp. E4415–E4422.

Yin, R. and Ulm, R. (2017), "How plants cope with UV-B: from perception to response.", *Current Opinion in Plant Biology*, Elsevier Ltd, Vol. 37, pp. 42–48.

Yoo, S.D., Cho, Y.H. and Sheen, J. (2007), "Arabidopsis mesophyll protoplasts: A versatile cell system for transient gene expression analysis", *Nature Protocols*, Vol. 2 No. 7, pp. 1565–1572.

Yoon, M.-K., Shin, J., Choi, G. and Choi, B.-S. (2006), "Intrinsically unstructured N-terminal domain of bZIP transcription factor HY5", *Proteins: Structure, Function, and Bioinformatics*, Vol. 65 No. 4, pp. 856–866.

Yoon, M.K., Kim, H.M., Choi, G., Lee, J.O. and Choi, B.S. (2007), "Structural basis for the conformational integrity of the Arabidopsis thaliana HY5 leucine zipper

homodimer", *Journal of Biological Chemistry*, Â© 2007 ASBMB. Currently published by Elsevier Inc; originally published by American Society for Biochemistry and Molecular Biology., Vol. 282 No. 17, pp. 12989–13002.

Yu, X., Klejnot, J., Zhao, X., Shalitin, D., Maymon, M., Yang, H., Lee, J., et al. (2007), "Arabidopsis cryptochrome 2 completes its posttranslational life cycle in the nucleus", *Plant Cell*, Vol. 19 No. 10, pp. 3146–3156.

Yu, Y., Wang, J., Zhang, Z., Quan, R., Zhang, H., Deng, X.W., Ma, L., et al. (2013), "Ethylene Promotes Hypocotyl Growth and HY5 Degradation by Enhancing the Movement of COP1 to the Nucleus in the Light", *PLoS Genetics*, Vol. 9 No. 12, available at:https://doi.org/10.1371/journal.pgen.1004025.

Zeidler, M., Zhou, Q., Sarda, X., Yau, C.-P. and Chua, N.-H. (2004), "The nuclear localization signal and the C-terminal region of FHY1 are required for transmission of phytochrome A signals.", *The Plant Journal : For Cell and Molecular Biology*, Vol. 40 No. 3, pp. 355–65.

Zhang, D., Qian, M., Yu, B. and Teng, Y. (2013), "Effect of fruit maturity on UV-B-induced post-harvest anthocyanin accumulation in red Chinese sand pear", *Acta Physiologiae Plantarum*, Vol. 35 No. 9, pp. 2857–2866.

Zhang, H., He, H., Wang, X., Wang, X., Yang, X., Li, L. and Deng, X.W. (2011), "Genome-wide mapping of the HY5-mediated genenetworks in Arabidopsis that involve both transcriptional and post-transcriptional regulation", *Plant Journal*, Vol. 65 No. 3, pp. 346–358.

Zhang, X., Huai, J., Shang, F., Xu, G., Tang, W., Jing, Y. and Lin, R. (2017), "A PIF1/PIF3-HY5-BBX23 transcription factor cascade affects photomorphogenesis", *Plant Physiology*, Vol. 174 No. 4, pp. 2487–2500.

Zhang, Y., Mayba, O., Pfeiffer, A., Shi, H., Tepperman, J.M., Speed, T.P. and Quail, P.H. (2013), "A Quartet of PIF bHLH Factors Provides a Transcriptionally Centered Signaling Hub That Regulates Seedling Morphogenesis through Differential Expression-Patterning of Shared Target Genes in Arabidopsis", edited by Copenhaver, G.P.*PLoS Genetics*, Vol. 9 No. 1, p. e1003244.

Zhao, L., Peng, T., Chen, C.Y., Ji, R., Gu, D., Li, T., Zhang, D., et al. (2019), "HY5 interacts with the histone deacetylase HDA15 to repress hypocotyl cell elongation in photomorphogenesis", *Plant Physiology*, Vol. 180 No. 3, pp. 1450–1466.

Zhao, L.H., Edward Zhou, X., Wu, Z.S., Yi, W., Xu, Y., Li, S., Xu, T.H., et al. (2013), "Crystal structures of two phytohormone signal-transducing α/β hydrolases: Karrikin-signaling KAI2 and strigolactone-signaling DWARF14", *Cell Research*, Vol. 23 No. 3, pp. 436–439.

Zheng, J., Hong, K., Zeng, L., Wang, L., Kang, S., Qu, M., Dai, J., et al. (2020), "Karrikin signaling acts parallel to and additively with strigolactone signaling to regulate rice mesocotyl elongation in darkness", *Plant Cell*, Vol. 32 No. 9, pp. 2780–2805.

Zhou, F., Lin, Q., Zhu, L., Ren, Y., Zhou, K., Shabek, N., Wu, F., et al. (2013), "D14-SCF D3 -dependent degradation of D53 regulates strigolactone signalling", *Nature*, Nature Publishing Group, Vol. 504 No. 7480, pp. 406–410.

Zhu, D., Maier, A., Lee, J.H., Laubinger, S., Saijo, Y., Wang, H., Qu, L.J., et al. (2008),

"Biochemical characterization of Arabidopsis complexes containing constitutively photomorphogenic1 and suppressor of PHYA proteins in light control of plant development", *Plant Cell*, Vol. 20 No. 9, pp. 2307–2323.

Zoulias, N., Brown, J., Rowe, J. and Casson, S.A. (2020), "HY5 is not integral to light mediated stomatal development in Arabidopsis", edited by Somers, D.E.*PLOS ONE*, Vol. 15 No. 1, p. e0222480.

Zuo, J., Niu, Q.W. and Chua, N.H. (2000), "An estrogen receptor-based transactivator XVE mediates highly inducible gene expression in transgenic plants", *Plant Journal*, Vol. 24 No. 2, pp. 265–273.

Zuo, Z., Liu, H., Liu, B., Liu, X. and Lin, C. (2011), "Blue Light-Dependent Interaction of CRY2 with SPA1 Regulates COP1 activity and Floral Initiation in Arabidopsis", *Current Biology*, Vol. 21 No. 10, pp. 841–847.

5 Supplementals

5.1 Supplemental information for chapter 2

5.1.1 Supplemental Figures

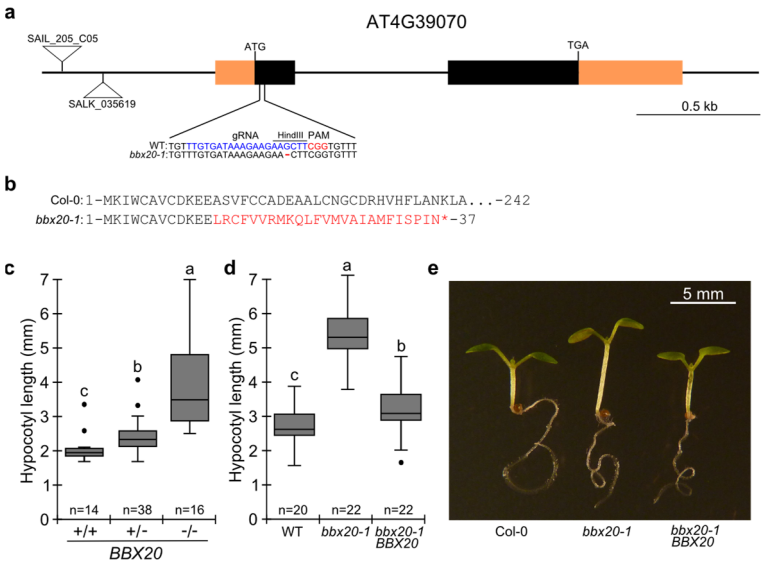

Supplemental Figure 5.1.1: Creation and validation of the *bbx20-1* mutant.

a) Schematic representation of the *BBX20* locus indicating two available T-DNA insertion lines and the sequence targeted by CRISPR/Cas9. Orange areas indicate 5' and 3' UTR while black areas indicate the two exons of *BBX20*. Blue and red text indicate the gRNA and PAM sequence, respectively, used for CRISPR/Cas9 induced mutagenesis of *BBX20*. The recovered *bbx20-1* mutant harbored a 1-bp deletion 4-bp upstream of the PAM sequence, resulting in the loss of a HindIII recognition sequence available in the WT. **b)** Expected amino acid sequence of the *bbx20-1* mutant caused by the 1-bp frameshift. Frameshifted amino acids are labelled in red and the asterisk indicates an early stop-codon. **c)** Hypocotyl measurements of 68 5-day-old seedlings from a *bbx20-1* heterozygote parental plant grown in 100 µmol m^{-2} s^{-1} of red light. After measurements of the individual hypocotyls, PCR based genotyping revealed 14 WT, 38 heterozygote and 16 *bbx20-1* homozygote seedlings allowing for grouping each measurement into the three genotypes. **d)** Hypocotyl measurements of Col-0, *bbx20-1* and T_1 *bbx20-1* seedlings complemented with a genomic *BBX20* construct, utilizing the pFAST vector system for identification of transgenic seeds, grown as in (c). **e)** Photo of representative seedlings from (d). Box plots represent medians and interquartile ranges with whiskers extending to the largest/smallest value and outliers are shown as dots. Different letters represent statistical significant differences ($p<0.05$) as determined by one-way ANOVA followed by Tukey's Post Hoc test.

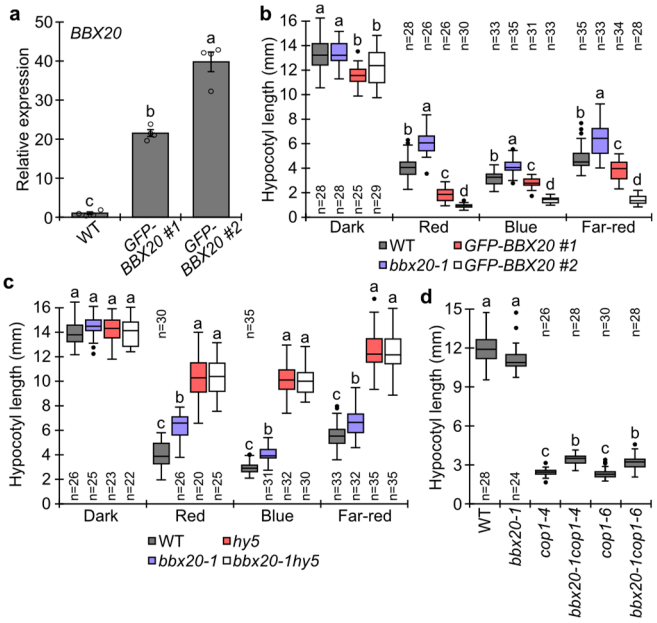

Supplemental Figure 5.1.2: BBX20 acts upstream of HY5 and downstream of COP1.

a) *BBX20* transcript levels relative to the reference genes *ACT2* and *EF1A* in 4-day-old WT and *35S::GFP-BBX20* transgenic seedlings grown in 75 µmol m^{-2} s^{-1} of constant white light. n=4 biological replicates indicated by open circles. Data represents means ± SE. **b-c)** Hypocotyl measurements of 5-day-old seedlings grown in darkness, monochromatic red (80 µmol m^{-2} s^{-1}), blue (14 µmol m^{-2} s^{-1}) and far-red (1 µmol m^{-2} s^{-1}) light. **d)** Hypocotyl measurements of 5-day-old seedlings grown in darkness. Box plots represent medians and interquartile ranges with whiskers extending to the largest/smallest value and outliers are shown as dots. Different letters represent statistical significant differences ($p<0.05$) as determined by one-way ANOVA followed by Tukey's Post Hoc test.

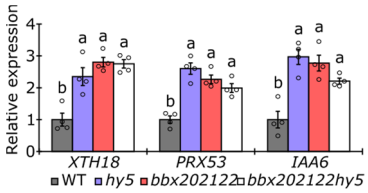

Supplemental Figure 5.1.3: Transcript analysis of genes inhibited by BBX20-22 and HY5.

Analysis of *XTH18*, *PRX53* and *IAA6* transcript abundance relative to the *GADPH* and *TFIID* reference genes in 4-day-old seedlings grown in 80 µmol m^{-2} s^{-1} of red light. Data represents means ± SE. n=4 independent biological replicates. Different letters denote statistical significant differences ($p<0.05$) as determined by one-way ANOVA followed by Tukey's Post Hoc test. Open circles indicate single biological measurements.

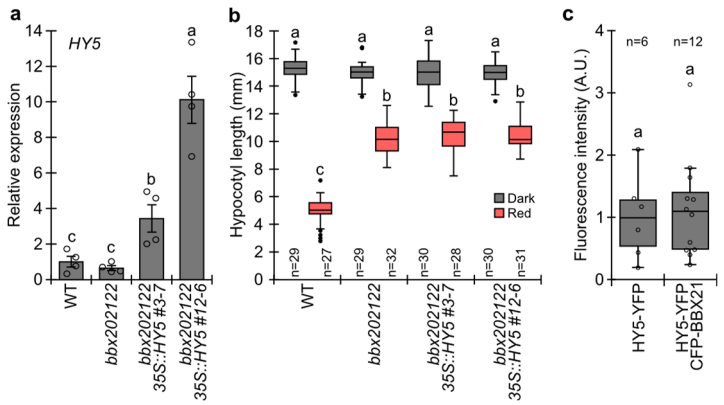

Supplemental Figure 5.1.4: The *bbx202122* phenotype is not due to reduced *HY5* transcript abundance.

a) Transcript levels of *HY5* relative to *GADPH* and *TFIID* in 4-day-old seedlings grown in 80 µmol m^{-2} s^{-1} of red light. n=4 biological replicates indicated by open circles. Data represents means ± SE. Different letters represent statistical significant differences ($p<0.05$) as determined by one-way ANOVA followed by Tukey's Post Hoc test. **b)** Hypocotyl measurements of 5-day old seedlings grown as in (a) or constant darkness. Different letters represent statistical significant differences ($p<0.05$) as determined by two-way ANOVA followed by Tukey's Post Hoc test. **c)** Quantification of fluorescence intensity of YFP in the nuclei of *bbx202122hy5hyh* protoplasts transiently expressing HY5-YFP with or without CFP-BBX21. Different letters represent statistical significant differences ($p<0.05$) as determined by Student's t-test. Box plots represent medians and interquartile ranges with whiskers extending to the largest/smallest value and outliers are shown as dots.

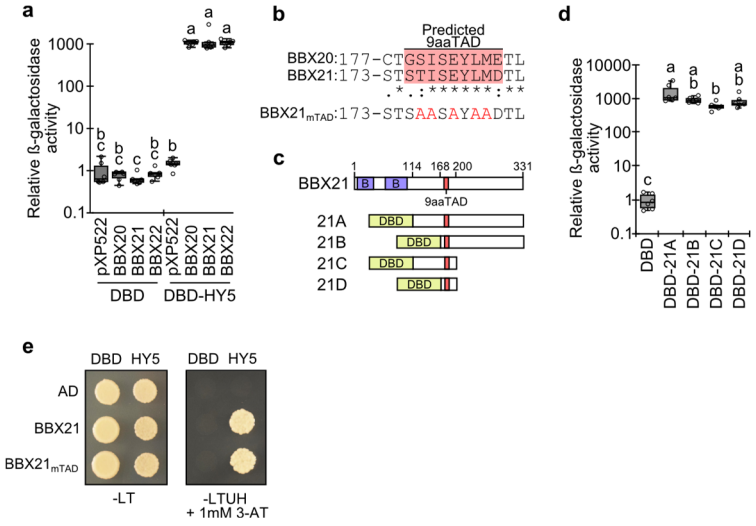

Supplemental Figure 5.1.5: A predicted 9aaTAD of BBX21 promotes transcription in yeast.

a) Liquid yeast two-hybrid β-galactosidase assay using DBD-HY5 as bait and BBX20, BBX21 or BBX22 as prey not fused to an additional activation domain. Box plots represent medians and interquartile ranges with whiskers extending to the largest/smallest value and outliers are shown as dots. n=6. **b)** Alignment of predicted TAD region of BBX20 and BBX21 using Clustal Omega (1.2.4). $BBX21_{mTAD}$ shows the sequence after the introduction of 5 alanine residues **c)** Graphical representation of four truncated BBX21 constructs, 21A-21D, all containing the predicted 9aaTAD region. B and DBD represent B-box domain and DNA-binding domain, respectively. **d)** Measurements of auto activation of 21A, 21B, 21C and 21D fragments in yeast. n=6. **e)** Yeast two-hybrid assay using HY5 as bait and BBX21 or $BBX21_{mTAD}$ as prey. –LW and –LWUH indicate media lacking either Leu, Trp or Leu, Trp, Ura, His, respectively. 3-AT represents the addition of 3-amino-1, 2,4-triazol to the growth medium. The experiment was repeated with similar results using two independent sets of primary transformants. Single measurements are shown as open circles and statistical groups are indicated by letters as determined by one-way ANOVA followed by Tukey's Post Hoc test.

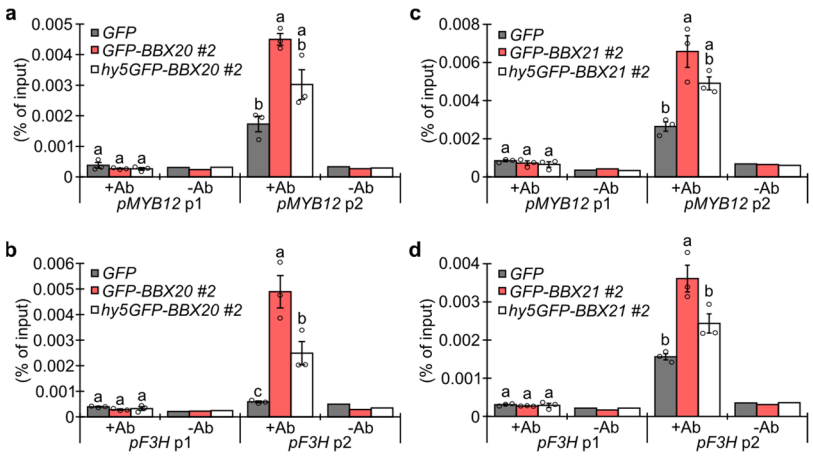

Supplemental Figure 5.1.6: BBX20 and BBX21 associates with DNA dependent on HY5 in *Arabidopsis*.

a-d) Chromatin immunoprecipitation using no antibody (-Ab) or an anti-GFP antibody (+Ab) on samples harvested from 4-day-old *35S::GFP*, *35S::GFP-BBX20 #2* and *hy5 35S::GFP-BBX20 #2* (a, b) or *35S::GFP*, *35S::GFP-BBX21 #2* and *hy5 35S::GFP-BBX21 #2* (c, d) transgenic seedlings grown in 80 µmol m^{-2} s^{-1} of red light. p1 and p2 denotes primer pairs amplifying a non-binding control region and HY5 binding region, respectively. n=3 biological replicates for +Ab samples and a single sample for -Ab). Data represents means ± SE. Single measurements are shown as open circles and statistical groups are indicated by letters as determined by one-way ANOVA followed by Tukey's Post Hoc test.

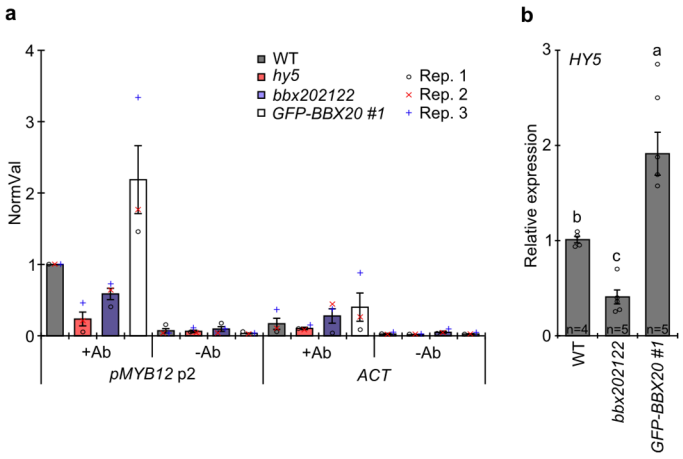

Supplemental Figure 5.1.7: HY5 binding to the *MYB12* promoter in *bbx202122* and *35S::GFP-BBX20 #1* correlate with *HY5* transcript levels.

a) Chromatin immunoprecipitation using no antibody (-Ab) or an anti-HY5 antibody (+Ab) on samples harvested from 4-day-old WT, *hy5*, *bbx202122* and *35S::GFP-BBX20 #1* seedlings grown in 80 µmol m^{-2} s^{-1} of red light. p2 denotes primer pairs amplifying a HY5 binding region of the *MYB12* promoter as shown in Figure 2.2a and *ACT* is used as negative control. n=3 independent biological replicates and each replicate was normalized to WT pMYB12 p2 +AB. Data represents means ± SE. Single measurements from each biological repeat is indicated by an open circle, cross and plus sign, respectively. **b)** Measurements of *HY5* transcript levels relative to *PP2A* in 4-day-old seedlings grown in 80 µmol m^{-2} s^{-1} of red light. Biological replicates indicated by open circles. Data represents means ± SE. Different letters represent statistical significant differences ($p<0.05$) as determined by one-way ANOVA followed by Tukey's Post Hoc test.

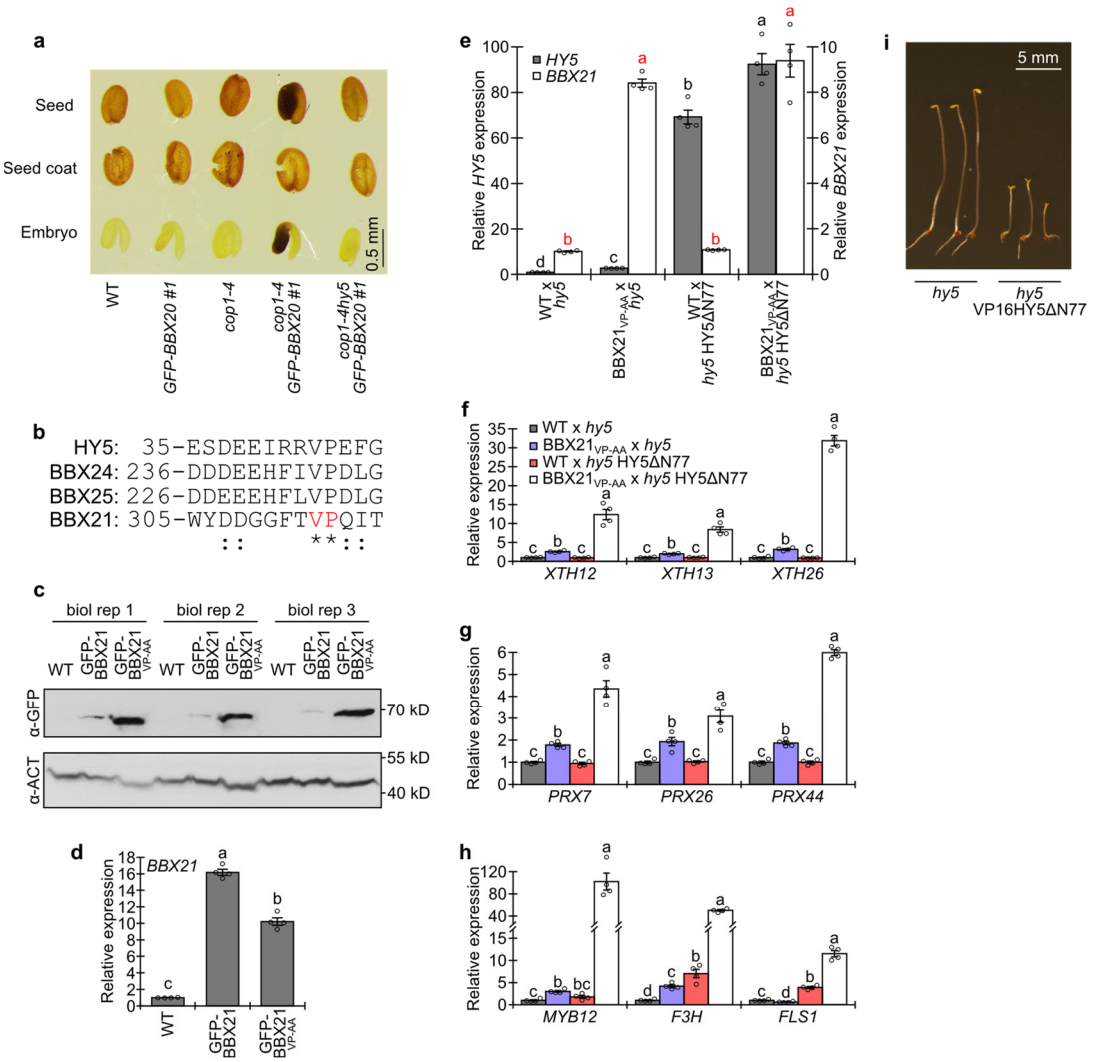

Supplemental Figure 5.1.8: Expression of BBX21$_{VP-AA}$ or a VP16 fusion is sufficient for HY5ΔN77 to promote photomorphogenesis.

a) Photo of representative seeds, dissected embryos and seed coats of indicated genetic background. Similar observations were made over multiple generations. **b)** Alignment of VP-domain containing amino acids 35-47 of HY5, 236-248 of BBX24, 226-238 of BBX25 and 305-317 of BBX21, respectively, using Clustal Omega (1.2.4). The Val-Pro pair labelled red in BBX21 was modified to Ala-Ala to generate BBX21$_{VP-AA}$. **c)** Immunoblot analysis of total protein samples collected from transgenic seedlings expressing *GFP-BBX21* and *GFP-BBX21$_{VP-AA}$* driven by the 35S promoter, grown for 4 days in darkness. Anti-GFP and anti-ACT antibodies were used to detect the BBX proteins and the ACT loading control, respectively. 3 independent biological replicates are shown. **d)** *BBX21* transcript levels relative to the *GADPH* and *TFIID* reference genes in WT, *35S::GFP-BBX21* and *35S::GFP-BBX21$_{VP-AA}$* seedlings grown in darkness for 4 days. n=4. **e)** *BBX21* transcript levels relative to the *GADPH* and *TFIID* reference genes in WT and *XVE::BBX21$_{VP-AA}$* seedlings grown in darkness for 4 days with 20 µM of 17-β-estradiol (+Est) or 0.1% ethanol (v/v) (Control). n=4 biological replicates. **f)** Transcript levels of *HY5* and *BBX21* shown as relative to the *GADPH* and *TFIID* reference genes in the indicated crosses between WT, *hy5*, *XVE::BBX21$_{VP-AA}$* and *hy5 35S::HY5ΔN77* grown for 4 days in darkness on 20 µM of 17-β-estradiol. Black and red letters indicate significance for *HY5* and *BBX21* levels, respectively. n=4 biological replicates indicated by open circles. **g-i)** Analysis of *XTH12*, *XTH13*, *XTH26* (g) *PRX7*, *PRX26*, *PRX44* (h) *MYB12*, *F3H* and *FLS1* (i) transcript abundance relative to *GADPH* and *TFIID* in 4 day old seedlings grown as in (f). n=4 biological replicates indicated by open circles. Data represents means ± SE. Different letters represent statistical significant differences ($p<0.05$) as determined by one-way (d, f-h) or two-way (e) ANOVA followed by Tukey's Post Hoc test. **j)** Photo of representative 5-day-old dark grown *hy5* mutant seedlings or T_1 *hy5* mutant seedlings transformed with *35S::VP16HY5ΔN77*.

5.1.2 Supplemental Data

Supplemental Data 5.1.1: Lists of *bbx202122* and *hy5* DEGs from RNA sequencing including a list of DEGs overlapping in the two mutants.

n=3 biological replicates. See Methods for details on statistical analysis. (Available online)

5.1.3 Supplemental Tables

Supplemental Table 5.1.1: List of primers used for cloning, qPCR and ChIP-qPCR analysis.

Cloning primers	**Sequence 5'-3'**
BBX20_LB_attB1	GGGGACAAGTTTGTACAAAAAAGCAGGCTTCATGAAGATTTGGTGTGCTG
BBX20_RBws_attB2	GGGGACCACTTTGTACAAGAAAGCTGGGTTCAAGAGAAGGGTTTGTGATC
gBBX20_R	GGGGACCACTTTGTACAAGAAAGCTGGGTCTCAACAATATGCTTTCCAG
gBBX20_F	GGGGACAAGTTTGTACAAAAAAGCAGGCTATATTGTACCATTTTCAATCAAG
BBX21_RP_VP-AA	TTACCAGAAAGATCTAAACTTTTTATTAGAAGAAAGAGGAGGAGGAGTGATCTGTGCGGCAGTGAAGC
BBX21_LB_attB1	GGGGACAAGTTTGTACAAAAAAGCAGGCTTCATGAAGATCAGGTGCGACGT
BBX21_RBws_attB2	GGGGACCACTTTGTACAAGAAAGCTGGGTTTACCAGAAAGATCTAAACTTTTTATTAGAAG
HY5RBws_attB2	GGGGACCACTTTGTACAAGAAAGCTGGGTTCAAAGGCTTGCATCAGCATT
HY5_DN77_LB_attB1	GGGGACAAGTTTGTACAAAAAAGCAGGCTTCAGGAAGCGAGGGAGGACAC
VP16attB1	GGGGACAAGTTTGTACAAAAAAGCAGGCTTCATGGCCCCCCCGACCGATG
VP16DN77_rev	GTGTCCTCCCTCGCTTCCTCCCACCGTACTCGTCAATTCCAAG
VP16DN77_fw	CTTGGAATTGACGAGTACGGTGGGAGGAAGCGAGGGAGGACAC
pMYB12_fwd_HindIII	TGACGTAAGCTTTCTTTCTTGAACATATACTTGTTACA
pMYB12_rev_EcoRI	TGACGTGAATTCTTTCTCCGGCGGTTATATGTG
pF3H_fwd_BamHI	TGACGTGGATCCGATCATTAATTTATCTTGTCTGCTTAA
pF3H_rev_EcoRI	TGACGTGAATTCTGTAATTACGAAGACAAAAGACTAA
B22LB_attB1	GGGGACAAGTTTGTACAAAAAAGCAGGCTTCATGAAGATTCAGTGTAACGTTTGTG
B22RBws_attB2	GGGGACCACTTTGTACAAGAAAGCTGGGTCTAGAACCGTCGCCGC
XbaI_BBX20f	TGACGTTCTAGATGAAGATTTGGTGTGCTG
XhoI_BBX20r	TGACGTCTCGAGTCAAGAGAAGGGTTTGTGATC
XbaI_BBX21f	TGACGTTCTAGATGAAGATCAGGTGCGACGT
XhoI_BBX21r	TGACGTCTCGAGTTACCAGAAAGATCTAAACTTTTTATTAGAAG
XbaI_BBX22f	TGACGTTCTAGATGAAGATTCAGTGTAACGTTTGTG
XhoI_BBX22r	TGACGTCTCGAGCTAGAACCGTCGCCGC
mTAD_f	AGCGCGGCTTCTGCGTATGCGGCGGATACGTTACCTGGTTGGCAC
mTAD_r	ATCCGCCGCATACGCAGAAGCCGCGCTTGTGGATCCCCACTGATTCA
BBX21_r_C-VP16	CATCGGTCGGGGGGGCCCAGAAAGATCTAAACTTTTTATTAGAAGAAAG
BBX21_f_C-VP16	CTTTCTTCTAATAAAAAGTTTAGATCTTTCTGGGCCCCCCCGACCGATG
VP16_r_attB2	GGGGACCACTTTGTACAAGAAAGCTGGGTTTACCCACCGTACTCGTCAATTC
BBX21-TAD_attB1	GGGGACAAGTTTGTACAAAAAAGCAGGCTTCTCGGTGAATCAGTGGGGATC
BBX21-TAD_attB2	GGGGACCACTTTGTACAAGAAAGCTGGGTTTAAGTAGGAAGAGAGGAATCGAGG
BBX21DN113_attB1	GGGGACAAGTTTGTACAAAAAAGCAGGCTTCTACAAACCTACTTCGAAATCTTCTTC
HY5LB_attB1	GGGGACAAGTTTGTACAAAAAAGCAGGCTTCATGCAGGAACAAGCGACTAGC
HY5RBns_attB2	GGGGACCACTTTGTACAAGAAAGCTGGGTTAAGGCTTGCATCAGCATTAGAAC
qPCR primers	**Sequence 5'-3'**
XTH12_F	CGTCACAGCTTACTACCTTTCTTC
XTH12_R	TGCATTTCGCGGTTACCTTTAC
XTH13_F	CGTCACTGCTTACTACCTTTCATC
XTH13_R	TGCATTTCACGGTTACCTTTGC
XTH18_F	CTCGAGGTGTTCCTGTAGAGTG
XTH18_R	ACACCGCATACATATGAGCAAC
XTH26_F	GAACCCATCCGAAGTTGTGTG
XTH26_R	AGCGTCCAGTTAGTCTTCACTC
PRX7_F	AAGACTTTCGCAGAGCAATCAC
PRX7_R	ATCTCTCCGACACGATCTTCAC
PRX26_F	CAGACTGCTTTGTTTCCGGATG
PRX26_R	ACCAGGACATCTCTGTTCCAAG
PRX44_F	GTGGGATTGTGTCTGGTTATGC
PRX44_R	CTCCTGATCTCTCCAGAACGTC
PRX53_F	TTCGTCCATTCCTTCTCCCATC
PRX53_R	AACGTATGCGCACCAGATAAG

MYB12_F	CCTCAAGCGTGGAAACATAACTCC	
MYB12_R	CGCGATTAGTGACCACCTGTTTC	
F3H_F	CAGGGACGAAGATGAACGGC	
F3H_R	AAGCAAAGAAGTCACGAGCG	
FLS1_F	TTAGGTGTACCGGCTCATACAG	
FLS1_R	TACCTCCCATTACTCAACCTCAG	
IAA6_F	GAAGATGAATCACTGCCGGTTG	
IAA6_R	GCCTATAGCTTTCGATGCTTCC	
BBX20_F	CCAAAACCCGACCAAAATCAG	
BBX20_R	AAGCAAATCCTCCACTCTCCA	
BBX21_F	AACAAGGACAGAACAACAAGAGA	
BBX21_R	TTAGAAGAAAGAGGAGGAGGAGTG	
HY5_F	CAGCAAGCAAGAGAGAGGAAA	*used in Supplemental Figure 5.1.4a, 5.1.8f
HY5_R	CAGCATTAGAACCACCACCA	*used in Supplemental Figure 5.1.4a, 5.1.8f
HY5q_F	CCATCAAGCAGCGAGAGGTCATCAA	*used in Supplemental Figure 5.1.7b
HY5q_R	CGCCGATCCAGATTCTCTACCGGAA	*used in Supplemental Figure 5.1.7b
ACT2_F	CTTGCACCAAGCAGCATGAA	
ACT2_R	CTTTGCACGCAGTGTATGCTC	
EF1a_F	TGAGCACGCTCTTCTTGCTTTCA	
EF1a_R	GGTGGTGGCATCCATCTTGTTACA	
GADPH_F	AGGTGCTTCCAGCTCTTAACG	
GADPH_R	TGCCTTCGGATTCCTCCTTG	
TFIID_F	GAATCACGGCCAACAATC	
TFIID_R	ACTCTTAGCCAAGTAGTGCTCC	
PP2A_F	TATCGGATGACGATTCTTCGTGCAG	
PP2A_R	GCTTGGTCGACTATCGGAATGAGAG	
ChIP-qPCR primers	**Sequence 5'-3'**	
p1_MYB12_F	GAGAAAACAAGGAACTAGGTCG	
p1_MYB12_R	TACCAACCACACACATCAAC	
p2_MYB12_F	CTCGGCACACACTAGAATTAG	
p2_MYB12_R	GAGGGAGAAGGAGATGATGAC	
p1_F3H_F	CTGTGATCTAGTGACCCTTTTG	
p1_F3H_R	ACGGCTCATCTTCCACTTTG	
p2_F3H_F	CGTGATTTCTCCACAGACC	
p2_F3H_R	GCTTTTTGGCTACATTCCAAC	
ip_ACT_F	GTTGGGATGAACCAGAAGGA	
ip_ACT_R	CTTACAATTTCCCGCTCTGC	

5.2 Supplemental information for chapter 3

5.2.1 Supplementary Figures

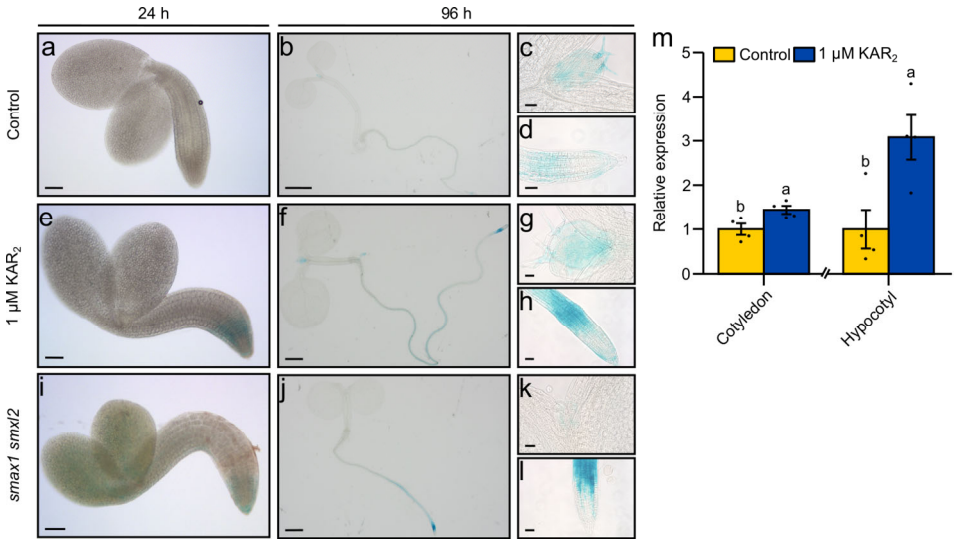

Supplemental Figure 5.2.1: *BBX20* promoter activity of a second transgenic line.

a – l GUS-staining of pBBX20::GUS-GFP line #2 grown for 24 h or 96 h in 80 µmol m^{-2} s^{-1} red light. The seeds were grown on control medium containing 0.1 % Acetone (a - d, i - l) or medium containing 1 µM KAR_2(e - h). Scale bars represent 50 µm (a, c, d, e, g, h, i, k, l), 500 µm (f, j) and 1 mm (b). **m** Transcript abundance of *BBX20* relative to *UBC21* and *PP2A* reference genes in cotyledons and hypocotyls of 4-day old WT seedlings grown in 80 µmol m^{-2} s^{-1} red light. n = 4 independent biological replicates are indicated by black dots. Bars represent the mean and error bars represent SE and different letters denote statistically significant differences as determined by two sample t-test within each tissue type, respectively ($p<0.05$).

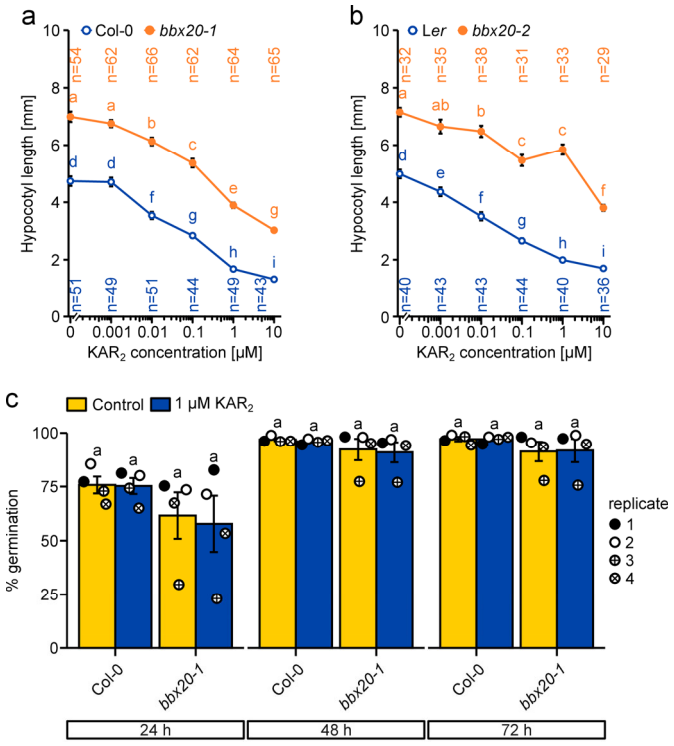

Supplemental Figure 5.2.2: KAR_2 response curves in *bbx20* mutants.

a-b Absolute hypocotyl length values corresponding to Fig. 2a (a) or Fig. 2c (b). Different letters denote statistically significant differences as determined by Wilcoxon rank sum test ($p<0.05$). **c** Germination rate of WT and *bbx20-1* seeds grown on medium containing 0.1 % Acetone (Control) or 1 µM KAR_2 for 24 h, 48 h or 72 h. Bars represent the mean and error bars represent SE and different letters denote statistically significant differences as determined by two-way ANOVA followed by Tukey test within each timepoint, respectively ($p<0.05$).

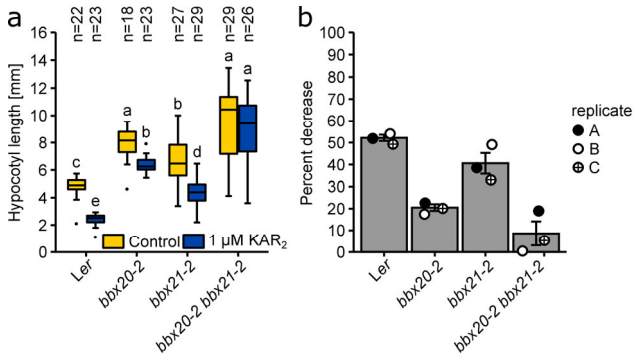

Supplemental Figure 5.2.3: Analysis of the KAR response of *bbx20* and *bbx21* mutants from the L*er* ecotype.

a Hypocotyl measurement of seedlings grown for 5 days on ½ MS medium containing 0.1 % Acetone (Control) or 1 µM Kar_2 in 70 µol m^{-2} s^{-1} red light. Box plots represent medians and interquartile ranges with whiskers extending to the largest/smallest value within 1.5*interquartile range and outliers are shown as dots. Different letters denote statistically significant differences as determined by two-way ANOVA followed by Tukey test (a) ($p<0.05$). **b** Average percent decrease of hypocotyl length in response to KAR treatment in three individual experiments. Bars represent the mean and error bars represent SE. Replicate C corresponds to the data shown in a.

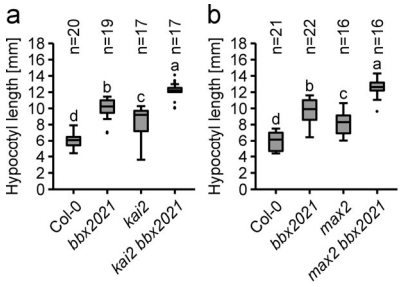

Supplemental Figure 5.2.4: Genetic interaction of *bbx2021* and *kai2* and *max2*.

a – b Hypocotyl measurements of 5-day old seedlings grown in 70 µmol m^{-2} s^{-1} red light. Box plots represent medians and interquartile ranges with whiskers extending to the largest/smallest value within 1.5*interquartile range and outliers are shown as dots. Different letters denote statistically significant differences as determined by one-way ANOVA followed by Tukey test (a,b).

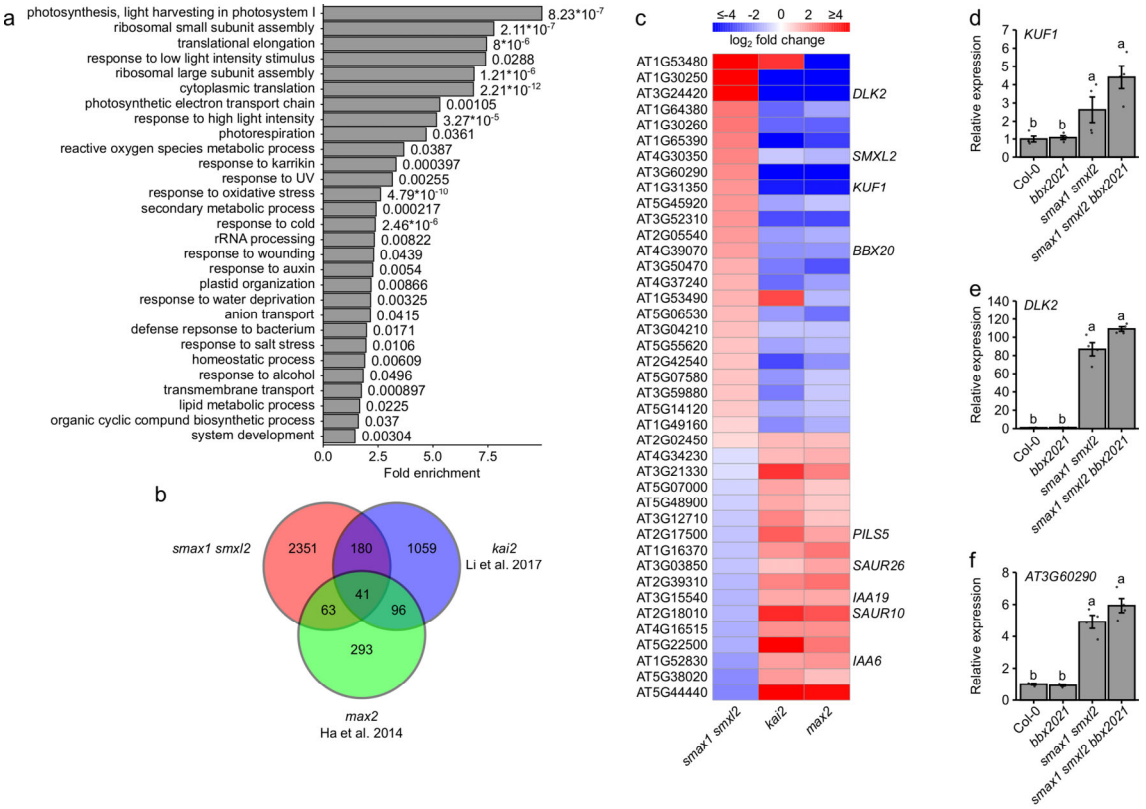

Supplemental Figure 5.2.5: Analysis of SMAX1 and SMXL2 regulated genes.

a Gene ontology analysis of genes deregulated in *smax1 smxl2*. **b** Venn diagram showing the overlap between DEGs in *smax1 smxl2*, *kai2* (Li *et al.*, 2017) and *max2* (Van Ha *et al.*, 2014). **c** Heatmap of the *smax1 smxl2*, *kai2* and *max2* overlap in b. The color scale represents the log_2 fold change relative to WT. **d - f** Transcript abundance of *DLK2, KUF1* and *AT3G60290* relative to *GADPH* and *TFIID* reference genes in 4-day old seedlings grown in 80 µmol m^{-2} s^{-1} red light. n = 4 independent biological replicates are indicated by black dots. Bars represent the mean and error bars represent SE and different letters denote statistically significant differences as determined by one-way ANOVA followed by Tukey's post hoc test ($p<0.05$).

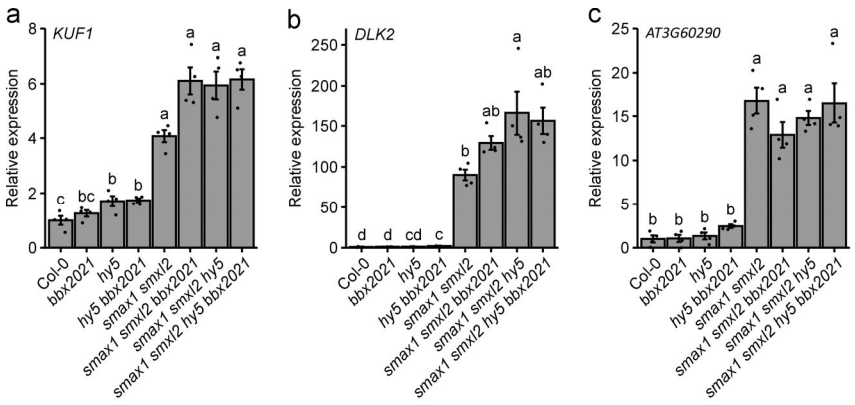

Supplemental Figure 5.2.6: Transcriptional regulation of *KUF1*, *DLK2* and *AT3G60290* in *smax1 smxl2 hy5 bbx2021*.

a - c Transcript abundance of *KUF1* (a), *DLK2* (b) and *AT3G60290* (c) relative to *GADPH* and *TFIID* reference genes in 4-day old seedlings grown in 80 µmol m^{-2} s^{-1} red light. n = 4 independent biological replicates are represented by black dots. Bars represent the mean and error bars represent SE and different letters denote statistically significant differences as determined by one-way ANOVA followed by Tukey's post hoc test ($p<0.05$).

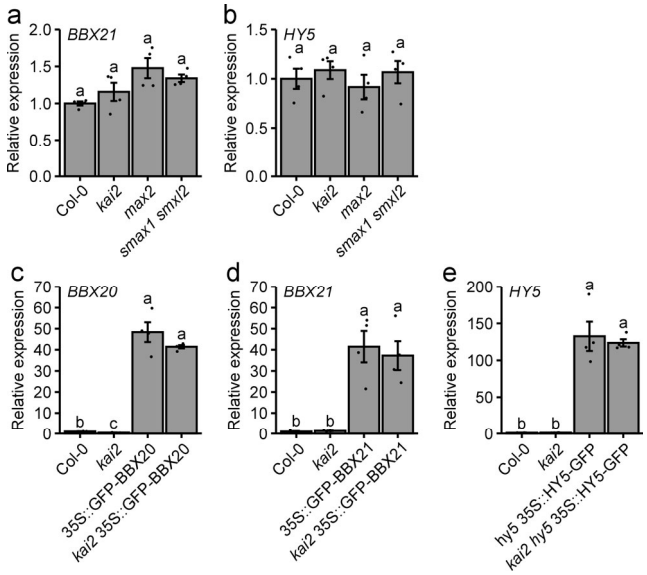

Supplemental Figure 5.2.7: *BBX21* and *HY5* transcript levels in KAR signaling mutants.

a - e Transcript abundance of *BBX21* (a, d), *HY5* (b, e) and *BBX20* (c) relative to *GADPH* and *TFIID* reference genes in 4-day old seedlings grown in 80 µmol m^{-2} s^{-1} red light. n = 4 independent biological replicates are represented by black dots. Bars represent the mean and error bars represent SE and different letters denote statistically significant differences as determined by one-way ANOVA followed by Tukey's post hoc test ($p<0.05$).

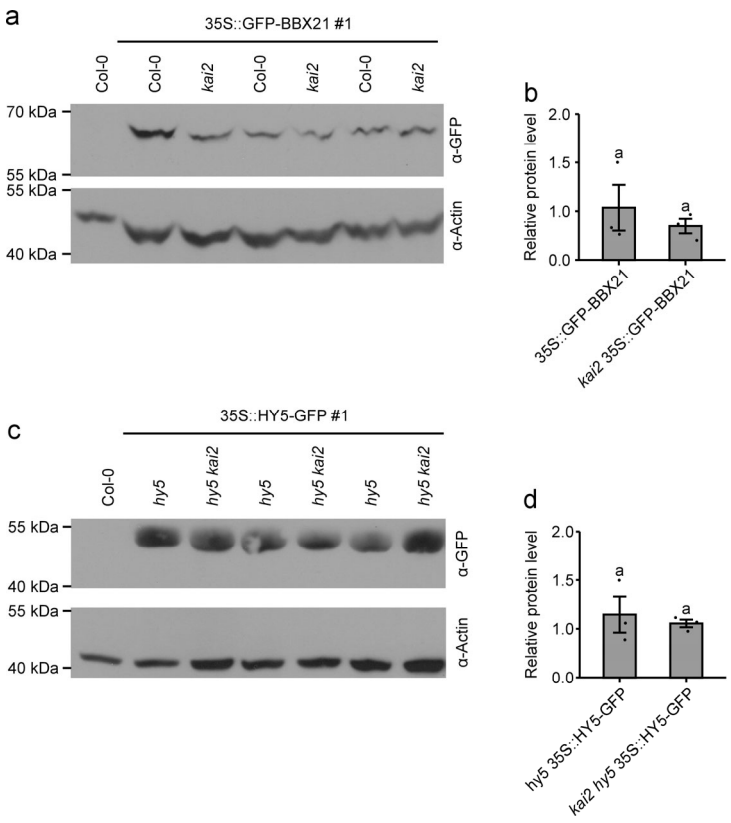

Supplemental Figure 5.2.8: Analysis of BBX21 and HY5 protein levels in the *kai2* mutant.

a, c Immunoblot analysis of total protein samples collected from Col-0 or *kai2* transgenic seedlings expressing GFP-BBX21 (a) or HY5-GFP (c) grown in 80 µmol m^{-2} s^{-1} red light for five days. Anti-GFP and anti-Actin antibodies were used to detect the recombinant proteins and the Actin loading control, respectively. Three independent biological replicates are shown. **b, d** Relative protein levels of BBX21 (b) and HY5 (d) relative to Actin, quantified from the immunoblot analysis in a and c. Bars represent the mean and error bars represent SE and different letters denote statistically significant differences as determined by two sample t-test ($p<0.05$).

5.2.2 Supplemental Data

Supplemental Data 5.2.1: DEGs of *bbx2021* and *smax1 smxl2*.

(Available online)

5.2.3 Supplemental Tables

Supplemental Table 5.2.1: Comparison of DEGs of *bbx2021* and *smax1 smxl2* with *HY5*-regulated genes.

Comparison of DEGs found in *bbx2021* and *smax1 smxl2* with publicly available transcriptome datasets containing *HY5*-regulated genes						
	DEGs of *bbx2021* identified in this study		DEGS of *smax1 smxl2* identified in this study		Zhao et al. 2019 DEGs of *hy5*	Bursch et al. 2020 DEGs of *hy5*
GeneID	log2 Fold Change	p adj.	log2 Fold Change	p adj.	DEGs found in the respective datasets are marked with +	

AT2G05440	-1.10E+00	2.02E-04	2.11E+00	1.32E-26	+	+
AT2G47460	-1.79E+00	1.16E-14	1.14E+00	3.15E-08	+	+
AT3G51240	-1.60E+00	4.96E-17	1.43E+00	1.35E-13	+	
AT3G52740	-1.07E+00	3.42E-05	1.30E+00	4.09E-11	+	+
AT5G02270	-1.40E+00	1.14E-53	7.29E-01	2.11E-15	+	+
AT5G05270	-8.42E-01	6.96E-06	1.37E+00	1.66E-21		
AT5G08640	-2.30E+00	8.89E-68	1.78E+00	3.81E-59	+	+
AT5G13930	-1.14E+00	3.07E-09	2.16E+00	7.85E-41	+	
AT5G44110	-1.49E+00	4.74E-41	7.80E-01	8.25E-12	+	+
AT1G21100	1.10E+00	2.80E-09	-8.03E-01	4.64E-03	+	+
AT4G12550	1.90E+00	2.37E-45	-2.29E+00	4.35E-35	+	+
AT4G15330	9.10E-01	5.81E-10	-9.66E-01	4.53E-08		
AT4G37700	7.09E-01	2.97E-02	-7.75E-01	3.84E-02	+	
AT5G23840	1.09E+00	2.44E-12	-9.18E-01	1.94E-05	+	
AT5G24410	1.35E+00	8.78E-09	-9.97E-01	3.20E-02	+	
AT5G46890	7.13E-01	7.65E-10	-1.17E+00	5.34E-30	+	
AT5G47450	1.11E+00	6.27E-20	-9.82E-01	1.18E-13	+	+
AT3G44970	-8.10E-01	2.08E-13	8.93E-01	1.75E-19	+	+
AT1G76930	7.86E-01	2.22E-05	1.46E+00	1.08E-25		
AT3G56400	1.27E+00	1.96E-07	1.14E+00	2.17E-05		
AT2G44460	-1.01E+00	1.61E-05	-1.68E+00	7.99E-19		
AT1G64795	-5.19E+00	3.42E-59	-5.68E+00	5.29E-26		+
AT1G70850	6.49E-01	7.16E-05	-1.17E+00	4.44E-22	+	
AT2G39310	6.35E-01	1.09E-06	-1.33E+00	1.14E-38	+	
AT3G49120	9.92E-01	1.94E-17	8.82E-01	3.06E-13		
AT1G14960	6.26E-01	1.26E-03	-8.76E-01	1.82E-09	+	+
AT4G15390	8.48E-01	3.70E-08	-1.08E+00	3.02E-14		
AT4G12545	1.01E+00	2.42E-14	-1.22E+00	9.15E-19	+	
AT5G60660	8.16E-01	3.89E-06	-1.45E+00	1.06E-23	+	
AT5G42580	8.50E-01	2.60E-04	-3.15E+00	1.42E-76	+	
AT5G42600	1.23E+00	1.90E-02	-3.59E+00	3.78E-47	+	
AT5G36130	8.56E-01	7.97E-06	-2.76E+00	1.17E-47		+
AT3G13610	6.84E-01	3.51E-02	-1.37E+00	8.30E-16		+
AT2G34500	7.36E-01	5.51E-09	-1.09E+00	4.71E-20	+	
AT5G36140	8.55E-01	2.72E-05	-3.63E+00	2.33E-55		+
AT4G23700	7.10E-01	2.43E-03	-1.80E+00	8.45E-33	+	
AT1G20160	1.01E+00	9.59E-09	-1.08E+00	2.15E-09	+	+
AT1G52400	1.03E+00	5.35E-06	-1.43E+00	4.03E-12		
AT1G10550	7.40E-01	1.05E-03	-1.35E+00	6.70E-13		
AT1G50560	6.02E-01	1.23E-02	-1.01E+00	1.28E-09	+	
AT2G28860	1.63E+00	5.01E-05	-1.77E+00	3.39E-05	+	
AT2G34350	8.58E-01	2.10E-02	-1.47E+00	6.87E-08	+	
AT5G15970	-8.32E-01	3.16E-09	1.53E+00	1.96E-38	+	+
AT2G43510	-8.18E-01	1.20E-08	7.05E-01	4.57E-06		+
AT3G21370	-1.41E+00	5.27E-23	-9.55E-01	3.99E-09	+	+

AT3G17609	-9.71E-01	2.34E-07	9.14E-01	2.28E-08	+	+
AT2G42530	-9.89E-01	1.93E-07	1.74E+00	1.03E-33		+
AT2G34080	-1.06E+00	1.77E-04	1.05E+00	3.76E-05	+	+

Supplemental Table 5.2.2: Comparison of DEGs of *smax1 smxl2* with *KAI2*- and *MAX2*-regulated genes

Comparison of DEGs found in smax1 smxl2 with publicly available transcriptome datasets containing *KAI2*- and *MAX2*-regulated genes				
	DEGS of *smax1 smxl2* identified in this study	*Li et al. 2017* DEGs in *kai2*	Van Ha et al. 2014 DEGs in *max2*	
GeneID	log2 Fold Change	log2 Fold Change	log2 Fold Change	Gene name
AT1G53480	6.188519454	3.943844268	-6.048491451	MRD1
AT1G30250	5.849038097	-9.37128452	-8.790467231	
AT3G24420	5.808455308	-8.974031407	-8.924526192	DLK2
AT1G64380	2.653394282	-2.902495807	-1.742994582	
AT1G30260	2.652267434	-2.915693746	-3.082810379	
AT1G65390	2.412905891	-5.04156156	-3.730506928	
AT4G30350	2.336844891	-1.080956881	-1.462485062	SMXL2
AT3G60290	2.284898979	-6.48442271	-5.866889042	
AT1G31350	2.092611945	-4.45695882	-4.563320089	KUF1
AT5G45920	2.027479143	-1.735120506	-1.135649782	
AT3G52310	2.022053322	-3.474208101	-3.585326735	ABCG27
AT2G05540	1.957018867	-1.920863748	-1.587404983	
AT4G39070	1.832701713	-2.153449514	-2.070222172	BBX20
AT3G50470	1.596396462	-2.531467053	-3.319721682	MLA10
AT4G37240	1.475561709	-2.821665934	-1.878632166	
AT1G53490	1.432963794	3.528246864	-1.357087734	
AT5G06530	1.335340658	-1.971068718	-2.783235571	ABCG22
AT3G04210	1.209076149	-1.103698109	-1.120936001	TN13
AT5G55620	1.18523245	-1.705386862	-1.358089122	
AT2G42540	1.163938651	-3.583176301	-2.17319995	
AT5G07580	1.139545589	-2.089943399	-1.061065768	ERF106
AT3G59880	1.115105901	-2.511155531	-1.020236342	
AT5G14120	1.009616774	-1.667198739	-1.183155411	
AT1G49160	0.850247423	-2.24716566	-1.533418623	
AT2G02450	0.789359097	1.344402782	1.248813876	
AT4G34230	-0.632297184	1.364124259	1.567355899	CAD5
AT3G21330	-0.663860438	3.984628174	2.456995605	
AT5G07000	-0.812465642	1.777240552	1.030491888	ST2B
AT5G48900	-0.916567801	1.615776314	1.008252373	
AT3G12710	-1.073763757	2.376629788	1.136864399	
AT2G17500	-1.14530081	3.154573812	1.781548731	PILS5

AT1G16370	-1.163823559	2.050201809	2.626905233	OCT6
AT3G03850	-1.18627915	1.178094603	1.731149433	SAUR26
AT2G39310	-1.33306864	2.302166277	2.73894095	
AT3G15540	-1.415921635	1.683254215	1.670903543	IAA19
AT2G18010	-1.479231725	4.189927955	3.34871286	SAUR10
AT4G16515	-1.511774404	2.191167498	2.153343924	
AT5G22500	-1.584867358	4.901396222	2.69886499	
AT1G52830	-1.947767653	1.889456993	2.069296691	IAA6
AT5G38020	-2.241224103	1.904208654	1.219662508	
AT5G44440	-2.379886892	10.02337263	4.733637808	

Supplemental Table 5.2.3: Primers used in this study.

Primer for genotyping			
gene	allele	name	sequence
BBX20	*bbx20-1* *bbx20-2*	cc_20_2_f	ggcattgaaagcaaaggagagagtag
		cc_20_2_r	ctcaggtcacccgaaacatccgttc
BBX21	*bbx21-1*	bbx21-1 LP	GGAACTACCGAACTATCATGGGCA
		bbx21-1 RP	GAAGCCACCATCATCATACCA
		LBb1.3	ATTTTGCCGATTTCGGAAC
	bbx21-2	bbx21-2 fwd	CGGTGAATCAGTGGGGATCC
		bbx21-2 rev	AGGAGGAGTGATCTGTGGGA
		DS3-1	ACCCGACCGGATCGTATCGGT
BBX22	*bbx22-1*	bbx22-1 LP	TGCTTAAACCATAAACCTCAAGC
		bbx22-1 RP	CCAAAAGCCACAAGATTCATC
		LBb1.3	ATTTTGCCGATTTCGGAAC
BBX23	*bbx23-1*	bbx23-1 LP	TATGATCCCACCACACATGTG
		bbx23-1 RP	TGGTTCAAATCCAACAAGGTC
		LBb1.3	ATTTTGCCGATTTCGGAAC
HY5	*hy5-215*	HY5_for3	TAAGAAAAATGCAGGAAC
		HY5_rev4	CTCATCGCTTTCAATTCC
		hy5-215_rev	CTCATCGCTTTCAATTCT
	hy5-1	hy5-1_wt_fw	TAAGAAAAATGCAGGAAC
		hy5-1_mut_fw	TAAGAAAAATGCAGGAAT
		hy5-1_rev	AGCTTCTCCTCCAAACT
HYH		hyh LP	ACTCGCATAAGAACATGTGGG
		hyh RP	ACCCACACGCTCTGTGAATAC
		p745 (wiscdslox)	AACGTCCGCAATGTGTTATTAAGTTGTC
KAI2	*htl-3*	kai2_wt_F	attaccgcgtcgtcctctacgac
		kai2_wt_R	tcggatggcttcgaatagttggtttaagtc
		Kai2_mut_F	CATCTGGTCGACGATTACCGCAAC
SMAX1	*smax1-2*	smax1-2 F	CATATGAGAGCTGGTTTAAGT
		smax1-2 R	CATATGTCATCGGGAAAACGC

		LBb1.3	ATTTTGCCGATTTCGGAAC
SMXL2	*smxl2-1*	smxl2-1 F	TGACATACACCGATCACCAC
		smxl2-1 R	GTATCATCATCCCACTTTGCATAC
		LB3	TAGCATCTGAATTTCATAACCAATCTCGATACAC
Primer for qPCR			
gene	geneID	name	sequence
BBX20	AT4G39070	BBX20_FP_2	CCAAAACCCGACCAAAATCAG
		BBX20_RP_2	AAGCAAATCCTCCACTCTCCA
BIC1	AT3G52740	BIC1_fwd	AAGAAGCATCGGAGAGAGATCG
		BIC1_rev	CTTCCTCTACGAGAGCAGTACG
ABCI20	AT5G02270	ABCI20_fwd	TGTTATCTCGGTGGCGAGTG
		ABCI20_rev	TTGGCCATCGGATACCTTGTG
FLS1	AT5G08640	FLS_FW	TTAGGTGTACCGGCTCATACAG
		FLS_REV	TACCTCCCATTACTCAACCTCAG
F3H	AT3G51240	F3H_FP_1	CAGGGACGAAGATGAACGGC
		F3H_RP_1	AAGCAAAGAAGTCACGAGCG
MYB12	AT2G47460	MYB12 2_fwd	GCATTCCACTTTGGGAAACAGGTG
		MYB12 3_rev	CGGAGACGTCTTGAGAGATGGATG
CHS	AT5G13930	CHS_FP_1	AGAAGGGTTGGAGTGGGGT
		CHS_RP_1	CGTAGGTAGGTAGGCAGATAGA
KUF1	AT1G31350	KUF1_FP	GGCGAAACGAAGAAGAACAG
		KUF1_RP	GTGGAGGAGGAAGCGGATAC
DLK2	AT3G24420	DLK2_FP	TTTCTCCTCATTCGTGGTCG
		DLK2_RP	GCTGTCTCGGGCTTCATCTT
AT3G60290	AT3G60290	2OG-FE-ox-family_fwd	TTACCTGCCGATGAGAAGATGC
		2OG-FE-ox-family_rev	TTTCCTTGTAGCAGGGAGGATTG
BBX21	AT1G75540	BBX21_FP_1	AACAAGGACAGAACAACAAGAGA
		BBX21_RP_1	TTAGAAGAAAGAGGAGGAGGAGTG
HY5	AT5G11260	HY5 1_fwd	ATGAGGAGATACGGCGAGTG
		HY5 1_rev	TCTGTTCCTCAACAACCTCTTCAG
TF2D	AT1G17440	TFIID_FW	GAATCACGGCCAACAATC
		TFIID_RV	ACTCTTAGCCAAGTAGTGCTCC
GADPH	AT1G42970	GADPH_FW	AGGTGCTTCCAGCTCTTAACG
		GADPH_RV	tgccttcggattcctccttg
UBC21	AT5G25760	UBC21_fw	CTCTTAACTGCGACTCAGGGAATC
		UBC21_rv	TGCCATTGAATTGAACCCTCTCAC
PP2A	AT1G69960	PP2A_fw	CCATTAGATCTTGTCTCTCTGCT
		PP2A_rv	GACAAAACCCGTACCGAG
Primer for Cloning			
		pBBX20_F	GGGGACAAGTTTGTACAAAAAAGCAGGCTgtccagtagtacatccatgtgac
		pBBX20_R	GGGGACCACTTTGTACAAGAAAGCTGGGTCTTTCTATTTTCTTTCCTCTCTGTATTAC